

**Biological evaluation of novel small molecule inhibitors against
*Mycobacterium tuberculosis***

by

Mr. Sagar Swami

10BB17J26055

A thesis submitted to the
Academy of Scientific & Innovative Research
for the award of the degree of
DOCTOR OF PHILOSOPHY
in
SCIENCE

Under the supervision of

Dr. Dhiman Sarkar



CSIR-National Chemical Laboratory, Pune



Academy of Scientific and Innovative Research

AcSIR Headquarters, CSIR-HRDC campus

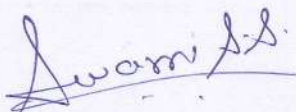
Sector 19, Kamla Nehru Nagar,

Ghaziabad, U.P. – 201 002, India

June-2022

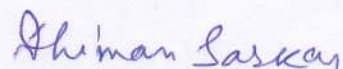
CERTIFICATE

This is to certify that the work incorporated in this Ph.D. thesis entitled, "Biological evaluation of novel small molecule inhibitors against *Mycobacterium tuberculosis*" submitted by Mr. Sagar Swami to the Academy of Scientific and Innovative Research (AcSIR) in fulfillment of the requirements for the award of the Degree of Doctor of Philosophy in Science, embodies original research work carried-out by the student. We, further certify that this work has not been submitted to any other University or Institution in part or full for the award of any degree or diploma. Research materials obtained from other sources and used in this research work have been duly acknowledged in the thesis. Images, illustrations, figures, tables, etc., used in the thesis from other sources, have also been duly cited and acknowledged.



Mr. Sagar Swami

Date: 03/06/2022

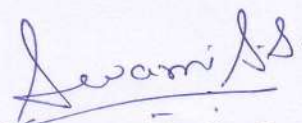


Dr. Dhiman Sarkar

Date: 03/06/2022

Statements of Academic Integrity

I, Mr. Sagar Swami, a Ph.D. student of the Academy of Scientific and Innovative Research (AcSIR) with Registration No. 10BB17J26055 hereby undertake that, the thesis entitled "Biological evaluation of novel small molecule inhibitors against *Mycobacterium tuberculosis*" has been prepared by me and that the document reports original work carried out by me and is free of any plagiarism in compliance with the UGC Regulations on "*Promotion of Academic Integrity and Prevention of Plagiarism in Higher Educational Institutions (2018)*" and the CSIR Guidelines for "*Ethics in Research and in Governance (2020)*".

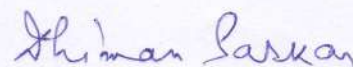


Signature of the Student

Date: 03/06/2022

Place: Pune

It is hereby certified that the work done by the student, under my supervision, is plagiarism-free in accordance with the UGC Regulations on "*Promotion of Academic Integrity and Prevention of Plagiarism in Higher Educational Institutions (2018)*" and the CSIR Guidelines for "*Ethics in Research and in Governance (2020)*".



Signature of the Supervisor

Name: Dr. Dhiman Sarkar

Date: 03/06/2022

Place: Pune

Acknowledgment

My journey to get a Ph.D. degree is a collective effort of many helping hands. This journey would not reach its destination without the support of numerous people who helped me and encouraged me in many ways. It is my privilege to write this section to express my sincere gratitude to all of them.

*First of all, I would like to express my gratitude to my research supervisor **Dr. Dhiman Sarkar** for giving me the first opportunity to do research under his supervision and guiding me to reach my destination during these five years. I thank him for the immense patience, encouragement, and guidance he has given me. He supported me a lot during my tough times and given many alternatives to come back on track and get the work done. As a supervisor, he helped me to develop my technical and scientific skills as an independent researcher by giving me complete freedom to think about problems, perform experiments and get the solutions to the problems. Whatever work discipline I learned during this journey, I will continue throughout my life. Because of his rigorous training during my Ph.D., I improved many skills, effectively conveyed my knowledge to the scientific community, and received awards. His guidance and encouragement helped me to develop confidence and solve problems. It was a great pleasure to complete my Ph.D. thesis under his supervision. I wish him good health and continuing success in his future accomplishments.*

*I thank **Dr. Aashish Lele** (Present Director) and **Dr. Ashwini Kumar Nangia** (Former Director) CSIR-National Chemical Laboratory for the outstanding leadership and the motivating atmosphere they provided in the institute. I've been fortunate to be a member of the NCL scientific community, which has developed a high degree of performance and potential in research that surpasses most other universities.*

*I gratefully acknowledge **Dr. Ashok Giri** (Chairperson), **Dr. Mahesh Kulkarni**, and **Dr. Moneesha Fernandes** for their valuable suggestions, timely evaluation, and critical comments on my work progress during the Doctoral Advisory Committee (DAC) meetings. I especially want to express my gratitude to Dr. Mahesh Kulkarni and his students, Dr. Reema Banarjee, Arvind, and Babasaheb, for their support in proteomics experiments and for allowing me to use their lab resources.*

*I am thankful to former and current heads of the Organic chemistry division (OCD), **Dr. Pradeep Tripathi**, **Dr. Subhash Chavan**, and **Dr. N. P. Argade**, for their excellent leadership and an inspirational working environment in the institute.*

*I also want to thank my collaborators, **Dr. Pratibha Shrivastava** (Agharkar Research Institute), **Dr. Surekha Satpute** (Department of Microbiology, Savitribai Phule Pune University), and **Dr. Anamik Shaha** (Former Vice-Chancellor of Gujrat Vidyapith, Ahmedabad) for giving me an opportunity to work with them. During the collaborative work, I learned how to communicate with team members, get the work done, and publish it effectively.*

I would also like to acknowledge all the stores & purchase section staff members, Admin, and technical divisions, for their friendly support during this journey. My sincere thanks to all the members of the SAC office for timely completing the documentary procedures as per guidelines.

*I am thankful to my other teachers **Dr. D. G. Kadam** (Former head of Microbiology department, Dayanand College Solapur), **Dr. S. N. Deshpande** (Associate Professor, Microbiology Department, Dayanand College Solapur), for creating interest in microorganisms. Because of their guidance, I learned to think scientifically. I got motivated to study further and find the answers to many scientific questions.*

*I am thankful to **Dr. Rahul Bhambure** for allowing me to use their LC-MS instrument and his students, **Dr. Tejas Chirmade** and **Deepa Mehta**, for their help in proteomics studies.*

*I want to thank my seniors, **Dr. Sampa Sarkar**, **Dr. Shamim Akhtar**, **Dr. Suvarna Gamble**, and **Dr. Meghna Athalye**, for their help and guidance. My special thanks to **Dr. Amit Choudhary** for teaching me screening techniques and publishing the work effectively. I also want to thank **Dr. Rahul Aher** for helping me in docking studies and many scientific discussions.*

*I am very thankful to my friend **Dr. Amar Yeware** for his support from the first day in the lab. His valuable suggestions and encouragement helped me a lot during this journey. I also thank my friend **Dr. Sonia Agrawal** who taught me the SDS-PAGE technique and helped me learn most of the techniques in the lab during my earlier days. As we are the last two members doing Ph.D., I am thankful to her for maintaining a healthy lab environment till the last day of the lab during this journey. I am thankful to our project trainees, Yash, Sushmita, Shibani, and Shakti, for maintaining a cheerful and healthy work atmosphere inside and outside the lab during their project tenure.*

*I am also thankful for **TheraIndx Lifescience Pvt. Ltd. Bangalore** for their help in in-vivo pharmacokinetic studies of novel antitubercular molecules.*

I would like to thank my dearest friends and batchmates (Jan. 2017 Ph.D. batch) Arvind, Babasaheb, Deepa, Kunthal, Bharat, Vasu, and Aabha, without whom this journey would not have been enjoyable and memorable.

*I am thankful to the **AcSIR** team for Ph.D. registration and **CSIR** for giving me this immense opportunity and providing the research fellowship during my Ph.D.*

*I express my deepest gratitude to all my family members who always had faith in me and were always supportive throughout my Ph.D. I especially want to thank my late mother, **Mrs. Vidya Swami**, and my late father, **Mr. Shivanand Swami**, for their blessings in completing this journey. I am thankful to my uncle **Mr. Sidhhayya Swami** who holds our hand in tough times, and because of his help, only I can reach this place. His perfection and sincerity have been my inspiration. I am thankful to my brother **Uday Swami** for always being with me and loving unconditionally.*

My special thanks to my late grandmother for the unforgettable memories with her from my childhood, and I know she will always be with me.

*The most important person in my life is my wife, **Deepali**. She is the pillar of our family. We started the same journey of Ph.D. I thank God Almighty for having such an excellent life partner. She supported me a lot in challenging and happy times during this journey of getting a Ph.D. Her countless efforts and unconditional love motivated me to reach the goal. I also thank her guide, **Dr. Vijay Bondre** (Encephalitis group, National Institute of Virology, ICMR Pune), for his help and timely encouragement during this journey.*

*I am also thankful to my mother-in-law **Smt. Sangeeta Narayan Mali** for endless support and giving valuable encouragement to complete this journey. I also thank **Dinesh** and **Namrata** for making this journey enjoyable.*

I know this is way too long, and I am still missing many people, but I just want to say that I am thankful to everyone and everything (even to my online guru “GOOGLE” and my laptop also, which, even after five years responding well) who contributed to star glazing my journey here in tiniest of thought and action.

Finally, I wish to thank God for giving me immense patience to complete my Ph.D. thesis.

*....**Sagar Swami***

Sr.No. Title/Sub-title	Page No.
I Contents	i-iii
II Abbreviations	iv-vi
Chapter 1: Overview of disease and drug discovery for tuberculosis	1-59
1. Introduction	2
1.1. Overview of tuberculosis	2
1.1.1. Taxonomy classification of <i>Mycobacterium tuberculosis</i>	2
1.1.2. Global implications of tuberculosis	2
1.1.3. Signs and Symptoms	3
1.1.4. Different types of tuberculosis	4
1.1.5. Transmission and pathogenesis of <i>Mycobacterium tuberculosis</i>	7
1.1.6. Microbiology of <i>Mycobacterium tuberculosis</i>	9
1.1.7. Diagnosis	11
1.1.8. Different physiological states of <i>Mycobacterium tuberculosis</i>	16
1.1.9. Treatment	18
1.2. Drug discovery in tuberculosis	23
1.2.1. The problem of MDR/XDR-TB	25
1.2.2. Major challenges in drug discovery against <i>Mycobacterium tuberculosis</i>	26
1.2.3. Different drug screening models	27
1.2.4. Global Alliance for TB Drug Development	36
1.2.5. Current status of drug discovery for tuberculosis and the importance of drug target identification	36
2. Thesis objectives	38
3. References	39

Chapter 2: Screening of novel small molecule inhibitors against the active and dormant stage of <i>Mycobacterium tuberculosis</i>	60-76
2.1. Introduction	61
2.2. Results	62
2.3. Discussion	68
2.4. Materials and Methods	71
2.5. References	74
Chapter 3. Identification of an intracellular protein target of different inhibitors in the active and dormant stage of <i>Mycobacterium tuberculosis</i>	77-145
3A. Identification of a protein target of RRA2 inhibitor within the active <i>Mycobacterium tuberculosis</i>	77-107
3.A.1. Introduction	78
3.A.2. Results	79
3.A.3. Discussion	93
3.A.4. Materials and Methods	95
3.A.5. References	101
3B. Identification of a protein target of RRA268 inhibitor within the dormant <i>Mycobacterium tuberculosis</i>	108-145
3.B.1. Introduction	109
3.B.2. Results	111
3.B.3. Discussion	126
3B.4. Materials and Methods	129
3.B.5. References	138

Chapter 4. Drug metabolism and pharmacokinetics study of novel hits against <i>Mycobacterium tuberculosis</i>	146-191
4.1. Introduction	147
4.2. Results	149
4.3. Discussion	174
4.4. Materials and Methods	177
4.5. References	186
III Abstract for Indexing	192
IV List of Publications	193
V List of Posters and Conferences	195
VI Copy of SCI Publications	

ABBREVIATIONS

TB	Tuberculosis
Mtb	<i>Mycobacterium tuberculosis</i>
BCG	Bacille Calmette–Guerin
HIV	Human immunodeficiency virus
AIDS	Acquired immunodeficiency syndrome
WHO	World health organization
PDIM	Phthiocerol dimycocerosate
SOD	Superoxide dismutase
ETH	Ergothioneine
ROS	Reactive oxygen species
RNS	Reactive nitrogen species
CO	Carbon monoxide
ZN	Ziehl–Neelsen
LJ	Lowenstein Jensen
CSF	Cerebrospinal fluid
LTBI	Latent tuberculosis infection
CXR	Chest X-ray
LRC	Low-resource countries
TST	Tuberculin skin test
PPD	Plasma protein derivative
CDC	Center for disease control
TU	Tuberculin unit
IGRA	Interferon-gamma release assay
IFN	Interferon
CFP	Culture filtrate protein
ESAT-6	Early secreted antigenic target 6
RD1	Region of difference 1
ELISA	Enzyme-linked immunosorbent assay
ELISPOT	Enzyme-linked immunosorbent spot
FDA	Food and Drug Administration
PBMCs	Peripheral blood mononuclear cells
MDR-TB	Multidrug-resistant tuberculosis
PTB	Pulmonary tuberculosis
μL	Microliter
ml	Milliliter
CFU	Colony-forming units
LF-LAM	Lateral flow lipoarabinomannan
CADx	Computer-Aided Detection
LTB	Latent tuberculosis
VBNC	Viable but non-culturable
DPI	Diphenyleneiodonium
NADH	Nicotinamide adenine dinucleotide hydrogen
DOTS	Directly observed treatment, short-course

XDR	Extensively drug-resistant
ESX-1	ESAT-6 secretion system-1
DST	Drug Susceptibility Testing
LORA	Low oxygen recovery assay
MBC	Minimal bactericidal concentration
PBS	Phosphate buffer saline
GFP	Green fluorescence protein
STR	Streptomycin
RPM	Revolutions per minute
BTZ	Benzothiazinone
MOXI	Moxifloxacin
MER	Meropenem
RIF	Rifampicin
NO	Nitric oxide
MIM	Macrophage infection models
MOI	Multiplicity of infection
NR	Nitrite reductase
ETC	Electron transport chain
XRMA	XTT reduction menadione assay
XTT	2,3-bis[2-methoxy-4-nitro-5-sulfophenyl]-2H-tetrazolium-5-carboxanilide
BS	Biosurfactant
IC ₅₀	Half maximal inhibitory concentration
DMAc	Dimethylacetamide
DMSO	Dimethyl sulfoxide
ATCC	American Type Culture Collection
MTCC	Microbial Type Culture Collection
MTT	3-(4,5-dimethylthiazol-2-yl)-2,5-diphenyl tetrazolium bromide
SAR	Structure-activity relationship
ADAS	Active and Dormant Anti-tubercular Screening
HPLC	High-performance liquid chromatography
Da/kDa	Dalton/Kilodalton
PLGS	ProteinLynx Global SERVER
SDS-PAGE	Sodium dodecyl sulfate-polyacrylamide gel electrophoresis
MSA	Multiple Sequence Alignment
PSA	Pairwise Sequence Alignment
kcal/mol	Kilocalorie per mole
LC-MS	Liquid chromatography-mass spectrometry
HSPs	Heat shock proteins
cpn	Chaperone
DC	Dendritic cells
PtpB	Protein tyrosine phosphatase B
FBS	Fetal bovine serum
PMA	Phorbol myristate acetate

THF	Tetrahydrofuran
UHPLC	Ultrahigh performance liquid chromatography
ESI ⁺	Electrospray ionization positive
PDB	Protein Data Bank
NAPs	Nucleoid-associated proteins
ADC	Albumin dextrose catalase
ADC	Albumin-dextrose-catalase
OD	Optical density
C _{max}	Peak concentration in plasma
NCA	Non-compartmental analysis
t _{1/2}	Elimination half-life
PAMPA	Parallel artificial membrane permeability
MTD	Maximum tolerated dose
P _{app}	Apparent permeability coefficient
SEM	Standard error of the means
AUC	Area Under the Plasma Concentration Time Curve
AUC _{0-t}	Area Under the Plasma Concentration Time Curve from t=0 to C _{last}
AUC _{0-∞}	Area Under the Plasma Concentration Time Curve from t=0 to infinity
AUC _{extr}	Extrapolated AUC from t _{last} to infinity
BLOQ	Below Limit of Quantitation
CMC	Carboxymethylcellulose
CC	Calibration curve
EDTA	Ethylenediaminetetraacetic acid
h	Hour(s)
K _{el}	First order Elimination rate constant
kg	Kilogram
LLOQ	Lower Limit of Quantitation
Min	Minute(s)
mg	Milligram
mg/kg	Milligram per kg
PK	Pharmacokinetics
R ²	Regression coefficient
t _{max}	Time of peak concentration in plasma
SD	Standard Deviation
CPCSEA	Committee for the Purpose of Control and Supervision of Experiments on Animals

Chapter 1

Introduction



***Overview Of Disease And Drug
Discovery For Tuberculosis***

1. Introduction

1.1. Overview of tuberculosis

Tuberculosis (TB) is a communicable disease frequently caused by the bacteria called *Mycobacterium tuberculosis* (Mtb). The bacteria most often affect the lungs but can harm any body part. The word Mycobacterium refers to a “fungus-like bacterium” [1]. It explains how the tubercle bacillus forms mold-like pellicles on the surface of a liquid medium. Robert Koch first reported the identification of Mtb by microscopic staining method on March 24, 1882.

Every year on March 24, we acknowledge “World Tuberculosis Day” to increase public awareness of the disease's terrible health, social, and economic effects and intensify efforts to combat the global TB pandemic. Mtb and members of the TB complex are important human pathogens (*Mycobacterium bovis*, *Mycobacterium bovis* bacille Calmette–Guerin (BCG), *Mycobacterium canettii*, *Mycobacterium africanum*, *Mycobacterium microti*, and *Mycobacterium pinnipedi*) also responsible for TB, which is one of the most explored human diseases. These mycobacteria are evolutionarily related, with more than 99.9% chromosomal identity, and they cause TB in mammalian hosts with similar pathophysiology. Mtb has only been found to survive and proliferate natively in humans.

1.1.1. Taxonomy classification of *Mycobacterium tuberculosis*

Kingdom	: Bacteria
Subkingdom	: Posibacteria
Phylum	: Actinobacteria
Subclass	: Actinobacteridae
Order	: Actinomycetales
Suborder	: Corynebacterineae
Family	: Mycobacteriaceae
Genus	: Mycobacterium
Species	: Mycobacterium tuberculosis

1.1.2. Global implications of tuberculosis

In 2020, about 1.5 million deaths occurred from a single disease, i.e., TB (including 2,14,000 people with HIV). It is the world's 13th most significant cause of mortality and the second leading communicable disease after COVID-19 (above HIV/AIDS) [2]. Globally, ~10 million

individuals will have TB by 2020, including 3.3 million women, 5.6 million males, and 1.1 million teenagers in the country. TB is seen in all nations worldwide and in all age groups of the population [3]. According to world health organization (WHO) estimations, the number of individuals developing TB and dying from the disease in 2021 and 2022 might be significantly higher.

Globally, in 2020, from the list of WHO regions, countries such as Africa (25 %), Western Pacific Asia (18%), and South-East Asia (43%) had the most TB cases, with lower numbers in the Eastern Mediterranean (8.3%), Europe (2.3%), and the Americas (3.0%). The other 30 countries with the highest TB burden reported for 86% of all projected incident cases worldwide, with eight nations of them (Figure 1) accounting for two-thirds of the worldwide total: China (8.5%), India (26%), Indonesia (8.4%), Pakistan (5.8%), the Philippines (6.0%), Nigeria (4.6%), Bangladesh (3.6%), and South Africa (3.3%). The eight nations (Figure 1) ranked first to eighth in terms of case counts, accounting for two-thirds of worldwide cases in 2020 [4].

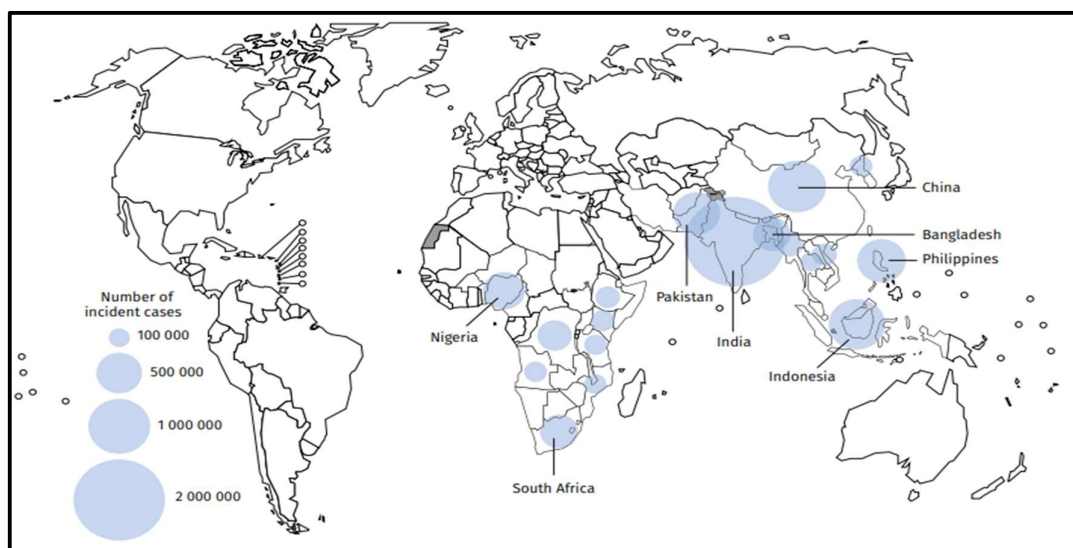


Figure 1. Prevalence of tuberculosis in 2020, based on nations having at least 100000 incident cases (Image reprinted with permission from “Global tuberculosis report 2021. Geneva: World Health Organization; 2021. Licence: CC BY-NC-SA 3.0 IGO”)

1.1.3. Signs and Symptoms

The symptoms of TB vary depending on where the bacilli are developing inside the body. In most cases, Mtb grows in the lungs (pulmonary TB) and may show symptoms such as a persistent cough for at least three weeks or longer, cough up blood, sputum, and chest pain

[5]. Common signs and symptoms include chills, fever, night sweats, swelling in the neck, lack of appetite, exhaustion, and weight loss [6]. Severe nail curling is also reported in some cases [7].

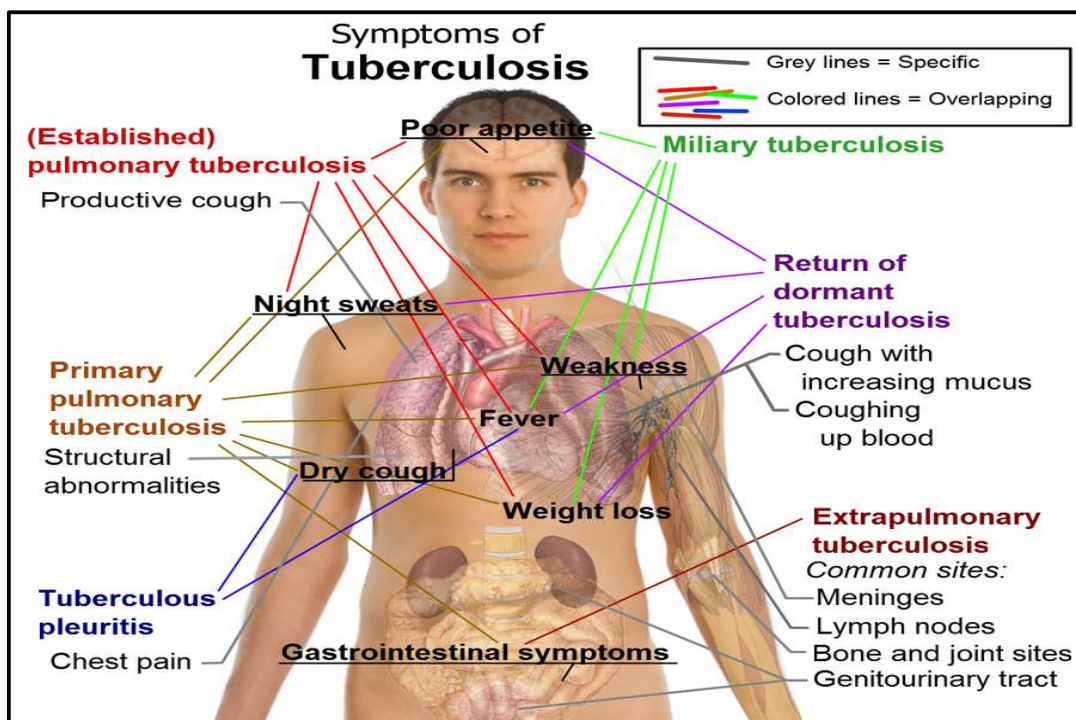


Figure 2. Symptoms of Tuberculosis (Image credit: <http://www.cchd.net/tuberculosis.html>)

1.1.4. Different types of tuberculosis

A. Pulmonary TB

When a person contracts TB, the Mtb bacilli predominantly target the lungs (in about 90 percent of cases), referred to as pulmonary Tb cases. About a quarter of the infected population may be asymptomatic and thus become the major hurdle in controlling the disease [8,9]. Chest discomfort and a continuing cough with sputum are common symptoms. Furthermore, pulmonary TB can develop into a long-term infection that results in significant disfiguring in the upper lobes of the lungs.

B. Extrapulmonary TB

Most pulmonary diseases require to spread out of the lung, and extrapulmonary tuberculosis (EPTB) responsible for a significant portion of TB cases globally. The predominance of these infections in vulnerable populations, such as children and those malnourished, is a characteristic feature of EPTB in all clinical forms [10]. In case of EPTB patients, Mtb can

infect a diverse spectrum of tissues and organs in addition to the lungs and lung parenchyma. Globally, extrapulmonary infections account for around ~15% of tuberculosis infections; these infections are challenging to identify, and since they may or may not be accompanied by pulmonary symptoms [11], treatment is more difficult in such patients. The same patient frequently has both pulmonary and extrapulmonary lesions present while still being known as having PTB [12]. The most common localization sites in the body are the pleura, lymph nodes, bone and joints, CNS, and abdomen (gastrointestinal and/or genitourinary system).

Lymphadenitis is often an infection of the cervical lymph nodes caused by broad hematogenous dissemination of the Mtb bacilli and is the most severe type of extrapulmonary infection seen in TB patients [13]. Numerous minor lesions of any form might develop due to bloodstream-mediated dissemination throughout the entire body. Mtb spreads to the nearby lymph nodes from a single initial lesion before moving through the lymphatic and circulatory systems to reseed the lungs[14]. An infection of the lung's mucous membranes frequently manifests as pleural effusions or collections of fluid between the membranes, and the lung is the second most typical cause of EPTB. Interestingly, these illnesses are more frequently linked to *Mycobacterium bovis*, a closely similar species, rather than Mtb, most likely due to the ingestion of tainted milk products [15]. Infection of the central nervous system is a different, less frequent, but potentially dangerous type of EPTB (CNS). This can manifest as encephalitis, TB meningitis, an abscess, or a tuberculoma [16]. Another typical form of EPTB is genitourinary (GU) TB. It comprises a range of clinical problems, including renal failure, infertility, persistent pelvic pain, single-organ TB localization, and complex GU disorders. TB disseminated locally elsewhere in the body generally comes second to GU TB [17]. The kidney, the epididymis, or the female genital organs are the main organs that Mtb bacilli reach through hematogenous dissemination [18].

Due to the extraordinarily wide range of indications and symptoms and the need for efficient diagnostic methods, diagnosing EPTB is challenging. Other factors, such as the location of involvement, the severity of the disease, and the host's immunological response, EPTB's clinical presentations, are incredibly variable. Since EPTB is frequently paucibacillary, collecting specimens suitable for microscopy, histology, culture, or molecular studies at the infection sites may be challenging. [19-21]. Imaging results are frequently non-specific, and serologic testing has been shown to be ineffective in diagnosing TB. The collection of samples for histology and microbiological examinations is not always simple. According to the WHO criteria of EPTB, a diagnosis of EPTB should be made based on one

specimen that tested positive for the disease on culture, positive histology results, or strong clinical evidence that EPTB is active [12]. Microscopy, culture, and nucleic-acid amplification procedures are examples of microbiological approaches. They are all helpful in diagnosing EPTB, and advancements in techniques such as closed automated nucleic acid amplification equipment and automated liquid culture have produced satisfactory or excellent outcomes. Nevertheless, difficulties persist, and the effectiveness of current microbiological approaches for diagnosing EPTB is still insufficient.

According to available data, Mtb actively stimulates angiogenesis to facilitate diffusion by forming new blood vessels [22,23]. Purified recombinant heparin-binding haemagglutinin adhesin (HbhA) (Mtb dissemination factor) vaccination prevents Mtb infection in mice and lowers the bacterial burden in the lungs and extrapulmonary organs [24,25], indicating that this research may have a variety of potential applications[26,27]. A combination regimen may have the ability to prevent dispersion since adding this antigen boosts the BCG vaccine's effectiveness [28]. Moreover, discovering a complete set of extrapulmonary and dissemination determinants for Mtb could advance our knowledge of the underlying molecular pathways, which will need to be confirmed and further examined in both small animal models and in vitro models. Another interesting report highlighted the importance of antigens actively transported to the lymph nodes by dendritic cells (DC) [29]. As they carry Mtb bacilli to the lymph nodes for presentation to immune cells, DC could offer a potential pathway for Mtb dissemination away from the initial site of infection. Treating extrapulmonary infections offers additional treatment problems because treating extrapulmonary infections does not necessarily result in patient testing positively for TB using a sputum smear test, the gold standard TB diagnostic test [30]. Furthermore, evidence indicates that Mtb actively promotes angiogenesis to create new blood vessels to aid diffusion and disseminate to new locations inside the body [31,32].

C. Miliary TB

Miliary TB develops when Mtb bacilli arrive in the blood circulation and spread throughout the body, where they proliferate and cause illness in various locations. In these cases, the Mtb can proliferate throughout the body in small clusters, affecting numerous organs simultaneously. Miliary TB, also known as "Disseminated tuberculosis," is an uncommon yet potentially more deadly and widespread type of TB that accounts for around 10% of all extrapulmonary TB cases [33-35].

1.1.5. Transmission and pathogenesis of *Mycobacterium tuberculosis*

According to Wells WF, the dried-out remnants of droplet nuclei that may carry harmful microbes are the carrier of airborne respiratory disease transmission [36]. Airborne infectious aerosols primarily transmit TB by droplet nuclei of size 0.5–5.0 μM in diameter. These aerosols are tiny enough to stay in the air for a longer time and distribute through air currents by coughing [37,38], sneezing [38], singing [39, 40], and talking [38,40] are only a few of the aerosol-generating respiratory activities that have been linked to the transmission of the disease. Interestingly, another study found that a single sneeze can release up to 40,000 droplets with an exit speed of a maximum of 4.5 meters/ second, which is one reason for disease transmission [41,42]. However, based on epidemic studies and observed connections, evidence for the relative relevance of these different respiratory activities is primarily hypothetical. TB is spread primarily by a sequence of variables, including live bacilli in the patient's sputum, spit aerosolization as droplet nuclei by patient coughing, sensitivity (immune status) of the exposed host, bacilli strength in the air, proximity, duration, and frequency of time the host breathes the air containing potential Mtb bacilli [43,37].

Pathogenesis of TB disease begins when a person inhales tubercle bacilli containing droplet nuclei from an infected person that reach the lungs' alveolar air sacs (Figure 3). Alveolar macrophages and other phagocytic immune cells identify and engulf these foreign tubercle bacilli; most of them are eliminated or suppressed by phagocytosis. During the early steps of infection, the macrophage engulfs the bacteria and is subsequently kept in a membrane-bound vesicle termed a phagosome that supports a primary cellular niche for Mtb to replicate [45,46]. Macrophages in the lungs release chemokines and cytokines that attract other phagocytic cells, such as monocytes, another alveolar, and macrophages neutrophils, forming structures called granuloma/tubercles. On the other hand, Mtb shifts to a latent or non-replicative state inside the granuloma to survive under harsh conditions. After this, a phagolysosome is formed when a phagosome fuses with a lysosome. Here, the cell tries to destroy the Mtb bacilli in the phagolysosome by using reactive oxygen species (ROS), reactive nitrogen species (RNS), carbon monoxide (CO), and an increased acidic environment.

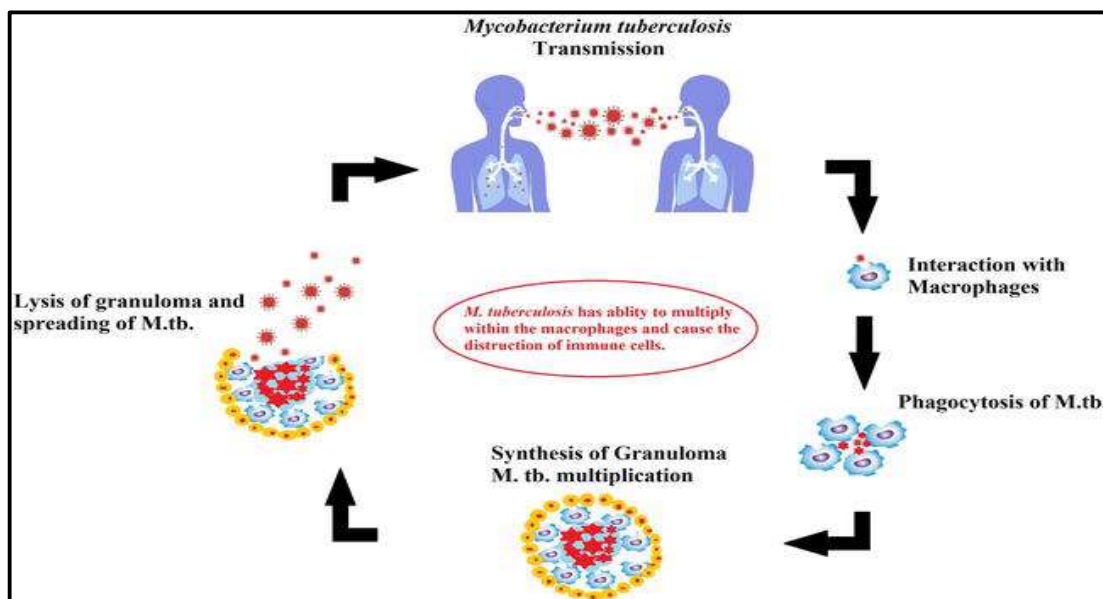


Figure 3. Transmission of *Mycobacterium tuberculosis* (Image credit- Dwivedi, Manish, and Priya Giri. *Molecular Epidemiology Study of Mycobacterium Tuberculosis Complex* (2021): 9.) [44]

On the other hand, Mtb possesses a thick, waxy mycolic acid capsule that shields it from these toxic substances. Mtb could proliferate inside macrophages, eventually killing the immune cells, although the precise mechanism of their survival within macrophages is unknown. In accordance with this, several findings are reported on the primary role of cell-wall related lipids (cycloprotonated mycolic acids, phthiocerol dimycocerosate (PDIM), etc.) [47,48], secretory antioxidant enzymes [superoxide dismutase (SodC, SodA), catalase (Kat), etc.] and secretory redox buffer ergothioneine (ERG) in delivering an excellent anatomical barrier to and detoxification of exogenous oxidants generated by the host [49]. Catalase-peroxidase, which helps the host cell survive oxidative stress, and lipoarabinomannan, which helps produce cytokines and resist oxidative stress, are two more virulence factors playing crucial in the survival of Mtb inside the host [50,51]. When macrophages die, a tiny number of the bacilli may proliferate intracellularly and be discharged into circulation. If alive, these bacilli can move to more distant tissues and organs via lymphatic routes or the circulation (including areas of the body in which TB disease is most likely to develop, such as regional lymph nodes, brain, bones and joints, the apex of the lung, and kidneys) leads to extrapulmonary TB. Because of this dissemination process, the immune system is primed beyond the alveolar barrier to trigger a systemic reaction to kill the circulating bacilli, and further may develop harmful effects on the body.

1.1.6. Microbiology of *Mycobacterium tuberculosis*

Mtb is an obligately aerobic, nonmotile bacillus, irregular rods 0.3-0.5 μ M in diameter, catalase-negative, non-spore-forming with a high cell wall content of high-molecular-weight lipids such as mycolic acid [5]. Growth is extremely slow, taking 16 to 20 hours to divide compared to less than an hour for most common bacterial infections such as *E.coli* (Generation time 20 min), and visible growth takes 3 to 8 weeks on solid media [52].

A. Microscopy

A hallmark of detection is still direct microscopy, wherein Mtb might seem slightly Gram-positive due to the mycolic acid in the cell wall, making the cells resistant to Gram staining [53]. The microbiological staining method such as Ziehl–Neelsen or Auramine O (diarylmethane) / auramine-rhodamine dyes are often used to detect acid-fast bacilli (AFB) / microorganisms, primarily Mycobacteria [54]. In Ziehl–Neelsen (ZN) staining procedure, the smear is fixed, dyed with carbol-fuchsin (a pink dye), and decolorized with acid-alcohol. Methylene-blue or other dyes are used to counterstain the smear. Only decolorized cells take up the counterstain and take on its color, resulting in a blue appearance, while acid-fast cells keep their red color (Figure 4.1 left) [55]. While, in the fluorescent Auramine O staining method, the sensitivity of mycolic acid in the cell walls for fluorochromes allows the Mtb bacilli to be identified using Auramine O. As opposed to standard ZN staining, utilizing fluorochromes during the observation of AFB has the benefit of allowing detection in a shorter period [56]. Light rays of a shorter wavelength travel through a smear dyed with an Auramine O dye, which collects shorter wavelength light rays and produces extended wavelength light rays in fluorescence microscopy. Fluorescent stain consists of Auramine O, and Rhodamine B dyes attach to the nucleic acids within the acid-fast bacilli and give yellow to orange color [57] (Figure 4.2 right).

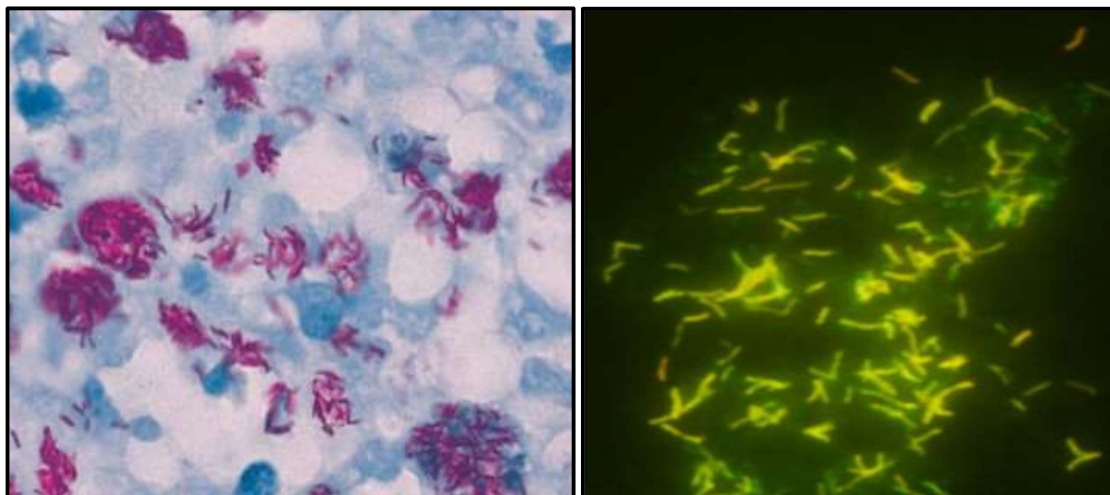


Figure 4. Acid-fast staining of Mtb bacilli. Mycobacteria are stained with Ziehl–Neelsen (left) and fluorescent auramine O (right) stain (Image credit-<http://www.medical-labs.net/giant-langhans-cell-and-mycobacterium-tuberculosis-2459/> and Caulfield, Adam J., and Nancy L. Wengenack. *Journal of Clinical Tuberculosis and Other Mycobacterial Diseases* 4 (2016): 33-43.) [58]

B. Culture

Mtb culture can be performed on both the solid and liquid medium in the laboratory. A liquid medium like Middlebrook 7H9 or 7H12, egg-based solid media like Lowenstein-Jensen (selective media), and solid agar-based media like Middlebrook 7H10 or 7H11 are often employed for growth [59]. The liquid medium, such as Dubos broth, septi-check, and Bactec 12 B also used in laboratories that allow optimum culture sensitivity. Liquid culture media is a gold standard for detecting very low bacterial loads and is primarily used in drug susceptibility testing [60]. A solid medium is less costly, but it takes longer for the bacillus to visible growth. A single Mtb organism has a generation period of 18–24 h at 37°C with adequate oxygen and nutrient availability and produces a white to a light-yellow colony on agar in 3–4 weeks, as shown in Figure 5. Liquid media is more costly than solid media but is more responsive and may develop organisms in as little as 10-14 days [61].

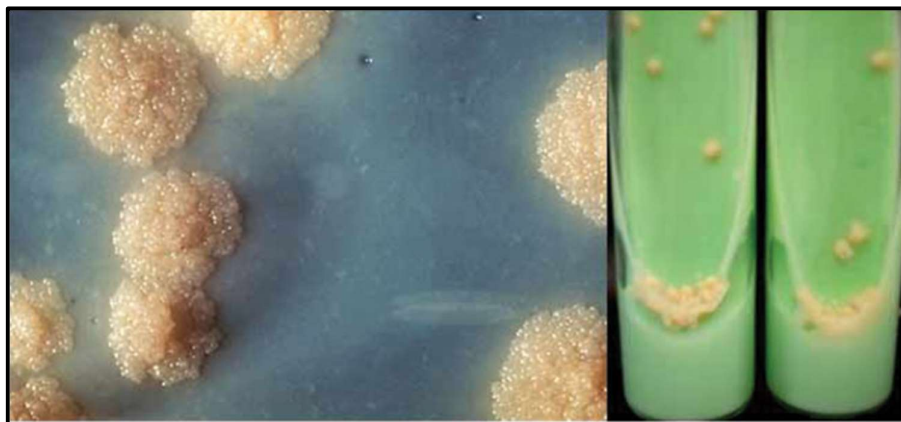


Figure 5. Cultural Characteristics of Mtb on Lowenstein Jensen (LJ) media

(Image credit-<https://microbenotes.com/lowenstein-jensen-lj-media/>)

1.1.7. Diagnosis

A conclusive diagnosis of TB needs the isolation of Mtb on culture media from the clinical specimen collected from the patient (usually sputum or cerebrospinal fluid (CSF), pus, biopsied tissue, etc.) as well as a consistent clinical symptom of the TB disease [62]. Also, laboratory testing has been used to check for and diagnose TB; a correct assessment is critical for determining suitable therapy and disease management. For the timely and effective detection of mycobacteria, particularly Mtb, it is now recommended that a mix of phenotypic and molecular assays can be employed [63]. The gold standard is still sputum smear microscopy and culture methods [64]. However, sputum smear selectivity for acid-fast bacteria is only ~50%, and sputum cultures have a somewhat significant turnaround time. As a result, several research has been conducted in an attempt to develop a quick and accurate TB diagnostic test. In the following, a short assessment will be given between traditional methods (all of which are growth-dependent) and new diagnostic methods to identify Mtb directly.

A. Old/Traditional methods

a] Medical consultation/symptoms

Some individuals infected with Mtb bacilli do not develop symptoms; this condition is called latent TB. Before becoming active, Mtb can remain in the latent stage for many years. A wide range of symptoms characterizes active TB [54,65,66]. While most symptoms are related to the respiratory system, they can also affect other body parts depending on where the Mtb grows-

1. Symptoms of TB in the lungs-Cough that lasts more than three weeks, coughing up blood or sputum (phlegm), and chest discomfort.
2. General indications of TB-Unusual tiredness, weakness, fever, chills, night sweats, appetite loss, and weight loss.
3. Organ-specific Symptoms-Blood in the urine and renal function loss if TB affects the kidneys, back pain, stiffness, muscular spasms, spinal irregularity if TB affects the spine, nausea, vomiting, disorientation, and loss of consciousness if TB affects the brain.

b] Chest X-ray

A routine chest X-ray (CXR) generally rules out pulmonary TB if the individual has no respiratory symptoms. Although CXR is an important method to identify TB pulmonary lesions, the activity of the infection cannot be determined with precision [67-69]. Chest radiographs are analyzed in medical care by trained physicians to identify TB. However, this is a time-consuming and subjective method that may lead to the wrong diagnosis in most cases. The availability of radiologists is often scarce in low-resource countries (LRCs), particularly in rural regions. The three essential technical criteria widely used in chest radiography analysis are the infected individual's inspiratory effort, the appropriateness of patient positioning/ rotation, and the extent of penetration or film blackening [70], as shown in Figure 6.

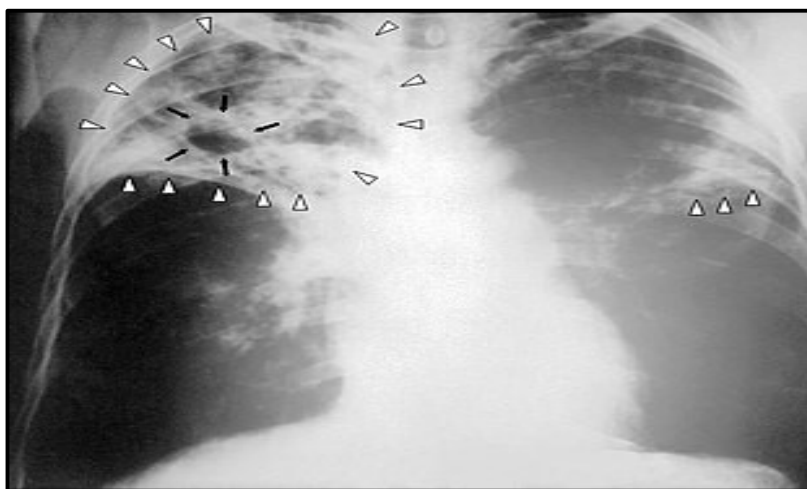


Figure 6. White arrowheads show infection in both lungs, and black arrows show the development of a cavity on a chest X-ray of an individual with advanced TB

(Image credit-https://en.wikipedia.org/wiki/Tuberculosis_radiology)

c] Tuberculin skin test

A tuberculin skin test (TST) is also known as the Mantoux /tuberculin sensitivity/ plasma protein derivative (PPD) test. This test is the most cost-effective, safe, and effective way to determine if someone has developed an immune response against Mtb. This reaction can occur if anyone has been exposed to active TB in the past or has taken the BCG tuberculosis vaccination and hence cannot differentiate between old and new infections. A negative test suggests that the individual has not yet been exposed to Mtb bacilli or his immune stem is not strong enough to respond to the injected PPD solution.

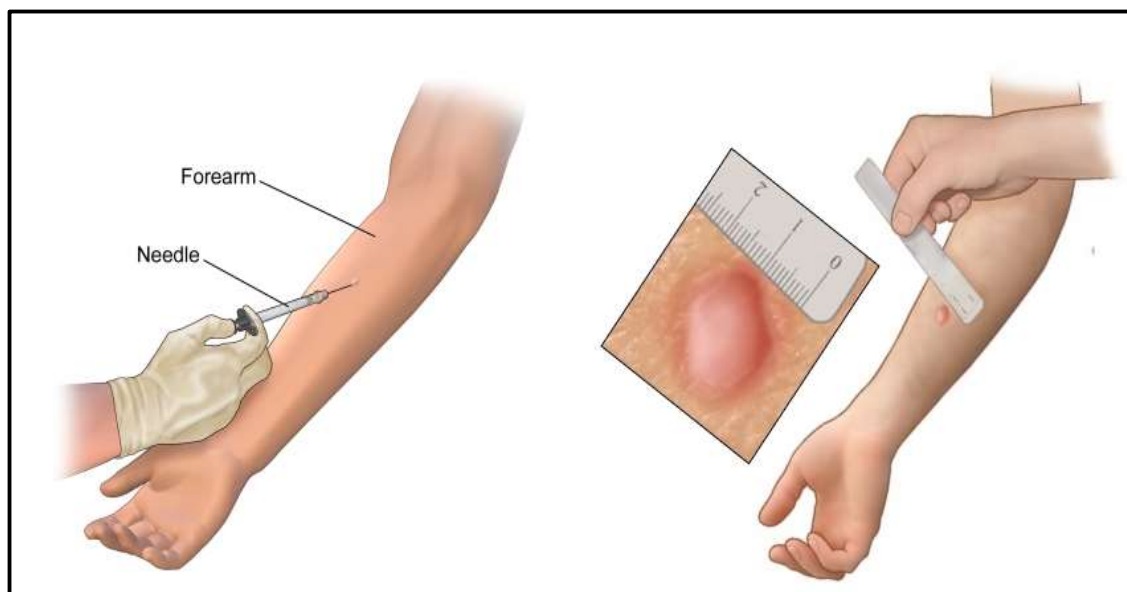


Figure 7. The Mantoux skin test consists of an intradermal injection of 0.1 mL of PPD solution. (Image credit <https://laboratorytests.org/mantoux-test/mantoux-test-2/>)

A positive TST reaction has been used as a marker of Mtb infection, appearing within 3 to 6 weeks, but sometimes up to 3 months, and remains positive lifetime even after medication [71]. This ‘tuberculin’ is a glycerol extract of the tubercle bacilli prepared by removing the bacteria, lowering the volume of broth to one-tenth by drying, and passing it through a sterilizing filter [72]. According to the center for disease control (CDC), a test recommended for India involves intradermal administration of 0.1mL of a liquid solution containing PPD RT23 with tween 80 (acting as a stabilizing agent) containing one standardized tuberculin unit (1TU) [73]. After injection, a delayed hypersensitivity reaction to PPD begins when the immune system attracts specialized immune cells called T-cells to the test site in a positive test. These T-cells have been sensitized by earlier infection attracted to the test site. These T-

cells release chemical messengers called lymphokines, attracting other lymphocytes and monocytes [74]. This further leads to local vasodilation (expansion of the diameter of blood vessels) and causes induration in 48-72 h (a hard, elevated region of 6 to 10mm in diameter with clearly defined edges at and around the injection site), which leads to edema shown in Figure 7, fibrin deposition, and recruitment of different types of inflammatory cells to the injection area.

d] Interferon-gamma release assay

Interferon-gamma release assay (IGRA/IFN- γ) is an in-vitro blood test of cell-mediated immune response that evaluate T-cell production of IFN- γ after stimulation with antigens unique to the Mtb (except BCG substrains); such as culture filtrate protein 10 (CFP10) and early secreted antigenic target 6 (ESAT-6). These antigens are encoded by genes in the Mtb genome's region of difference 1 (RD1) locus [75,76]. Currently, two IGRAs are recommended in many developed countries to diagnose TB-

1. The QuantiFERON-TB Gold In-Tube (QFT) test [77,78] is an enzyme-linked immunosorbent assay (ELISA)-based, whole-blood test that uses peptides from the RD-1 antigens from CFP-10 and ESAT-6 in a tube format.
2. T-SPOT.TB assay [79,80], a form of an enzyme-linked immunosorbent spot (ELISPOT) (Collectis/Qiagen, Carnegie, Australia). Both tests are recognized for usage in Europe and authorized by Health Canada and the US Food and Drug Administration (FDA). This assay was performed on calculated and normalized peripheral blood mononuclear cells (PBMCs) incubated with CFP-10 and ESAT-6 peptides.

B. New diagnostic methods

I] Xpert MTB/RIF

The WHO approved the Xpert MTB/RIF test in 2010 for the first diagnostic testing of persons suspected of multidrug-resistant tuberculosis (MDR-TB) or HIV-associated tuberculosis [81,82]. The Xpert Mtb/RIF assay is a single test used for identifying Mtb and detecting RIF resistance within two hours, directly from sputum samples. It is an automated molecular technique based on nested PCR. Moreover, it includes PCR amplification of the “RIF resistance-determining region” of the Mtb *rpoB* gene and later probing this region to identify mutations responsible for RIF resistance. About 95% of the RIF-resistant TB cases contain mutations in the 81-bp region [83]. As per reports, in affected individuals with

culture-positive pulmonary TB (PTB), the sensitivity was 78.2 to 90 %, while the specificity was >98 %. While, in the case of children, the sensitivity dropped from 76 to 65% [84,85]. The test process can be done on clinical specimens directly, such as unprocessed sputum pellets or sputum samples (also known as sputum sediment), made after disinfecting and concentrating sputum [86].

II] Xpert MTB/ RIF Ultra/ Xpert Ultra

Even though the Xpert MTB/RIF test has improved TB and rifampicin resistance diagnosis, its sensitivity is limited in smear-negative participants with pulmonary tuberculosis illness or individuals with HIV. Xpert MTB/RIF Ultra/ Xpert Ultra was established to circumvent this constraint. It has a larger chamber (50µL) for DNA amplification than Xpert, permitting double the sample volume to reach the PCR reaction [87]. Bahr and colleagues compared Xpert Ultra to Xpert for detecting Mtb in cerebrospinal fluid, suggesting that Xpert Ultra had greater sensitivity than the culture method [88]. Analytical experiments indicated that Xpert Ultra had a lower detection limit of 15.6 bacterial colony forming units (cfu) per ml than Xpert, which shown 12.6 cfu/ml [89]. If MTB is identified (category "trace"), no conclusions on rifampicin resistance can be drawn, and the data are given as "MTB detected, trace, RIF undetermined" [90]. In 2018, the WHO recommended that Xpert Ultra be used for TB diagnosis. It could be thoroughly evaluated in various epidemiological and geographical situations with various patient groups, particularly among extrapulmonary TB patients [91].

III] Genexpert OMNI

Given the worries linked with the need for continuous power supply and the need for a physical lab with the traditional GeneXpert platform, Cepheid has developed the world's most portable point-of-care diagnostic test [92]. This compact, lightweight gadget expands access to speedy, accurate, and possibly life-saving TB testing in some of the world's most remote locations. The GeneXpert® Omni is battery-powered and has four hours of battery life, web-enabled, and wireless, enabling real-time transmission of the instrument and test data [93]. The GeneXpert® Omni is projected to significantly expand GeneXpert® technology's reach by providing reliable testing for life-threatening illnesses such as TB, drug-resistant TB, HIV, and Ebola [94]. Because of the device's portability, testing may be done on-demand at the patient's home rather than at a centralized healthcare organization.

IV] Lateral flow lipoarabinomannan commercial tests (LF-LAM)

The glycolipid lipoarabinomannan (LAM) is found in the outer cell wall of mycobacteria and can estimate up to 15% of the total bacterial weight [95]. A proof of concept for an ELISA-based urine detection method was reported in 2001 [96]. LAM is a carbohydrate antigen containing glycosidic linkages that humans do not metabolize due to a lack of suitable enzymes. Hence, LAM may be excreted by the kidneys of individuals with active TB cases and found antigenically intact in urine samples. The quantity of LAM in the urine should theoretically represent the bacterial load, metabolic activity, and breakdown rate, allowing for detection using sensitive immunological methods. The success rate of LF-LAM is highly correlated with autopsy findings of renal or disseminated TB [97], confirmed mycobacterial blood culture [98], and in positive Xpert cases of concentrated urine samples [99].

V] Digital Chest X-ray (CXR)

Recently, Computer-Aided Detection (CADx) system was also reported, which might assist physicians and radiologists in better understanding active TB patients [100]. This CXR system uses image analysis techniques to improve, segment, and categorize CXR pictures of suspected TB patients in order to advise further diagnosis and check whether the individual is infected or not based on CXR readings.

1.1.8. Different physiological states of *Mycobacterium tuberculosis*

There are various physiological states of mycobacteria inside the host as follows-

A. Active-TB/Aerobic /Replicating stage bacilli-

Mtb is an obligately aerobic organism that can attack any body part but primarily targets the lungs [101]. The disease is transmitted as a highly infectious aerosol from the lungs of individuals with active TB. However, if positively diagnosed with TB, they can show the symptoms and are responsible for further disease transmission. In many individuals, any inhaled Mtb bacilli are killed instantly by the body's immune system. Nevertheless, in some cases, depending on the immune status of the individuals, these Mtb bacilli may dominate the host and start replication. Acid-fast staining and chest x-ray are the most common diagnostic tests physicians recommend to identify active-TB in these situations. A physiological pH of 6-7 and a nutrient-rich environment favor the Mtb bacilli for multiplication in aerobic conditions. Active, drug-susceptible TB disease is commonly treated with drugs such as Rifampicin and Isoniazid. Most other available drugs act mainly

against the active stage of Mtb; hence, in most cases, TB is curable and preventable with proper treatment strategies.

B. Dormant-TB /Anaerobic /Hypoxia /Latent/Non-Replicating stage bacilli

The World Health Organization classifies latent TB (LTB) as an asymptomatic condition of a sustained immunological reaction to Mtb antigen stimulation without clinically evident active TB [102,103]. Generally, in LTB cases, individuals who inhale the Mtb bacilli through aerosols do not always feel sick and are not contagious. They are unable to spread the Mtb bacilli to others. There is no standard gold test for LTB, and they frequently have a normal CXR, negative IGRA, and a negative sputum test. The TST is typically the only way to determine whether someone has LTB. According to current estimates, LTB affects almost a quarter of the world's population [104]. The length of latency varies, and healthy people can have a lifetime risk of the disease progressing to active TB [105]. However, reactivation occurs in a limited percentage of cases (5–15%), usually within the first 2–5 years after infection [106,107]. The process through which a subclinical latent infection becomes acute TB illness is known as reactivation. As a result, people with LTB are a key source of new active TB cases [108].

C. Viable but non-culturable /cultivable *Mycobacterium tuberculosis*

Many bacteria like Mtb use the viable but non-culturable (VBNC) state as a unique survival strategy for responding to harsh environmental circumstances. When the VBNC concept was first introduced 30 years ago, numerous questions about its significance were raised because there was no clear distinction between dying cells and bacteria's adaptive strategies for dealing with stressful environments [109]. VBNC cells are generally found and associated with sputum samples of TB patients, which could lead to false-negative results during diagnosis [92]. VBNC cells are not considered dead due to many differences despite their inability to grow on ordinarily permissive conditions. VBNC cells have an intact membrane that contains undamaged genetic information, whereas dead cells have a broken membrane that cannot maintain chromosomal and plasmid DNA [110,111].

In general, VBNC Cells such as *M.smegmatis* are reported to be more resistant to high temperatures [112]. The increased resistance might be due to decreased metabolic rate and increased cell wall strength by enhanced peptidoglycan cross-linking. Mtb is known to enter a VBNC condition during host infection and resuscitate (i.e., human lungs). It is also widely known that these latent bacteria may produce active TB if the selective pressures for latency

are removed, primarily in the form of immunosuppression on the contrary. VBNC Cells are not the same as latent infection, and latency or dormancy is a VBNC stage of Mtb that contributes to approximately two million Mtb carriers worldwide [113]. The role of selective pressure for latency was studied recently and identified that, at a concentration of 10mm, nitrite induces rapid non-culturability of Mtb at the aerobic stage. [114]. Moreover, diphenyleneiodonium (DPI), an inhibitor of NADH Oxidase, was also reported to induce the VBNC stage in Mtb [115]. These data suggest that a particular chemical compound alters the physiology of Mtb from active to VBNC state in Mtb and can easily be studied in in-vitro conditions.

1.1.9. Treatment

Successful TB treatment is still challenging due to the unique shape and chemical nature of the mycobacterial cell wall, which prevents medications from entering and renders many antibiotics ineffective [116]. For several years, the WHO has addressed the global problem of poor TB control; and recommended a new integrated care program called directly observed treatment, short-course (DOTS) in 1994 [117-119]. The DOTS strategy's major goals are to promote adherence to approved chemotherapy and treatment completion, which ultimately help to control disease and prevent drug resistance. The strategy is divided into five key aspects: 1. Governmental support, 2. microscopic observation of sputum samples for acid-fast-bacilli from suspected TB patients, 3. DOTS-based short-course treatments, 4. a continuous supply of high-quality medicines and diagnostic supplies, 5. monitoring of program performance and reporting system of treatment outcome. The current therapeutic regimen employs a combination of medications that have been found to improve the disease's susceptibility to therapy and decrease the length of time it takes to cure it [120].

A. Drugs/antibiotics for TB

Although very successful, current TB treatment regimens are far from optimal. The time it takes to cure a patient with the best combination of available treatments cannot be decreased to less than six months. RIF and INH are the two most common drugs used presently, with RIF being the more important drug that helps to reduce treatment time and assures positive outcomes [121,118].

I] First-line antitubercular drugs

First-line treatment includes medicines of the first choice for treating a specific ailment because it is thought to be the most appropriate cure for that disease with greater efficacy and the fewest adverse effects. The list of first-line antitubercular drugs and their mechanism of action are mentioned in Table 1.

Table 1. First-line antitubercular drugs and their mechanism of action

Class of AntiTB Drug	Mode of action	Target	Inhibition spectrum against Mtb		Site of action	Acting pH
			Active State	Dor-mant State		
Rifampicin	Bactericidal	Blocks mRNA synthesis (transcription) by inhibiting the bacterial DNA-dependent RNA polymerase	High	Low	Both intracellular and extracellular	Both alkaline and acidic medium
Isoniazid	Bactericidal	Inhibits synthesis of mycolic acid synthesis-essential for mycobacterial cell wall	High	Low	Both intracellular and extracellular	Both alkaline and acidic medium
Pyrazinamide	Bactericidal	Disrupts mycobacterial cell membrane	Low	High	Intracellular bacilli	Acidic medium
Ethambutol	Bacteriostatic	Inhibits Mycobacterial Arabinosyl transferase- Inhibits synthesis of cell membrane	High	Low	Both intracellular and extracellular	Both alkaline and acidic medium
Streptomycin	Bactericidal	Binds to the 16s rRNA interferes with translation proofreading, and thereby inhibits protein synthesis	High	Moderate	Extracellular bacilli	Alkaline medium

II] Second-line antitubercular drugs

In 2019, the WHO released new unified recommendations on the second-line medications that should be used to treat drug-resistant TB [122]. In 2020, there will also be a substantial modification to the guidelines. The latest unified recommendations have significantly altered the approach to treating MDR/ extensively drug-resistant (XDR)-TB [123]. According to the new WHO drug classification system (2016) [91], patients with rifampicin-resistant TB or

MDR-TB need a treatment plan (based on safety, efficacy, and cost) with at least five effective TB medicines during the acute stage of TB: one is pyrazinamide, and four core second-line TB drugs (Table 2), one each from groups A and B and at least two from group C. While the use of second-line TB drugs, rare side effects are reported which are relatively frequent, and they are easy to deal with symptomatic therapy. Unfortunately, specific side effects include nephrotoxicity from aminoglycosides, cardiotoxicity from fluoroquinolones, gastrointestinal toxicity from ethionamide or para-aminosalicylic acid, and central nervous system toxicity from Cycloserine, which can be life-threatening [124]. Patients at a higher risk of harmful effects may benefit from a baseline examination. Hence, it is important to have regular clinical and laboratory evaluations during therapy to avoid significant side effects.

Table 2. Summary of the existing classifications of second-line anti-tuberculosis drug

WHO 2016 TB drugs classification	
Group A Fluoroquinolones	<ul style="list-style-type: none"> • Levofloxacin • Moxifloxacin • Gatifloxacin
Group B Second-line injectable agents	<ul style="list-style-type: none"> • Amikacin • Capreomycin • Kanamycin (Streptomycin)
Group C Other core second-line agents	<ul style="list-style-type: none"> • Ethionamide/protionamide • Cycloserine/terizidone • Linezolid • Clofazimine
Group D Add-on agents (not core MDR-TB regimen components)	D1 <ul style="list-style-type: none"> • Pyrazinamide • Ethambutol • High-dose isoniazid
	D2 <ul style="list-style-type: none"> • Bedaquiline • Delamanid
	D3 <ul style="list-style-type: none"> • p-Aminosalicylic acid • Imipenem–cilastatin • Meropenem • Amoxicillin-clavulanate • (Thioacetazone)

III] Vaccines for Tuberculosis

Robert Koch was the first to use semi-purified culture filtrates of Mtb, “the old tuberculin,” as a therapeutic vaccination for TB patients [125]. Later, Albert Calmette and Camille Guerin of the Pasteur Institute were the first to discover the BCG vaccine in 1921. It was developed from a live-attenuated strain of *Mycobacterium bovis* bacillus Calmette-Guerin (BCG), a related strain of Mtb [126]. Extensive genomic studies have revealed that the deletion of a region of deletion 1 (RD1) is a 10.7kb fragment responsible for virulence in Mtb and *M bovis*. RD1 codes for the ESAT-6 secretion system-1 (ESX-1) encode for two important Mtb immunogenic proteins, ESAT6 and CPF-10. It has been discovered that the absence of the RD1 region is the primary cause of virulence [127]. Since 1921, the BCG vaccine has been given to roughly 100 million children globally [128], avoiding 120000 childhood deaths annually [129].

The current BCG vaccine provides excellent protection, but only for a short time. It is ineffective in people who have already been exposed to mycobacterial antigens (whether by prior BCG vaccination, contact with environmental Mtb bacilli, or latent TB disease) [130]. The BCG vaccine schedule protects newborn newborns and children (not adults) against severe TB; it has an established safety record after more than 4 billion injections, although there are concerns about safety in HIV-positive neonates [131,132]. Despite its extensive usage in newborns, BCG does not effectively prevent adult pulmonary illness, and as a result, the worldwide incidence of TB has not decreased [133]. This finding most likely reflects a lack of efficacy in adults, particularly in the scenario of previous exposure to mycobacteria in the environment. BCG immunization does not provide enough protection against young and adult TB, the most common type of illness. It is effective against the most severe types of TB, including TB meningitis and miliary TB, in 70-80% of cases [134]. However, it is less effective in preventing TB, which affects the lungs.

People who have previously had the BCG vaccine may be suggested for TST to check their previous exposure to mycobacteria. Occasionally, vaccination may result in a positive skin test for TB, which indicates the result might be due to the BCG vaccination or infection with mycobacteria. It is difficult to identify whether a person has a latent tuberculosis infection or has developed a TB illness. In such cases, other tests, such as a chest x-ray and a sputum sample, are required to determine whether or not the person has TB. A meta-analysis of randomized experiments and case-control studies found that the effectiveness of the BCG

vaccine against pulmonary TB in newborns and adolescents is around 50%, with a range of 0-80% [135]. In addition, differential efficacy of the BCG vaccine suggests that Tb vaccines may be feasible, and three different vaccine development strategies [136] could be used-

1. To produce a better BCG vaccine that includes safe and long-acting recombinant BCG strains or attenuated Mtb.
2. To use a prime-boost method, in which a new vaccine, generally viral vectored or protein adjuvant, is given as a booster dose later.
3. To produce therapeutic vaccinations to shorten the length of Tb treatment, which usually includes immunotherapeutic vaccines.

Several first-generation vaccines have reached Phase IIb human clinical trials, and some second-generation vaccines are completing preclinical testing and preparing to start Phase I trials (Table 3).

Table 3. Profile of several therapeutic vaccine candidate products for TB

Candidates	Mechanisms	Development status
Viral Vector		
MVA85A	Recombinant vaccinia virus encoding tuberculosis antigens 85A	Phase II
AERAS-402/Crucell Ad35	Recombinant adenovirus (serotype 35) encoding tuberculosis antigens 85A, 85B, and TB10.4	Phase II
Ad5Ag85A	Recombinant adenovirus (serotype 5) encoding tuberculosis antigens 85A	Phase I
rHCMV	Recombinant human cytomegalovirus (new platform)	In development
Recombinant Protein		
Mtb72F/AS02A	A fusion protein of TB virulence factors Mtb32 and Mtb39 in AS02A adjuvant	Phase II
Hybrid-1	Fusion protein of TB antigens 85B and ESAT-6, formulated with IC-31 or CAF01 adjuvants	Phase I
H4/AERAS-404	Fusion protein of TB antigens 85B and TB10.4 formulated in IC-31 adjuvant	Phase I
H56	Fusion protein of TB antigens 85B and ESAT-6 with latent stage antigen Rv2660c formulated with IC-31 adjuvant	Phase I
HBHA	Protein formulation of a heparin-binding hemagglutinin	In development
Recombinant BCG		
VPM1002	Recombinant, urease C deficient BCG	Phase I/II

	expressing listeriolysin for phagosomal escape	
AERAS-422	Recombinant BCG expressing perfringolysin (for phagosomal escape) and overexpressing antigens 85A, 85B, TB10.4, and Rv3407	Phase I
Attenuated Mtb		
MTBVAC01	Recombinant Mtb with <i>phoP</i> gene deletion, preventing transcription of virulence factors	Phase I
Δ leuD/ Δ panCD	Recombinant, auxotrophic Mtb with deletion for leucine and pantothenate	Preclinical
Other		
RUTI	Formulation of detoxified, fractionated Mtb cells	Phase II
<i>Mycobacterium smegmatis</i>	Bacilli genetically similar to Mtb but avirulent, engineered to express TB antigens	Phase I
<i>Mycobacterium vaccae</i>	Bacilli are genetically similar to Mtb but avirulent	Phase III
DNA vaccines	Plasmid DNA encoding a variety of Mtb antigens	In development

(Credit- Grave, A., and David Hokey. *J Bioterr Biodef S 1* (2011): 2) [137]

1.2. Drug discovery in tuberculosis

Although still being severely underfunded, drug discovery and development for TB have advanced dramatically in the last 10–20 years [138]. Over the last decade, the number of candidates in the TB medication research pipeline has increased (<https://www.newtbdrugs.org>). However, very few candidates can fulfill adequate treatment safety and efficacy requirements. Drug discovery is a lengthy process that might take up to 15-20 years to complete. Screening for therapeutically active compounds is usually the first step in the early drug discovery process. Only one out of thousands of drugs that are in the pipeline will reach the level of commercial approval.

Furthermore, only a few drug candidates out of thousands of drugs make it to preclinical testing. These drugs/compounds must have a therapeutic impact on the condition in question, and testing for safety and effectiveness begins when they are identified. The drug discovery process is divided into several stages and actions. Early Drug Discovery, Preclinical Phase, Clinical Phases, and Regulatory Approval are the four primary stages of the early drug discovery process.

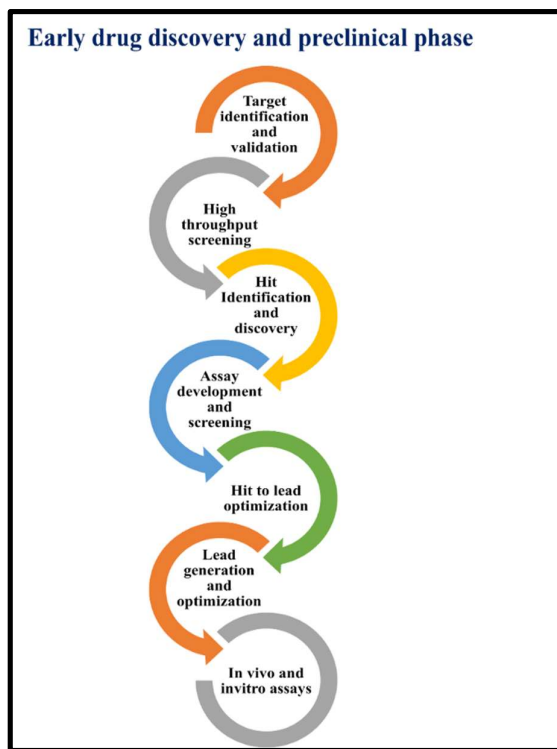


Figure 8. A general outline of the early stages of drug discovery

Various actions and tests are included in the early drug discovery process. Researchers work together to find and optimize possible leads for a specific target. In order to treat a disease, the leads must elicit the desired impact on a specific biological target involved in the condition. Researchers currently employ in silico platforms, biochemical tests, cell cultures, and numerous animal models in their research. The general outline in the early phases of drug discovery (as shown in Figure 8) includes identifying and validating the target using different experimental methods to ensure its activity. Then this is further taken to high-throughput screening, wherein the number of similar scaffolds of the drugs was evaluated for their efficacy in a single time. Before further clinical trials, the identified hits were assessed and optimized by using different in-vitro, ex-vivo, and in-vivo screening assay methods.

The history of anti-TB drug discovery starts with streptomycin. Selman Waksman developed streptomycin, a drug that works against Mtb, in 1943 [139]. In November 1949, streptomycin was administered to the first human patient infected with TB and cured. Following that, it was discovered that some patients treated with only streptomycin got ill again because the tubercle bacillus had evolved resistance to the antibiotic. To overcome this issue, rifampicin was launched towards the end of the 1960s, as shown in Figure 9. Using combination

therapy, drug-resistant and drug-susceptible TB decreased in developed countries. Hence, drugs in combination are given, such as rifampicin, ethambutol, pyrazinamide, and isoniazid, to treat drug-sensitive TB cases [140]. However, with the development of resistance to these drugs since 2000, there has been a rise in MDR/XDR TB cases, creating a necessity for developing new drugs. From 2005 onwards, three oral drugs, bedaquiline, pretomanid, and linezolid, are recommended to treat such patients. These drugs have shown better results with respect to efficacy against Mtb.

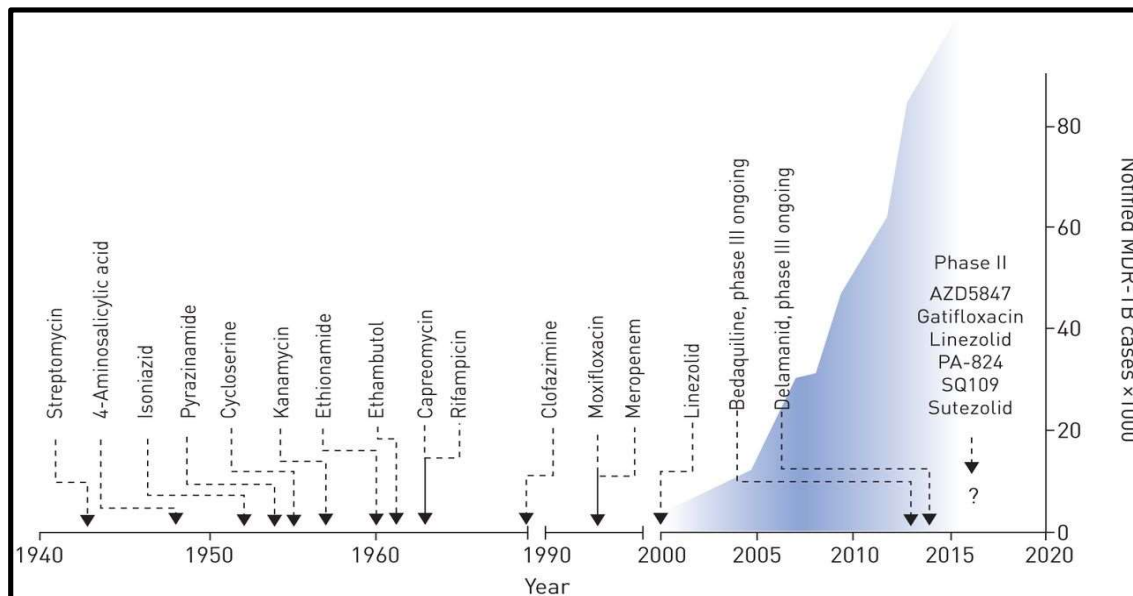


Figure 9. Discovery timeline of currently available TB drugs

(Image reprinted with permission from “Ioana Diana Olaru, Florian von Groote Bidlingmaier, Jan Heyckendorf, Wing Wai Yew, Christoph Lange, Kwok Chiu Chang European Respiratory Journal 45 (4) 1119-1131”) [141]

1.2.1. The problem of MDR/XDR-TB

Multidrug-resistant tuberculosis (MDR-TB) has emerged globally in the last 20 years [142,143], followed by XDR- TB [144,145]. In 2008, the WHO projected those 4,40,000 incidences of MDR TB happened (3.6% of total incident TB episodes) [146]. Unlike other bacterial pathogens, the sensitivity of various strains of TB to the medicines employed in first-line therapy is typically relatively different. The frontline drugs consist of a six-month course of four combined medications, such as isoniazid, rifampicin, ethambutol, and pyrazinamide, used to treat sensitive TB cases. While in some cases, Mtb develops resistance to these existing drugs, and thus, drug resistance in TB is the key problem in the treatment

[2]. MDR-TB is a kind of TB caused by microorganisms that are resistant to the two most effective first-line anti-TB medications, isoniazid, and rifampicin. MDR-TB can be treated and restored to normal conditions using second-line medicines. The organisms that cause XDR-TB are resistant to some of the most potent anti-TB medications. XDR-TB strains emerged after the mishandling of people with MDR-TB. Second-line treatment options are limited, requiring extensive chemotherapy (up to 2 years of treatment) using expensive and toxic medications [147]. Drug Susceptibility Testing (DST) was the first approach for detecting MDR-TB and XDR-TB to assess how well antitubercular medications limit Mtb growth [148].

1.2.2. Major challenges in drug discovery against *Mycobacterium tuberculosis*

There are numerous challenges in identifying suitable antitubercular agents. These include-

1. The extremely slow growth rate of Mtb with a mean generation time of 20-24 hrs.
2. Mtb is a respiratory pathogen, so it should be strictly handled under strict safety conditions (preferably under Biosafety Level-3 conditions), which requires expensive facilities.
3. The cell wall of Mtb is thick and waxy, making it a barrier that prevents many small molecules, such as drugs, from entering into the bacteria. Hence, this is the major reason for the failure of drugs that cannot access the desired target(s).
4. Over time, Mtb has evolved to develop efflux pumps that have been the main reason for the problem of drug resistance to most available drugs [149].
5. The Mtb was found in diverse microenvironments and different physiological states as active and dormant/ latent stages in a single patient. This creates the urgent need for effective drugs in diverse internal environments and should be effective against multiple physiologically different states [150].
6. Drugs must be safe for long periods, with no notable adverse effects or drug-drug interactions, due to the lengthy therapy necessary to cure TB.
7. Coinfection with HIV/AIDS further restricts the usage of standard drug regimens, which ultimately complicates the disease condition.

Researchers have used a range of screening procedures to find interesting molecule series for development in an attempt to address these difficulties.

1.2.3. Different drug screening models

Several in-vitro, ex-vivo, and in-vivo animal models have been developed to better understand host-pathogen interaction and mimic the bacilli's dormant state.

A. In-vitro models for the active stage of *Mycobacterium tuberculosis*

Because TB is such a complicated illness, no individual in-vitro screening model can be offered to guess in vivo effectiveness.

1. High throughput assays based on carbon source variation

Various alternate carbon and non-carbon sources are used by Mtb bacilli, such as glucose, fatty acid, butyrate, cholesterol, and palmitate during infection [151-156]. Based on these sources, multiple assays are developed to measure the growth of bacilli in the presence of the compound. Examples include virulent Mtb recombinant strains that produce far-red fluorescent reporters and employ fluorescence to monitor in-vitro growth [157]. This assay is used explicitly for screening drugs against the aerobic stage Mtb, using glucose as the sole carbon source. Another assay uses butyrate as a carbon source. Because butyrate is a short-chain fatty acid, it requires bacteria to employ the glyoxylate shunt and beta-oxidation routes, both of which are thought to be effective throughout the infection [158]. Furthermore, when cholesterol is used as a carbon source, it forces Mtb to use a whole set of degradative enzymes simply expressed in cholesterol exposure. Using Almar blue assay and cholesterol as carbon source, the assay is used to screen active compounds against active stage Mtb [159].

B. In-vitro models for the dormant stage of *Mycobacterium tuberculosis*

1. Nutrient starvation models

One simple in-vitro model based on complete nutrient starvation was proposed by Betts et al. to explore granulomas and the influence of granulomas on Mtb metabolism [160]. This model is modified from the earlier Loebel nutritional deprivation model [161]. Mtb bacilli are resuspended in simple phosphate-buffered saline and incubated for six weeks at 37 °C. In this condition, Mtb stops growing, slows down its respiration, and is resistant to frontline drugs such as isoniazid, rifampicin, and metronidazole. Further microarray study revealed indications of transcription machinery slowing, cell division, energy consumption, lipid production, stimulation of the stringent response, and numerous other genes that might be involved in long-term survival inside the host. The bacteria may survive for months after they have been formed. Compounds may be added into the wells containing starved cells, and

growth was assessed over time. This time-consuming technique needs 4–5 weeks to confirm viability by colony counts. Mtb cultures starved in distilled water showed altered cell morphology and staining characteristics. However, when reintroduced to nutrient-rich media, they regained acid fastness and began to thrive, even after two years of starvation [162].

Another starvation model has been modified for high throughput applications using a defined medium without any carbon source [163]. Bacilli were starved in a medium lacking carbon source for five weeks before being subjected to chemicals in a 384-well format. The growth of cells is evaluated utilizing fluorescence from a GFP reporter following a time of outgrowth with the complete medium. A secondary test was conducted utilizing identical conditions and a luminous strain (expressing luciferase) for a 96-well format. The major disadvantage of this assay is reproducibility. Another study showed that after an initial 2 to 3-log reduction in cfu, *Mycobacterium smegmatis* has been alive for over 650 days, displaying greater stress resistance, higher mRNA stability, and an overall decrease in protein synthesis [164].

2. Low oxygen-based models

Hypoxia is a well-known characteristic of TB granulomas. The classic Wayne hypoxia model is based on tubercle bacilli cultured in a deep liquid medium with extremely moderate stirring to maintain uniform dispersion while managing O₂ depletion [165]. At least two phases of nonreplicating persistence were seen in this model. When the dropping dissolved O₂ level reached 1% saturation, the change into the first stage, called NRP stage 1, happened abruptly. Significant CFU numbers and DNA synthesis accompanied the modest rise in turbidity during this microaerophilic stage. While the bacilli remained in this condition, a high rate of glycine dehydrogenase synthesis was begun and maintained, and a constant ATP concentration was maintained. The bacilli quickly changed to an anaerobic stage, called NRP stage 2, when the dissolved O₂ content of the culture dropped below roughly 0.06 % saturation, with no further rise in turbidity and a significant decrease in glycine dehydrogenase concentration. Bacilli in NRP stage 2 could live anaerobically partly because they had spent enough transit time in NRP stage 1. The Mtb bacilli, when entered in non-replicative states, showed resistance to the antibiotics such as isoniazid and rifampicin, but they became susceptible to metronidazole [166]. Another model was established using the same basis, known as low oxygen recovery assay (LORA). This assay is used for drug screening wherein the bacilli are forced to enter the non-replicating stage in low oxygen conditions using a fermenter. Then, the bacteria are exposed to compounds for ten days in 96

well formats [167]. The necessity for fermentation apparatus is one drawback of this test; however, this may be overcome by utilizing the Wayne model (discussed above) to grow hypoxic bacteria in glass tubes.

In a simplified modification of the low oxygen experiment, bacterial cultures are seeded into 96-well plates and covered with paraffin [168]. The use of paraffin prevents oxygen from entering the medium, and hypoxic conditions occur due to bacterial respiration after 11–13 days. At this time, compounds can be added to the plates containing bacterial culture, and the growth of bacteria can be assessed after 15–20 days of incubation, in this case, employing an RFP reporter. The practice of using paraffin may help lessen edge effects caused by medium evaporation. Although theoretically accessible, this test takes a longer time to get the screening results.

3. Lipid-rich environment based models

Mtb survives in a lipid-rich environment and has adapted to it. The bacteria are also known to influence the host's lipid equilibrium. As a result, tests that include lipids can be effective. A lipid-rich variant of the Wayne hypoxia model was employed to determine chemical potency [169,165,170]. Bacteria are cultivated in this model in media enriched with cholesterol, stearic acid, palmitic acid, and oleic acid, all of which are present in the sputum [170]. Compounds are added after 14 days after achieving the non-replicating bacilli, and colony counts monitor live bacteria throughout the test. After analysis, it was found that the bacilli used in this test are found to be more drug-resistant to existing medicines like moxifloxacin and rifampicin. Tolerance was not primarily related to hypoxia because the bacteria were more vulnerable to the same drugs as glucose was the carbon source, indicating that lipids had a significant impact [170].

4. Low pH models

This model employs low pH incubation conditions to generate a non-replicating condition in Mtb bacilli [171]. The Mtb strain expressing luciferase was employed in this model. Under test conditions, the assay first established the linear connection between luminescence and viable bacteria (as measured by CFU). In order to create a reproducible experiment, the assay parameters are optimized in 96-well plates. After which, the bacilli were exposed to test compounds for seven days in phosphate-citrate buffer, pH 4.5; live bacteria were evaluated by luminescence. The minimal bactericidal concentration at pH 4.5 (MBC4.5) was discovered to represent >2 logs of reduction of bacilli. Furthermore, the usefulness of the test

model with control drugs has been validated. The pH homeostasis assay uses a reporter strain with a pHLUOR (ratiometric GFP responsive to pH) to quantify intrabacterial pH after two days of exposure to test compounds at pH 4.5; it has been extended to 96-well and 384-well formats, offering for screening and dose-response analysis [172,173].

5. Streptomycin auxotroph dormancy models

In this model, strain 18b of Mtb was used. Streptomycin-dependent strain 18b is an experimentally isolated strain that can only survive in the presence of streptomycin [174]. Removing streptomycin from the medium and allowing the bacteria to enter a viable but non-cultivable condition gives a simple method to achieve a non-replicating state of Mtb bacilli. Another advantage of this model is that the strain is classified as avirulent since it cannot cause infection without streptomycin. However, it may be employed in in-vivo studies if the animals are administered with antibiotics.

In another dormancy model, the 18b strain of Mtb, streptomycin (STR)-dependent mutant, was used for screening compounds against nongrowing cells [175]. The optimal circumstances for 18b cells to reproduce in the presence of STR and survive but not proliferate after STR removal were discovered. Mtb 18b strain was sensitive to INH and RIF in the presence of the antibiotic, as well as the new medicines under clinical trials such as PA-824, TMC207, benzothiazinone (BTZ), moxifloxacin (MOXI), and meropenem (MER). After removing STR, the strain was less susceptible to the cell wall inhibitors INH and BTZ but more susceptible to RIF and PA-824. In contrast, MOXI and MER were equally susceptible in both situations. After in vivo treatment of chronically infected mice with five of these medicines, the same potency ranking was reported against nonreplicating *M. tuberculosis* 18b. Despite the growth halt, strain 18b maintains high metabolic activity in-vitro, and the resazurin reduction test results remain positive. This technique was found suitable for high-throughput screening using strain 18b to uncover novel inhibitors of dormant Mtb after being adapted to a 96-well format.

6. Multiple stress model

A single experiment may be used to investigate many stimuli in these conditions, which can subsequently be deconvoluted to discover which condition is significant. This is a very efficient technique for large numbers of molecules. The multiple stress model proposed by Deb and his associates contains numerous environmental stimuli related to the infection, including low oxygen (5%), low nutrients (0.1X strength Dubos medium), high CO₂ (10%),

and low pH (5.0) [176]. In this condition, bacteria stop replication, gathers triacylglycerol, and become more antibiotic-resistant. The metabolic activity of these non-replicating bacteria is assessed using the redox dye Alamar blue to develop an assay suitable for drug assessment, although three days of outgrowth following drug exposure is necessary for this experiment [176].

A second multi-stress model generates a non-replicating state by combining moderate hypoxia, low pH, and butyrate as a source of nitric oxide, carbon, and reactive nitrogen intermediates [177]. Each stress condition was chosen based on its relevance to the infectious environment. Although it requires a time of expansion, this assay is suitable for high-throughput assessment and dosage response curves. The outgrowth time in liquid media is eliminated in an upgraded version of the procedure wherein the bacteria are seeded onto a medium supplemented with charcoal for 7–10 days, and further metabolic activity is measured using resazurin [178,179]. Although this approach still depends on outgrowth to create enough signal, the use of charcoal eliminates chemical leftovers, eliminating false positives resulting from action against active bacteria. Furthermore, because it consistently identifies a 2–3 log reduction in CFUs, this approach may be used to estimate the MBC of test compounds during screening [178].

7. The rifampicin persister model

Although an increased dose of rifampicin has shown the potential to improve TB control by reducing treatment time, the effects of the elimination rate of persistent bacteria remain unknown. To address this issue, Hu et al. developed this model [180]. In this model, rifampin (100g/ml) was added to a 100-day-old stationary phase Mtb culture and incubated for five days. "They discovered that bacilli could grow in a fresh 7H9 liquid media but could not form colonies on an agar plate." This trait is analogous to the Cornell model's latent bacilli. This model introduced a minor modification of PZA combined with RIF, demonstrating that additional bacterial population eradication and remaining bacilli closely resembled dormant bacilli. Rifampin-resistant bacilli were shown to be capable of metabolizing C14-palmitate and producing mRNA for sigB, rpoB, and hspX.

8. Nitrite induces Viable but non-cultivable dormancy

Nitrite-treated Mtb cells generate dose-dependent nitric oxide (NO) within the cell [114]. In this model, nitrite is utilized to induce dormancy in Mtb; after this, a viable but non-cultivable dormancy phenomenon is achieved in Mtb cells when exposed to 10mM nitrite.

Further experimental results showed that MRA2164 and MRA0854 genes were considerably upregulated following nitrite exposure in search of the conserved sequence of NO-producing enzymes in the bacterial system [181]. Furthermore, the purified recombinant MRA2164 protein has considerable NO synthesizing activity and is nitrite-dependent. Compared to wild-type bacilli, knocking down the MRA2164 gene at the mRNA level resulted in a much lower NO level and a recovery of replicative competence. As a result, nitrite promotes dormancy in Mtb cells by inducing MRA2164 gene expression and NO generation to sustain a non-replicative state in Mtb. This nitrite-treated dormancy model might aid in screening novel compounds against TB, particularly for screening compounds against the latent phenotype of the Mtb bacilli.

B. Ex-vivo models for screening of compounds

1. Macrophage infection models

Due to the simplicity of preparations, homogeneity of culture, and capacity to grow high cell numbers necessary for primary screenings, cell lines are commonly employed for intracellular experiments. Mostly murine cell lines such as RAW264.7 [182,183] and J774 [184] and human cell lines such as A549 and THP-1 are used for macrophage infection models (MIM) for Mtb [185-187]. Phagocytic potential, pre-activation, an appropriate multiplicity of infection (MOI), and test time will differ for each cell line for the individual assay. Because infected macrophages cannot stay alive for lengthy times, shorter experiments are typically used. MIM is primarily used for screening and dose-response analysis of compounds.

In nitrite reductase (NR) assay, the kinetics of nitrate reduction by Mtb during growth is studied [188]. A steady increase in NR was found during the growth of Mtb in THP-1 macrophages. NR in a culture medium with 50 mM nitrate was shown to be ideal on the fifth day after Mtb infection. This macrophage-based test yielded an S/N ratio of 5.4 and a Z-factor of 0.965, indicating a reliable assay technique. To confirm the method, standard antitubercular inhibitors such as isoniazid, rifampicin, ethambutol, streptomycin, and pyrazinamide were added at their IC₉₀ value on the day of infection. When these inhibitors were given to the culture on the fifth day following infection, they could not kill the bacilli. The bacilli were destroyed quickly after adding pentachlorophenol and rifampicin on the fifth day of infection. Overall, the NR assay utilizing Mtb infected with THP-1 macrophages

provides a unique, cost-effective method for screening both active and dormant stage-specific compounds against TB.

In a novel red fluorescence protein-based microplate assay for drug screening, inhibitors were added during inoculation, primarily representing active stage inhibitors rather than dormant ones [189]. The culture was coated with paraffin to create hypoxia, allowing chemicals to be added at any point throughout the 96-well plate's incubation. The red fluorescent protein's sustained expression in bacilli under both actively growing and dormant circumstances aids in quantifying the bacilli growth and inhibition kinetics in the medium. Additionally, this assay's Z' factor and S/N ratios were 0.91–0.94 and > 27, respectively, confirming the protocol's sturdiness. This newly designed drug-screening technique provides an accessible, low-cost, safe, high-throughput approach for finding new antitubercular inhibitors against active and dormant TB.

2. Vitamin C induced dormancy model /A multistress redox model

Vitamin C, often known as ascorbic acid, is an antioxidant and oxygen scavenger used in combination medication therapy. This approach addresses current intracellular models' limitations [190]. Taneja NK et al. showed in 2010 that adding 10mM vitamin C after infection inhibited intracellular mycobacterial development. Resistance to INH and increased DevRS/DosT signaling were found in mycobacterial growth arrest with dormancy. Vitamin C was discovered to change the physiology of Mtb in-vitro, causing it to stop multiplying. According to a recent study, Vitamin C adapted mycobacteria with dormancy traits such as growth standstill, loss of acid-fast staining, size reduction, resistance to first-line TB medicines, a protective response to oxidative stress, and reductive stress dissipation through triglyceride accumulation. When Vitamin C was added in in-vitro condition, it was found to induce the VBNC stage in Mtb, but when it was removed, the active form of growth was returned [191]. Hence, the Vitamin C-induced dormancy model is a redox model with several stressors. This model, which is an alternate explanation of non-replicating persistence, was utilized to screen compounds against the VBNC stage of Mtb.

C. In-vivo models

Various animal models have been used for the in-vivo screening of compounds and specifically to study the dormancy phenotype of Mtb.

1. The mouse model of mycobacterial persistence/ Cornell model/ The treated model

McCune and colleagues at Cornell University established the Cornell dormancy model in the 1950s, which offered the initial experimental in-vivo proof of the survival of latent bacilli [192]. Because dormant TB is the outcome of complicated host-pathogen interactions, simulating this condition may be difficult [193,194]. In the past, mice have long been employed in genetic studies because of their ease, the logarithmic expansion of mice for genetic research, and technological advantages like the accessibility of numerous strains and affordable reagents. Nevertheless, TB in mice varies from human TB in several ways; for example, the bacillary load can be quite high in sensitive mice and is not removed through the host. Similarly, the immunological responses in the form of granuloma in mice vary from that in humans since there is no calcification or caseation [195]. In this case, mice are injected intravenously with a high dose of virulent Mtb and then treated with antibiotics to decrease the bacterial load to low or undetectable. Although no living mycobacteria are discovered after therapy, the infection might reactivate spontaneously, a situation known as pseudosterilization or reaction to immunosuppressive medications like corticosteroids. Bacteria from the Cornell model have been found to be drug resistant. The low bacterial load in the mice is identical to paucibacillary latent human TB, making this model appealing. However, using antibiotics to reduce mycobacterial burden does not replicate Mtb's natural pathogenic entry, making it a controversial microbiological tool for latency and immunological study.

2. The low dose Chronic Murine model/ The Untreated Mouse model

A low dosage of Mtb infection administered by aerosol or intravenous route generates a gradual but consistent rise in bacterial counts in the lungs in this model [196]. Infection is confined primarily by the host immune response, which resembles latency in humans after an initial acute phase of bacterial proliferation. The bacillary count plateau is proportional to the initial inoculum size [175]. Unlike latent TB infections in humans, this model produces a significant bacillary load, and the animals die due to lung disease produced by the inflammatory response. This model of a chronic infectious condition has been adopted for its convenience and development of extended chronic TB, although it does not reflect genuine latency [197].

3. Guinea pig persister model

This model of experimental airborne TB was developed to test the efficiency of chemotherapeutic regimens against pathogenic tubercle bacilli. The bacilli of high and low virulence are used for in vivo studies during the early phase of treatment in a guinea pig model [198]. Primary lung lesions and metastatic sites in the lung and spleen caused by spontaneously occurring bacillaemia were studied. Three treatment combinations, INH+EMB, RIF+INH, and EMB+RIF therapies, were started four weeks after infection and continued for eight weeks. Despite slight variations in the time it took for a significant bactericidal effect to appear, the microbial population's rate declined. All three treatment combinations significantly reduced the number of Mtb H37Rv retrieved from primary lung lesions, main lesion-free lung lobes, and the spleen. The degree of calcification of original lung lesions and the number of surviving bacilli were related to X-rays of excised inflated lung lobes.

4. Zebrafish model

The zebrafish, also known as *Danio rerio*, is gaining popularity as an animal model in TB research [199]. The similarities in histology and pathology between *Mycobacterium marinum* infection in zebrafish and Mtb infection in humans have led to this change. The advantages of using a zebrafish model are its small size, low cost, transparency, and ease of handling. The zebrafish model infected with *Mycobacterium marinum* is helpful for testing novel human TB vaccines, high-throughput small-molecule screening, repurposing known medications with potential antitubercular action, and assessing novel antitubercular molecules for hepatotoxicity.

Overall, the processes through which tubercle bacilli can live in a latent condition inside a human host are unknown. Developing new models and analyzing active and dormant TB infections is limited by the lack of understanding. In order to have a high predicted sterilizing index, continuous efforts are needed to develop better in-vivo, ex-vivo, and in-vitro models of persistent/latent Mtb. These objectives must be met to reach the global targets of combating TB with new, effective, and shorter regimens that demonstrate powerful sterilizing properties in dormancy models. Furthermore, these models will aid in the prevention of infection in latently infected populations.

1.2.4. Global Alliance for TB Drug Development

The Global Alliance for TB Drug Development (TB Alliance), established in 2000, is a non-profit organization committed to speeding up the research and developing fast-acting, low-cost medications to combat TB [200]. The TB Alliance has an internal team of about 50 people and a global network of partners and collaborators. It is a virtual drug R&D organization that interacts with the academic, corporate, public, and charitable sectors to contribute to and improve the TB drug pipeline and stimulate and facilitate worldwide efforts to find novel TB medicines. The TB Alliance uses the experience and resources of an extensive and diversified network of partners while lowering R&D expenditures, such as overhead and infrastructure investments, through a range of license and collaboration agreements. Three clinical-stage compounds are now completing late-stage research in the TB Alliance catalog. Moxifloxacin is a known antibiotic being evaluated for a TB indication; the other two, TMC207 and PA-824, are unique chemical entities [201].

There are five strategic goals for the TB Alliance [202]-

1. Find and obtain promising compounds.
2. Oversee the development of potential medications in the preclinical stage.
3. Be the driving force behind clinical studies and regulatory approval.
4. Make sure it is affordable, adaptable, and accessible (AAA strategy).
5. Assemble expertise and resources for the development of TB drugs.

The TB Alliance's success may motivate funders to provide more significant financing for future projects.

1.2.5. Current status of drug discovery for tuberculosis and the importance of drug target identification

Over the last decade, the number of candidates in the TB drug research pipeline has increased (<https://www.newtbdrugs.org>). However, the dropout rate for drug development is relatively high, demanding continuing research for new active molecules to treat TB effectively. The CDC has suggested two treatment regimens for latent TB infections in the United States. The first treatment is RIF-based and lasts 3–4 months, whereas the second is INH monotherapy and lasts 6–9 months. Rifapentine and Rifampin are also included in these courses. PZA, EMB, and the other medications described above are used in other nations for at least six

months [203]. At present, there are four drugs in combination used to treat TB patients. The use of the combination strategy is primarily based on differences in the cellular targets, as mentioned in Table 4.

Table 4. Current antituberculosis regimes with their cellular targets

Drug	Chemical class	Cellular targets
Isoniazid	Isonicotinic acid	Enoyl-ACP reductase, mycolic acid elongation
Rifampicin	Rifamycin	DNA-primed RNA polymerase
Pyrazinamide	Pyrazine	Multiple drug targets and multiple mechanisms of action such as fatty acid biosynthesis/membrane depolarization/ribosomal protein S1 (Rps A), protein translation, and the ribosome-sparing processes of translation
Ethambutol	Ethylenediamine	Cell wall arabinan deposition

In a significant majority of patients with extremely drug-resistant forms of tuberculosis, triple combinations of bedaquiline, pretomanid, and linezolid drugs resulted in a positive outcome six months after the completion of therapy; however, some related adverse effects were noted [204]. Bedaquiline and linezolid have been used more often to treat MDR and XDR tuberculosis over the duration of this study. The WHO recently published guidelines that recommend these two medications as the first-line treatment for MDR tuberculosis throughout an 18-month course of therapy [205]. Moreover, the pretomanid-containing regimen (Nix-TB), which also contained BDQ, and linezolid used in combination, was reported to show almost 90% treatment success with highly resistant TB. The MIC values reported for pretomanid are in the range of 0.015–0.25 µg/ml for drug-sensitive strains and 0.03–0.53 µg/ml for drug-resistant strains [206].

Combining high doses of 8-methoxyquinolones, rifamycins, nitroimidazoles, and a diarylquinoline (bedaquiline) are now being evaluated in phases IIb and III clinical trials. Other compounds (for example, new oxazolidinones and ethylenediamines) are still in the early phases of clinical trials [207].

The majority of antitubercular drugs target one of three pathways: 1. cell wall synthesis, 2. Electron transport chain (ETC), and 3) Transcription and translation processes [208]. Generally, a 'druggable' target is a peptide, nucleic acid, or protein whose activity may be influenced by a drug, for example, biological entities such as an antibody or recombinant protein or a small molecular weight synthetic compound. The ability to investigate novel targets for creating antibiotics throughout the Mtb genome has become possible because of the accessibility of the whole genomic sequence for Mtb [158,209]. Novel biochemical entities and targets should help avoid drug resistance and enhance current therapies. For an antibiotic to be developed, it must be susceptible to medications and drug-effective in in-vivo conditions [210]. Overall, screening of novel compounds using suitable models and identifying the drug target may help understand the mechanism of action of the candidate compound and give the confidence to proceed further for in-vivo studies.

2. Thesis objectives

It takes a lengthy, challenging, and expensive technique to develop a new drug/treatment and bring it to market. The first step in this process is drug discovery, which requires finding interesting molecules with a significant biological advantage. The initial phases of drug discovery are mainly accomplished by compound screening and end with target identification and its characterization. Most of the proposed drugs against TB failed in early clinical trials for two main reasons: efficacy and safety. To overcome this problem, novel screening methods, such as phenotypic screening or whole cell-based in-vitro screening techniques, are available to evaluate small molecules potential against TB. The first study, frequently conducted in academia, produces data to support a hypothesis that inhibiting or activating a protein or pathway would significantly impact a disease state. This activity identifies a target that may require additional validation before moving on to the lead discovery phase to justify a drug discovery program. Our present study tried to identify novel small molecule inhibitors and their target from a different class of compounds against TB using established screening methods against both active and dormant stages of Mtb.

The present study has been commenced with specific objectives as mentioned below-

1. Overview of disease and drug discovery for tuberculosis
2. Screening of novel small molecule inhibitors against an active and dormant stage of *Mycobacterium tuberculosis*

3. Identification of intracellular protein target of different inhibitors within the active and dormant stage of *Mycobacterium tuberculosis*

3. A. Identification of intracellular protein target of RRA2 inhibitor within the active *Mycobacterium tuberculosis*

3. B. Identification of intracellular protein target of RRA268 inhibitor within the dormant *Mycobacterium tuberculosis*

4. Drug metabolism and pharmacokinetics study of novel triazole hits against *Mycobacterium tuberculosis*.

The current study will help us to understand the potential of the synthesized compounds against different stages of Mtb and discard the rest. Further target identification and characterization allow for the prediction of increased confidence in the relationship between the target and the disease and explore their mechanistic relationships within complex biological systems of an organism.

3. References

1. Gangadharam, Pattisapu RJ, and P. Anthony Jenkins. *Mycobacteria: I basic aspects*. Vol. 1. Springer Science & Business Media, 1997.
2. Global tuberculosis report 2021. Geneva: World Health Organization; 2021. Licence: CC BY-NC-SA 3.0 IGO.
3. Ledesma, Jorge R., Jianing Ma, Avina Vongpradith, Emilie R. Maddison, Amanda Novotney, Molly H. Biehl, Kate E. LeGrand et al. "Global, regional, and national sex differences in the global burden of tuberculosis by HIV status, 1990–2019: results from the Global Burden of Disease Study 2019." *The Lancet Infectious Diseases* 22, no. 2 (2022): 222-241.
4. Yerramsetti, Sita, Ted Cohen, Rifat Atun, and Nicolas A. Menzies. "Global estimates of paediatric tuberculosis incidence in 2013–19: a mathematical modelling analysis." *The Lancet Global Health* 10, no. 2 (2022): e207-e215.
5. Bennett, John E., Raphael Dolin, and Martin J. Blaser. *Mandell, Douglas, and Bennett's Principles and Practice of Infectious Diseases E-Book*. Elsevier Health Sciences, 2019.
6. Mortaz, Esmaeil, Mohammad Reza Masjedi, Atefeh Abedini, Soheila Matroodi, Arda Kiani, Dina Soroush, and Ian M. Adcock. "Common features of tuberculosis and sarcoidosis." *International Journal of Mycobacteriology* 5 (2016): S240-S241.

7. Gibson, Peter G., Michael Abramson, Richard Wood-Baker, Jimmy Volmink, Michael Hensley, and Ulrich Costabel, eds. *Evidence-based respiratory medicine*. John Wiley & Sons, 2008.
8. Lawn, S. D., and A. I. Zumla. "Seminar tuberculosis." *Lancet* 378, no. 9785 (2011): 57-72.
9. Behera, D. *Textbook of Pulmonary Medicine* Volumes 1 and 2. Jaypee Brothers Pvt. Limited, 2010.
10. Cegielski, J. P., and D. N. McMurray. "The relationship between malnutrition and tuberculosis: evidence from studies in humans and experimental animals." *The international journal of tuberculosis and lung disease* 8, no. 3 (2004): 286-298.
11. WHO Global Tuberculosis Report 2019. Geneva: World Health Organization (2019).
12. World Health Organization. Tuberculosis diagnostics – Xpert MTB/RIF Test; (2013).
13. Peto, Heather M., Robert H. Pratt, Theresa A. Harrington, Philip A. LoBue, and Lori R. Armstrong. "Epidemiology of extrapulmonary tuberculosis in the United States, 1993–2006." *Clinical Infectious Diseases* 49, no. 9 (2009): 1350-1357.
14. Diacon, A. H., B. W. Van de Wal, C. Wyser, J. P. Smedema, J. Bezuidenhout, C. T. Bolliger, and G. Walzl. "Diagnostic tools in tuberculous pleurisy: a direct comparative study." *European Respiratory Journal* 22, no. 4 (2003): 589-591.
15. De la Rúa-Domenech, Ricardo. "Human Mycobacterium bovis infection in the United Kingdom: incidence, risks, control measures and review of the zoonotic aspects of bovine tuberculosis." *Tuberculosis* 86, no. 2 (2006): 77-109.
16. Rock, R. B., M. Olin, and C. Baker. "a, Molitor, TW, Peterson, PK, 2008. Central nervous system tuberculosis: pathogenesis and clinical aspects." *Clin. Microbiol. Rev* 21 (2008): 243-261.
17. Abbara, Aula, and Robert N. Davidson. "Etiology and management of genitourinary tuberculosis." *Nature Reviews Urology* 8, no. 12 (2011): 678-688.
18. Gatongi, D. K., and V. Kay. "Endometrial tuberculosis presenting with postmenopausal pyometra." *Journal of obstetrics and gynaecology* 25, no. 5 (2005): 518-520.
19. Golden, Marjorie P., and Holenarasipur R. Vikram. "Extrapulmonary tuberculosis: an overview." *American family physician* 72, no. 9 (2005): 1761-1768.
20. Sester, Martina, Giovanni Sotgiu, Christoph Lange, Claudia Giehl, Enrico Girardi, Giovanni Battista Migliori, Aik Bossink et al. "Interferon- γ release assays for the

- diagnosis of active tuberculosis: a systematic review and meta-analysis." *European Respiratory Journal* 37, no. 1 (2011): 100-111.
21. Norbis, Luca, Paolo Miotto, Riccardo Alagna, and Daniela M. Cirillo. "Tuberculosis: lights and shadows in the current diagnostic landscape." *New Microbiol* 36, no. 2 (2013): 111-20.
 22. Oehlers, Stefan H., Mark R. Cronan, Ninecia R. Scott, Monica I. Thomas, Kazuhide S. Okuda, Eric M. Walton, Rebecca W. Beerman, Philip S. Crosier, and David M. Tobin. "Interception of host angiogenic signalling limits mycobacterial growth." *Nature* 517, no. 7536 (2015): 612-615.
 23. Polena, Helena, Frédéric Boudou, Sylvain Tilleul, Nicolas Dubois-Colas, Cécile Lecointe, Niaina Rakotosamimanana, Mattia Pelizzola et al. "Mycobacterium tuberculosis exploits the formation of new blood vessels for its dissemination." *Scientific reports* 6, no. 1 (2016): 1-11.
 24. Parra, Marcela, Thames Pickett, Giovanni Delogu, Veerabadran Dheenadhayalan, Anne-Sophie Debrie, Camille Locht, and Michael J. Brennan. "The mycobacterial heparin-binding hemagglutinin is a protective antigen in the mouse aerosol challenge model of tuberculosis." *Infection and Immunity* 72, no. 12 (2004): 6799-6805.
 25. Schepers, Kinda, Violette Dirix, F. Mouchet, V. Verscheure, S. Lecher, C. Locht, and F. Mascarot. "Early cellular immune response to a new candidate mycobacterial vaccine antigen in childhood tuberculosis." *Vaccine* 33, no. 8 (2015): 1077-1083.
 26. De Maio, Flavio, Valentina Palmieri, Marco De Spirito, Giovanni Delogu, and Massimiliano Papi. "Carbon nanomaterials: a new way against tuberculosis." *Expert Review of Medical Devices* 16, no. 10 (2019): 863-875.
 27. Reljic, R., C. Di Sano, C. Crawford, F. Dieli, S. Challacombe, and J. Ivanyi. "Time course of mycobacterial infection of dendritic cells in the lungs of intranasally infected mice." *Tuberculosis* 85, no. 1-2 (2005): 81-88.
 28. Guerrero, Gloria G., Ann-Sophie Debrie, and Camille Locht. "Boosting with mycobacterial heparin-binding haemagglutinin enhances protection of Mycobacterium bovis BCG-vaccinated newborn mice against M. tuberculosis." *Vaccine* 28, no. 27 (2010): 4340-4347.
 29. Humphreys, Ian R., Graham R. Stewart, David J. Turner, Janisha Patel, Danai Karamanou, Robert J. Snelgrove, and Douglas B. Young. "A role for dendritic cells in the

- dissemination of mycobacterial infection." *Microbes and Infection* 8, no. 5 (2006): 1339-1346.
30. Zürcher, Kathrin, Marie Ballif, Sasisopin Kiertiburanakul, Henri Chenal, Marcel Yotebieng, Beatriz Grinsztejn, Denna Michael et al. "Diagnosis and clinical outcomes of extrapulmonary tuberculosis in antiretroviral therapy programmes in low-and middle-income countries: a multicohort study." *Journal of the International AIDS Society* 22, no. 9 (2019): e25392.
31. Oehlers, Stefan H., Mark R. Cronan, Ninecia R. Scott, Monica I. Thomas, Kazuhide S. Okuda, Eric M. Walton, Rebecca W. Beerman, Philip S. Crosier, and David M. Tobin. "Interception of host angiogenic signalling limits mycobacterial growth." *Nature* 517, no. 7536 (2015): 612-615.
32. Polena, Helena, Frédéric Boudou, Sylvain Tilleul, Nicolas Dubois-Colas, Cécile Lecointe, Niaina Rakotosamimanana, Mattia Pelizzola et al. "Mycobacterium tuberculosis exploits the formation of new blood vessels for its dissemination." *Scientific reports* 6, no. 1 (2016): 1-11.
33. Sharma, Surendra K., Alladi Mohan, and Abhishek Sharma. "Challenges in the diagnosis & treatment of miliary tuberculosis." *The Indian journal of medical research* 135, no. 5 (2012): 703.
34. Mert, Ali, Muammer Bilir, Fehmi Tabak, Resat Ozaras, Recep Ozturk, Hakan Senturk, Hilal Aki, Nur Seyhan, Tuncer Karayel, and Yildirim Aktuglu. "Miliary tuberculosis: clinical manifestations, diagnosis and outcome in 38 adults." *Respirology* 6, no. 3 (2001): 217-224.
35. Sharma, Surendra K., and Alladi Mohan. "Miliary tuberculosis." *Tuberculosis and Nontuberculous Mycobacterial Infections* (2017): 491-513.
36. Wells, William Firth. "Airborne Contagion and Air Hygiene. An Ecological Study of Droplet Infections." *Airborne Contagion and Air Hygiene. An Ecological Study of Droplet Infections*. (1955).
37. Loudon, Robert G., and Sharon K. Spohn. "Cough frequency and infectivity in patients with pulmonary tuberculosis." *American Review of Respiratory Disease* 99, no. 1 (1969): 109-111.
38. Duguid, J. P. "The size and the duration of air-carriage of respiratory droplets and droplet-nuclei." *Epidemiology & Infection* 44, no. 6 (1946): 471-479.

39. Bates, Joseph H., William E. Potts, and Margaret Lewis. "Epidemiology of primary tuberculosis in an industrial school." *New England Journal of Medicine* 272, no. 14 (1965): 714-717.
40. Loudon, Robert G., and Rena Marie Roberts. "Singing and the dissemination of tuberculosis." *American Review of Respiratory Disease* 98, no. 2 (1968): 297-300.
41. Somogyi, Ron, Alex E. Vesely, Takafumi Azami, David Preiss, Joseph Fisher, Joe Correia, and Robert A. Fowler. "Dispersal of respiratory droplets with open vs closed oxygen delivery masks: implications for the transmission of severe acute respiratory syndrome." *Chest* 125, no. 3 (2004): 1155-1157.
42. Tang, Julian W., Andre D. Nicolle, Christian A. Klettner, Jovan Pantelic, Liangde Wang, Amin Bin Suhaimi, Ashlynn YL Tan et al. "Airflow dynamics of human jets: sneezing and breathing-potential sources of infectious aerosols." *PloS one* 8, no. 4 (2013): e59970.
43. Gunnels, Janice J., Joseph H. Bates, and Hermione Swindoll. "Infectivity of sputum-positive tuberculous patients on chemotherapy." *American Review of Respiratory Disease* 109, no. 3 (1974): 323-330.
44. Dwivedi, Manish, and Priya Giri. "Challenges in Drug Discovery against Tuberculosis." *Molecular Epidemiology Study of Mycobacterium Tuberculosis Complex* (2021): 9.
45. Dinan, Adam M., Pin Tong, Amanda J. Lohan, Kevin M. Conlon, Aleksandra A. Miranda-CasoLuengo, Kerri M. Malone, Stephen V. Gordon, and Brendan J. Loftus. "Relaxed selection drives a noisy noncoding transcriptome in members of the Mycobacterium tuberculosis complex." *MBio* 5, no. 4 (2014): e01169-14.
46. Ahmad, Suhail. "Pathogenesis, immunology, and diagnosis of latent Mycobacterium tuberculosis infection." *Clinical and Developmental Immunology* (2011).
47. Yuan, Ying, Richard E. Lee, Gurdyal S. Besra, John T. Belisle, and C. E. Barry. "Identification of a gene involved in the biosynthesis of cyclopropanated mycolic acids in Mycobacterium tuberculosis." *Proceedings of the National Academy of Sciences* 92, no. 14 (1995): 6630-6634.
48. Murry, Jeffrey P., Amit K. Pandey, Christopher M. Sasseti, and Eric J. Rubin. "Phthiocerol dimycocerosate transport is required for resisting interferon- γ -independent immunity." *The Journal of infectious diseases* 200, no. 5 (2009): 774-782.

49. Kumar, Ashwani, Aisha Farhana, Loni Guidry, Vikram Saini, Mary Hondalus, and Adrie JC Steyn. "Redox homeostasis in mycobacteria: the key to tuberculosis control?." *Expert reviews in molecular medicine* 13 (2011).
50. Roy Chowdhury, Roshni, Francesco Vallania, Qianting Yang, Cesar Joel Lopez Angel, Fatoumatta Darboe, Adam Penn-Nicholson, Virginie Rozot et al. "A multi-cohort study of the immune factors associated with M. tuberculosis infection outcomes." *Nature* 560, no. 7720 (2018): 644-648.
51. Githinji, Leah N., Diane M. Gray, and Heather J. Zar. "Lung function in HIV-infected children and adolescents." *Pneumonia* 10, no. 1 (2018): 1-10.
52. Jindal, S. K. "Textbook of Pulmonary and Critical Care Medicine Vols 1 and 2." (2011).
53. Fu, L. M., and C. S. Fu-Liu. "Is Mycobacterium tuberculosis a closer relative to Gram-positive or Gram-negative bacterial pathogens?." *Tuberculosis* 82, no. 2-3 (2002): 85-90.
54. Cudahy, Patrick, and Sheela V. Sheno. "Diagnostics for pulmonary tuberculosis." *Postgraduate medical journal* 92, no. 1086 (2016): 187-193.
55. Shepard, C. C., and D. H. McRae. "A method for counting acid-fast bacteria." *International Journal of Leprosy* 36, no. 1 (1968): 78-82.
56. Ramírez-Rueda, R. Y. "Mycobacterium tuberculosis: clinical and microbiological aspects." *In The Microbiology of Respiratory System Infections*, pp. 153-166. Academic Press, 2016.
57. Kommareddi, Santi, Carlos R. Abramowsky, Gary L. Swinehart, and Linda Hrabak. "Nontuberculous mycobacterial infections: comparison of the fluorescent auramine-O and Ziehl-Neelsen techniques in tissue diagnosis." *Human pathology* 15, no. 11 (1984): 1085-1089.
58. Caulfield, Adam J., and Nancy L. Wengenack. "Diagnosis of active tuberculosis disease: From microscopy to molecular techniques." *Journal of Clinical Tuberculosis and Other Mycobacterial Diseases* 4 (2016): 33-43.
59. Fitzgerald, D. W., T. R. Sterline, and D. W. Haas. "251-Mycobacterium tuberculosis." *Bennett JE, Dolin R, Blaser MJ. Mandell, Douglas, and Bennett's principles and practice of infectious diseases. Elsevier Saunders* (2015): 2787.
60. Lewinsohn, David M., Michael K. Leonard, Philip A. LoBue, David L. Cohn, Charles L. Daley, Ed Desmond, Joseph Keane et al. "Official American Thoracic Society/Infectious Diseases Society of America/Centers for Disease Control and Prevention clinical practice

- guidelines: diagnosis of tuberculosis in adults and children." *Clinical Infectious Diseases* 64, no. 2 (2017): e1-e33.
61. Chihota, V. N., A. D. Grant, K. Fielding, B. Ndibongo, A. Van Zyl, D. Muirhead, and G. J. Churchyard. "Liquid vs. solid culture for tuberculosis: performance and cost in a resource-constrained setting." *The international journal of tuberculosis and lung disease* 14, no. 8 (2010): 1024-1031.
62. Kumar, V., A. K. Abbas, N. Fausto, R. Mitchell, and Robbins Basic Pathology. "Saunders." *The Curtis center, Philadelphia, Pennsylvania-2004* 7 (2007): 614.
63. Winn, Washington C. *Koneman's color atlas and textbook of diagnostic microbiology*. Lippincott williams & wilkins, 2006.
64. Heifets, Leonid B., and Robert C. Good. "Current laboratory methods for the diagnosis of tuberculosis." *Tuberculosis: pathogenesis, protection, and control* (1994): 85-110.
65. Cheng, Jun, Lixia Wang, Hui Zhang, and Yinyin Xia. "Diagnostic value of symptom screening for pulmonary tuberculosis in China." *PloS one* 10, no. 5 (2015): e0127725.
66. Department of disease control, Chinese Ministry of Health. Guidelines for implementing the national tuberculosis control program in China. Beijing: Beijing Union Medical College Press; 2009 (ISBN 978-7-81136-190-2).
67. Konstantinos, Anastasios. "Testing for tuberculosis." (2010).
68. Silverman, Charlotte. "An appraisal of the contribution of mass radiography in the discovery of pulmonary tuberculosis." *American review of tuberculosis* 60, no. 4 (1949): 466-482.
69. Van't Hoog, Anna H., Helen K. Meme, Kayla F. Laserson, Janet A. Agaya, Benson G. Muchiri, Willie A. Githui, Lazarus O. Odeny, Barbara J. Marston, and Martien W. Borgdorff. "Screening strategies for tuberculosis prevalence surveys: the value of chest radiography and symptoms." *PloS one* 7, no. 7 (2012): e38691.
70. Naing, Wai Yan Nyein, and Zaw Z. Htike. "Advances in automatic tuberculosis detection in chest x-ray images." *Signal & Image Processing* 5, no. 6 (2014): 41.
71. Hsu, Katharine HK. "Tuberculin reaction in children treated with isoniazid." *American Journal of Diseases of Children* 137, no. 11 (1983): 1090-1092.
72. Monaghan, M. L., M. L. Doherty, J. D. Collins, J. F. Kazda, and P. J. Quinn. "The tuberculin test." *Veterinary microbiology* 40, no. 1-2 (1994): 111-124.
73. Chadha, Vineet K. "Tuberculin test." *The Indian Journal of Pediatrics* 68, no. 1 (2001): 53-58.

74. Beck, J. Swanson. "Skin changes in the tuberculin test." *Tubercle* 72, no. 2 (1991): 81-87.
75. Mahairas, Gregory G., Peter J. Sabo, Mark J. Hickey, Devinder C. Singh, and C. Kendall Stover. "Molecular analysis of genetic differences between *Mycobacterium bovis* BCG and virulent *M. bovis*." *Journal of bacteriology* 178, no. 5 (1996): 1274-1282.
76. Sørensen, Anne L., Sadamu Nagai, Gunnar Houen, Peter Andersen, and Ase B. Andersen. "Purification and characterization of a low-molecular-mass T-cell antigen secreted by *Mycobacterium tuberculosis*." *Infection and immunity* 63, no. 5 (1995): 1710-1717.
77. Lighter, Jennifer, Mona Rigaud, Roger Eduardo, Chia-Hui Peng, and Henry Pollack. "Latent tuberculosis diagnosis in children by using the QuantiFERON-TB Gold In-Tube test." *Pediatrics* 123, no. 1 (2009): 30-37.
78. Takasaki, Jin, Toshie Manabe, Eriko Morino, Yoshikazu Muto, Masao Hashimoto, Motoyasu Iikura, Shinyu Izumi, Haruhito Sugiyama, and Koichiro Kudo. "Sensitivity and specificity of QuantiFERON-TB Gold Plus compared with QuantiFERON-TB Gold In-Tube and T-SPOT. TB on active tuberculosis in Japan." *Journal of infection and chemotherapy* 24, no. 3 (2018): 188-192.
79. Meier, T., H-P. Eulenbruch, P. Wrighton-Smith, G. Enders, and T. Regnath. "Sensitivity of a new commercial enzyme-linked immunospot assay (T SPOT-TB) for diagnosis of tuberculosis in clinical practice." *European Journal of Clinical Microbiology and Infectious Diseases* 24, no. 8 (2005): 529-536.
80. Wagstaff, Antona J., and Jean-Pierre Zellweger. "T-SPOT™. TB." *Molecular Diagnosis & Therapy* 10, no. 1 (2006): 57-63.
81. World Health Organization. *Automated real-time nucleic acid amplification technology for rapid and simultaneous detection of tuberculosis and rifampicin resistance: Xpert MTB*. No. WHO/HTM/TB/2013.16. World Health Organization, 2013.
82. World Health Organization. *Rapid implementation of the Xpert MTB/RIF diagnostic test: technical and operational 'How-to'; practical considerations*. No. WHO/HTM/TB/2011.2. World Health Organization, 2011.
83. Van Der Zanden, A. G. M., E. M. Te Koppele-Vije, N. Vijaya Bhanu, D. Van Soolingen, and L. M. Schouls. "Use of DNA extracts from Ziehl-Neelsen-stained slides for molecular detection of rifampin resistance and spoligotyping of *Mycobacterium tuberculosis*." *Journal of clinical microbiology* 41, no. 3 (2003): 1101-1108.
84. Lawn, Stephen D., Peter Mwaba, Matthew Bates, Amy Piatek, Heather Alexander, Ben J. Marais, Luis E. Cuevas et al. "Advances in tuberculosis diagnostics: the Xpert MTB/RIF

- assay and future prospects for a point-of-care test." *The Lancet infectious diseases* 13, no. 4 (2013): 349-361.
85. Pham, Thu Hang, Jonathan Peter, Fernanda CQ Mello, Tommy Parraga, Nguyen Thi Ngoc Lan, Pamela Nabeta, Eloise Valli et al. "Performance of the TB-LAMP diagnostic assay in reference laboratories: Results from a multicentre study." *International journal of infectious diseases* 68 (2018): 44-49.
86. Blakemore, Robert, Elizabeth Story, Danica Helb, JoAnn Kop, Padmapriya Banada, Michelle R. Owens, Soumitesh Chakravorty, Martin Jones, and David Alland. "Evaluation of the analytical performance of the Xpert MTB/RIF assay." *Journal of clinical microbiology* 48, no. 7 (2010): 2495-2501.
87. Cresswell, Fiona V., Lillian Tugume, Nathan C. Bahr, Richard Kwizera, Ananta S. Bangdiwala, Abdu K. Musubire, Morris Rutakingirwa et al. "Xpert MTB/RIF Ultra for the diagnosis of HIV-associated tuberculous meningitis: a prospective validation study." *The Lancet infectious diseases* 20, no. 3 (2020): 308-317.
88. Bahr, Nathan C., Lillian Tugume, Radha Rajasingham, Reuben Kiggundu, Darlisha A. Williams, Bozena Morawski, David Alland, David B. Meya, Joshua Rhein, and David R. Boulware. "Improved diagnostic sensitivity for tuberculous meningitis with Xpert® MTB/RIF of centrifuged CSF." *The international journal of tuberculosis and lung disease* 19, no. 10 (2015): 1209-1215.
89. Chakravorty, Soumitesh, Ann Marie Simmons, Mazhgan Rowneki, Heta Parmar, Yuan Cao, Jamie Ryan, Padmapriya P. Banada et al. "The new Xpert MTB/RIF Ultra: improving detection of Mycobacterium tuberculosis and resistance to rifampin in an assay suitable for point-of-care testing." *MBio* 8, no. 4 (2017): e00812-17.
90. World Health Organization. "WHO meeting report of a technical expert consultation: non-inferiority analysis of Xpert MTB/RIF Ultra compared to Xpert MTB/RIF. Geneva: World Health Organization; 2017." (2017).
91. Falzon, Dennis, Holger J. Schünemann, Elizabeth Harausz, Licé González-Angulo, Christian Lienhardt, Ernesto Jaramillo, and Karin Weyer. "World Health Organization treatment guidelines for drug-resistant tuberculosis, 2016 update." *European Respiratory Journal* 49, no. 3 (2017).
92. Osman, Jheni. *100 Ideas That Changed the World*. Random House, 2011.
93. UPDATE, SEMI-ANNUAL. "Tuberculosis Diagnostic Technology and Market Landscape." (2013).

94. Georghiou, Sophia B., Riccardo Alagna, Daniela M. Cirillo, Sergio Carmona, Morten Ruhwald, and Samuel G. Schumacher. "Equivalence of the GeneXpert System and GeneXpert Omni System for tuberculosis and rifampicin resistance detection." *PLoS one* 16, no. 12 (2021): e0261442.
95. Hunter, Shirley Wu, and P. J. Brennan. "Evidence for the presence of a phosphatidylinositol anchor on the lipoarabinomannan and lipomannan of *Mycobacterium tuberculosis*." *Journal of Biological Chemistry* 265, no. 16 (1990): 9272-9279.
96. Hamasur, Beston, Judith Bruchfeld, Melles Haile, Andrzej Pawlowski, Bjarne Bjorvatn, Gunilla Källenius, and Stefan B. Svenson. "Rapid diagnosis of tuberculosis by detection of mycobacterial lipoarabinomannan in urine." *Journal of microbiological methods* 45, no. 1 (2001): 41-52.
97. Cox, Janneke A., Robert L. Lukande, Sam Kalungi, Eric Van Marck, Koen Van de Vijver, Andrew Kambugu, Ann M. Nelson, Robert Colebunders, and Yukari C. Manabe. "Is urinary lipoarabinomannan the result of renal tuberculosis? Assessment of the renal histology in an autopsy cohort of Ugandan HIV-infected adults." *PLoS One* 10, no. 4 (2015): e0123323.
98. Nakiyingi, Lydia, V. Mischka Moodley, Yukari C. Manabe, Mark P. Nicol, Molly Holshouser, Derek T. Armstrong, Widaad Zemanay et al. "Diagnostic accuracy of a rapid urine lipoarabinomannan test for tuberculosis in HIV-infected adults." *Journal of acquired immune deficiency syndromes* (1999) 66, no. 3 (2014): 270.
99. Peter, Jonathan G., Grant Theron, Tapuwa E. Muchinga, Ureshnie Govender, and Keertan Dheda. "The diagnostic accuracy of urine-based Xpert MTB/RIF in HIV-infected hospitalized patients who are smear-negative or sputum scarce." *PloS one* 7, no. 7 (2012): e39966.
100. Chan, Heang Ping. "Computer Aided Diagnosis: Concepts and Applications." (2017).
101. Torfs, Eveline, Tatiana Piller, Paul Cos, and Davie Cappoen. "Opportunities for overcoming *Mycobacterium tuberculosis* drug resistance: emerging mycobacterial targets and host-directed therapy." *International journal of molecular sciences* 20, no. 12 (2019): 2868.
102. Dye, Christopher, Suzanne Scheele, Vikram Pathania, and Mario C. Raviglion. "Global burden of tuberculosis: estimated incidence, prevalence, and mortality by country." *Jama* 282, no. 7 (1999): 677-686.

103. World Health Organization. *Guidelines on the management of latent tuberculosis infection*. World Health Organization, 2015.
104. Houben, Rein MGJ, and Peter J. Dodd. "The global burden of latent tuberculosis infection: a re-estimation using mathematical modelling." *PLoS medicine* 13, no. 10 (2016): e1002152.
105. Parrish, Nikki M., James D. Dick, and William R. Bishai. "Mechanisms of latency in *Mycobacterium tuberculosis*." *Trends in microbiology* 6, no. 3 (1998): 107-112.
106. Comstock, George W., Verna T. Livesay, and SHIRLEY F. WOOLPERT. "The prognosis of a positive tuberculin reaction in childhood and adolescence." *American journal of epidemiology* 99, no. 2 (1974): 131-138.
107. Vynnycky, E., and P. E. M. Fine. "The natural history of tuberculosis: the implications of age-dependent risks of disease and the role of reinfection." *Epidemiology & Infection* 119, no. 2 (1997): 183-201.
108. Shea, Kimberly M., J. Steve Kammerer, Carla A. Winston, Thomas R. Navin, and C. Robert Horsburgh Jr. "Estimated rate of reactivation of latent tuberculosis infection in the United States, overall and by population subgroup." *American journal of epidemiology* 179, no. 2 (2014): 216-225.
109. Pinto, Daniela, Mário A. Santos, and Lélia Chambel. "Thirty years of viable but nonculturable state research: unsolved molecular mechanisms." *Critical reviews in microbiology* 41, no. 1 (2015): 61-76.
110. Heidelberg, J. F., M. Shahamat, M. Levin, I. Rahman, G. Stelma, C. Grim, and R. R. Colwell. "Effect of aerosolization on culturability and viability of gram-negative bacteria." *Applied and Environmental Microbiology* 63, no. 9 (1997): 3585-3588.
111. Cook, K. L., and C. H. Bolster. "Survival of *Campylobacter jejuni* and *Escherichia coli* in groundwater during prolonged starvation at low temperatures." *Journal of applied microbiology* 103, no. 3 (2007): 573-583.
112. Anuchin, Aleksey M., Andrey L. Mulyukin, Natalya E. Suzina, Vitaly I. Duda, Galina I. El-Registan, and Arseny S. Kaprelyants. "Dormant forms of *Mycobacterium smegmatis* with distinct morphology." *Microbiology* 155, no. 4 (2009): 1071-1079.
113. Gengenbacher, Martin, and Stefan HE Kaufmann. "Mycobacterium tuberculosis: success through dormancy." *FEMS microbiology reviews* 36, no. 3 (2012): 514-532.

114. Gample, Suwarna P., Sonia Agrawal, and Dhiman Sarkar. "Evidence of nitrite acting as a stable and robust inducer of non-cultivability in Mycobacterium tuberculosis with physiological relevance." *Scientific reports* 9, no. 1 (2019): 1-12.
115. Yeware, Amar, Suwarna Gample, Sonia Agrawal, and Dhiman Sarkar. "Using diphenyleneiodonium to induce a viable but non-culturable phenotype in Mycobacterium tuberculosis and its metabolomics analysis." *PloS one* 14, no. 8 (2019): e0220628.
116. Lawn, S. D., and A. I. Zumla. "Seminar tuberculosis." *Lancet* 378, no. 9785 (2011): 57-72.
117. Raviglione, Mario C., and Antonio Pio. "Evolution of WHO policies for tuberculosis control, 1948–2001." *The Lancet* 359, no. 9308 (2002): 775-780.
118. Maher, Dermot, Pierre Chaulet, Sergio Spinaci, and A. Harries. "Treatment of tuberculosis: guidelines for national programmes." *Geneva: World Health Organization* (1997).
119. World Health Organization. An expanded DOTS framework for effective tuberculosis control. WHO Stop TB Department, Geneva, 2002 (WHO/ CDS/TB/2002.297).
120. Mitchison, D. A. "Basic concepts in the chemotherapy of tuberculosis." *In Mycobacteria*, pp. 15-50. Springer, Boston, MA, 1998.
121. Dye, Christopher, Geoffrey P. Garnett, Karen Sleeman, and Brian G. Williams. "Prospects for worldwide tuberculosis control under the WHO DOTS strategy." *The Lancet* 352, no. 9144 (1998): 1886-1891.
122. World Health Organization. *WHO consolidated guidelines on drug-resistant tuberculosis treatment*. No. WHO/CDS/TB/2019.7. World Health Organization, 2019.
123. Pontali, Emanuele, Mario C. Raviglione, and Giovanni Battista Migliori. "Regimens to treat multidrug-resistant tuberculosis: past, present and future perspectives." *European Respiratory Review* 28, no. 152 (2019).
124. Ramachandran, Geetha, and Soumya Swaminathan. "Safety and tolerability profile of second-line anti-tuberculosis medications." *Drug safety* 38, no. 3 (2015): 253-269.
125. Kaufmann, Stefan HE, and Florian Winau. "From bacteriology to immunology: the dualism of specificity." *Nature immunology* 6, no. 11 (2005): 1063-1066.
126. Calmette, A., and Harry Plotz. "Protective inoculation against tuberculosis with BCG." *American Review of Tuberculosis* 19, no. 6 (1929): 567-572.
127. Pym, Alexander S., Priscille Brodin, Laleh Majlessi, Roland Brosch, Caroline Demangel, Ann Williams, Karen E. Griffiths, Gilles Marchal, Claude Leclerc, and

- Stewart T. Cole. "Recombinant BCG exporting ESAT-6 confers enhanced protection against tuberculosis." *Nature medicine* 9, no. 5 (2003): 533-539.
128. Roy, Partho, Johan Vekemans, Andrew Clark, Colin Sanderson, Rebecca C. Harris, and Richard G. White. "Potential effect of age of BCG vaccination on global paediatric tuberculosis mortality: a modelling study." *The Lancet Global Health* 7, no. 12 (2019): e1655-e1663.
129. Ragonnet, Romain, James M. Trauer, Nicholas Geard, Nick Scott, and Emma S. McBryde. "Profiling Mycobacterium tuberculosis transmission and the resulting disease burden in the five highest tuberculosis burden countries." *BMC medicine* 17, no. 1 (2019): 1-12.
130. Brewer, Timothy F. "Preventing tuberculosis with bacillus Calmette-Guerin vaccine: a meta-analysis of the literature." *Clinical Infectious Diseases* 31, no. Supplement_3 (2000): S64-S67.
131. Azzopardi, Peter, C. M. Bennett, S. M. Graham, and T. Duke. "Bacille Calmette-Guérin vaccine-related disease in HIV-infected children: a systematic review." *The International journal of tuberculosis and lung disease* 13, no. 11 (2009): 1331-1344.
132. Hesseling, Anneke C., Ben J. Marais, Robert P. Gie, H. Simon Schaaf, Paul EM Fine, Peter Godfrey-Faussett, and Nulda Beyers. "The risk of disseminated Bacille Calmette-Guerin (BCG) disease in HIV-infected children." *Vaccine* 25, no. 1 (2007): 14-18.
133. Fine, Paul EM. "Variation in protection by BCG: implications of and for heterologous immunity." *The Lancet* 346, no. 8986 (1995): 1339-1345.
134. Rodrigues, Laura C., Vinod K. Diwan, and Jeremy G. Wheeler. "Protective effect of BCG against tuberculous meningitis and miliary tuberculosis: a meta-analysis." *International journal of epidemiology* 22, no. 6 (1993): 1154-1158.
135. Colditz, Graham A., Timothy F. Brewer, Catherine S. Berkey, Mary E. Wilson, Elisabeth Burdick, Harvey V. Fineberg, and Frederick Mosteller. "Efficacy of BCG vaccine in the prevention of tuberculosis: meta-analysis of the published literature." *Jama* 271, no. 9 (1994): 698-702.
136. Ahsan, Mohamed Jawed. "Recent advances in the development of vaccines for tuberculosis." *Therapeutic advances in vaccines* 3, no. 3 (2015): 66-75.
137. Grave, A., and David Hokey. "Tuberculosis vaccines: review of current development trends and future challenges." *J Bioterr Biodef S* 1 (2011): 2.

138. World Health Organization. *Progress report on access to hepatitis C treatment: focus on overcoming barriers in low-and middle-income countries*. No. WHO/CDS/HIV/18.4. World Health Organization, 2018.
139. Wainwright, Milton. "Streptomycin: discovery and resultant controversy." *History and philosophy of the life sciences* (1991): 97-124.
140. Calvori, Clara, Laura Frontali, Louisa Leoni, and Giorgio Tecce. "Effect of rifamycin on protein synthesis." *Nature* 207, no. 4995 (1965): 417-418.
141. Olaru, Ioana Diana, Florian von Groote-Bidlingmaier, Jan Heyckendorf, Wing Wai Yew, Christoph Lange, and Kwok Chiu Chang. "Novel drugs against tuberculosis: a clinician's perspective." *European Respiratory Journal* 45, no. 4 (2015): 1119-1131.
142. Centers for Disease Control (CDC). "Nosocomial transmission of multidrug-resistant tuberculosis among HIV-infected persons--Florida and New York, 1988-1991." *MMWR. Morbidity and mortality weekly report* 40, no. 34 (1991): 585-591.
143. Frieden, Thomas R., Timothy Sterling, Ariel Pablos-Mendez, James O. Kilburn, George M. Cauthen, and Samuel W. Dooley. "The emergence of drug-resistant tuberculosis in New York City." *New England journal of medicine* 328, no. 8 (1993): 521-526.
144. Shah, N.S., Wright, A., Bai, G.H., Barrera, L., Boulahbal, F., Martín-Casabona, N., Drobniewski, F., Gilpin, C., Havelková, M., Lepe, R. and Lumb, R., 2007. Worldwide emergence of extensively drug-resistant tuberculosis. *Emerging infectious diseases*, 13(3), p.380.
145. Gandhi, Neel R., Anthony Moll, A. Willem Sturm, Robert Pawinski, Thiloshini Govender, Umesh Laloo, Kimberly Zeller, Jason Andrews, and Gerald Friedland. "Extensively drug-resistant tuberculosis as a cause of death in patients co-infected with tuberculosis and HIV in a rural area of South Africa." *The Lancet* 368, no. 9547 (2006): 1575-1580.
146. WHO, Geneva. "Multidrug and extensively drug-resistant TB (M/XDR-TB): 2010 global report on surveillance and response." *WHO/HTM/TB/2010.3* (2010).
147. Sarathy, J. P., F. Zuccotto, H. Hsinpin, L. Sandberg, L. E. Via, G. A. Marriner, T. Masquelin, P. Wyatt, P. Ray, and V. Dartois. "Prediction of drug penetration in tuberculosis lesions. *ACS Infect Dis* 2: 552–563." (2016).
148. Richter, Elvira, Sabine Rüsç-Gerdes, and Doris Hillemann. "Drug-susceptibility testing in TB: current status and future prospects." *Expert Review of Respiratory Medicine* 3, no. 5 (2009): 497-510.

149. Rodrigues, Liliana, Diana Machado, Isabel Couto, Leonard Amaral, and Miguel Viveiros. "Contribution of efflux activity to isoniazid resistance in the Mycobacterium tuberculosis complex." *Infection, Genetics and Evolution* 12, no. 4 (2012): 695-700.
150. Zuniga, Edison S., Julie Early, and Tanya Parish. "The future for early-stage tuberculosis drug discovery." *Future microbiology* 10, no. 2 (2015): 217-229.
151. Muñoz-Elías, Ernesto J., and John D. McKinney. "Mycobacterium tuberculosis isocitrate lyases 1 and 2 are jointly required for in vivo growth and virulence." *Nature medicine* 11, no. 6 (2005): 638-644.
152. Pandey, Amit K., and Christopher M. Sassetti. "Mycobacterial persistence requires the utilization of host cholesterol." *Proceedings of the National Academy of Sciences* 105, no. 11 (2008): 4376-4380.
153. Marrero, Joeli, Carolina Trujillo, Kyu Y. Rhee, and Sabine Ehrh. "Glucose phosphorylation is required for Mycobacterium tuberculosis persistence in mice." *PLoS pathogens* 9, no. 1 (2013): e1003116.
154. Muñoz-Elías, Ernesto J., Anna M. Upton, Joseph Cherian, and John D. McKinney. "Role of the methylcitrate cycle in Mycobacterium tuberculosis metabolism, intracellular growth, and virulence." *Molecular microbiology* 60, no. 5 (2006): 1109-1122.
155. Muñoz-Elías, Ernesto J., and John D. McKinney. "Carbon metabolism of intracellular bacteria." *Cellular microbiology* 8, no. 1 (2006): 10-22.
156. Marrero, Joeli, Kyu Y. Rhee, Dirk Schnappinger, Kevin Pethe, and Sabine Ehrh. "Gluconeogenic carbon flow of tricarboxylic acid cycle intermediates is critical for Mycobacterium tuberculosis to establish and maintain infection." *Proceedings of the National Academy of Sciences* 107, no. 21 (2010): 9819-9824.
157. Ollinger, Juliane, Anuradha Kumar, David M. Roberts, Mai A. Bailey, Allen Casey, and Tanya Parish. "A high-throughput whole cell screen to identify inhibitors of Mycobacterium tuberculosis." *PLoS One* 14, no. 1 (2019): e0205479.
158. Early, Julie V., Allen Casey, Maria Angeles Martinez-Grau, Isabel C. Gonzalez Valcarcel, Michal Vieth, Juliane Ollinger, Mai Ann Bailey et al. "Oxadiazoles have butyrate-specific conditional activity against Mycobacterium tuberculosis." *Antimicrobial agents and chemotherapy* 60, no. 6 (2016): 3608-3616.
159. VanderVen, Brian C., Ruth J. Fahey, Wonsik Lee, Yancheng Liu, Robert B. Abramovitch, Christine Memmott, Adam M. Crowe et al. "Novel inhibitors of cholesterol degradation in Mycobacterium tuberculosis reveal how the bacterium's metabolism is

- constrained by the intracellular environment." *PLoS pathogens* 11, no. 2 (2015): e1004679.
160. Betts, Joanna C., Pauline T. Lukey, Linda C. Robb, Ruth A. McAdam, and Ken Duncan. "Evaluation of a nutrient starvation model of Mycobacterium tuberculosis persistence by gene and protein expression profiling." *Molecular microbiology* 43, no. 3 (2002): 717-731.
161. Loebel, R. O., E. Shorr, and H. B. Richardson. "The influence of foodstuffs upon the respiratory metabolism and growth of human tubercle bacilli." *Journal of bacteriology* 26, no. 2 (1933): 139-166.
162. Nyka, W. "Studies on the effect of starvation on mycobacteria." *Infection and immunity* 9, no. 5 (1974): 843-850.
163. Grant, Sarah Schmidt, Tomohiko Kawate, Partha P. Nag, Melanie R. Silvis, Katherine Gordon, Sarah A. Stanley, Edward Kazyskaya et al. "Identification of novel inhibitors of nonreplicating Mycobacterium tuberculosis using a carbon starvation model." *ACS chemical biology* 8, no. 10 (2013): 2224-2234.
164. Smeulders, Marjan J., Jacquie Keer, Richard A. Speight, and Huw D. Williams. "Adaptation of Mycobacterium smegmatis to stationary phase." *Journal of bacteriology* 181, no. 1 (1999): 270-283.
165. Wayne, Lawrence G., and Ladonna G. Hayes. "An in vitro model for sequential study of shiftdown of Mycobacterium tuberculosis through two stages of nonreplicating persistence." *Infection and immunity* 64, no. 6 (1996): 2062-2069.
166. Wayne, Lawrence G., and Hilda A. Sramek. "Metronidazole is bactericidal to dormant cells of Mycobacterium tuberculosis." *Antimicrobial agents and chemotherapy* 38, no. 9 (1994): 2054-2058.
167. Cho, Sang Hyun, Saradee Warit, Baojie Wan, Chang Hwa Hwang, Guido F. Pauli, and Scott G. Franzblau. "Low-oxygen-recovery assay for high-throughput screening of compounds against nonreplicating Mycobacterium tuberculosis." *Antimicrobial agents and chemotherapy* 51, no. 4 (2007): 1380-1385.
168. Yeware, Amar, and Dhiman Sarkar. "Novel red fluorescence protein based microplate assay for drug screening against dormant Mycobacterium tuberculosis by using paraffin." *Tuberculosis* 110 (2018): 15-19.

169. Wayne, Lawrence G. "In vitro model of hypoxically induced nonreplicating persistence of *Mycobacterium tuberculosis*." *In Mycobacterium tuberculosis protocols*, pp. 247-269. Humana Press, 2001.
170. Aguilar-Ayala, Diana Angelica, Margo Cnockaert, Peter Vandamme, Juan Carlos Palomino, Anandi Martin, and Jorge Gonzalez-Y-Merchand. "Antimicrobial activity against *Mycobacterium tuberculosis* under in vitro lipid-rich dormancy conditions." *Journal of medical microbiology* 67, no. 3 (2018): 282-285.
171. Early, Julie V., Steven Mullen, and Tanya Parish. "A rapid, low pH, nutrient stress, assay to determine the bactericidal activity of compounds against non-replicating *Mycobacterium tuberculosis*." *PLoS One* 14, no. 10 (2019): e0222970.
172. Darby, Crystal M., Helgi I. Ingólfsson, Xiuju Jiang, Chun Shen, Mingna Sun, Nan Zhao, Kristin Burns et al. "Whole cell screen for inhibitors of pH homeostasis in *Mycobacterium tuberculosis*." *PloS one* 8, no. 7 (2013): e68942.
173. Early, Julie, Juliane Ollinger, Crystal Darby, Torey Alling, Steven Mullen, Allen Casey, Ben Gold et al. "Identification of compounds with pH-dependent bactericidal activity against *Mycobacterium tuberculosis*." *ACS infectious diseases* 5, no. 2 (2018): 272-280.
174. Campos-Neto, Antonio. "Mycobacterium tuberculosis strain 18b, a useful non-virulent streptomycin dependent mutant to study latent tuberculosis as well as for in vivo and in vitro testing of anti-tuberculosis drugs." *Tuberculosis (Edinburgh, Scotland)* 99 (2016): 54-55.
175. Sala, Claudia, Neeraj Dhar, Ruben C. Hartkoorn, Ming Zhang, Young Hwan Ha, Patricia Schneider, and Stewart T. Cole. "Simple model for testing drugs against nonreplicating *Mycobacterium tuberculosis*." *Antimicrobial agents and chemotherapy* 54, no. 10 (2010): 4150-4158.
176. Deb, Chirajyoti, Chang-Muk Lee, Vinod S. Dubey, Jaiyanth Daniel, Bassam Abomoelak, Tatiana D. Sirakova, Santosh Pawar, Linda Rogers, and Pappachan E. Kolattukudy. "A novel in vitro multiple-stress dormancy model for *Mycobacterium tuberculosis* generates a lipid-loaded, drug-tolerant, dormant pathogen." *PloS one* 4, no. 6 (2009): e6077.
177. Gold, Ben, Thulasi Warriar, and Carl Nathan. "A multi-stress model for high throughput screening against non-replicating *Mycobacterium tuberculosis*." *In Mycobacteria protocols*, pp. 293-315. Humana Press, New York, NY, 2015.

178. Gold, Ben, Julia Roberts, Yan Ling, Landys Lopez Quezada, Jou Glasheen, Elaine Ballinger, Selin Somersan-Karakaya, Thulasi Warriar, and Carl Nathan. "Visualization of the charcoal agar resazurin assay for semi-quantitative, medium-throughput enumeration of mycobacteria." *JoVE (Journal of Visualized Experiments)* 118 (2016): e54690.
179. Gold, Ben, Julia Roberts, Yan Ling, Landys Lopez Quezada, Jou Glasheen, Elaine Ballinger, Selin Somersan-Karakaya, Thulasi Warriar, J. David Warren, and Carl Nathan. "Rapid, semiquantitative assay to discriminate among compounds with activity against replicating or nonreplicating *Mycobacterium tuberculosis*." *Antimicrobial agents and chemotherapy* 59, no. 10 (2015): 6521-6538.
180. Hu, Yanmin, Alexander Liu, Fatima Ortega-Muro, Laura Alameda-Martin, Denis Mitchison, and Anthony Coates. "High-dose rifampicin kills persisters, shortens treatment duration, and reduces relapse rate in vitro and in vivo." *Frontiers in microbiology* 6 (2015): 641.
181. Agrawal, Sonia, Suwarna Gample, Amar Yeware, and Dhiman Sarkar. "Novel gene similar to nitrite reductase (NO forming) plays potentially important role in the latency of tuberculosis." *Scientific reports* 11, no. 1 (2021): 1-13.
182. Manning, Alyssa J., Yulia Ovechkina, Amanda McGillivray, Lindsay Flint, David M. Roberts, and Tanya Parish. "A high content microscopy assay to determine drug activity against intracellular *Mycobacterium tuberculosis*." *Methods* 127 (2017): 3-11.
183. Christophe, Thierry, Mary Jackson, Hee Kyoung Jeon, Denis Fenistein, Monica Contreras-Dominguez, Jaeseung Kim, Auguste Genovesio et al. "High content screening identifies decaprenyl-phosphoribose 2' epimerase as a target for intracellular antimycobacterial inhibitors." *PLoS pathogens* 5, no. 10 (2009): e1000645.
184. Stanley, Sarah A., Sarah Schmidt Grant, Tomohiko Kawate, Noriaki Iwase, Motohisa Shimizu, Carl Wivagg, Melanie Silvis et al. "Identification of novel inhibitors of *M. tuberculosis* growth using whole cell based high-throughput screening." *ACS chemical biology* 7, no. 8 (2012): 1377-1384.
185. Sorrentino, Flavia, Ruben Gonzalez del Rio, Xingji Zheng, Jesus Presa Matilla, Pedro Torres Gomez, Maria Martinez Hoyos, Maria Esther Perez Herran, Alfonso Mendoza Losana, and Yossef Av-Gay. "Development of an intracellular screen for new compounds able to inhibit *Mycobacterium tuberculosis* growth in human macrophages." *Antimicrobial agents and chemotherapy* 60, no. 1 (2016): 640-645.

186. Zheng, Xingji, and Yossef Av-Gay. "System for efficacy and cytotoxicity screening of inhibitors targeting intracellular Mycobacterium tuberculosis." *JoVE (Journal of Visualized Experiments)* 122 (2017): e55273.
187. Larsson, Marie C., Maria Lerm, Kristian Ängeby, Michaela Nordvall, Pontus Juréen, and Thomas Schön. "A luciferase-based assay for rapid assessment of drug activity against Mycobacterium tuberculosis including monitoring of macrophage viability." *Journal of microbiological methods* 106 (2014): 146-150.
188. Sarkar, Sampa, and Dhiman Sarkar. "Potential use of nitrate reductase as a biomarker for the identification of active and dormant inhibitors of Mycobacterium tuberculosis in a THP1 infection model." *Journal of Biomolecular Screening* 17, no. 7 (2012): 966-973.
189. Taneja, Neetu Kumra, Sakshi Dhingra, Aditya Mittal, Mohit Naresh, and Jaya Sivaswami Tyagi. "Mycobacterium tuberculosis transcriptional adaptation, growth arrest and dormancy phenotype development is triggered by vitamin C." *PloS one* 5, no. 5 (2010): e10860.
190. Sikri, Kriti, Priyanka Duggal, Chanchal Kumar, Sakshi Dhingra Batra, Atul Vashist, Ashima Bhaskar, Kritika Tripathi, Tavpritesh Sethi, Amit Singh, and Jaya Sivaswami Tyagi. "Multifaceted remodeling by vitamin C boosts sensitivity of Mycobacterium tuberculosis subpopulations to combination treatment by anti-tubercular drugs." *Redox biology* 15 (2018): 452-466.
191. McCune, Robert M., Floyd M. Feldmann, and Walsh McDermott. "Microbial persistence: II. Characteristics of the sterile state of tubercle bacilli." *The Journal of experimental medicine* 123, no. 3 (1966): 469-486.
192. Saunders, Bernadette M., and Warwick J. Britton. "Life and death in the granuloma: immunopathology of tuberculosis." *Immunology and cell biology* 85, no. 2 (2007): 103-111.
193. Zhang, Ying. "Persistent and dormant tubercle bacilli and latent tuberculosis." *Front Biosci* 9, no. 1 (2004): 1136-56.
194. Sugawara, Isamu, Hiroyuki Yamada, and Satoru Mizuno. "Pathological and immunological profiles of rat tuberculosis." *International journal of experimental pathology* 85, no. 3 (2004): 125-134.
195. Orme, Ianm. "A Mouse Model of the Recrudescence of Latent Tuberculosis in the Elderly1-3." *Age* 18, no. 22 (1988): 24.

196. Sever, John L., and Guy P. Youmans. "Enumeration of viable tubercle bacilli from the organs of nonimmunized and immunized mice." *American Review of Tuberculosis and Pulmonary Diseases* 76, no. 4 (1957): 616-635.
197. Stead, William W., Gerald R. Kerby, Donald P. Schlueter, And Clarence W. Jordahl. "The clinical spectrum of primary tuberculosis in adults: confusion with reinfection in the pathogenesis of chronic tuberculosis." *Annals of internal medicine* 68, no. 4 (1968): 731-745.
198. Smith, D. W., V. Balasubramanian, and E. Wiegshauss. "A guinea pig model of experimental airborne tuberculosis for evaluation of the response to chemotherapy: the effect on bacilli in the initial phase of treatment." *Tubercle* 72, no. 3 (1991): 223-231.
199. Bouz, Ghada, and Nada Al Hasawi. "The zebrafish model of tuberculosis-no lungs needed." *Critical reviews in microbiology* 44, no. 6 (2018): 779-792.
200. Ginsberg, A. "The TB Alliance: overcoming challenges to chart the future course of TB drug development. *Future Med Chem* 3: 1247–1252." (2011).
201. Gardner, Charles A., Tara Acharya, and Ariel Pablos-Méndez. "The global alliance for tuberculosis drug development—accomplishments and future directions." *Clinics in chest medicine* 26, no. 2 (2005): 341-347.
202. Global Alliance for TB Drug Development. Overview of the TB Alliance program. Available at: <http://www.tballiance.org>. Accessed March 4, 2005
203. Sterling, Timothy R., Gibril Njie, Dominik Zenner, David L. Cohn, Randall Reves, Amina Ahmed, Dick Menzies et al. "Guidelines for the treatment of latent tuberculosis infection: recommendations from the National Tuberculosis Controllers Association and CDC, 2020." *American Journal of Transplantation* 20, no. 4 (2020): 1196-1206.
204. Conradie, Francesca, Andreas H. Diacon, Nosipho Ngubane, Pauline Howell, Daniel Everitt, Angela M. Crook, Carl M. Mendel et al. "Treatment of highly drug-resistant pulmonary tuberculosis." *New England Journal of Medicine* 382, no. 10 (2020): 893-902.
205. World Health Organization. WHO consolidated guidelines on drug-resistant tuberculosis treatment. No. WHO/CDS/TB/2019.7. *World Health Organization*, 2019.
206. Perveen, Summaya, Diksha Kumari, Kuljit Singh, and Rashmi Sharma. "Tuberculosis drug discovery: Progression and future interventions in the wake of emerging resistance." *European Journal of Medicinal Chemistry* (2021): 114066.
207. J Sloan, Derek, Geraint R Davies, and Saye H Khoo. "New drugs and treatment regimens." *Current respiratory medicine reviews* 9, no. 3 (2013): 200-210.

208. Shetye, Gauri S., Scott G. Franzblau, and Sanghyun Cho. "New tuberculosis drug targets, their inhibitors, and potential therapeutic impact." *Translational Research* 220 (2020): 68-97.
209. Yuan, Tianao, and Nicole S. Sampson. "Hit generation in TB drug discovery: from genome to granuloma." *Chemical reviews* 118, no. 4 (2018): 1887-1916.
210. Harvey, Alan L., RuAngelie Edrada-Ebel, and Ronald J. Quinn. "The re-emergence of natural products for drug discovery in the genomics era." *Nature reviews drug discovery* 14, no. 2 (2015): 111-129.

Chapter 2

Screening of novel small molecule inhibitors against active and dormant stage of Mycobacterium tuberculosis

2.1. Introduction:

Tuberculosis (TB) is a significant health hazard and a leading cause of death from a single infection. Around 10 million people got infected, and around 1.4 million deaths were reported in 2019 [1]. WHO recommended DOTS therapy (Directly observed treatment, short-course), which includes a six-month drug regime of first-line drugs (isoniazid, rifampicin, pyrazinamide, and ethambutol) for treatment of TB [2,3]. Although the recommended drugs are highly effective, due to prolonged treatment duration, non-adherence of patients to the prescribed regimen, high cost, and adaptive nature of *Mycobacterium tuberculosis* (Mtb), the eradication of TB is a remote possibility. For centuries, TB has emerged as a vital cause of ill health and the prime cause of death due to a single infectious agent after HIV/AIDS. Although in the last decade, various newly discovered leads have been developed [4,5]. However, it took almost five decades to successfully approve three drugs: bedaquiline, delamanid, and pretomanid [6]. New strains of the extensively drug-resistant (XDR) and multidrug-resistant (MDR) are resistant to the existing drugs and have further aggravated the situation [1]. Drugs having a broader and often unexpected range of biological activity may cause adverse effects, rendering their usage unsuitable for treatment. Therefore, there is a burning demand for a new class of anti-mycobacterial agents with a different mode of action which further led chemists to explore a wide range of chemical structures. Our present investigation has been addressed to find new chemical entities with effective anti-tubercular and anti-bacterial activity.

The main problems in antitubercular discovery are the existence of Mtb in heterogeneous populations in the human host (i.e., active and dormant stages of growth) and the lack of an effective drug screening method that can identify the potential candidates amongst the synthesized derivatives [7]. There is currently no single model that can adequately mimic the in-vivo situations in which Mtb is present in TB patients due to the complexity and variability of Mtb infection. Furthermore, there is no "standard" screening technique for generating hit compounds to develop anti-TB drugs. Hence, simple in-vitro tests that may quickly identify effective compounds and predict in-vivo activity in humans are needed to create novel medications. To address this problem, our lab has developed some in-vitro screening methods such as XTT reduction menadione assay (XRMA) [8], a whole cell-based high-throughput screening protocol [9], a protocol based on high-throughput screening on the biosynthetic activity of Mtb glutamine synthetase [10], and novel red fluorescence protein-based microplate-based assay [11] for drug screening against active and

dormant stage of Mtb. Some of the research groups working in the TB area have synthesized some molecules/compounds and are interested in checking their activity against different stages of Mtb.

In the present study, we have evaluated the biological potential of different categories of a small number of synthesized chemical and natural derivatives to find new chemical entities with effective anti-tubercular and anti-bacterial activity. Natural compounds include biosurfactants (BS) and derivatives of podocarflavone A, while chemical compounds include phenanthridine-trione-epoxide conjugates, pyrazole derivatives of 5-Chloro-2-Methoxy Phenyl Hydrazide, and pyrazole scaffolds hybrid with 1,4-dihydropyridine and 4-hydroxy coumarin are evaluated for their biological potential using established in-vitro screening methods in our lab (as discussed above). We performed in-vitro screening of these compounds against active and dormant stages of Mtb. The same molecules were further evaluated to check the specificity by in-vitro screening method against different bacteria.

2.2. Results

2.2.1. Biological evaluation of Biosurfactant

Table 1. Antitubercular activity

Compound Code	MIC (μM)
BS	286.8 \pm 3
Rifampicin	0.048 \pm 0.012

Table 2. Antibacterial activity

Compound Code	Anti-bacterial activity			
	<i>Staphylococcus aureus</i>	<i>Bacillus subtilis</i>	<i>Escherichia coli</i>	<i>Pseudomonas aeruginosa</i>
	MIC (μM)	MIC (μM)	MIC (μM)	MIC (μM)
BS	>300	>300	>300	>300
Ampicillin	11.47 \pm 0.71	24.41 \pm 0.37	9.95 \pm 2.57	20.77 \pm 1.54
Kanamycin	19.11 \pm 1.58	12.32 \pm 1.30	8.29 \pm 1.94	5.90 \pm 0.20

Table 3. Cytotoxic activity of biosurfactant

Cell Line	GI ₅₀ (μ M)	PTX Standard (μ M)
MCF-7	76.33 \pm 10.83	0.001 \pm 0.003
HeLa	73.86 \pm 7.51	0.007 \pm 0.01
HCT	55.71 \pm 9.06	1.97 \pm 0.21

2.2.2. Biological evaluation of Podocarflavone A and its analogs against *Mycobacterium tuberculosis*

Table 4. Antitubercular activity

Compound Code	IC ₅₀ (μ M)	MIC (μ M)
7a	175.90	>300
8a	60.11	>300
7b	104.80	227.99
8b	71.55	>300
7c	89.56	>300
8c	61.77	>300
7d	133.09	>300
8d	36.47	231.29
7e	66.50	188.97
8e	45.38	>300
Rifampicin	-	0.042
Isoniazid	-	0.077

Table 5. Antibacterial activity

Compound Code	Gram +ve Bacteria				Gram -ve Bacteria			
	<i>S.aureus</i>		<i>B.subtilis</i>		<i>E.coli</i>		<i>Ps.aeruginosa</i>	
	(μ M)		(μ M)		(μ M)		(μ M)	
	IC ₅₀	MIC	IC ₅₀	MIC	IC ₅₀	MIC	IC ₅₀	MIC
7a	>300	>300	>300	>300	>300	>300	>300	>300
8a	114.49	>300	109.09	>300	>300	>300	>300	>300
7b	>300	>300	>300	>300	>300	>300	>300	>300
8b	>300	>300	>300	>300	>300	>300	>300	>300

7c	>300	>300	>300	>300	>300	>300	>300	>300
8c	>300	>300	>300	>300	>300	>300	>300	>300
7d	>300	>300	>300	>300	>300	>300	>300	>300
8d	57.98	220.80	64.83	155.67	>300	>300	>300	>300
7e	>300	>300	>300	>300	>300	>300	>300	>300
8e	198.54	>300	>300	>300	>300	>300	>300	>300
Ampicillin	-	3.63	-	28.41	-	8.04	-	15.19
Kanamycin	-	19.98	-	5.42	-	6.06	-	5.20

2.2.3. Biological evaluation of Phenanthridin-trione-epoxide conjugates against *Mycobacterium tuberculosis*

Table 6. Anti-tubercular activity

Compo und Code	Active Stage Mtb		Dormant Stage Mtb		Compo und Code	Active Stage Mtb		Dormant Stage Mtb	
	MIC	IC ₅₀	MIC	IC ₅₀		MIC	IC ₅₀	MIC	IC ₅₀
	(μ M)	(μ M)	(μ M)	(μ M)		(μ M)	(μ M)	(μ M)	(μ M)
RM 33	>100	>100	>100	>100	RM68	>100	>100	>100	>100
RM 49	>100	>100	>100	>100	RM 71	>100	>100	>100	>100
RM 58	23.5\pm 0.95	1.86\pm 0.27	24.18\pm 0.47	6.98\pm 0.63	RM 73	15.27\pm 4.27	3.19\pm 0.27	21.4\pm 0.66	6.33 \pm 0.01
RM 59	>100	>100	>100	>100	RM 74	>100	>100	>100	>100
RM 60	4.78\pm 0.75	1.15\pm 0.27	18.38\pm 0.24	2.45\pm 0.24	RM 75	5.79\pm 0.58	1.71\pm 0.23	21.10 \pm0.79	2.07 \pm 0.16
RM 61	5.33\pm 1.24	1.47\pm 0.07	21.51\pm 0.63	2.70\pm 0.060	Rifampicin	0.0071 \pm 0.003	-	0.056 \pm 0.06 8	-
RM 65	18.6\pm 1.25	4.64\pm 0.11	32.56\pm 0.94	5.02\pm 0.51	Isoniazid	1.96 \pm 0.029	-	0.53 \pm 0.021	-
RM 67	>100	>100	>100	>100	-	-	-	-	-

Table 7. Antibacterial activity

Compound Code	Gram-positive bacteria				Gram-negative bacteria			
	<i>S.aureus</i>		<i>B.subtillis</i>		<i>E.coli</i>		<i>Ps. aeruginosa</i>	
	(μ M)		(μ M)		(μ M)		(μ M)	
	MIC	IC ₅₀	MIC	IC ₅₀	MIC	IC ₅₀	MIC	IC ₅₀
RM 33	>100	>100	>100	>100	>100	>100	>100	>100
RM 49	>100	>100	>100	>100	>100	>100	>100	>100
RM 58	>100	>100	>100	>100	>100	>100	>100	>100
RM 59	>100	>100	>100	>100	>100	>100	>100	>100
RM 60	60.81±0.94	19.24±1.21	67.34±11.91	17.92±1.28	>100	>100	>100	>100
RM 61	69.97±1.56	23.41±1.35	>100	21.88±4.18	>100	>100	>100	>100
RM 65	>100	32.25±2.42	>100	30.61±2.23	>100	>100	>100	>100
RM 67	>100	>100	>100	>100	>100	>100	>100	>100
RM 68	>100	>100	>100	>100	>100	>100	>100	>100
RM 71	>100	>100	>100	>100	>100	>100	>100	>100
RM 73	>100	63.94±3.12	>100	42.88±0.53	>100	>100	>100	>100
RM 74	>100	>100	>100	>100	>100	>100	>100	>100
RM 75	66.89±1.12	20.09±0.63	64.91±1.41	20.30±0.54	>100	>100	>100	>100
Ampicillin	-	11.47±2.11	-	24.41±0.37	9.96±2.57	-	20.77±1.54	-
Kanamycin	-	19.11±1.59	-	12.32±1.30	8.29±1.94	-	5.90±0.20	-

2.2.4. Biological evaluation of Pyrazole derivatives of 5-Chloro-2-Methoxy Phenyl Hydrazide

Table 8. Anti-tubercular activity

Percent inhibition of active and dormant state of *M. tuberculosis* in the presence of a compound at a single concentration (30 μ g/ml)

Sr. No.	Compound Code	(Dormant State)	(Active State)	Sr. No.	Compound Code	(Dormant State)	(Active State)
		% Inhibition	% Inhibition			% Inhibition	% Inhibition
		Avg	Avg			Avg	Avg

1	1a	12.96± 3.22	10.56±10.41	8	2d	22.90±0.74	80.77± 1.37
2	1b	30.21± 12.71	18.95±5.78	9	2e	14.37±2.61	10.07± 9.57
3	1c	17.55± 3.69	28.63±6.90	10	2f	40.21±4.23	55.70± 4.50
4	1d	21.06± 9.10	-1.32±7.33	11	2g	42.01±0.24	45.56± 0.71
5	2a	5.42± 10.00	-1.62±4.00	12	2j	33.02±1.72	79.54± 3.79
6	2b	34.05± 5.37	20.47±5.78	13	2i	1.82±11.33	-2.24± 4.71
7	2c	10.70± 8.09	28.36±12.60	-	-	-	-

Table 9. Secondary screening of selected compounds for anti-tubercular activity

Compound Code	(Dormant State) μM		(Active State) μM	
	IC ₅₀	MIC	IC ₅₀	MIC
2d	>10	>10	0.512	>10
2f	>10	>10	>10	>10
2j	>10	>10	>10	>10
Rifampicin	-	0.053	-	0.042
Isoniazid	-	0.089	-	0.077

Table 10. Antibacterial activity

The preliminary anti-bacterial activity of compounds against a Gram-positive and Gram-negative bacterium at a single concentration (30 μg/ml)

Sr. No.	Compound Code	Anti-microbial activity			
		Gram-positive bacteria		Gram-negative bacteria	
		% GI <i>Staphylococcus aureus</i>	% GI <i>Bacillus subtilis</i>	% GI <i>Pseudomonas aeruginosa</i>	% GI <i>Escherichia coli</i>
1	1a	11.05	24.18	-22.24	0.32
2	1b	7.67	51.99	-19.18	21.14
3	1c	17.19	-56.91	-21.88	-4.31
4	1d	0.82	53.14	-29.70	-17.81
5	2a	0.75	41.72	-12.42	23.16
6	2b	-1.35	38.44	-5.29	-8.13
7	2c	5.37	35.55	-16.04	14.42
8	2d	10.84	-5.55	-18.31	14.12
9	2e	5.59	43.80	-24.83	1.32

10	2f	4.94	49.59	-20.92	-16.66
11	2g	15.64	16.15	-24.63	0.79
12	2j	6.32	18.50	-39.63	2.60
13	2i	3.67	45.77	-10.10	-16.23

2.2.5. Biological evaluation of pyrazole scaffolds hybrid with 1,4-dihydropyridine and 4-hydroxy coumarin

Table 11. Anti-tubercular activity

Primary screening of synthesized compounds was done at 30 µg/ml for anti-tubercular activity against active and dormant stages of Mtb

Compound Code	(Dormant State Mtb) % Inhibition	(Active State Mtb) % Inhibition	Compound Code	(Dormant State Mtb) % Inhibition	(Active State Mtb) % Inhibition
	Avg	Avg		Avg	Avg
4a	45.91±2.08	31.091±3.14	4l	33.361±3.92	8.461±3.23
4b	60.461±6.34	21.711±1.72	4m	26.161±1.52	14.091±5.15
4c	45.431±1.16	35.361±3.65	4n	31.991±8.39	25.151±1.3
4d	62.741±10.12	47.781±7.39	4o	36.361±6.18	19.951±2.02
4e	30.021±11.08	32.941±4.25	6a	28.99±2.40	26.85±5.02
4f	71.731±0.36	44.451±6.17	6c	31.38±4.11	29.87±5.26
4g	65.551±0.54	11.851±7.55	6e	22.06±1.70	32.48±5.52
4h	46.191±1.54	24.641±8.07	6f	31.79±7.15	19.11±2.92
4i	70.551±0.41	53.731±18.36	6g	86.72±0.17	81.39±13.22
4j	28.691±3.98	34.51±3.53	6h	83.24±6.57	75.69±10.41
4k	63.841±0.6	36.791±11.95	-	-	-

Table 12. Secondary screening of selected compounds for anti-tubercular activity against active and dormant stages of *Mycobacterium tuberculosis*

Compound Code	(Dormant State Mtb) µM		(Active State Mtb) µM	
	IC ₅₀	MIC	IC ₅₀	MIC
4b	>10	>10	>10	>10
4d	>10	>10	>10	>10
4f	>10	>10	>10	>10
4g	>10	>10	>10	>10
4i	>10	>10	>10	>10
4k	>10	>10	>10	>10

6g	9.54	>10	3.86	5.24
6h	0.50	>10	3.60	5.03
Rifampicin	-	0.069	-	0.053

Table 13. The preliminary anti-bacterial activity of compounds against a Gram-positive and Gram-negative bacterium at a single concentration (30 µg/ml)

Compound Code	Anti-microbial activity			
	% GI <i>Pseudomonas aeruginosa</i>	% GI <i>Staphylococcus aureus</i>	% GI <i>Bacillus subtilis</i>	% GI <i>E.coli</i>
4a	-42.39	13.49	49.71	24.45
4b	-58.65	-7.71	-49.82	-2.01
4c	-53.55	11.2	41.83	38.5
4d	-7.31	12.73	-53.31	15.17
4e	3.1	6.49	-96.28	9.53
4f	-35.89	13.08	-27.04	11.18
4g	-58.64	15.09	-1.75	11.87
4h	-48.67	9.28	30.18	14.16
4i	-57.05	12.66	-50.89	4.35
4j	-10.7	-4.94	-12.53	7.33
4k	-46.78	12.39	15.44	-6.27
4l	-27.1	1.8	-26.64	24.88
4m	-1.32	2.17	-71.22	13.18
4n	-9.3	0.02	-40.59	24.96
4o	-35.19	6.13	-60.66	21.24
6a	-52.25	6.28	-10.9	-2.32
6c	-52.18	4.96	-46.12	18.97
6e	-65.97	97.73	-18.91	40.45
6f	-41.93	6.76	-79.11	-16.28
6g	-57.64	99.44	99.07	9.99
6h	-33.19	99.38	41.23	41.98

2.3. Discussion

Drug discovery and development in TB are still challenging due to the shortage of predictive animal models, multiple physiological states, and an organism's slow growth rate. Therefore, it is mandatory to broaden the target areas to discover the drugs with a new mode of action [12,13]. Initially, the present study was carried out to identify new small molecule inhibitors/compounds for their anti-tubercular activity. The inhibitors were further screened

for their anti-bacterial activity to ensure their specificity. In the first section, we have explored one of the possibilities in the drug regimen using BS produced by *P. maritimus*. The in-vitro XRMA activity of BS was confirmed against Mtb, wherein; it was agreed that the current anti-tubercular activity is reporting a higher MIC at $286.8 \pm 3 \mu\text{M}$ ($160.8 \pm 1.64 \mu\text{g/ml}$) concentration as compared with the standard drug Rifampicin exhibited $0.04 \mu\text{g/ml}$ or $0.048 \pm 0.012 \mu\text{M}$. However, it is important to note that the standard or reference drugs have undergone extensive research and chemical modifications, e.g., Rifampicin is chemically derived from natural product Rifamycins initially isolated from *Streptomyces mediterani* in 1957 [14,15]. The early members of the family are undesirable for therapeutic applications due to poor potency, solubility, bioavailability, and short half-life compared with the current advanced stage of Rifampicin. So, as per our study, the higher MIC may be reduced by future developments through chemical modifications in natural products or making synthetic derivatives of it. Further study is required in this area.

Further, to ensure specificity of BS, tested against *Escherichia coli*, *Pseudomonas aeruginosa*, *Staphylococcus aureus*, and *Bacillus subtilis* and found no significant inhibition up to $100 \mu\text{g/ml}$ concentration. The cytotoxic effect of BS derived from marine microbes has been reported earlier [16], but the terpene containing BS has not yet been previously acknowledged. In this work, we report the cytotoxic activity of terpene containing BS of Planococcus and displayed significant cytotoxicity against MCF-7 ($\text{GI}_{50} 78.29 \mu\text{M} \pm 10.97 \mu\text{M}$), HeLa ($\text{GI}_{50} 75.75 \mu\text{M} \pm 7.70 \mu\text{M}$) and HCT ($\text{GI}_{50} 57.13 \mu\text{M} \pm 9.14 \mu\text{M}$) cell lines. This is the first report on BS produced by *P. maritimus* for its anti-tubercular agent, to the best of our knowledge. Such natural compounds have been explored for positive synergistic results of the existing anti-tubercular agents.

The effects of Podocarflavone A on Mtb have not been reported to date. The present study investigated this for the first time. We examined the effects of Podocarflavone A and its analogs by in-vitro anti-tubercular screening. From our preliminary studies, Compounds **8a**, **8d**, and **8e** against *M. tuberculosis* using XRMA protocol exhibited promising antimycobacterial activity with significant IC_{50} values, confirming the drug likeliness properties against Mtb. Compounds **8a**, **8d**, and **8e** showed antibacterial activity with considerable IC_{50} against the *Staphylococcus aureus*; Compounds **8a** and **8d** showed inhibition against *Bacillus subtilis*, exploring the specificity against Gram-positive bacterial strains.

The preliminary in-vitro antitubercular screening results warrant Phenanthridin-trione-epoxide conjugates as highly potent antitubercular agents. In light of these findings, antitubercular activity can be enhanced by opting appropriate substitution of 1,10 Phenanthroline and propargyl bromide in its structure. Compound **RM58**, **RM60**, **RM61**, **RM65**, **RM73**, and **RM75** showed a significant inhibitory effect (<30 μ M) against both active and dormant stages of Mtb. The same tested compounds such as **RM58**, **RM60**, **RM61**, **RM65**, **RM73**, and **RM75**, showed antibacterial activity with considerable IC_{50} against the *Staphylococcus aureus* and *Bacillus subtilis*, further exploring the specificity against Gram-positive bacterial strains.

While performing a biological evaluation of some pyrazole derivatives of 5-Chloro-2-Methoxy Phenyl Hydrazide, we have screened new series of (5-chloro-2-methoxyphenyl)(5-alkyl-3-(substituted)(phenyl/alkyl)-1H-pyrazol-1-yl) methanones with regio isomer B as a significant product using dimethylacetamide (DMAc) in an acidic medium. These compounds were screened for their antitubercular activity and antibacterial activity. The results showed that compounds **2d**, **2f**, and **2h** show good antitubercular activity in the active stage. In contrast, no significant activity in the dormant stage of Mtb. Further evaluation against gram-positive and gram-negative bacteria demonstrated no activity, suggesting that the compounds **2d**, **2f**, and **2h** are more specifically inhibiting the active stage of Mtb. Furthermore, compound **2d** exhibited significant antitubercular activity from the secondary analysis on the active stage of Mtb with IC_{50} of 0.512 μ M. These results encourage further screening and may be a good antitubercular candidate in the pyrazole class.

The biological evaluation of pyrazole scaffolds hybrid with 1,4-dihydropyridine and 4-hydroxy coumarin data suggested that 2 compounds, **6g** and **6h**, exhibited a significant inhibitory effect on both active and dormant stages of Mtb. In contrast, the compound **6g** showed significant inhibition against *Staphylococcus aureus* and *Bacillus subtilis*, further exploring the lead compound's specificity. These agents could perform better when combined as hybrid molecules in a synergistic combination. The probable mode of action and its antimycobacterial potential need further studies to explore these hybrid pyrazole molecules as a lead molecule against tuberculosis and antimicrobial agents.

In conclusion, this work explores the biological evaluation of different classes and the nature of compounds that can be explored further as drug targets for developing novel drugs against TB. The inhibitory potential of the candidate molecules identified in the present study effectively supports their antituberculosis properties and hence can be considered the

best candidates against Mtb. However, further efficacy studies are required to confirm the actual potential of these molecules for in-vivo clinical trials.

2.4. Materials and Methods:

2.4.1. Chemicals and materials

All the chemicals such as XTT, DMSO, rifampicin, isoniazid, and *M phlei* media components such as KH_2PO_4 , trisodium citrate, and MgSO_4 , asparagine, and glycerol were purchased from Sigma Aldrich, USA. Dubos medium was purchased from DIFCO, USA. Stock solutions (10mg/ml) of all the newly synthesized compounds were freshly prepared in DMSO (Sigma Aldrich) and used on the same day after mixing.

2.4.2. Organism/ cell line and media used

M. tuberculosis H37Ra (ATCC 25177), obtained from the Microbial Type Culture Collection (MTCC; Chandigarh, India). MCF-7 (breast cancer cell line), HeLa (Human cervical cancer cell line), and HCT (colon cancer cell line) were obtained from the National Center for Cell Science (NCCS), Pune, India. Four bacterial strains (Gram-negative strains: *Escherichia coli* (NCIM 2065; ATCC 8739) and *Pseudomonas aeruginosa* (NCIM 5029; ATCC 27853); Gram-positive strains: *Staphylococcus aureus* (NCIM 2901; ATCC 29737) and *Bacillus subtilis* (NCIM 2920; ATCC 605) were procured from National Collection of Industrial Microorganisms (NCIM) NCL Pune and grown in Luria Bertani medium from High Media, India. The stock was maintained at $-70\text{ }^\circ\text{C}$ and sub-cultured once in a liquid Dubos broth with 5 % glycerol, and 10 % Albumin dextrose catalase (ADC) enrichment medium, incubated in a shaker incubator rotating at a speed of 150 rpm at $37\text{ }^\circ\text{C}$ till the logarithmic phase ($\text{OD}_{620} \sim 1.0$) was reached.

2.4.3. Cultivation of aerobic bacilli

For aerobic cultivation, bacterial cultures were grown in a defined *M. phlei* medium within a 100 ml flask under aerobic conditions in a shaker incubator (Thermo Electron Corporation Model 481) maintained with shaking conditions at 150 rpm and $37\text{ }^\circ\text{C}$ on an orbital shaker (Thermo Electron Model No.131 481; Thermo Electron Corp., Marietta, OH). Once the cultures reached OD_{620} of 1.0, 1 % of bacterial culture was used as inoculum to determine anti-tubercular activity.

2.4.4. Anti-tubercular activity

A) For In-vitro screening against active stage Mtb-

For anti-tubercular activity screening, stock solutions of all the synthesized compounds were freshly prepared in DMSO and evaluated for their in-vitro anti-tubercular activity against the active stage Mtb using an established microplate-based technique using tetrazolium salt 2,3-bis[2-methoxy-4-nitro-5-sulphophenyl]-2H-tetrazolium-5-carboxanilide (XTT) and menadione to determine the viability of Mtb [8]. Briefly, 2.5 μ L of the test solutions at different concentrations between 100-0 μ g/ml were added to 247.5 μ L of *M. phlei* medium containing bacilli and incubated for 8 days for the active stage at 37 °C to study the dose-response effect. Post incubation, an XRMA assay was performed. The plate was read on SpectraMax Plus 384, Molecular Devices, Inc., using a 470 nm filter against a blank prepared from cell-free wells. MIC and IC₅₀ values of the selected compound were calculated from their dose-response curves by using OriginPro 2019b software. The assay was carried out in triplicates, and the percentage inhibition was calculated using a similar formula as per the described method below in the calculation of percent inhibition. The data shown are representative of three independent experiments.

B) For In-vitro screening against dormant stage Mtb-

A modified approach previously published was used to obtain anaerobic bacilli in microplate format [8]. Once the Mtb culture reaches 1.0 OD, at this stage, in the *M. phlei* medium, Mycobacterium cells generally aggregated under aerobic conditions. The flask containing log phase cells was intermittently sonicated at 50 kHz for 2-5 minutes (unless all aggregates were appropriately dissolved) in a water bath sonicator before incubation in the presence of appropriate compound concentration for screening. These sonicated cells were utilized as an inoculant in the wells of a microplate. 250 μ L of culture with $\sim 10^5$ cells/ml was added to each well of 96 well plates that were kept at 0.5 HSR. By using a microplate sealer (Nunc Inc.), the air supply to the dormant Mtb culture in the microplate was stopped in aseptic conditions. After that, the plate was incubated at 37 °C in a CO₂ incubator for 12 days. Post incubation, an XRMA assay was performed as mentioned above (In-vitro screening against active stage Mtb). MIC and IC₅₀ values of the selected compound were calculated from their dose-response curves by using OriginPro 2019b software. The assay was carried out in triplicates, and the percentage inhibition was calculated using a similar formula as per the described

method below in the calculation of percent inhibition. The data shown are representative of three independent experiments.

2.4.5. Anti-bacterial activity

To determine specificity, we have used optical density-based measurements to assess bacterial growth inhibition for screening compounds for their anti-bacterial activity against Gram-positive and Gram-negative bacteria [17]. All the synthesized compounds were screened for their in-vitro anti-bacterial activity in 96-well plates against four bacterial strains (Gram-negative strains: *Escherichia coli* (NCIM 2065; ATCC 8739) and *Pseudomonas aeruginosa* (NCIM 5029; ATCC 27853); Gram-positive strains: *Staphylococcus aureus* (NCIM 2901; ATCC 29737) and *Bacillus subtilis* (NCIM 2920; ATCC 605). Once the cultures reached OD₆₂₀ of 1, 0.1 % of bacterial culture was used as inoculum to determine anti-bacterial activity. The synthesized compounds were screened to monitor the dose-response effect and incubated for 8 h at 37 °C. Post-incubation OD₆₂₀ was measured for both Gram-positive and Gram-negative bacteria. Here reference drugs in clinical use, Ampicillin, and Kanamycin served as standard. The data shown are representative of three independent experiments.

2.4.6. Cytotoxicity of the active molecules

The cytotoxicity compound was examined by examining their effect on the proliferation of MCF-7 (breast cancer cell line), HeLa (Human cervical cancer cell line), and HCT (colon cancer cell line) as per earlier described 3-(4,5-dimethylthiazol-2-yl)-2,5-diphenyl tetrazolium bromide (MTT) assay [18,19]. Briefly, growing cells from individual cell lines (1x10⁶ cells/ml) were used to monitor the dose-response effect of the inhibitors. DMSO was used as vehicle control. The 96 well-plates were then incubated for 72 h in the incubator (37 °C, 5% CO₂, 95% humidity) to adhere to the well bottom. After adding MTT dye solution (50 µg/ml) to each well, the plate was incubated for 1h in an incubator. 200 µL of isopropanol was added to each well and kept for 4 h to dissolve the formazan crystal. The read-out was taken after 72 h of incubation at 490nm. The GI₅₀ values of the selected compound were calculated from their dose-response curves by using OriginPro 2019b software. The assay was carried out in triplicates, and the percentage inhibition was calculated using a similar formula as per the described method below in the calculation of percent inhibition. The data shown are representative of three independent experiments.

2.4.7. Calculation of percent inhibition

The percentage inhibition was calculated using the following equation: percentage inhibition = [(Average absorbance of control- Average absorbance of the test sample)/ (Average absorbance of control - Average absorbance of blank)] X 100, where control denotes the medium with bacilli together with the vehicle, test denotes the medium with bacilli together with compound and blank denotes the cell-free medium.

2.5. References:

1. World Health Organization. "Global tuberculosis report 2020. Geneva: World Health Organization; 2020.232 p. License: CC BY-NC-SA 3.0 IGO."
2. Dye, Christopher, Geoffrey P. Garnett, Karen Sleeman, and Brian G. Williams. "Prospects for worldwide tuberculosis control under the WHO DOTS strategy." *The Lancet* 352, no. 9144 (1998): 1886-1891.
3. Dover, Lynn G., and Geoffrey D. Coxon. "Current status and research strategies in tuberculosis drug development: miniperspective." *Journal of medicinal Chemistry* 54, no. 18 (2011): 6157-6165.
4. Chauhan, Prem MS, Naresh Sunduru, and Moni Sharma. "Recent advances in the design and synthesis of heterocycles as anti-tubercular agents." *Future Medicinal Chemistry* 2, no. 9 (2010): 1469-1500.
5. Campaniço, André, Rui Moreira, and Francisca Lopes. "Drug discovery in tuberculosis. New drug targets and antimycobacterial agents." *European journal of medicinal chemistry* 150 (2018): 525-545.
6. Tiberi, S., M. Muñoz-Torrico, R. Duarte, M. Dalcolmo, L. D'Ambrosio, and G-B. Migliori. "New drugs and perspectives for new anti-tuberculosis regimens." *Pulmonology* 24, no. 2 (2018): 86-98.
7. Grzelak, Edyta M., Mary P. Choules, Wei Gao, Geping Cai, Baojie Wan, Yuehong Wang, James B. McAlpine et al. "Strategies in anti-Mycobacterium tuberculosis drug discovery based on phenotypic screening." *The Journal of antibiotics* 72, no. 10 (2019): 719-728.
8. Singh, Upasana, Shamim Akhtar, Abhishek Mishra, and Dhiman Sarkar. "A novel screening method based on menadione mediated rapid reduction of tetrazolium salt for testing of anti-mycobacterial agents." *Journal of microbiological methods* 84, no. 2 (2011): 202-207.

9. Khan, Arshad, and Dhiman Sarkar. "A simple whole cell-based high throughput screening protocol using Mycobacterium bovis BCG for inhibitors against dormant and active tubercle bacilli." *Journal of microbiological methods* 73, no. 1 (2008): 62-68.
10. Singh, Upasana, and Dhiman Sarkar. "Development of a simple high-throughput screening protocol based on biosynthetic activity of Mycobacterium tuberculosis glutamine synthetase for the identification of novel Inhibitors." *Journal of biomolecular screening* 11, no. 8 (2006): 1035-1042.
11. Yeware, Amar, and Dhiman Sarkar. "Novel red fluorescence protein based microplate assay for drug screening against dormant Mycobacterium tuberculosis by using paraffin." *Tuberculosis* 110 (2018): 15-19.
12. Koul, Anil, Eric Arnoult, Nacer Lounis, Jerome Guillemont, and Koen Andries. "The challenge of new drug discovery for tuberculosis." *Nature* 469, no. 7331 (2011): 483-490.
13. Rawat, Diwan S. "Antituberculosis drug research: a critical overview." *Medicinal research reviews* 33, no. 4 (2013): 693-764.
14. Sensi, P. "History of the development of rifampin." *Reviews of infectious diseases* 5, no. Supplement_3 (1983): S402-S406.
15. Bhowon, Minu Gupta, Sabina Jhaumeer Laulloo, and Henri Li Kam Wah. *Chemistry for a Clean and Healthy Planet*. Edited by Ponnadurai Ramasami. Springer, 2019.
16. Waters, Amanda L., Russell T. Hill, Allen R. Place, and Mark T. Hamann. "The expanding role of marine microbes in pharmaceutical development." *Current opinion in biotechnology* 21, no. 6 (2010): 780-786.
17. Campbell, Jennifer. "High-throughput assessment of bacterial growth inhibition by optical density measurements." *Current protocols in chemical biology* 2, no. 4 (2010): 195-208.
18. Nigam, Preeti, Shobha Waghmode, Michelle Louis, Shishanka Wangnoo, Pooja Chavan, and Dhiman Sarkar. "Graphene quantum dots conjugated albumin nanoparticles for targeted drug delivery and imaging of pancreatic cancer." *Journal of Materials Chemistry B* 2, no. 21 (2014): 3190-3195.
19. Molinari, Aurora, Alfonso Oliva, Claudia Ojeda, José M. Miguel del Corral, M. Angeles Castro, Carmen Cuevas, and Arturo San Feliciano. "Synthesis and Cytotoxic Evaluation of 6-(3-Pyrazolylpropyl) Derivatives of 1, 4-Naphthohydroquinone-1, 4-diacetate." *Archiv der Sagar Swami, Ph.D. Thesis, AcSIR, CSIR-NCL Pune-2022*

Pharmazie: *An International Journal Pharmaceutical and Medicinal Chemistry* 342, no. 10 (2009): 591-599.

Chapter 3. A

Identification of intracellular protein target of RRA2 inhibitor within active Mycobacterium tuberculosis

3.A.1. Introduction:

Tuberculosis is a major public health problem in developing countries and requires innovative treatment to eradicate this infection [1-3]. Past 20 years, the advent of new technologies has failed to provide many novel anti-tubercular molecules or molecular targets [4]. Considering the biological relevance of azoles, 1,2,4-triazoles have recently shown anti-tubercular action against *Mycobacterium tuberculosis* (Mtb). Rifampicin and isoniazid are the two most common drugs used presently, with rifampicin being the more important drug in terms of lowering treatment time and ensuring positive results. [5]. Furthermore, the possibility of azoles exerting anti-tubercular activity by inhibiting CYP51 and CYP121 through a process wherein the heterocyclic nitrogen (N3: imidazole or N4: 1,2,4-triazole) joins to the sixth coordination position of the heme iron atom of porphyrin in the enzyme's substrate-binding site was highlighted. [6-10]. The 1,2,4-triazole core has drawn good interest due to its diversified pharmacological activities and low toxicity. This core is known as a therapeutic drug in the market, including triazolam, voriconazole, itraconazole, fluconazole, etizolam, alprazolam, and so forth [11-13]. Numerous groups worldwide have synthesized novel triazole derivatives and analyzed them for anti-mycobacterial activity [14-16]. The hydrogen bond acceptor subunit, the positioning in the aromatic ring, and the surface topography of the triazole and phenyl rings have been significant for anti-tubercular action in structure-activity relationship (SAR) investigations of this compound class. Interestingly, minor structural changes to the 1,2,4-triazole scaffold have been observed to inhibit different molecular targets (e.g., CYP51 and CYP121) [16-18].

One of the key features of Mtb is that it exists in two different physiological states, such as the actively replicating stage and non-replicating dormancy state and remains to survive in the host tissues for prolonged periods without showing symptoms of the disease [19,20]. The existing regimen includes frontline drugs such as rifampicin, isoniazid, ethambutol, and pyrazinamide, recommended for active TB cases and still in use since 1960. One of the reasons for the success of these drugs lies in stringent preclinical and clinical drug development procedures and knowledge of their mechanism of action. Furthermore, target identification and characterization are essential stages in the initial phases of drug discovery [21,22]. A target is a general term that can refer to a wide variety of biological things, such as proteins, genes, and RNA. Specifically, in TB research, most of the compounds fail in the early phases due to a lack of understanding of the drug target and its effects on the active and dormant stages of Mtb. For example, drugs that act on the active stage but fail to act on the

dormant stage of Mtb. Therefore, predicting the targets of novel hits and their characterization on specific stages of Mtb may give the confidence to proceed further for in-vivo studies.

We have recently reported the biological activity of the 1,2,4-triazole derivatives against Mtb and *M. bovis* BCG [23,24]. Some hits have shown stage-specific inhibition in in-vitro and ex-vivo assays against Mtb. However, these compounds' target and action mechanisms are not yet identified. Interestingly our present in-vitro and ex-vivo studies have shown that RRA2 effectively inhibits the active and dormant stage of Mtb bacilli. In this study, we selected some of the hits (RRA2, RRA3, and RRA7) from our previous study and identified the intracellular target GroEL2 as a potential target for the RRA2 inhibitor.

3.A.2. Results:

3.A.2.1. Identification of triazolethiol actives against *M.bovis* BCG

Earlier research from our lab identified 54 derivatives of 1,2,4-triazolethiol from our in-house chemical library [25]. The same were screened using a simple and rapid bioassay, i.e., Active and Dormant Anti-tubercular Screening (ADAS) [26] protocol (described in method section) with a range of concentration of 0-100 µg/ml against *M. bovis* BCG. Secondary screening from the same study found that 17 active compounds showed >90% inhibition. In particular, three of them (RRA2, RRA3, and RRA7) showed >98% inhibition in this detection method. In this study, from secondary screening from our lab results of the earlier study [25], we selected RRA2, RRA3, and RRA7 as lead compounds within 54 derivatives and pursued for further characterization.

3.A.2.2. Determination of MIC of RRA2, RRA3, and RRA7 against *M. bovis* BCG

The MIC values of RRA2, RRA3, and RRA7 were determined against aerobically growing *M. bovis* BCG 2.31, 2.35, and 2.61 µg/ml, respectively (Table 1). In Wayne's tube culture, the three leads were separately applied to hypoxia-induced dormant bacilli [27]. The tube model of dormancy allows for adding chemicals at any stage of the culture without disrupting the oxygen environment. RRA2, RRA3, and RRA7 (at their MIC concentration) reduced the viability of dormant Mtb bacilli by 0.91±0.2, 1.20±0.4, and 1.1±0.2 logs CFU, respectively (Table 1). Despite the presence of propargyl or allyl groups in these three lead triazole compounds, they were unable to suppress bacilli, which suggested that a different substituent at the C-5 position may be responsible for its activity. At the C-5 position, several groups

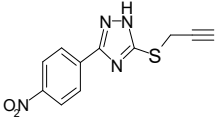
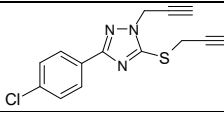
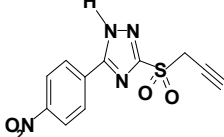
were attempted, but only p-nitrophenyl (RRA2) exhibited the necessary activity. The allyl group might be substituted for the propargyl moiety in compound RRA3 to maintain the level of inhibition against the bacilli. This p-nitrophenyl compound's sulfone derivative (RRA7) was similarly effective against actively proliferating *M. bovis* BCG, suggesting that sulphur oxidation did not affect its biological activity.

3.A.2.3. The spectrum of activity against *M. tuberculosis*, *M. smegmatis*, and *E. coli*

To further confirm the spectrum of activity of RRA2, RRA3, and RRA7 were assayed against an actively growing and hypoxic Wayne's tube model (dormant bacilli) of Mtb culture. The MIC values of RRA2, RRA3, and RRA7 were obtained at 2.0 ± 0.2 , 2.27 ± 0.1 , and 2.45 ± 0.2 $\mu\text{g/ml}$, respectively against aerobic Mtb bacilli (Table 1). The calculated reduction of viable cell counts of dormant Mtb bacilli were found to be 0.82 ± 0.1 , 1.43 ± 0.4 , and 0.91 ± 0.2 log CFU values, respectively. The inductive impact of the group linked to the para position of the phenyl ring connected to the C-5 position of 1,2,4-triazolethiol is important in making the potent inhibitory effect against the bacilli according to the inhibitory effect of these compounds against both Mtb and *M. bovis* BCG. Earlier research with well-known anti-fungal triazole medications revealed that mycobacteria are targeted by 14- α -demethylase, a cytochrome P-450 protein family member. Remarkably, our lead compounds were ineffective against *M. smegmatis*, despite the fact that *M. smegmatis* contains 51 copies of those proteins, while *M. bovis* BCG and Mtb only have 22 copies [28,29].

Furthermore, the lead compounds were also assayed against gram-negative bacteria *E. coli* as a test organism to check their specificity against nonmycobacterial species. None of the lead compounds had any considerable effect on the growth of any organism up to the concentration of 100 $\mu\text{g/ml}$ (Table 1). Hence, the result confirmed that the effectiveness of RRA2, RRA3, and RRA7 were specific for non-mycobacterial species *M. bovis* BCG and *M. tuberculosis*. Interestingly, RRA2 showed more potency against an actively growing and hypoxic Wayne's tube model (dormant bacilli) of Mtb culture and was further used for its target identification from whole-cell Mtb culture [30]. Rifampicin, metronidazole, isoniazid, and itaconic anhydride were used as standards (positive controls) in these assays [30].

Table 1: Secondary screening characterization and MIC identification of identified lead molecules

Compound code	Compound Structure	MIC ^c against active stage ^c (µg/ml)			Inhibition against dormant stage ^d (CFU/ml)		
		<i>M. bovis</i> BCG	<i>M. tuberc</i> ulosis	<i>M. smeg</i> matis	<i>E. coli</i>	<i>M. bovis</i> BCG	<i>M. tuberculosis</i>
RRA2		2.31± 0.3	2.0± 0.2	>100	>100	0.91± 0.2	0.82±0.1
RRA3		2.35± 0.1	2.27± 0.1	>100	>100	1.2± 0.4	1.43±0.4
RRA7		2.61± 0.4	2.45± 0.2	>100	>100	1.1± 0.2	0.91±0.2
Rifampicin ^a		0.22± 0.2	0.12± 0.05	0.23± 0.2	0.51 ±0.1	0.64± 0.3	0.53±0.1
Isoniazid ^a		0.31± 0.1	0.25± 0.01	0.31± 0.1	2.1± 0.1	0.66± 0.1	0.75±0.1
Metronidazole ^b		>100	>100	>100	>100	0.56± 0.4	0.61±0.4
Itaconic anhydride ^b		>100	>100	>100	>100	0.94± 0.2	0.93±0.1

^a positive control for the active stage of *M. tuberculosis*

^b positive control for the dormant stage of *M. tuberculosis*

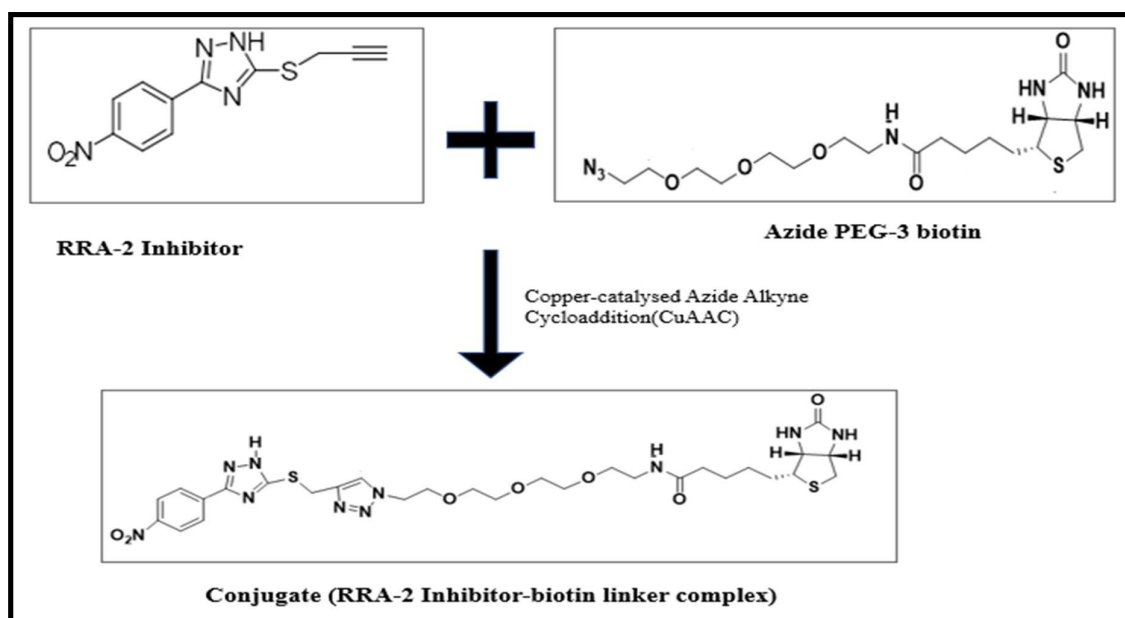
^c Concentration of compounds exhibiting 90% inhibition on mycobacterial growth.

^d CFU counts were determined after four days of treatment with compounds

3.A.2.4. Formation of conjugate RRA2 inhibitor Biotin-linker complex via Copper Catalysed Azide Alkyne Cycloaddition reaction

RRA2 compound possesses an acetylenic group in the side chain, which could be utilized in a copper-catalyzed alkyne-azide cycloaddition reaction, i.e., ‘click chemistry,’ with Azide-PEG3-Biotin to form a covalent linkage (Scheme 1). The reaction mixture (biotin-linker-RRA2) was purified using preparative HPLC, and mass was confirmed via Mass Spectrometry.

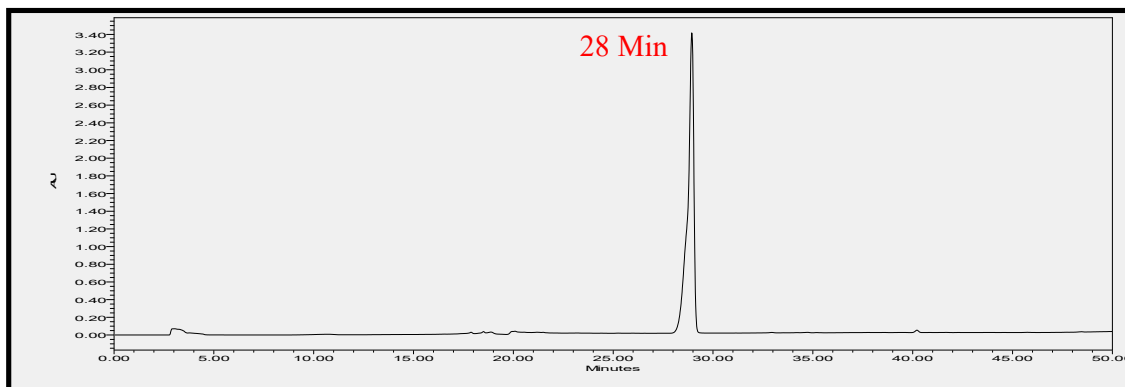
Scheme 1: Proposed mechanism for the formation of conjugate RRA2 inhibitor Biotin-linker complex via copper catalysed Azide Alkyne Cycloaddition reaction



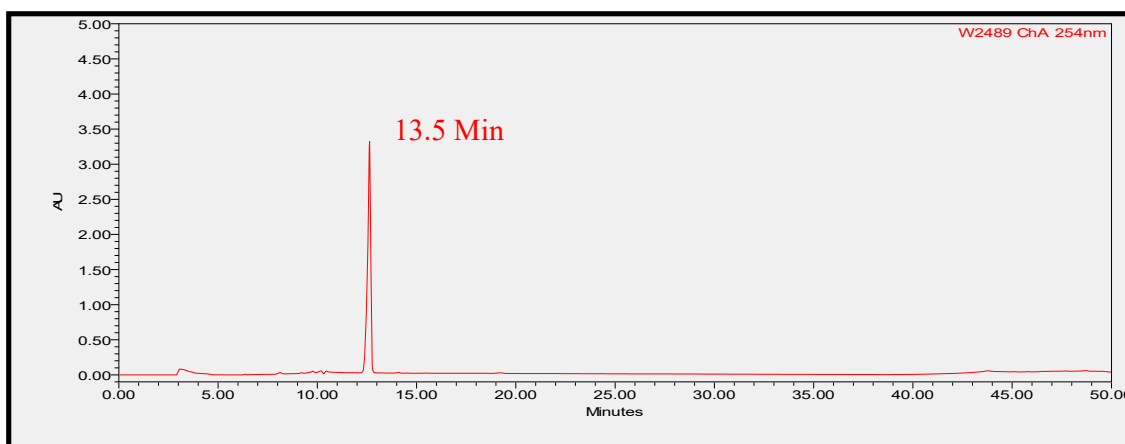
3.A.2.5. Purification of Biotin Linker-Inhibitor complex by HPLC

The reaction product (RRA2 compound and Biotin-linker conjugate) was collected in a 2 ml Eppendorf tube and allowed for solvent drying up in speed vac. for 30 min. The contents in the tube dissolved with DMSO and further filtered from the rest of the substances by the preparative HPLC method, as shown in Figure 1. The retention time of the RRA2 inhibitor and biotin-linker were first standardized as 28 Min. and 13.5 Min., respectively. One foreign pick was identified at 7 Min. retention time when the reaction product was injected and separated through the HPLC column using similar conditions. This foreign peak (Figure 1C) represented the neat conjugate (inhibitor-biotin linker complex) and was collected for further experiments.

A) Chromatogram of RRA2 inhibitor



B) Chromatogram of Azide PEG-3 Biotin



C) Chromatogram of Conjugate

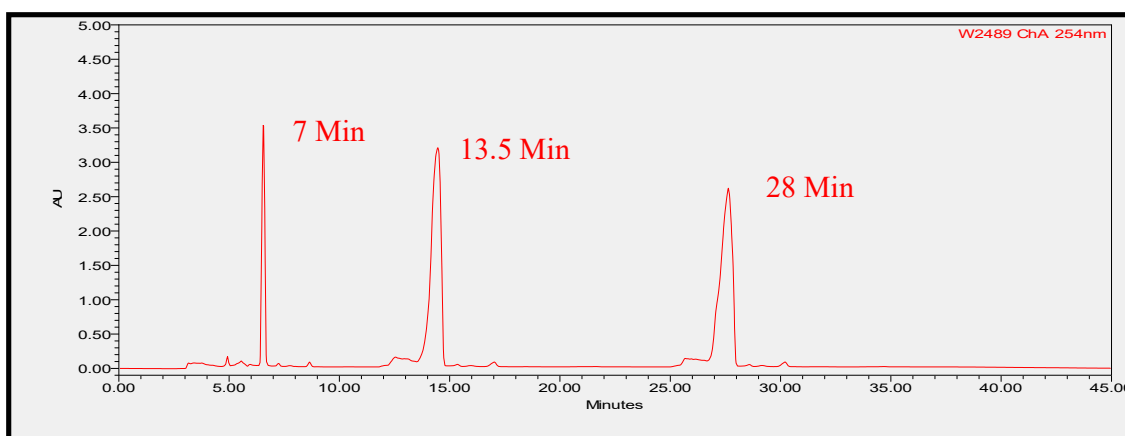


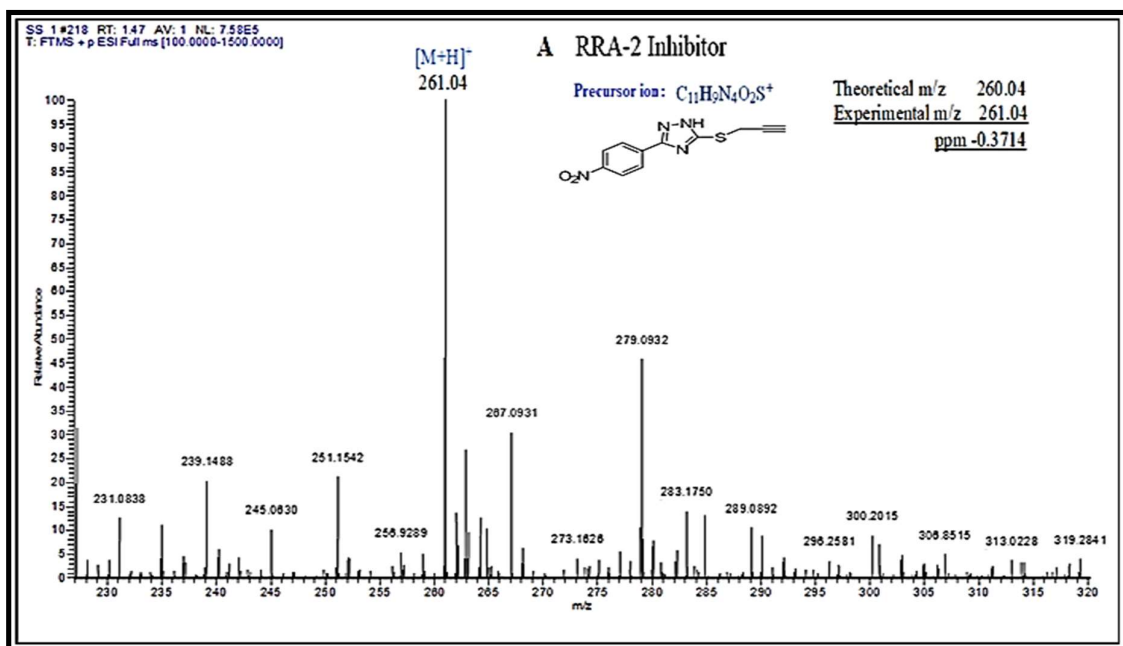
Figure 1. HPLC profile analysis. Chromatogram of RRA2 Inhibitor at MIC (A), biotin at 1mg/ml (B), and the reaction mixture of biotin-inhibitor conjugates, i.e., product (C), were

analyzed by preparative HPLC. The chromatograms represent a result obtained from three identical sets of each experiment. The details about the chromatography are provided in the “Materials and Methods” section.

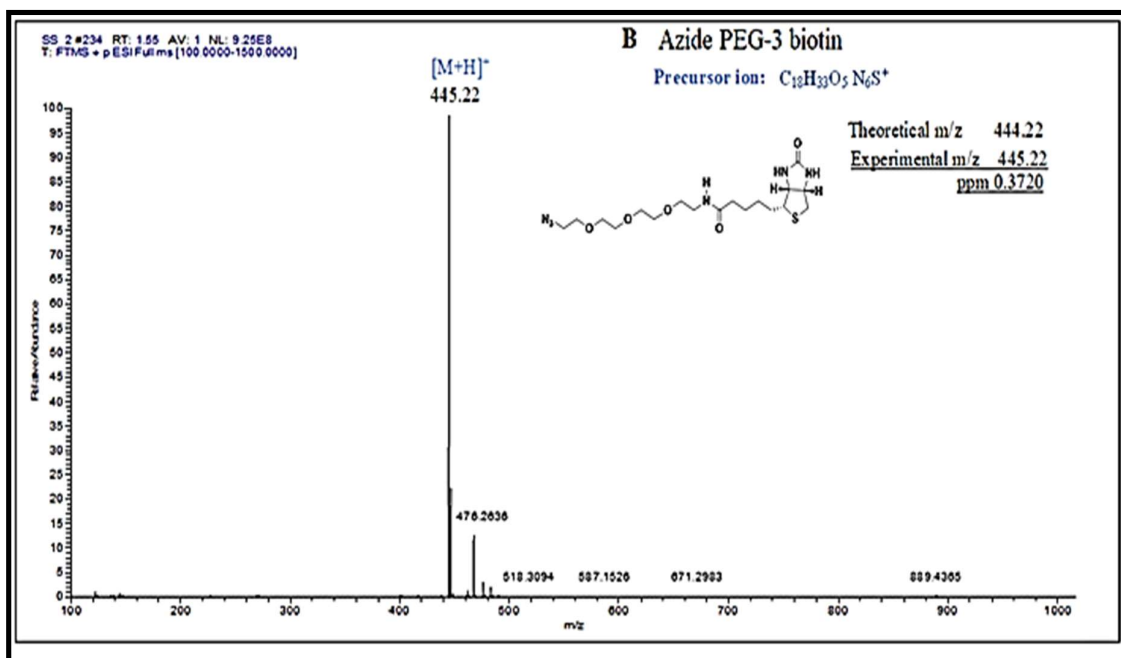
3.A.2.6. Confirmation of conjugate by HR-MS Analysis

The new peak at 7 min separated during the HPLC analysis was collected and allowed for solvent evaporation in speed vac. for 30 min and further subjected to HR-MS analysis for estimation of molecular mass of the conjugate. The HR-MS analysis of the new peak was found to have a molecular mass of 705.25 Da, shown in Figure 2, C, confirming the formation of the Biotin linker-inhibitor conjugate from copper-catalyzed alkyne-azide cycloaddition reaction. Then, the product was collected and put together to do further experiments.

A) HR mass spectra for RRA2 inhibitor



B) HR mass spectra for Azide PEG-3 Biotin



C) HR mass spectra for Conjugate (inhibitor-biotin linker complex)

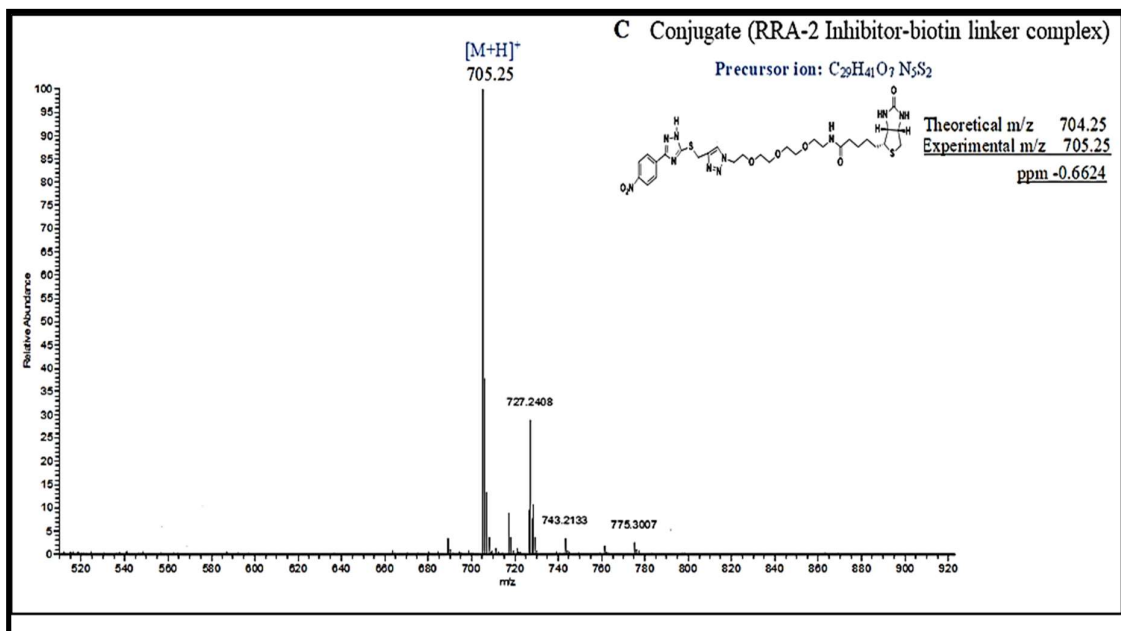


Figure 2. Mass confirmation by HR-MS analysis. HR mass spectra were obtained of only RRA2 inhibitor (A), only Azide-PEG3-Biotin-linker (B), and conjugate (inhibitor-biotin linker complex) (C). The chromatograms represent a result obtained from three identical sets of each experiment.

3.A.2.7. Identification of target protein for RRA2 from the whole-cell extract of *Mycobacterium tuberculosis* by using conjugate (biotin linker-inhibitor)

In order to aid future lead optimization of the RRA2 scaffold, the specific target of the RRA2 compound was identified with whole-cell Mtb culture. Affinity pooling may be a classic and simple strategy for finding a protein target amongst the several methodologies established for finding the target of a novel compound. The purified biotin-linker-RRA2 conjugate was added to the Mtb whole-cell extract.

Proteins hooked with RRA2 were then pulled down via MagnaBind Streptavidin beads (Thermo Fisher Scientific) and washed with PBS 2-3 times to remove undesirable nonspecific proteins. SDS-PAGE result indicated a significant protein band at ~60 kDa molecular weight (Figure 3). As a control, we added our biotin-linked-RRA2 to a whole Mtb cell culture previously treated with RRA2. Notably, no band was seen (in the control lane) on the SDS-PAGE, presumably as RRA2 was already bound to the target protein's active site, leaving no room for conjugate (biotin linked-RRA2) binding and subsequent pull-down.

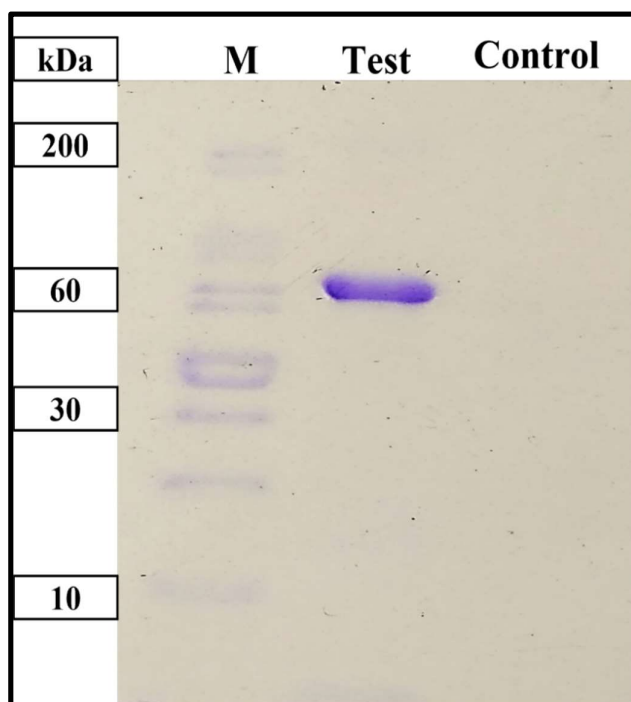


Figure 3. Separation of target protein isolated from Mtb whole-cell extract on SDS-PAGE. The gel image represents the final target protein sample obtained in addition to conjugate (biotin linker-RRA2) from the whole-cell extract previously treated with RRA2

compound (Control), untreated with RRA2 compound (Test), and M is represented by molecular weight protein markers.

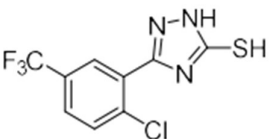
Table 2. Identification of target protein by LC-MS/MS Method

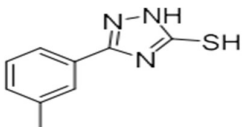
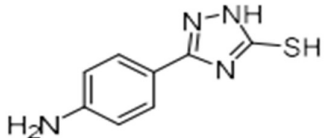
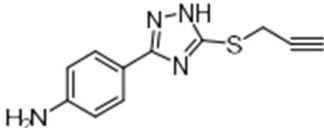
Accession	Entry	Description	mW (Da)	pI (pH)	PLGS Score	Peptides	Coverage (%)
P9WPE7	CH602_ MYCTU	60 kDa chaperonin 2 OS=Mycobacterium tuberculosis (strain ATCC 25618 / H37Ra) OX=83332 GN=groEL2 PE=1 SV=1	56692	4.92	1380	25	50.18

3.A.2.8. Target Specificity analysis

To determine the target specificity of RRA2, four-hit derivatives of 1,2,4-triazolethiols (RRA79, RRA242, RRA267, and RRA268) were selected from an in-house library (Table 3). These derivatives also have significant inhibitory activity against the active and dormant stage of Mtb. Therefore, these four compounds are specific compounds of either the bacilli's active or dormant stage.

Table 3: Anti-mycobacterial activity of synthesized triazoles derivatives against the active and dormant stage of *Mycobacterium tuberculosis*

Compound Code	Structure	Molecular weight (Dalton)	MIC (µg/ml)		
			In-vitro active stage inhibitor	In-vitro dormant stage inhibitor	Ex vivo dormant stage inhibitor
RRA 79		279	>100	2.5±0.03	0.1±0.03

RRA 242		191	>100	>100	3.0±0.06
RRA 267		192	>100	0.5±0.02	0.3±0.04
RRA 268		230	>100	0.1±0.01	0.4±0.05
Rifampicin	NA	NA	0.04± 0.03	0.06± 0.06	0.08± 0.12
Isoniazid	NA	NA	0.06± 0.04	0.08± 0.03	0.09± 0.05

To confirm the specificity of the RRA2 compound, the purified biotin-linker-RRA2 conjugate was separately added to the Mtb whole cell culture, which has already been treated with RRA2 compound (control) and without RRA2 compound (test) along with four similar scaffolds of 1,2,4-triazolethiols compounds (Table 3). A similar protocol was used to pull the purified target protein (mentioned in the above section) and performed the SDS-PAGE analysis. Presumably, if all or any of the compounds had the same target as RRA2, it should not show any band in the SDS-PAGE because the target site is not available to bind to purified conjugate.

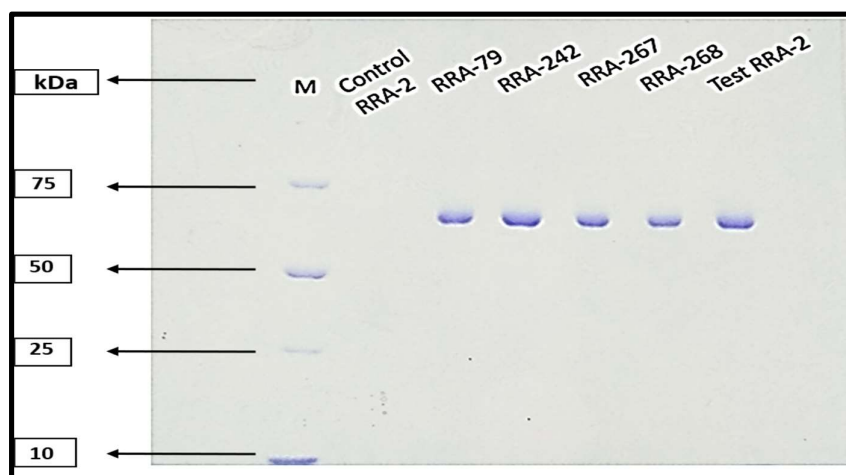
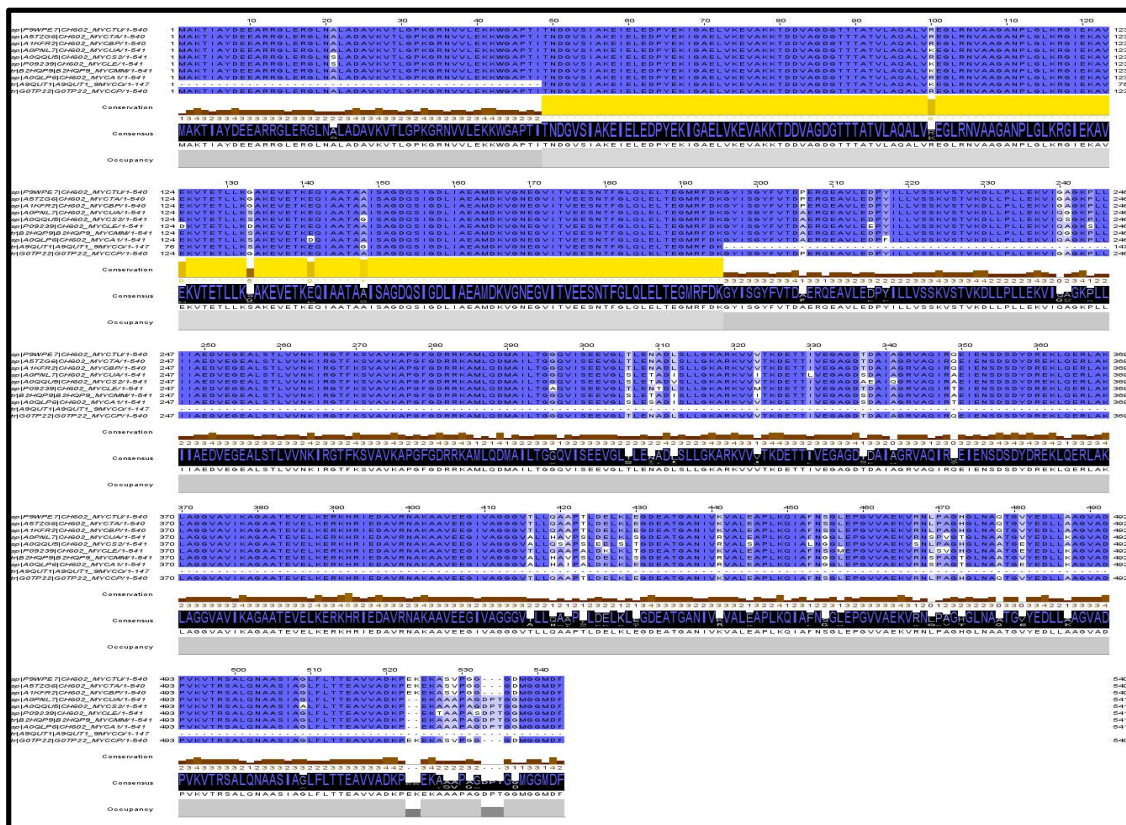


Figure 4. Target specificity analysis of RRA2 in the presence of four similar scaffolds of 1,2,4-triazolethiols compounds by SDS-PAGE. M represents different molecular weight

protein markers, whole-cell culture treated with purified conjugate mixture added to previously treated with RRA2 compound (control), RRA79, RRA242, RRA267, and RRA268. Here, the test is the whole-cell extracts that were previously untreated with an RRA2 compound.

Interestingly, Figure 4 showed the cleared bands with all four compounds like test samples of RRA2 except in the control sample. Even though the other four similar scaffolds of 1,2,4-triazolethiols compounds had an inhibitory effect against the active and dormant stage of Mtb, but their protein target sites were different. This result demonstrated the robust specificity of the RRA2 target.

3.A.2.9. Multiple Sequence Alignment of GroE12 protein from different species of Mycobacteria

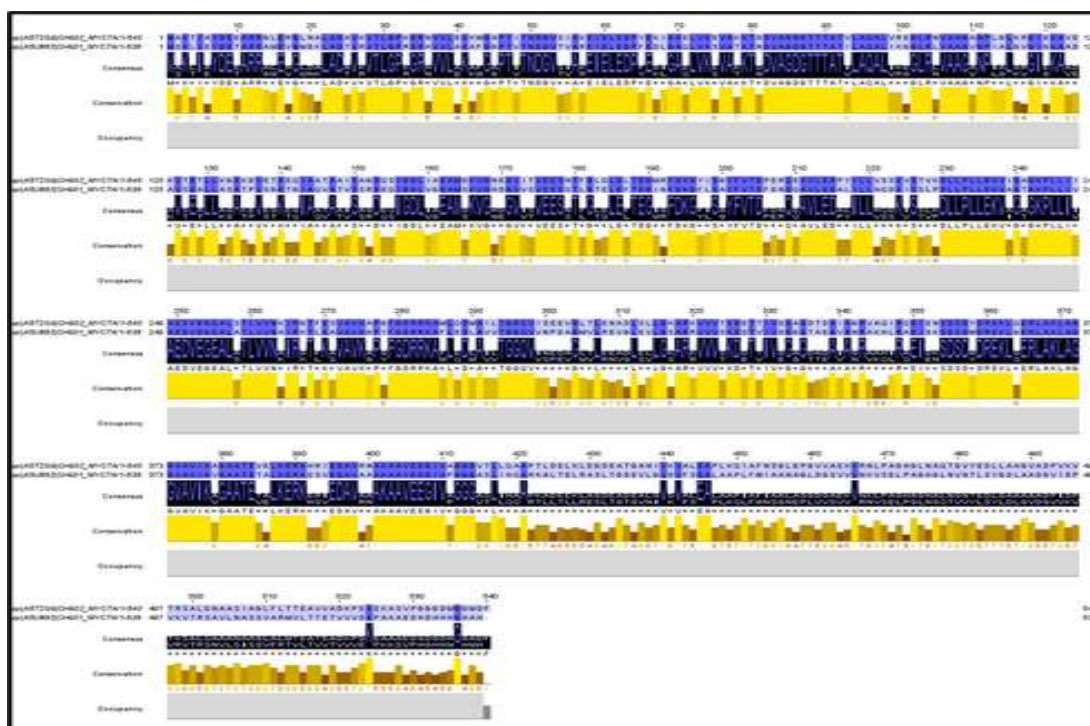


Seq. Order: 1. *M. tuberculosis* H37RV; 2. *M. tuberculosis* H37Ra; 3. *M. bovis*; 4. *M. ulcerans*; 5. *M. smegmatis*; 6. *M. leprae*; 7. *M. marinum*; 8. *M. avium*; 9. *M. abscessus*; 10. *M. canettii*

Figure 5. Multiple Sequence Alignment of GroE12 protein from different species of Mycobacteria

The Multiple Sequence Alignment (MSA) was manually edited in Jalview software V 2.11.2.0, a tool written in Java to analyze the residue conservation patterns (the analysis method is written in the materials and methods section). Once the sequence of GroEL2 protein from 10 closely related Mycobacterial species has been clustered, the conservation patterns can be calculated and shown for each group (Figure 5). Each column in the alignment or group is given a score from 0 to 10 based on the common Physico-chemical properties of the residues (highlighted in brown color). The height of consensus between the sequence is related to the sequence similarity highlighted in blue color. Multiple sequence alignment (MSAs) is often used to measure common features between sequence conservation of protein domains, tertiary and secondary structures, and even individual amino acids or nucleotides to find sequence similarity, homology, and evolutionary association. The degree of protein sequence similarity is represented in dark blue to no color, whereas the dark blue color between the sequences represents 100 % similarity. In contrast, the regions where there is no blue color indicates that there is no similarity between the sequence.

3.A.2.10. Pairwise Sequence Alignment of GroE11 and GroE12 protein from *Mycobacterium tuberculosis* H37Ra



```

Score = 15940.0
Length of alignment = 539
Sequence sp|ASU892|CH601_MYCTA/1-539 (Sequence length = 539)
Sequence sp|ASTZG6|CH602_MYCTA/1-536 (Sequence length = 540)

sp|ASU892|CH601_MYCTA/1-539 MSKLI EYDETARRAMEVGM DKLADTVRVTLGPRGRHVV LAKAFG
sp|ASTZG6|CH602_MYCTA/1-536 MAKTIAYDEEARRGLERGLNALADAVKVTLPKGRNVVLEKKWVG

sp|ASU892|CH601_MYCTA/1-539 GPTVTNDGVTVAREIELEDPFEDLGAQLVKS VATKTNDVAGDGT
sp|ASTZG6|CH602_MYCTA/1-536 APTITNDGVSIAKEIELEDPYEKIGAE LVKEVAKKTDDVAGDGT

sp|ASU892|CH601_MYCTA/1-539 TTATILAQALIKGGLRLVAAGVNP IALGVGIGKAADAVSEALLA
sp|ASTZG6|CH602_MYCTA/1-536 TTATVLAQALVREGLRNVAAGANPLGLKRGIEKAVEKVTETLLK

sp|ASU892|CH601_MYCTA/1-539 SATPVSGKGTGIAQVATVSSRDEQIGDLVGEAMSKVGH DGVVSVVE
sp|ASTZG6|CH602_MYCTA/1-536 GAKEVETKEQJAATAAISAGDQSIGDLIAEAMD KVGNEGVTVE

sp|ASU892|CH601_MYCTA/1-539 ESSTLGTLEFTEGIGFDKGFLSAYFV TDFDNQQAVLEDA LILL
sp|ASTZG6|CH602_MYCTA/1-536 ESNTFGLQLELTEGMRFDKGYISGYFVT DPERQEAVLEDPYILL

sp|ASU892|CH601_MYCTA/1-539 HQDKISSLPDLLP LLEK VAGTGKPLLIUAE DVEGEALATLVVNA
sp|ASTZG6|CH602_MYCTA/1-536 VSSKVSTV KDLLP LLEK VIGAGKPLLIIEA DVEGEALSTLVV NK

sp|ASU892|CH601_MYCTA/1-539 IRKTLKAVAVKGPYFGDRRKAFLE DLAVVTGGQV VNP DAGM VLR
sp|ASTZG6|CH602_MYCTA/1-536 IRGTFKSVAVKAPGFGDRRKAM LQDMAILTGGQVISEEVGLTLE

sp|ASU892|CH601_MYCTA/1-539 EVGLEVLGSARRVVVSKDDTVIVDGGGTAEAVANRAKH LRAEID
sp|ASTZG6|CH602_MYCTA/1-536 NADLSLLGKARKVVVTKDETTIVEGAGD TDAIAGRVAQIRQEIE

sp|ASU892|CH601_MYCTA/1-539 KSDSDWDREKLG ER LAKLAGG VAVIKVGAATETALKERKESVED
sp|ASTZG6|CH602_MYCTA/1-536 NSDSDYDREK LQERLAKLAGG VAVIKAGAAATEVELKERKHRIED

sp|ASU892|CH601_MYCTA/1-539 AVAAAKAAVEEGIVP GGGASLIHQARKALTELRASLTGDEV LGV
sp|ASTZG6|CH602_MYCTA/1-536 AVRNAKAAVEEGIVAGGGV TLL-QAAPTLD ELK--LEGDEATGA

sp|ASU892|CH601_MYCTA/1-539 DVFSEALAAPLFWIAANAGLDG SVVVNKVSELPAGHGLNVNTLS
sp|ASTZG6|CH602_MYCTA/1-536 NIVKVALEAPLQK IAFNSGLEPGVVAEKVRNLPAGHGLNAQTGV

sp|ASU892|CH601_MYCTA/1-539 YGDLAADGVIDPVKVT R S AVL NASSVARMVLT TETV VVDKPAKA
sp|ASTZG6|CH602_MYCTA/1-536 YEDLLAAGVADPVKVT R S ALQNAASIAGLFLTTEAVVADKPEKE

sp|ASU892|CH601_MYCTA/1-539 EDHDDHHHGH AH
sp|ASTZG6|CH602_MYCTA/1-536 KASVPGGGGDMG
Percentage ID = 61.04

```

Figure 6. Pairwise Sequence Alignment (PSA) of GroE11 and GroE12 protein from *Mycobacterium tuberculosis*

The pairwise sequence similarity of GroE11 and GroE12 protein from the *Mycobacterium tuberculosis* H37 Ra strain was done using Jalview software V 2.11.2.0. The percentage identity score from our pairwise sequence similarity analysis was 61.04 from the pairwise alignment study of the GroE11 and GroE12 protein from Mtb, as shown in Figure 6.

3.A.2.11. Potential Binding mode of RRA2

We conducted preliminary molecular docking to determine where RRA2 might interact with GroE12. There were two major sites, which are also the hinge sites of the protein [31], where compounds could potentially interact with GroE12 (Figure 7. A). The first is where ATP has been proposed to interact and was crystallized in the analogous *E. Coli* GroE11 protein (PDB:1KP8) [32]. The second was where Mg was found in the *M. tuberculosis* GroE12 X-ray

structure (PDB:3rtk) [33]. Both sites were utilized to dock RRA2. Interestingly, the RRA2 compound was able to have a consistent binding mode in both sites. Although the Mg site scored lower across the board than the ATP site (Table 4), for the RRA2 complex, the ATP site was lower energy than the Mg site (-13355.62 kcal/mol for ATP site vs. -13292.40 kcal/mol for the Mg site).

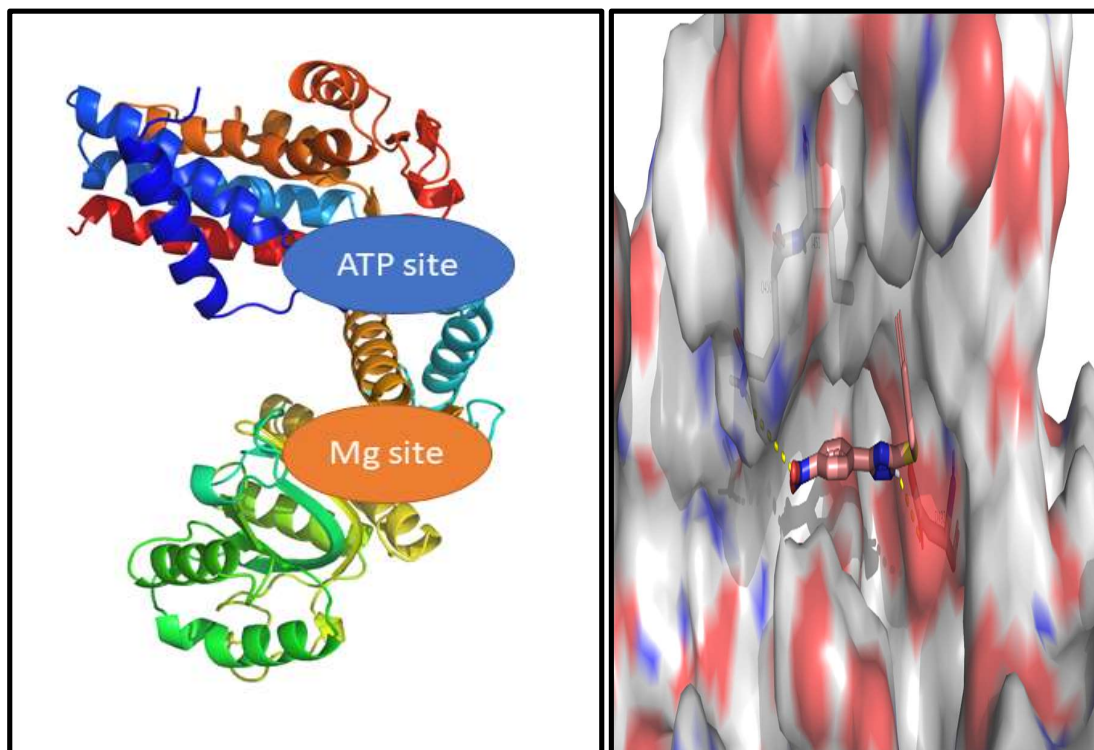


Figure 7. A. Structure of GroEl2 colored orientation of RRA2 (peach) in the ATP site of GroEl2

Figure 7. B. Proposed docking via rainbow from N to C terminus

Figure 7. Prediction of target protein GroEl2 by Molecular Modelling

Table 4. Docking scores

Shown is the docking score for the highest-ranked solution. Notably, the lower the score, the better the dock is proposed to be.

Compound code	ATP site (kcal/mol)	Mg site (kcal/mol)
RRA2	-4.893	-3.608

Furthermore, numerous studies have suggested that movement in the equatorial domain, which binds ATP, is essential for its function [33]. Therefore, it would be expected that a compound binding in this region would interfere with ATP binding and affect the function of GroEl2. This suggests that the ATP site is the likely binding site for this compound class. In this site, RRA2 is positioned with I451 stacking over the phenyl group and putative hydrogen bonds between the nitro moiety of RRA2 to Q450 and the triazine D483 (Figure 7 B). The alkyne is pointed out of the pocket, having little effect on the interaction energy. This is important as it is essential to be exposed for the biotin-linking experiment to be viable. Although beyond the scope of this work, future experiments (e.g., mutagenesis, X-ray crystallization) will be needed to confirm this binding mode.

3.A.3. Discussion

Triazoles have long been known for their antifungal, antiviral, and plant growth-regulating properties. However, in recent years, their anti-mycobacterial potential has gained recognition. [6]. Only fluconazole and tebuconazole have been shown to have anti-mycobacterial action without increasing MIC values or specificity [34]. Furthermore, they have no significant effect on dormant tubercle bacilli. In this work, alkyl-substituted 1,2,4-triazolethiols and hybrids were prepared and investigated for anti-tuberculous efficacy. Out of 54 compounds were selected as primary screen hits. All 17 hits in previous studies were chosen based on their effectiveness against *M. bovis* BCG's aerobic replicating stage. Only three lead compounds (RRA2,3,7) were shown to have a meaningful influence on actively replicating bacilli after considering their dose-dependent effect. [23].

Biotinylated RRA2 conjugate was used for pulling down the target protein GroEl2 from *Mtb* whole-cell extract and confirmed by SDS-PAGE (Figure 3) and Liquid chromatography-mass spectrometry (LC-MS) analysis, as shown in Table 2. Earlier research reported that GroEl2 has homology with members of a family of heat shock proteins (HSPs) that is known as the chaperonin-60 (Cpn60/GroEl) family, which serves as an essential molecular chaperone (Cpn) for maintaining cellular homeostasis in normal and stressed conditions among different proteins. *Mtb* contains two copies of the *cpn60* gene [35]. One of these, *cpn60.1*, is an operon with *cpn 10*, while the second *cpn60.2* occurs independently on the chromosome. The regulation of HSPs in *Mtb* has shown overexpression of the two *Cpn60s* upon thermal shock [36] and phagocytosis by macrophages [37]. These reports

suggest that the Cpn60 of Mtb contributes to its defense response against external stress conditions.

Furthermore, evidence uncovered that both proteins Cpn 60.1 (GroEL1) and 60.2 (GroEL2) of Mtb are highly antigenic and potent cytokine inducers [38,39]. Earlier studies also focused on the role of the full-length (FL) Mtb protein GroEL2, indicating that a cleaved form of GroEL2 [GroEl(cl)] predominates in wild-type and that the cleavage of the same protein GroEL2 tends to inhibit the innate immune response to infection [40]. Furthermore, the FL GroEL2 protein produced strong proinflammatory responses from dendritic cells (DC) and promoted its maturation and antigen presentation to T cells [41]. Similar to GroEL2(cl), Fong et. al. [42] reported that HSP70 is secreted from cells and can activate the immunoreceptors on monocytes and neutrophils. So, targeting GroEL2 may open up new avenues for treating TB. In this concern, a series of inhibitors were also reported for dual-targeting GroEL/ES along with protein tyrosine phosphatase B (PtpB), which act as virulence factors and show effective inhibition against active and dormant stages of TB [43].

Interestingly, our present in-vitro and ex vivo studies showed that RRA2 efficiently inhibits the active and dormant stages of Mtb bacilli, as shown in Table 1. Despite the presence of propargyl or allyl groups in other triazole structures (RRA3 and RRA7), they were unable to inhibit bacilli, indicating that a distinct substituent at the C-5 position is responsible for its activity. At the C-5 position, several groups were attempted, but only p-nitrophenyl (RRA2) demonstrated the necessary activity. This p-nitrophenyl compound's sulfone derivative (RRA7) was similarly effective against actively growing *M. bovis* BCG, indicating that oxidation of Sulphur did not affect its biological activity. However, both compounds were similarly effective against *M. tuberculosis*.

RRA2, RRA3, and RRA7 were ineffective against *M. smegmatis* and *E. coli*, suggesting that they had a tuberculosis-specific action. The inhibitory result of these compounds against *M. bovis* BCG and *M. tuberculosis* revealed that the inductive consequence of the group connected to the para position of the phenyl ring connected to the C-5 position of 1,2,4-triazolethiol is critical in the making of the potent inhibitory effect against the bacilli. The replacement of the propargyl moiety by the allyl group in the latter molecule (RRA3) may keep the degree of inhibition against the bacilli. In comparison to existing anti-tubercular medicines, these three compounds are structurally unique. The efficacy of these three compounds on both stages of Mtb has generated doubts regarding their

ability to block 14-demethylase. These compounds were ineffective against *M. smegmatis*, which has the same target enzyme as *M. smegmatis*. [44].

Our findings summarized three nontoxic lead compounds (RRA2, RRA3, and RRA7) of 1,2,4-triazolethiols (alkyl-substituted) that significantly inhibit the active and dormant stage *M. tuberculosis* and *M. bovis* BCG bacilli. They were more specific against Mtb bacilli than *M. smegmatis* and *E. coli*. Among these three lead compounds, due to higher efficacy and presence of alkyne group in its structure, RRA2 was used for pool down technique for target identification. Using the LC-MS approach, we identified GroEl2, a chaperonin, as the target of the RRA2 compound in active stage Mtb and confirmed it through molecular modeling studies. Multiple sequence alignment studies highlighted the difference in GroEL1 and GroEL2 protein sequences within Mtb H37Ra species, indicating the possibility of an inhibitor that could be explicitly inhibited to Mtb strains. The outcome of this study disclosed that the consolidated analysis was found to be supportive of explaining the efficacy of RRA2 in inhibiting Mtb cells for interpreting their possible mechanism of action. Therefore, the RRA2 compound could be a potential candidate molecule before the *in vivo* trial studies.

3.A.4. Materials and methods

3.A.4.I. Bacterial strains, media, and inoculum preparation

M. bovis BCG (ATCC 35,745) and *M. smegmatis* (ATCC 607) were obtained from Astra Zeneca, Bangalore, India, and *M. tuberculosis* H37Ra (ATCC 25,177) was obtained from Microbial Type Culture Collection, Chandigarh, India. *E. coli* strain DH5 α was obtained from the National Collection of Industrial Microorganisms (NCIM), Pune, India. RPMI 1640 cell culture media and fetal bovine serum (FBS) were purchased from GIBCO, USA. All the chemicals were purchased from Sigma Aldrich USA. Unless mentioned, Dubos albumin agar powder and other chemicals were purchased from DIFCO, USA. All mycobacterial strains were subcultured routinely in Dubos albumin agar slants or plates. The liquid inoculum was prepared in Dubos broth with 5 % glycerol, and 10 % Albumin dextrose catalase (ADC) enrichment medium, incubated in a shaker incubator rotating at a speed of 150 rpm at 37 °C till the logarithmic phase (OD₆₂₀ ~ 1.0) was reached. 1% of 1.0 OD₆₂₀ of the culture was used as the standard inoculum size for all the experiments, yielding final inoculum of approximately 10⁵ CFU/ml.

3.A.4.II. Inhibitory effect of active molecules against intracellular *Mycobacterium tuberculosis* inside THP-1 macrophage

THP-1 was used to examine the inhibitory activity of the compounds against intracellular bacilli by following a method described earlier [1,45,46]. Briefly, 3 mL of THP-1 cells ($\sim 5 \times 10^4$ cells/ml) were treated with 100 nM of phorbol myristate acetate (PMA) in a culture flask for 24 h to convert them into macrophages. These macrophages were further incubated for 12 h with *M. tuberculosis* at MOI (multiplicity of infection) of 1: 100 for infection. Extracellular bacilli were removed by washing twice with sterile PBS and adding fresh medium to adhered cells. Compounds were then added to these infected macrophages at different concentrations. In order to check the effect of inhibitors on the growth of intracellular bacilli, compounds were added at 0 h (for identification of active stage inhibitors) and after 120 h (for identification of dormant stage inhibitors) of infection; unless mentioned otherwise, the effect of the compound was monitored by determining the bacterial load within macrophage by lysing them with hypotonic buffer (10 mM HEPES, 1.5 mM MgCl₂ and 10 mM KCl) at different time points and spreading 100 μ L of the samples on Dubos agar plates to enumerate colonies after 21 days.

3.A.4.III. Preparation of Conjugate (RRA2-biotin linker complex)

Copper-catalyzed alkyne-azide cycloaddition protocol was used to prepare biotin-linked RRA2 conjugate (RRA2-biotin linker complex) [47,48]. Briefly, Azide-PEG3-Biotin (5 mg/0.011 mmol) was dissolved in 0.5 mL anhydrous Tetrahydrofuran (THF) in a 5 mL round bottom test tube at room temperature. 0.5 mL copper sulphate solution (125 mmol) was added to this 5 mL test tube and mixed properly. Next, 10 mg of sodium ascorbate was added, and this complete solution was stirred on a magnetic stirrer at room temperature. A 2:1 ratio of RRA2 and Biotin was used for the reaction. So, 10 mg of the inhibitor was added to this reaction mixture, and the reaction was allowed to proceed and stirred for 8 h at room temperature.

3.A.4.IV. Purification of Biotin Linker-Inhibitor complex by HPLC

Chromatographic separation and analysis of the product and components of the reaction were done using reverse-phase X bridge C₁₈ (5 μ m, 46x250 mm) column in preparative HPLC (binary pump-1525, UV detector-2489, sampler-2707, Waters, India). Organic solvents employed to prepare mobile phases were HPLC-grade, and the HPLC column used was reverse-phase X bridge C₁₈ (5 μ M, 46x250 mm). The optimized mobile phase composition

used was in, 'A' solution - water (100, 60, 60, 45, 40, 0) % and 'B' solution – acetonitrile (0, 40, 40, 55, 60, 100) %. The analysis was carried out in gradient elution mode with a 1 mL/min flow rate with column run-off monitored at 254 nm wavelength. The retention time for inhibitor RRA2 (Figure 1, A) and Azide-PEG3-biotin (Figure 1, B) were observed at 28 min and 13.5 min, respectively, which could help in comparison with the reaction mixture of the conjugate (Figure 1, C). After injecting the conjugate reaction mixture into the column, one foreign peak was observed at a 7 min retention time along with the biotin and inhibitor peak. This foreign peak (Figure 1, C) represented the neat conjugate (inhibitor-biotin linker complex) and was collected for further experiments.

3.A.4.V. Mass confirmation by HR-MS analysis

HR-MS analysis was done by the modified method, as reported earlier [49]. The purified inhibitor-biotin linker complex was dissolved in acetonitrile (mass spectrometry grade) followed by separation using the Accela ultrahigh performance liquid chromatography (UHPLC) system (Thermo Fisher, Waltham, USA) using a C18 Hypersil Gold column (3 μ m, 3 \times 100mm, Thermo fisher) coupled with a Q Executive- Orbitrap mass spectrometer (Thermo Fisher, Germany). The separation is carried out in optimized mobile phase composition of solvent A (acetonitrile with 0.1% of formic acid) against 70-30% of solvent B (water with 0.1% of formic acid) at a flow rate of 500 μ L/min and a temperature of 45 $^{\circ}$ C for 5 min. The molecular weight was identified by electrospray ionization positive (ESI+) mode with a mass scan range set from 100 to 1500 m/z. The data acquisition and processing were performed using the Thermo Scientific Xcalibur software (version 3.0). The tandem mass spectrometry (data-dependent MS/MS) data were collected with collision energy between 30 and 40 eV. The raw data from the instrument were converted to the mzxml file format using ProteoWizard. The mass confirmation was carried out with the HPLC purified fractions for RRA2 Inhibitor (Figure 2, A), Azide-PEG3 Biotin (Figure 2, B), and neat conjugate (Figure 2, C), respectively, were then analyzed for mass confirmation by HR-MS method. The RRA2 Inhibitor (Figure 2, A) and Azide-PEG3-Biotin (Figure 2, B) showed their corresponding mass of 261.04 Da and 445.22 Da. The mass of neat conjugate was found at 705.25 Da, confirming the separation of the Biotin linker-inhibitor conjugate from the mixture. The confirmed conjugate mass from HR-MS analysis helped to process for the next step of the experiment.

3.A.4.VI. Binding of conjugate RRA2-Biotin complex with crude whole cell extract of *Mycobacterium tuberculosis*

The RRA2-Biotin conjugate obtained from HPLC purification was allowed to dry up the solvent in speed vac for 30 min, dissolved in 100µL DMSO, and added to the whole-cell extract of aerobic Mtb culture. For whole-cell extract preparation, 5 mL spheroplast solution (0.0006%) was added in ~1.0 OD Mtb culture and incubated for 12-16 h. This Biotin linker-inhibitor conjugate was also added to the control culture, which was already treated with an RRA-2 inhibitor. To bind to the target protein, both control and test samples were kept for 30 minutes in an incubator shaker at 37 °C and 150 RPM. Both the cultures were sonicated in protein extraction buffer (100mM HEPES buffer, 5 mM EDTA 1 %, SDS, 100 mM NaCl 0.5%, Triton X-100, and freshly prepared 1% protease inhibitor cocktail) at 45 Hz with 10 Sec. pulse ON and 5 Sec. pulse OFF in ice-cold condition for 15 min and centrifuged the cell extract at 14,000 rpm for 1 h at 4 °C to get the intracellular protein in supernatant. The supernatant containing the target protein with Biotin-Inhibitor conjugate was taken out and dialyzed against PBS to remove the excess unbound Biotin-Inhibitor conjugate and inhibitor molecules at 25°C for 3 h.

3.A.4.VII. Purification of RRA2-Biotin conjugate tagged target Proteins by MagnaBind™ Streptavidin Beads

MagnaBind Streptavidin Beads are convenient for affinity purification or separation methods involving biotin-labeled molecules obtained from Thermo Scientific MagnaBind Streptavidin Beads (Cat. No. 21344) were added in the supernatant containing the target protein already bound with Biotin-Inhibitor conjugate allowed to pull down by using an external magnetic field overnight at 4 °C. Then, the beads were washed with sterile PBS 2-3 times to remove the unwanted proteins. To release our target protein attached with Biotin-Inhibitor conjugate, we added an excess of free 10 mM biotin molecule in shaking condition at 25 °C for 30 min. before dialysis against water at 25 °C for 3 h. Dialyzed sample was collected and further processed for protein precipitation.

3.A.4. VIII. Chloroform-Methanol Precipitation of Target proteins

The chloroform-methanol precipitation method was followed to remove salt and detergents. 100 µL sample was added to 400 µL methanol, vortexed well, then 100 µL chloroform was added and vortexed. 300 µL Milli Q water was added and again vortexed for 2 min. Spin was given for 1 min at 14,000g. Removed the top aqueous layer (protein is

between layers), then 400 μ L methanol was added and vortexed. 2 min at 14,000 g spin was given and removed the MeOH without disturbing the pellet. The sample was dried in speed-Vac. and 1X sample buffer (125 mM Tris•HCl, pH 6.8, 20% Glycerol, 1% SDS, 10% β -Mercaptoethanol, 0.5 mg/ml Bromophenol Blue) was added for SDS PAGE [50].

3.A.4.VIX. Protein estimation

Protein quantification was done by the Bradford method (Bio-Rad Protein Assay; Cat. No. 500-0006) according to the manufacturer's instructions (Bio-Rad, Hercules, CA) [51].

3.A.4.X. SDS-PAGE and Proteomic Analysis of Captured Proteins

Individual proteins in the sample were separated by carrying out SDS-PAGE [52]. Briefly, 80 μ g (5 μ L) of each protein sample was first mixed with 1X loading (sample) buffer containing 5% β -mercaptoethanol (Sigma, MO, USA). The samples were then incubated for 10 min at 80 °C. Next, 20 μ L (64 μ g) samples were loaded onto 12.5% Bis-Tris pre-cast polyacrylamide gels, and the SDS-PAGE was carried out using Mini-PROTEAN® Electrophoresis System-Bio-Rad (Cat. No.1658000). After electrophoresis, the gel was subjected to Coomassie staining for overnight. Protein bands seen within the gel were appropriately cut and subjected to trypsin digestion using the earlier protocol [53], followed by peptide extraction and proteomic analysis in Liquid chromatography-mass spectrometry (LC-MS).

3.A.4.XI. Target specificity analysis

To determine the target specificity of RRA2, four-hit derivatives of 1,2,4-triazolethiols (RRA79, RRA242, RRA267, and RRA268) were selected from an in-house library (Table 3). These derivatives also have significant inhibitory activity against active and dormant stages of Mtb. Therefore, all these four compounds are specific compounds of either the active stage or dormant stage of the bacilli. To confirm the specificity of the RRA2 compound, the purified biotin linker-RRA2 conjugate was separately added to the Mtb whole-cell culture, which has already been treated with RRA2 compound (control) and without RRA2 compound (test) along with four similar scaffolds of 1,2,4-triazolethiols compounds (Table 3). A similar protocol was used to pull the purified target protein (mentioned in the above section) and perform the SDS-PAGE. Presumably, if all or any of the compounds had the same target as RRA2, it should not show any band in the SDS-PAGE because the target site is not available to bind to purified conjugate.

3.A.4.XII. LC-MS analysis

2 μL digested peptides with a final concentration of 100 ng/ μL were analyzed by nano LC-MS using nanoACQUITY online coupled to SYNAPT HDMS system (Waters Corporation, MA, USA) equipped with a nanolockspray ion source with a flow rate of 300 nL/ min (external lock mass standard: Glu-fibrinopeptide) [54]. Peptide samples were injected online onto a 5 μm Symmetry C18 trapping column (180 μM x 2 cm length) at a flow rate of 15 $\mu\text{L}/\text{min}$. Peptides were separated by in-line gradient elution onto BEH (Bridged Ethyl Hybrid) C18 1.7 μM x 75 μM x 150 mm nanoACQUITY analytical column at a flow rate of 300 nL/ min using a linear gradient from 5 to 40% B over 35 min (A. 0.1% formic acid in water, B. 0.1% formic acid in acetonitrile). The acquisition was performed in positive V mode in a mass range of 50-1990 m/z with a scan time of 1 second with alternating low (5 eV) and high (15-40 eV) collision energy. MS data were processed with ProteinLynx Global Server (PLGS version 2.4. Waters Corporation, MA, USA). The processed data were allowed to search against the *Mycobacterium tuberculosis* H37Ra subset of the UniProt database containing all 44,987 protein entries for protein identification described by Silva et. al. [55].

3.A.4.XIII. Multiple Sequence Alignment of GroEl2 protein from different species of Mycobacteria

Multiple sequence alignment (MSAs) is often used to measure common features between sequence conservation of protein domains, tertiary and secondary structures, and even individual amino acids or nucleotides to find sequence similarity, homology, and evolutionary association. The Multiple Sequence Alignment (MSA) was manually edited using default parameters in Jalview software V 2.11.2.0 [56]. FASTA files of GroEl2 were imported from the UniProt database for 10 closely related Mycobacterial species. (1. *M. tuberculosis* H37RV; 2. *M. tuberculosis* H37Ra; 3. *M. bovis*; 4. *M. ulcerans*; 5. *M. smegmatis*; 6. *M. leprae*; 7. *M. marinum*; 8. *M. avium*; 9. *M. abscessus*; 10. *M. canetti*)

3.A.4.XIV. Pairwise Sequence Alignment of GroEl1 and GroEl2 protein from *Mycobacterium tuberculosis*

To identify the pairwise sequence similarity of GroEl1 and GroEl2 protein from Mtb strain was done using FASTA files of GroEl1 and GroEl2 were imported from UniProt database using Jalview software V 2.11.2.0. Every unique pair of sequences is implemented in MUSCLE [57], ClustalW [58], and computes the identity of each pair of sequences.

3.A.4.XV. Molecular Modelling

The crystal structure of M.tuberculosis GroEl2 (PDB: 1KP8) was downloaded from the Protein Data Bank (rcsb.org). All docking was conducted within Maestro v12.0.012 (Schrodinger LLC, New York, NY, 2020). Specifically, the protein was prepared using the Protein Preparation Wizard. Site ID was used to find potential binding pockets. The Receptor Grid-Generation was used to create a docking receptor using default parameters. Ligands were drawn in Maestro v12.0.012 (Schrodinger LLC, New York, NY, 2020) and prepared using ILgprep from the Schrodinger suite. These compounds were then docked into each receptor using the standard precision docking in Glide, with 10 poses to be written out for each ligand. Docks were then visually analyzed for their ability to cluster and their interactions. The energy was calculated using the refine protein-ligand complex within Prime (Schrödinger, LLC, New York, NY, 2020). Figures 7, A, and B were constructed using The PyMOL Molecular Graphics System, Version 4.6.0, Schrodinger, LLC.

3.A.5. References

1. Muñoz-Elías, Ernesto J., Juliano Timm, Tania Botha, Wai-Tsing Chan, James E. Gomez, and John D. McKinney. "Replication dynamics of Mycobacterium tuberculosis in chronically infected mice." *Infection and immunity* 73, no. 1 (2005): 546-551.
2. Rogerson, Brian J., Yu-Jin Jung, Ronald LaCourse, Lynn Ryan, Nicholas Enright, and Robert J. North. "Expression levels of Mycobacterium tuberculosis antigen-encoding genes versus production levels of antigen-specific T cells during stationary level lung infection in mice." *Immunology* 118, no. 2 (2006): 195-201.
3. McCune, Robert M., Floyd M. Feldmann, and Walsh McDermott. "Microbial persistence: II. Characteristics of the sterile state of tubercle bacilli." *The Journal of experimental medicine* 123, no. 3 (1966): 469-486.
4. Cong, Feng, Atwood K. Cheung, and Shih-Min A. Huang. "Chemical genetics-based target identification in drug discovery." *Annual review of pharmacology and toxicology* 52 (2012): 57-78.
5. Chaudhary, Preeti M., Sayalee R. Chavan, M. Kavitha, Shailaja P. Maybhate, Sunita R. Deshpande, Anjali P. Likhite, and P. R. Rajamohan. "Structural elucidation of propargylated products of 3-substituted-1, 2, 4-triazole-5-thiols by NMR techniques." *Magnetic Resonance in Chemistry* 46, no. 12 (2008): 1168-1174.

6. Bellamine, Aouatef, Galina I. Lepesheva, and Michael R. Waterman. "Fluconazole binding and sterol demethylation in three CYP51 isoforms indicate differences in active site topology." *Journal of lipid research* 45, no. 11 (2004): 2000-2007.
7. Song, Ming-Xia, and Xian-Qing Deng. "Recent developments on triazole nucleus in anticonvulsant compounds: a review." *Journal of enzyme inhibition and medicinal chemistry* 33, no. 1 (2018): 453-478.
8. Slivka, Mikhailo V., Natalia I. Korol, and Maksym M. Fizer. "Fused bicyclic 1, 2, 4-triazoles with one extra sulfur atom: Synthesis, properties, and biological activity." *Journal of Heterocyclic Chemistry* 57, no. 9 (2020): 3236-3254.
9. Vanjare, Balasaheb D., Prasad G. Mahajan, Nilam C. Dige, Hussain Raza, Mubashir Hassan, Yohan Han, Song Ja Kim, Sung-Yum Seo, and Ki Hwan Lee. "Novel 1, 2, 4-triazole analogues as mushroom tyrosinase inhibitors: synthesis, kinetic mechanism, cytotoxicity, and computational studies." *Molecular Diversity* 25, no. 4 (2021): 2089-2106.
10. Dunford, Adrian J., Kirsty J. McLean, Muna Sabri, Harriet E. Seward, Derren J. Heyes, Nigel S. Scrutton, and Andrew W. Munro. "Rapid P450 heme iron reduction by laser photoexcitation of Mycobacterium tuberculosis CYP121 and CYP51B1: analysis of CO complexation reactions and reversibility of the P450/P420 equilibrium." *Journal of Biological Chemistry* 282, no. 34 (2007): 24816-24824.
11. Kharb, Rajeev, Prabodh Chander Sharma, and Mohammed Shahar Yar. "Pharmacological significance of triazole scaffold." *Journal of enzyme inhibition and medicinal chemistry* 26, no. 1 (2011): 1-21.
12. Pagniez, Fabrice, Nicolas Lebouvier, Young Min Na, Isabelle Ourliac-Garnier, Carine Picot, Marc Le Borgne, and Patrice Le Pape. "Biological exploration of a novel 1, 2, 4-triazole-indole hybrid molecule as antifungal agent." *Journal of enzyme inhibition and medicinal chemistry* 35, no. 1 (2020): 398-403.
13. Kaur, P., and A. Chawla. "1, 2, 4-Triazole: a review of pharmacological activities." *Int. Res. J. Pharm* 8, no. 7 (2017): 10-29.
14. Guardiola-Diaz, Hebe M., Lisa-Anne Foster, Darren Mushrush, and Alfin DN Vaz. "Azole-antifungal binding to a novel cytochrome P450 from Mycobacterium tuberculosis: implications for treatment of tuberculosis." *Biochemical pharmacology* 61, no. 12 (2001): 1463-1470.

15. Gülerman, N. N., H. N. Doğan, S. Rollas, C. Johansson, and C. Celik. "Synthesis and structure elucidation of some new thioether derivatives of 1, 2, 4-triazoline-3-thiones and their antimicrobial activities." *Il Farmaco* 56, no. 12 (2001): 953-958.
16. Akhtar, Tashfeen, Shahid Hameed, Khalid M. Khan, Ajmal Khan, and Muhammad Iqbal Choudhary. "Design, synthesis, and urease inhibition studies of some 1, 3, 4-oxadiazoles and 1, 2, 4-triazoles derived from mandelic acid." *Journal of Enzyme Inhibition and Medicinal Chemistry* 25, no. 4 (2010): 572-576.
17. Wu, Jingde, Xinyong Liu, Xianchao Cheng, Yuan Cao, Defeng Wang, Zhong Li, Wenfang Xu, Christophe Pannecouque, Myriam Witvrouw, and Erik De Clercq. "Synthesis of novel derivatives of 4-amino-3-(2-furyl)-5-mercapto-1, 2, 4-triazole as potential HIV-1 NNRTIs." *Molecules* 12, no. 8 (2007): 2003-2016.
18. Moulin, Aline, Luc Demange, Joanne Ryan, Céline M'Kadmi, Jean-Claude Galleyrand, Jean Martinez, and Jean-Alain Fehrentz. "Trisubstituted 1, 2, 4-triazoles as ligands for the ghrelin receptor: on the significance of the orientation and substitution at position 3." *Bioorganic & medicinal chemistry letters* 18, no. 1 (2008): 164-168.
19. Gomez, James E., and John D. McKinney. "*M. tuberculosis* persistence, latency, and drug tolerance." *Tuberculosis* 84, no. 1-2 (2004): 29-44.
20. Gengenbacher, Martin, and Stefan HE Kaufmann. "*Mycobacterium tuberculosis*: success through dormancy." *FEMS microbiology reviews* 36, no. 3 (2012): 514-532.
21. Hughes, James P., Stephen Rees, S. Barrett Kalindjian, and Karen L. Philpott. "Principles of early drug discovery." *British journal of pharmacology* 162, no. 6 (2011): 1239-1249.
22. Blake, Robert A. "Target validation in drug discovery." In *High Content Screening*, pp. 367-377. Humana Press, 2007.
23. Sonawane, Amol D., Navnath D. Rode, Laxman Nawale, Rohini R. Joshi, Ramesh A. Joshi, Anjali P. Likhite, and Dhiman Sarkar. "Synthesis and biological evaluation of 1, 2, 4-triazole-3-thione and 1, 3, 4-oxadiazole-2-thione as antimycobacterial agents." *Chemical Biology & Drug Design* 90, no. 2 (2017): 200-209.
24. Rode, Navnath D., Amol D. Sonawane, Laxman Nawale, Vijay M. Khedkar, Ramesh A. Joshi, Anjali P. Likhite, Dhiman Sarkar, and Rohini R. Joshi. "Synthesis, biological evaluation, and molecular docking studies of novel 3-aryl-5-(alkyl-thio)-1H-1, 2, 4-triazoles

derivatives targeting Mycobacterium tuberculosis." *Chemical Biology & Drug Design* 90, no. 6 (2017): 1206-1214.

25. Sarkar, Sampa "Biochemical studies on the role of *M. tuberculosis* nitrate reductase during survival in host macrophages." Savitribai Phule Pune University, <http://hdl.handle.net/10603/139717> (2011).

26. Khan, Arshad, and Dhiman Sarkar. "A simple whole cell based high throughput screening protocol using Mycobacterium bovis BCG for inhibitors against dormant and active tubercle bacilli." *Journal of microbiological methods* 73, no. 1 (2008): 62-68.

27. Wayne, Lawrence G., and Charles D. Sohaskey. "Non-replicating persistence of Mycobacterium tuberculosis." *Annual Reviews in Microbiology* 55, no. 1 (2001): 139-163.

28. Jackson, Colin J., David C. Lamb, Timothy H. Marczylo, Josie E. Parker, Nigel L. Manning, Diane E. Kelly, and Steven L. Kelly. "Conservation and cloning of CYP51: a sterol 14 α -demethylase from Mycobacterium smegmatis." *Biochemical and biophysical research communications* 301, no. 2 (2003): 558-563.

29. Poupin, Pascal, Véronique Ducrocq, Sylvie Hallier-Soulier, and Nicole Truffaut. "Cloning and characterization of the genes encoding a cytochrome P450 (PipA) involved in piperidine and pyrrolidine utilization and its regulatory protein (PipR) in Mycobacterium smegmatis mc2155." *Journal of bacteriology* 181, no. 11 (1999): 3419-3426.

30. Sarkar D, Sarkar, S A Method of Screening Anti-Tubercular Compound. WIPO Patent Appl WO 2012/123971 A2 (2012).

31. Qamra, Rohini, and Shekhar C. Mande. "Crystal structure of the 65-kilodalton heat shock protein, chaperonin 60.2, of Mycobacterium tuberculosis." *Journal of bacteriology* 186, no. 23 (2004): 8105-8113.

32. Wang, J., and D. C. Boisvert. "Structural basis for GroEL-assisted protein folding from the crystal structure of (GroEL-KMgATP) 14 at 2.0 Å resolution." *Journal of molecular biology* 327, no. 4 (2003): 843-855.

33. Shahar, Anat, Meira Melamed-Frank, Yechezkel Kashi, Liat Shimon, and Noam Adir. "The dimeric structure of the Cpn60. 2 chaperonin of Mycobacterium tuberculosis at 2.8 Å reveals possible modes of function." *Journal of molecular biology* 412, no. 2 (2011): 192-203.

34. Aggarwal, Ranjana, and Garima Sumran. "An insight on medicinal attributes of 1, 2, 4-triazoles." *European journal of medicinal chemistry* 205 (2020): 112652.
35. Kong, Tim Hing, A. R. Coates, P. D. Butcher, C. J. Hickman, and T. M. Shinnick. "Mycobacterium tuberculosis expresses two chaperonin-60 homologs." *Proceedings of the National Academy of Sciences* 90, no. 7 (1993): 2608-2612.
36. Stewart, Graham R., Lorenz Wernisch, Richard Stabler, Joseph A. Mangan, Jason Hinds, Ken G. Laing, Douglas B. Young, and Philip D. Butcher. "Dissection of the heat-shock response in Mycobacterium tuberculosis using mutants and microarrays." *Microbiology* 148, no. 10 (2002): 3129-3138.
37. Monahan, Irene M., Joanna Betts, Dilip K. Banerjee, and Philip D. Butcher. "Differential expression of mycobacterial proteins following phagocytosis by macrophages. " *Microbiology* 147, no. 2 (2001): 459-471.
38. Lewthwaite, Jo C., Anthony RM Coates, Peter Tormay, Mahavir Singh, Paolo Mascagni, Stephen Poole, Michael Roberts, Lindsay Sharp, and Brian Henderson. "Mycobacterium tuberculosis chaperonin 60.1 is a more potent cytokine stimulator than chaperonin 60.2 (Hsp 65) and contains a CD14-binding domain." *Infection and immunity* 69, no. 12 (2001): 7349-7355.
39. Young, DOUGLAS B., and THOMAS R. Garbe. "Heat shock proteins and antigens of Mycobacterium tuberculosis." *Infection and immunity* 59, no. 9 (1991): 3086-3093.
40. Naffin-Olivos, Jacqueline L., Maria Georgieva, Nathan Goldfarb, Ranjna Madan-Lala, Lauren Dong, Erica Bizzell, Ethan Valinetz et al. "Mycobacterium tuberculosis Hip1 modulates macrophage responses through proteolysis of GroEL2." *PLoS pathogens* 10, no. 5 (2014): e1004132.
41. Georgieva, Maria, Jonathan Kevin Sia, Erica Bizzell, Ranjna Madan-Lala, and Jyothi Rengarajan. "Mycobacterium tuberculosis GroEL2 modulates dendritic cell responses." *Infection and immunity* 86, no. 2 (2018): e00387-17.
42. Fong, Jerry J., Karthik Sreedhara, Liwen Deng, Nissi M. Varki, Takashi Angata, Qinglian Liu, Victor Nizet, and Ajit Varki. "Immunomodulatory activity of extracellular Hsp70 mediated via paired receptors Siglec-5 and Siglec-14." *The EMBO journal* 34, no. 22 (2015): 2775-2788.

43. Washburn, Alex, Sanofar Abdeen, Yulia Ovechkina, Anne-Marie Ray, Mckayla Stevens, Siddhi Chitre, Jared Sivinski, et al. "Dual-targeting GroEL/ES chaperonin, and protein tyrosine phosphatase B (PtpB) inhibitors: A polypharmacology strategy for treating Mycobacterium tuberculosis infections." *Bioorganic & medicinal chemistry letters* 29, no. 13 (2019): 1665-1672.
44. Sarkar, D. Nitrite-Reductase (Nirb) as Potential Anti-Tubercular Target and a Method to Detect the Severity of Tuberculosis Disease. World Intellectual Property Organization Patent WO 2014/132263 A1, (2014).
45. Mcdonough, Kathleen A., Y. Kress, and B. R. Bloom. "Pathogenesis of tuberculosis: interaction of Mycobacterium tuberculosis with macrophages." *Infection and immunity* 61, no. 7 (1993): 2763-2773.
46. Sarkar, Sampa, and Dhiman Sarkar. "Potential use of nitrate reductase as a biomarker for the identification of active and dormant inhibitors of Mycobacterium tuberculosis in a THP1 infection model." *Journal of Biomolecular Screening* 17, no. 7 (2012): 966-973.
47. Meldal, Morten, and Christian Wenzel Tornøe. "Cu-catalyzed azide-alkyne cycloaddition." *Chemical reviews* 108, no. 8 (2008): 2952-3015.
48. Hong, Vu, Stanislav I. Presolski, Celia Ma, and M. G. Finn. "Analysis and optimization of copper-catalyzed azide-alkyne cycloaddition for bioconjugation." *Angewandte Chemie* 121, no. 52 (2009): 10063-10067.
49. Dan, Vipin Mohan, Vinodh JS, Sandesh CJ, Rahul Sanawar, Asha Lekshmi, R. Ajay Kumar, T. R. Santhosh Kumar, Uday Kiran Marelli, Syed G. Dastager, and M. Radhakrishna Pillai. "Molecular networking and whole-genome analysis aid discovery of an angucycline that inactivates mTORC1/C2 and induces programmed cell death." *ACS chemical biology* 15, no. 3 (2020): 780-788.
50. Wessel, D. M., and U. I. Flügge. "A method for the quantitative recovery of protein in dilute solution in the presence of detergents and lipids." *Analytical biochemistry* 138, no. 1 (1984): 141-143.
51. Bradford, N. J. A. B. "A rapid and sensitive method for the quantitation microgram quantities of a protein isolated from red cell membranes." *Anal. Biochem* 72, no. 248 (1976): e254.

52. Vila, Andrew, Keri A. Tallman, Aaron T. Jacobs, Daniel C. Liebler, Ned A. Porter, and Lawrence J. Marnett. "Identification of protein targets of 4-hydroxynonenal using click chemistry for ex vivo biotinylation of azido and alkynyl derivatives." *Chemical research in toxicology* 21, no. 2 (2008): 432-444.
53. Shevchenko, Andrej, Henrik Tomas, Jan Havli, Jesper V. Olsen, and Matthias Mann. "In-gel digestion for mass spectrometric characterization of proteins and proteomes." *Nature protocols* 1, no. 6 (2006): 2856-2860.
54. Ramdas, Vidya, Rashmi Talwar, Vijay Kanoje, Rajesh M. Loriya, Moloy Banerjee, Pradeep Patil, Advait Arun Joshi et al. "Discovery of Potent, Selective, and State-Dependent NaV1. 7 Inhibitors with Robust Oral Efficacy in Pain Models: Structure–Activity Relationship and Optimization of Chroman and Indane Aryl Sulfonamides." *Journal of medicinal chemistry* 63, no. 11 (2020): 6107-6133.
55. Silva, Jeffrey C., Richard Denny, Craig Dorschel, Marc V. Gorenstein, Guo-Zhong Li, Keith Richardson, Daniel Wall, and Scott J. Geromanos. "Simultaneous qualitative and quantitative analysis of the Escherichia coli proteome: A sweet tale." *Molecular & cellular proteomics* 5, no. 4 (2006): 589-607.
56. Waterhouse, Andrew M., James B. Procter, David MA Martin, Michèle Clamp, and Geoffrey J. Barton. "Jalview Version 2—a multiple sequence alignment editor and analysis workbench." *Bioinformatics* 25, no. 9 (2009): 1189-1191.
57. Edgar, Robert C. "MUSCLE: multiple sequence alignment with high accuracy and high throughput." *Nucleic acids research* 32, no. 5 (2004): 1792-1797.
58. Larkin, Mark A., Gordon Blackshields, Nigel P. Brown, R. Chenna, Paul A. McGettigan, Hamish McWilliam, Franck Valentin et al. "Clustal W and Clustal X version 2.0." *Bioinformatics* 23, no. 21 (2007): 2947-2948.

Chapter 3. B

*Identification of protein target for
RRA268 inhibitor within dormant
Mycobacterium tuberculosis*

3.B.1. Introduction:

Tuberculosis (TB) has been a major cause of death in developing and under-developing countries for many years [1,2]. About one-third of the world's population infected with Mtb exists in the dormant stage, with a 2-23% reactivation rate of cases [3,4]. TB is a treatable disease in most cases, but limited access to health care is a major hurdle for many people in emerging countries. Furthermore, the rise of drug-resistant strains against available drugs faces the risk of losing control of the disease. There are reports on drug-induced dormancy of the bacilli by creating stress using current first-line drugs such as rifampicin, isoniazid, streptomycin, and ethambutol [5-8]. Another problem is that the exposure of these frontline anti-TB drugs against dormant stage Mtb creates drug tolerance.

When Mtb encounters bactericidal drugs, tolerant Mtb cells are thus killed at a slower rate than the fully susceptible population from which they arose [9]. Various mechanisms are proposed by which Mtb can adapt to such conditions, including thickening of the cell wall, activation of efflux pumps, and altered expression of transcriptional regulators [10,11]. This is creating a question mark on the currently available anti-tubercular drug regimen. Moreover, the heterogeneity of mycobacterial populations in a single patient may also contribute to the inconsistency in treatment responses to the available drug regimen [12,13]. Under such conditions, there is an urgent need to adopt new strategies for controlling TB. Current regimens are afflicted with issues of patient nonfulfillment, insufficient health care mistakes, and increasing cases of drug-resistant strains, creating a significant need to create new strategies and drugs for cost-effective medication.

We have recently reported the biological activity of the 1,2,4-triazole derivatives against *Mycobacterium tuberculosis* and *M. bovis* BCG [14,15]. In continuation of our earlier findings, we pursued selected hits from this scaffold to further characterization for identification of their potential target in Mtb cell. In our earlier research, some hits have shown stage-specific inhibition in in-vitro and ex-vivo assays against Mtb; hence in the present study, we have a specific interest in further characterizing the selected hits against dormant stage Mtb. Furthermore, the availability of the classic Wayne hypoxia model to get the dormant Mtb culture that may mimic the internal environment of necrotic and cellular granulomas, respectively, motivated us to explore the possible target for the hits that specifically act on dormant stage Mtb. This hypoxia model is widely used and ideal for assessing novel compounds' activity under various hypoxic settings [16-18].

Azoles are one of the significant groups of nitrogen-containing heterocycles that showed numerous biological actions, for instance, anti-malarial, anti-bacterial, anti-HIV, anti-inflammatory, anti-fungal, and anti-TB properties [19,23]. Specifically, triazoles, including 1,2,3,-triazole, benzotriazole, triazolopyrimidines, and their derivatives, come up with interest in medicinal chemistry because of their stability towards metabolic degradation and ability to form hydrogen bond favoring the binding of biomolecular targets. Some drugs now available in market for use are based on triazoles exclusively of 1,2,3-triazole moiety such as antibiotic Cefatrizine, an anti-fungal agent, anti-bacterial agent Tazobactam, anti-cancer agent Carboxyamido-triazole (CAI) as well as anti-HIV agent (2',5'-bis-O-(tert-butyl)dimethylsilyl)-beta-D-ribofuranosyl]-3'-spiro-5''-(4''-amino-1'',2''-oxathiole-2'',2''-dioxide) thymine) TSAO [19-21]. The presence of azole moiety in the core structure of these drugs suggests that the azole scaffolds have a higher potential to develop anti-tubercular drugs. Furthermore, triazole derivatives are also considered as a new category of effective anti-TB agents due to their potential activities. Isoniazid (INH) is the best example of a triazole derivative used as an anti-tubercular drug [23].

Earlier efforts were made to develop drugs that act on the active stage Mtb. However, there is a lack of interest in controlling dormant/latent-TB infections, which is the leading cause of delayed treatment and rapid development of drug resistance. Slow in-vitro growth, a downshift in metabolic pathways, altered staining features, inability to be cultured on a solid medium, and resistance to standard antimycobacterial drugs are all characteristics of dormant bacilli [7]. Most of the population is infected with dormant Mtb, and chances of approximately 10 % dormant Mtb to reactivate, resulting in active, infectious TB cases throughout their life after the initial infection [24]. If we can control this dormant Mtb population, it will definitely help reduce the development of drug resistance and treatment time. Various new drugs are available on the market used explicitly to treat dormant-TB cases. Examples include the novel nitroimidazole PA-824 has exhibited excellent potency against dormant stage Mtb, and a well-accepted report in phase II scientific trial for treating TB-infected patients. In the meantime, 6-nitroimidazo(2,1-b)(1,3)oxazole delamanid (OPC67683) has newly received authorization for use against MDR-TB [25,26]. These findings suggest that compounds that are active against the dormant stage of Mtb could reduce the treatment time, and hence more attention is required during drug development that can act on dormant stage Mtb. Despite such developments in in-vitro and in-vivo studies, the challenge of discovering and confirming targets is reflected in the failure rate of drug

candidates in clinical trials due to inadequate knowledge of the mechanism of action and lack of information about the target in the pathogen.

We recently reported that RRA2 binds with intracellular GroEL2 protein as a potential target to exert its effect on both active and dormant Mtb bacilli [27]. Interestingly, other potent inhibitors from the same triazole scaffold do not bind the same target GroEL2 protein. Many of these compounds also showed a difference in stage specificity with respect to the change in the substitutions in the six-membered heterocyclic ring of the triazole moiety. This prompted us to extend our search for novel targets against other inhibitors of the same triazole class. Herein, we have explored the spectrum of activity of different RRA compounds against Gram-positive and Gram-negative bacterial strains. The same compounds were further evaluated for their cytotoxicity against standard cancer cell lines to ensure toxicity. In this study, we have used the RRA268 inhibitor to identify its protein target based on its significant inhibition, specifically against the dormant Mtb. Our results identified DNA binding protein HU as a primary target of RRA 268 inhibitor, which could be further used to develop therapies against TB.

3.B.2. Results:

3.B.2.1. Identification of 1,2,4-triazole derivatives against the active and dormant stage of *Mycobacterium tuberculosis*

From our triazole derivatives, we identified similar scaffolds of eight derivatives of 1,2,4-triazolethiol based on their inhibition against active and dormant stage Mtb. In the present study, the dose-dependent effect of the same eight derivatives (RRA2, RRA3, RRA4, RRA121, RRA267, RRA268, RRA226, and RRA232) were further screened using an in-vitro assay (XTTRMA assay) [28], and ex-vivo assay (nitrate reductase NR assay) [29] against the dormant stage Mtb (described in method section). From the screening results of Table 1, we have selected RRA268 because it acts against the dormant stage Mtb bacilli estimated from both the in-vitro and ex-vivo assay methods.

Table 1: Antimycobacterial activity of synthesized 1,2,4-triazole derivatives against the active and dormant stage of *Mycobacterium tuberculosis*

Compound Code	In-vitro activity against active stage Mtb	In-vitro activity against dormant stage Mtb	Ex-vivo activity against dormant stage Mtb
	MIC ($\mu\text{g/ml}$)	MIC ($\mu\text{g/ml}$)	MIC ($\mu\text{g/ml}$)
RRA2	15.67±1.65	9.64±07	6.09±2.55
RRA3	27.54±3.56	>30	>30
RRA4	>30	>30	>30
RRA121	>30	>30	>30
RRA226	>30	>30	>30
RRA232	>30	>30	>30
RRA267	0.46±0.01	>30	0.29±0.15
RRA268	>30	0.11±0.06	0.34±0.12
Rifampicin ^a	0.05±0.04	0.064±0.05	0.09±0.10
Isoniazid ^a	0.12±0.04	-	-

^a Positive control drugs; std 1) Rifampicin, 2) Isoniazid

3.B.2.2. The spectrum of activity of 1,2,4-triazole derivatives against non-mycobacterial species

The increasing gap between the use of anti-bacterial agents and their effectiveness against various pathogenic bacteria is due to widespread and unorganized use, which is a significant problem in controlling the disease [30]. Drugs having a broader and often unexpected range of biological activity may cause adverse effects, rendering their usage unsuitable for treatment. Thus, there is an urgent need to discover new compounds with proven antimicrobial activity, especially those with 1,2,4-triazole derivatives. In continuation of our work on evaluating the compounds against mycobacteria, we are interested in examining the

spectrum of activity of 1,2,4-triazole derivatives against different bacterial strains. Hence, eight derivatives (RRA2, RRA3, RRA4, RRA121, RRA267, RRA268, RRA226, and RRA232) that are used for anti-tubercular activity study were further screened for their spectrum of inhibitory activity against four bacterial strains, Gram-negative strains- *Escherichia coli*, *Pseudomonas aeruginosa* and Gram-positive strains- *Staphylococcus aureus* and *Bacillus subtilis*. None of the tested compounds had any significant effect on the growth of either tested bacterial strains up to the concentration of >100 µg/ml given in Table 2, which suggests that the compound's higher specificity toward Mtb can be explored further for potential anti-TB agents.

Table 2: Anti-bacterial activity of synthesized 1,2,4-triazole derivatives against non-mycobacterial species

Sr.No	Compound Code	Anti-bacterial Activity			
		Gram +ve bacteria MIC (µg/ml)		Gram - ve bacteria MIC (µg/ml)	
		<i>Staphylococcus aureus</i>	<i>Bacillus subtilis</i>	<i>Escherichia coli</i>	<i>Pseudomonas aeruginosa</i>
1	RRA2	>100	>100	>100	>100
2	RRA3	>100	>100	>100	>100
3	RRA4	>100	>100	>100	>100
4	RRA121	>100	>100	>100	>100
5	RRA226	>100	>100	>100	>100
6	RRA232	>100	>100	>100	>100
7	RRA267	>100	>100	>100	>100
8	RRA2268	>100	>100	>100	>100
	Ampicillin ^a	4.07±0.25	8.59±0.13	4.48±0.90	7.39±0.54
	Kanamycin ^a	9.48±0.77	5.68±0.63	3.97±0.94	2.92±0.10

^a Positive control drugs- 1) Ampicillin, 2) Kanamycin

3.B.2.3. In-vitro cytotoxicity of 1,2,4-triazole derivatives against human cancer cell lines

In-vitro toxicity screening models are based on the alteration of cell viability in several human cell lines [31]. These tests must be well-characterized and accurate predictors of in-vivo effects, with a low rate of false-positive or negative outcomes. Hits should be assessed for cytotoxicity before moving on in the discovery process. Herein, the eight derivatives of 1,2,4-triazole (RRA2, RRA3, RRA4, RRA121, RRA267, RRA268, RRA226, and RRA232) were further screened for in-vitro cytotoxicity against four human cancer cell lines namely, THP-1 (Human leukemia monocytic cell line), A549 (Human lung cancer cell line), PANC-1

(Human pancreatic cancer cell line), and HeLa (Human cervical cancer cell line) by 3-(4,5-dimethylthiazol-2-yl)-2,5-diphenyltetrazolium bromide (MTT) assay method [32,33]. None of the tested compounds had any significant cytotoxic effect on the growth of either tested human cancer cell line up to the concentration of >100 µg/ml given in Table 3, which suggests that the compounds are safe to use and can be explored further for potential anti-TB candidates.

Table 3: In-vitro cytotoxicity of synthesized 1,2,4-triazole derivatives against different human cancer cell lines

Sr. No	Compound Code	Cytotoxic- activity % GI ₅₀ ^a			
		THP-1 (Human leukemia monocytic cell line)	A549 (Human lung cancer cell line)	PANC-1 (Human pancreatic cancer cell line)	HeLa (Human cervical cancer cell line)
		(µg/ml)	(µg/ml)	(µg/ml)	(µg/ml)
1	RRA2	>100	>100	>100	>100
2	RRA3	>100	>100	>100	>100
3	RRA4	>100	>100	>100	>100
4	RRA121	>100	>100	>100	>100
5	RRA226	>100	>100	>100	>100
6	RRA232	>100	>100	>100	>100
7	RRA267	>100	>100	>100	>100
8	RRA268	>100	>100	>100	>100
	Paclitaxel ^b	0.093±0.3	0.084±0.07	5.394±0.18	0.077±0.04

^a Inhibitor concentrations responsible for 50 % growth inhibition were assessed by MTT assay at 72 h. The values were calculated with data from at least three independent experiments.

^b Positive control drug

3.B.2.4. Growth patterns in active and dormant cultures of *Mycobacterium tuberculosis*

At intervals, Wayne tubes containing Mtb culture were taken out for growth measurement at OD₆₂₀, and methylene blue decolorization was also monitored for up to 24 days (Figure 1.A. and 1.B.). Active Mtb culture growth was monitored simultaneously at OD₆₂₀ for 24 days. Similar patterns of growth curves were observed in both the replicates of active and dormant in-vitro cultures. Initial growth patterns were similar for up to 4 days in both active and dormant Mtb cultures (Figure 1.A.), but from 9th day onwards, growth remained at a stationary phase in the hypoxic culture tubes. Significant decolorization and reduction of methylene blue was observed on day 12 (Figure 1.B.), indicated achieving hypoxia confirmation as per the report mentioned earlier [35,57].

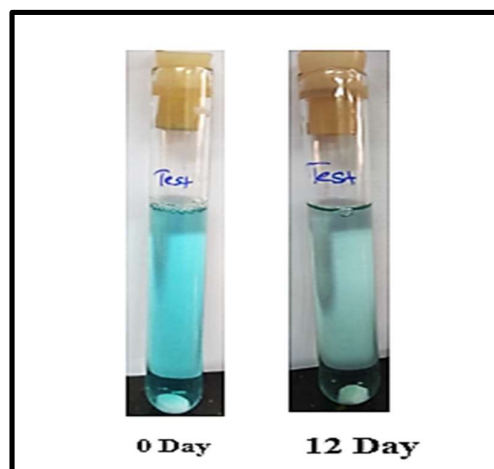
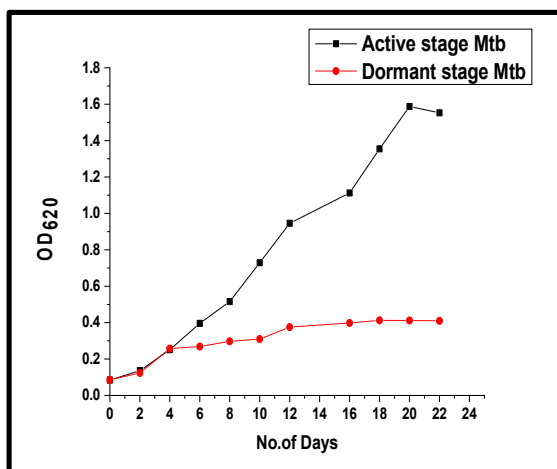


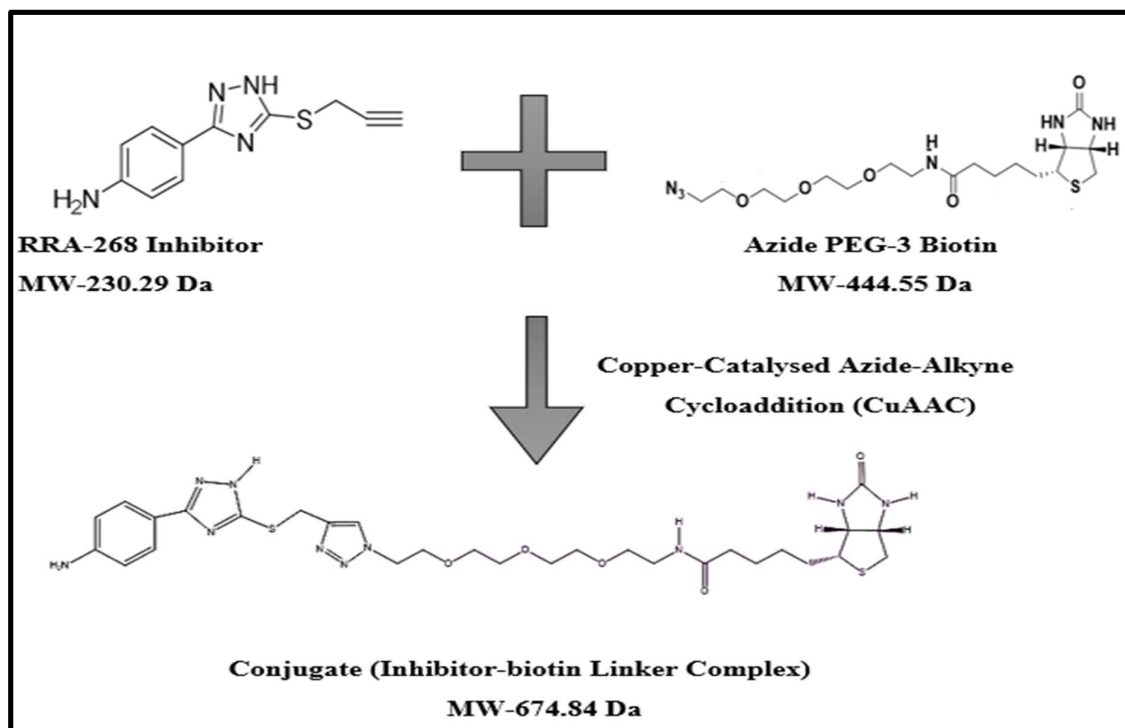
Figure 1. A. Growth curves for Mtb active and dormant cultures in duplicate over time course studied using Wayne hypoxia model [34]. Mean values with standard error from triplicate cultures are shown

Figure 1.B. O₂ depletion was monitored by reduction and decolorization of the methylene blue indicator [35]. Cultures were stirred with magnetic beads (8mm) at OD₆₂₀ are shown.

3.B.2.5. Synthesis of conjugate RRA268 compound and Biotin-linker conjugate

RRA268 compound possesses an acetylenic group in the side chain, which could be utilized in a copper-catalyzed alkyne-azide cycloaddition reaction, i.e., ‘click chemistry,’ with azide group present in one terminal of Azide-PEG3-Biotin to form a covalent linkage (Scheme 1). The conjugate (biotin-linker-RRA268) was purified using a preparative HPLC method, and then the mass was confirmed using Mass Spectrometric analysis.

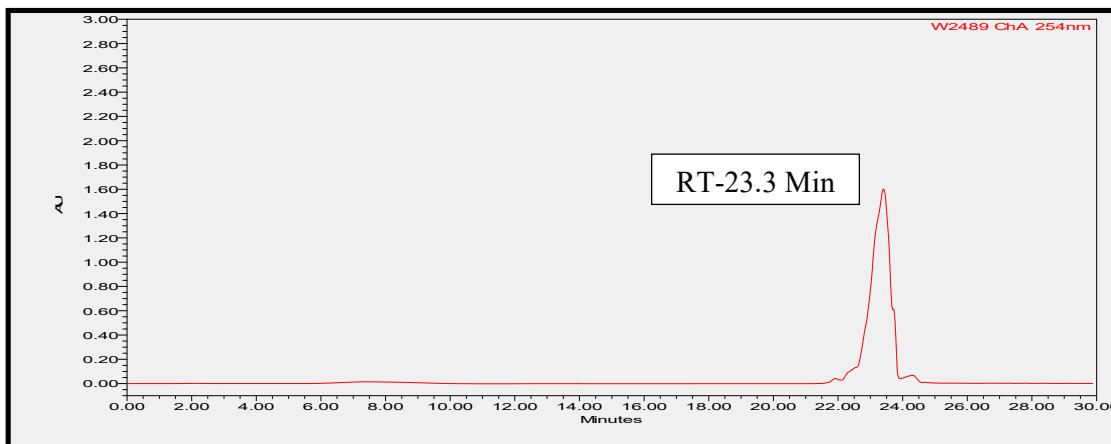
Scheme 1: Proposed mechanism for the synthesis of RRA268 compound Biotin-linker conjugate using copper-catalyzed Azide Alkyne Cycloaddition reaction



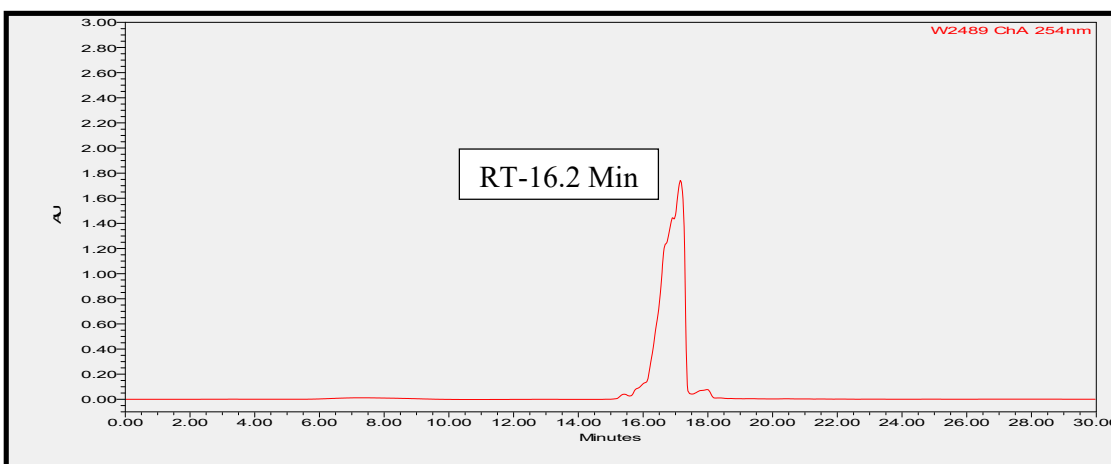
3.B.2.6. Purification of Biotin Linker-Inhibitor complex by HPLC

The reaction product (RRA268 compound and Biotin-linker conjugate) was collected in a 2 ml Eppendorf tube and allowed for solvent drying up in speed vac. for 30 min. The contents in the tube dissolved with DMSO and further purified from the rest of the substances by the preparative HPLC method, as shown in Figure 2. The retention time of the RRA268 inhibitor and biotin-linker were first standardized as 23.3 Min and 16.2 Min, respectively. One foreign pick was identified with an 11.5minute retention time (Figure 2. C) when the reaction product was injected and separated through the HPLC column using similar conditions.

A) Chromatogram of RRA268 inhibitor



B) Chromatogram of Azide PEG-3 Biotin



C) Chromatogram of Conjugate (inhibitor-biotin linker complex)

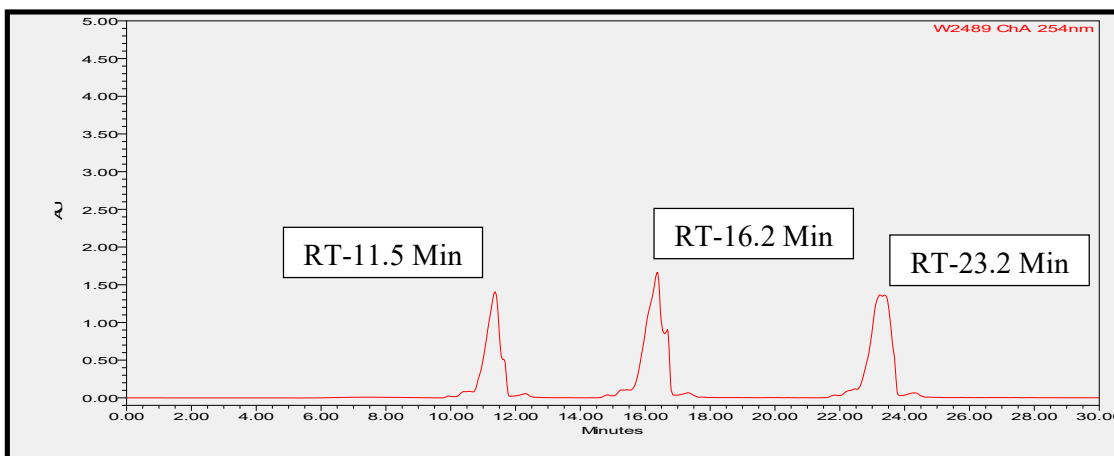


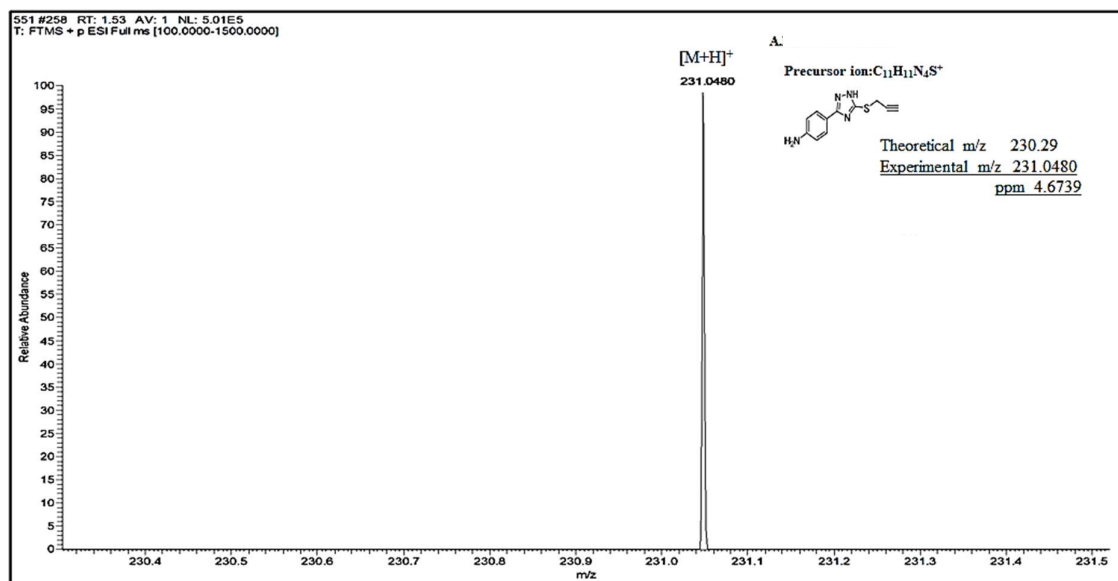
Figure 2. HPLC profile analysis Conjugate. Chromatogram of RRA268 at MIC concentration of 9.64 $\mu\text{g/ml}$ concentration (A), Azide PEG-3 biotin at 1 mg/ml (B), and the

reaction mixture containing biotin-inhibitor conjugate (C) were analyzed by preparative HPLC. The chromatograms represent a result obtained from three identical sets of each experiment. The details about the chromatography are provided in the “Materials and Methods” section.

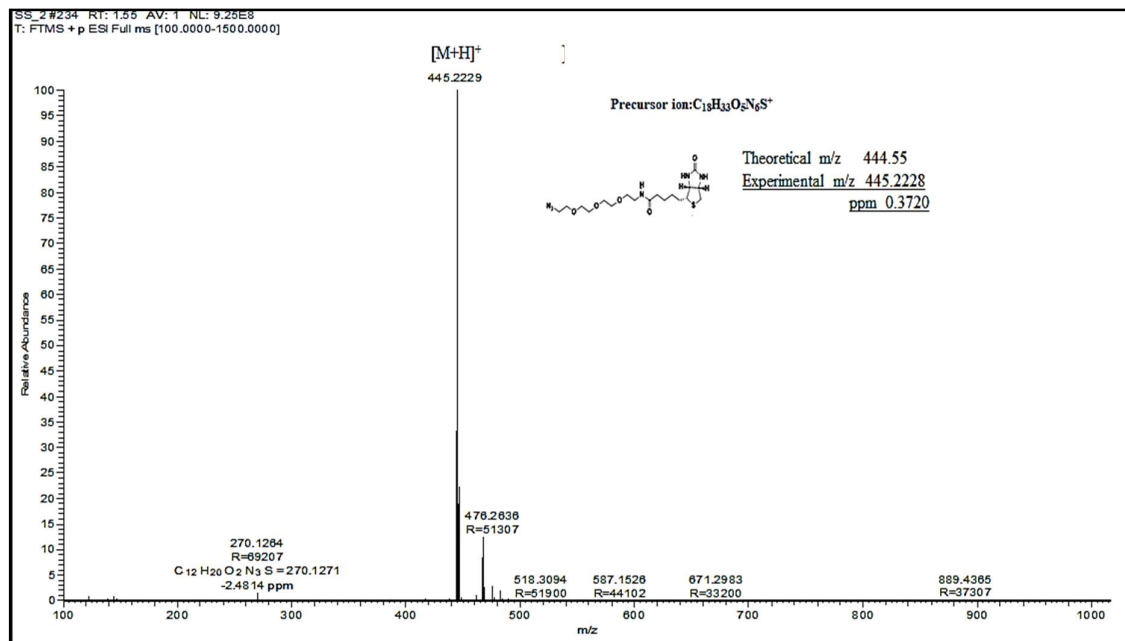
3.B.2.7. Confirmation of conjugate by HR-MS Analysis

The new peak at 11.5 min (Figure 3) separated during the HPLC analysis was collected and allowed for solvent evaporation in speed vac. for 30 min and further subjected to HR-MS analysis for estimation of molecular mass of the conjugate. The HR-MS analysis of the new peak was found to have a molecular mass of 675.51 Da, shown in Figure 3, C, confirming the formation of the Biotin linker-inhibitor conjugate from copper-catalyzed alkyne-azide cycloaddition reaction. Then, the product was collected and put together to do further experiments.

A) HR mass spectra for RRA268 inhibitor



B) HR mass spectra Azide PEG-3 Biotin



C) HR mass spectra for Conjugate (inhibitor-biotin linker complex)

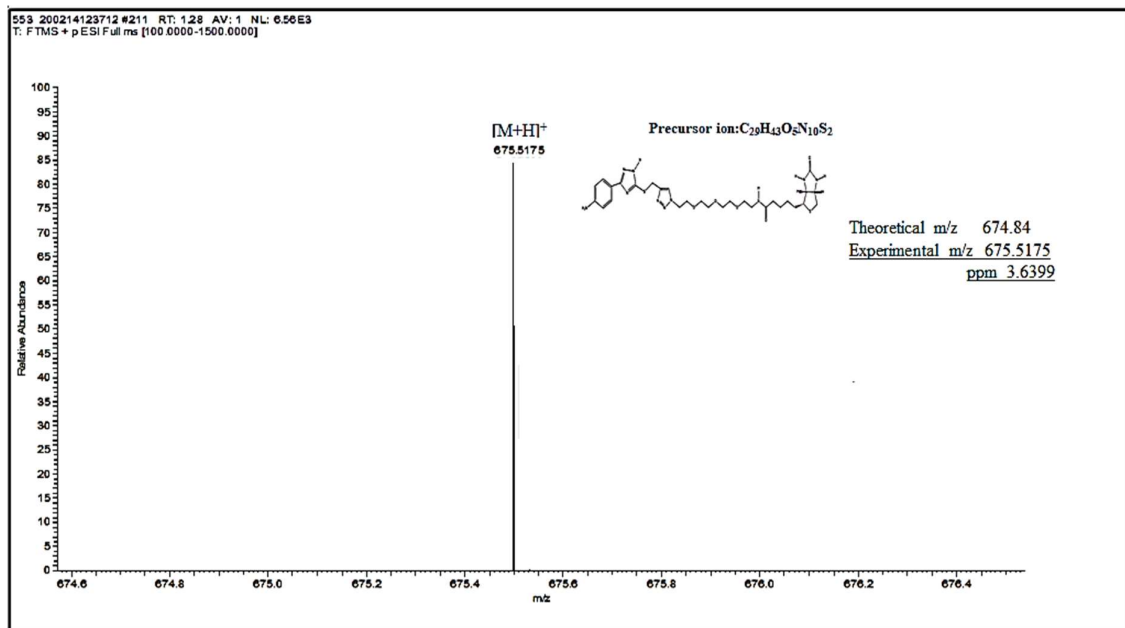


Figure 3. Mass confirmation by HR-MS analysis. HR mass spectra were obtained of only the HPLC peak elutes collected from RRA268 inhibitor (A), only Azide-PEG3-Biotin-linker (B), and conjugate (inhibitor-biotin linker complex) (C). The chromatograms represent a result obtained from three identical sets of each experiment.

3.B.2.8. Identification of target protein for RRA268 inhibitor from *Mycobacterium tuberculosis*

In order to aid future lead optimization of the RRA268 scaffold, the identification of the specific target of the RRA268 inhibitor was carried out using dormant Mtb culture. Due to the higher efficacy against dormant stage Mtb and the presence of the alkyne group, RRA 268 was selected to identify its specific target from the dormant stage of Mtb culture. Affinity pooling may be a classic and simple strategy for finding a protein target among the several approaches known for identifying the target of a novel compound [36,37].

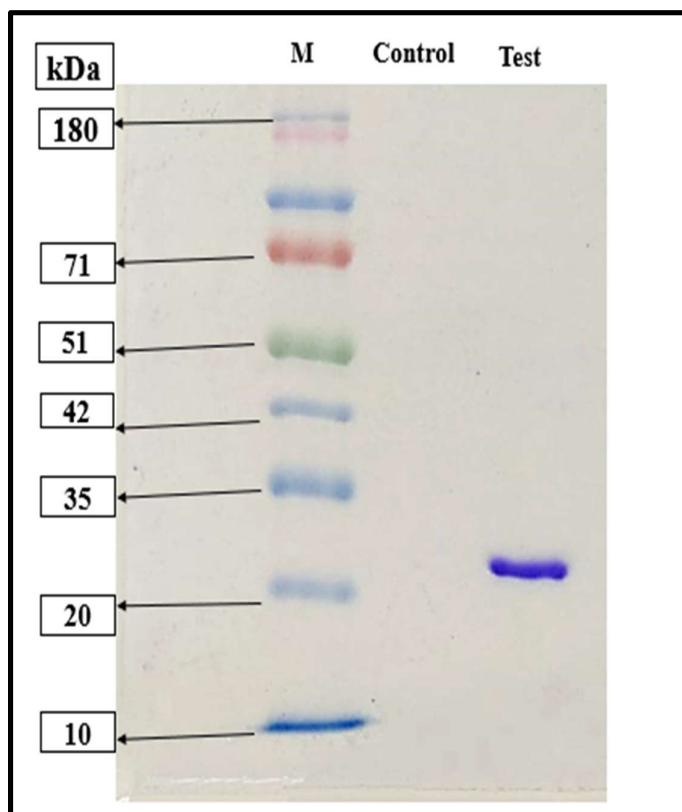


Figure 4. SDS-PAGE analysis of target protein isolated from *Mycobacterium tuberculosis*. The gel image represents the target protein obtained after being previously treated with RRA268 compound (Control), untreated with RRA268 compound (Test), and molecular weight protein markers (M).

SDS-PAGE analysis indicated a significant protein band at ~ 23 kDa molecular weight (Figure 4). As a control, we added biotin-linked-RRA268 to dormant Mtb culture previously treated with RRA268. Notably, no band was seen on the control lane, presumably

as RRA268 was already bound to the target protein's active site, leaving no room for conjugate (biotin-linked-RRA268) binding and subsequent pull-down.

Table 4. Identification of protein by LC-MS/MS Method

Accession	Entry	Description	mW (Da)	pI (pH)	PLGS Score	Peptides	Theoretical Peptides	Coverage (%)	Protein ID
A5U6Z 7	A5U6Z7 - MYCTA	DNA binding protein HU homolog OS <i>Mycobacterium tuberculosis</i> strain ATCC 25177 H37Ra OX 419947 G	22173	12.3589	1159.66	8	11	33.1776	3006

Table 5. Fragments Generated for the identified protein

Sequence	Retention Time (min)
(R)QATAAVENVVDTIVR(A)	9.7767
(K)AATKAPAR(K)	19.2952
(K)AELIDVLTQK(L)	9.2762
(K)GDSVTITGFGVFEQR(R)	9.8563
(K)AATKAPAKK(A)	18.9162
(R)LPAEGPAVK(R)	19.9649
(K)LGSDR(R)	16.6312
(I)TGFGVFEQR(R)	9.8616

3.B.2.9. Target Specificity analysis

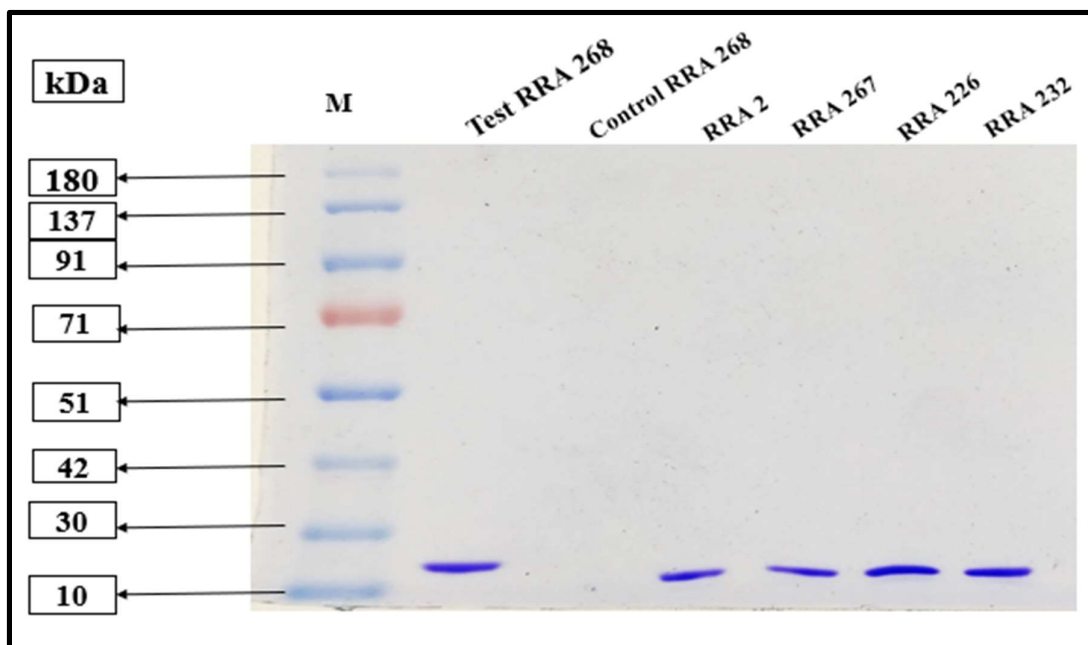


Figure 5. SDS-PAGE analysis of target protein by competing for the conjugate with other compounds. The purified conjugate was treated with the dormant Mtb culture already treated with RRA268 (control), RRA2, RRA267, RRA226, and RRA232, respectively. M represents different molecular weight protein markers. The result shown here is representative of three identical experiments.

Interestingly, each lane of Figure 5 showed a clear band at ~ 23 kDa representing the protein of the same molecular weight obtained in the presence of all four different compounds like test samples of RRA268 except in the control sample. Even though the other four representatives belonged to the same scaffold of 1,2,4-triazole, they had shown varied inhibitory effects against the active and dormant stage of Mtb. Compounds RRA226 and RRA232 are not inhibitors of Mtb, so they were used as a placebo and allowed to compete with the target protein. Even though the inhibitors RRA2 and RRA267 were allowed to compete with the target binding site, they showed similar results to the placebos. As the inhibitors (Compounds RRA2 and RRA267) are not competing with the RRA268 binding site of the target protein, it is concluded that their protein target sites are different. This result demonstrated the robust target specificity of the compound RRA268.

3.B.2.10. Multiple Sequence Alignment of DNA binding protein HU from different species of Mycobacteria

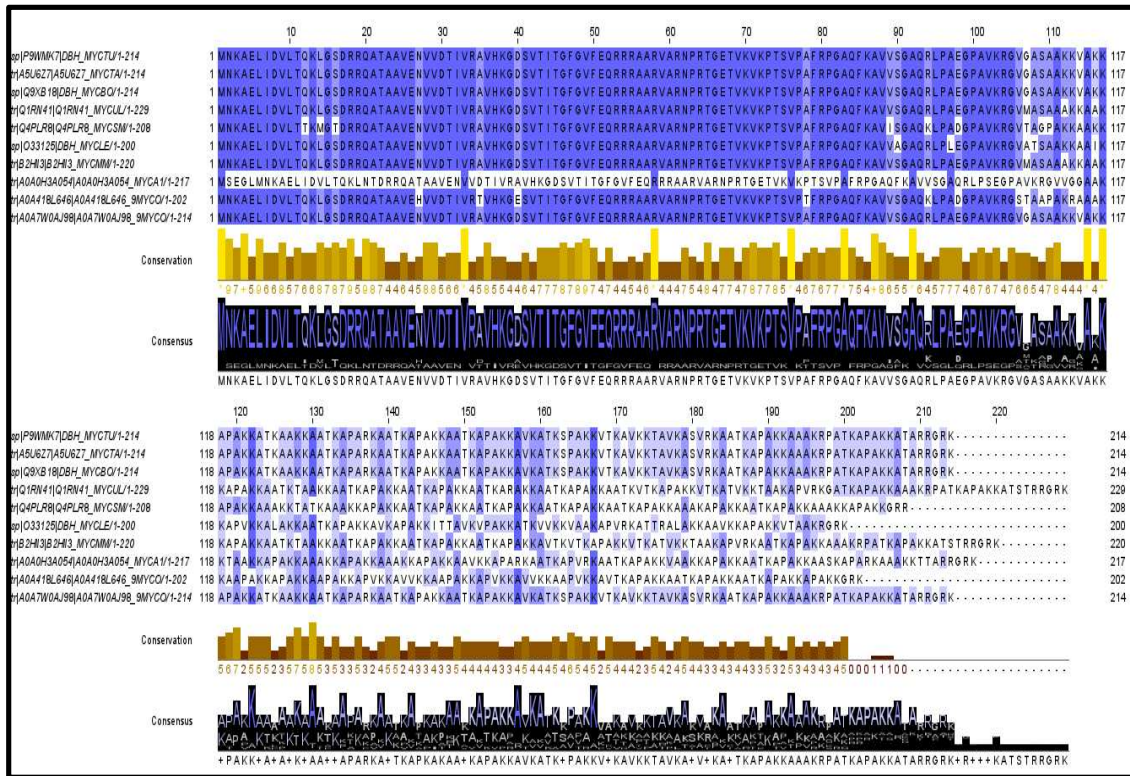


Figure 6 Multiple Sequence Alignment of DNA binding protein HU from different species of Mycobacteria Seq. Order: 1. *M. tuberculosis* H37RV; 2. *M. tuberculosis* H37Ra; 3. *M. bovis*; 4. *M. ulcerans*; 5. *M. smegmatis*; 6. *M. leprae*; 7. *M. marinum*; 8. *M. avium*; 9. *M. abscessus*; 10. *M. canettii*.

The Multiple Sequence Alignment (MSA) was manually edited in Jalview software V 2.11.2.0, a tool written in Java to analyze the residue conservation patterns (the analysis method is written in the materials and methods section). Once the sequence of DNA binding protein HU from 10 closely related Mycobacterial species has been clustered, the conservation patterns can be calculated and shown for each group (Figure 6). Each column in the alignment or group is given a score from 0 to 10 based on the common Physico-chemical properties of the residues (highlighted in Yellow color). The height of consensus between the sequence is related to the sequence similarity highlighted in multiple colors. MSA is often used to measure common features between sequence conservation of protein domains, tertiary and secondary structures, and even individual amino acids or nucleotides to find sequence similarity, homology, and evolutionary association. The degree of protein sequence

similarity is represented in dark blue to no color, where the dark blue color between the sequences represents 100 % similarity. In contrast, the regions where there is no blue color indicates that there is no similarity between the sequence.

3.B.2.11. Pairwise Sequence Alignment of DNA binding protein HU between *Mycobacterium tuberculosis* H37Rv and H37Ra

The pairwise sequence alignment (PSA) analysis between DNA binding protein HU from *Mycobacterium tuberculosis* H37 Ra and Rv strains was done using Jalview software V 2.11.2.0. The percentage identity score from our PSA was found to be 100. 100 % Sequence similarity (Figure 7) indicates that the proteins have identical sequences. In other words, RRA268 could be used to interact with the same target in the *Mycobacterium tuberculosis* H37Rv strain with equal efficiency and kill the pathogen in the animal model.

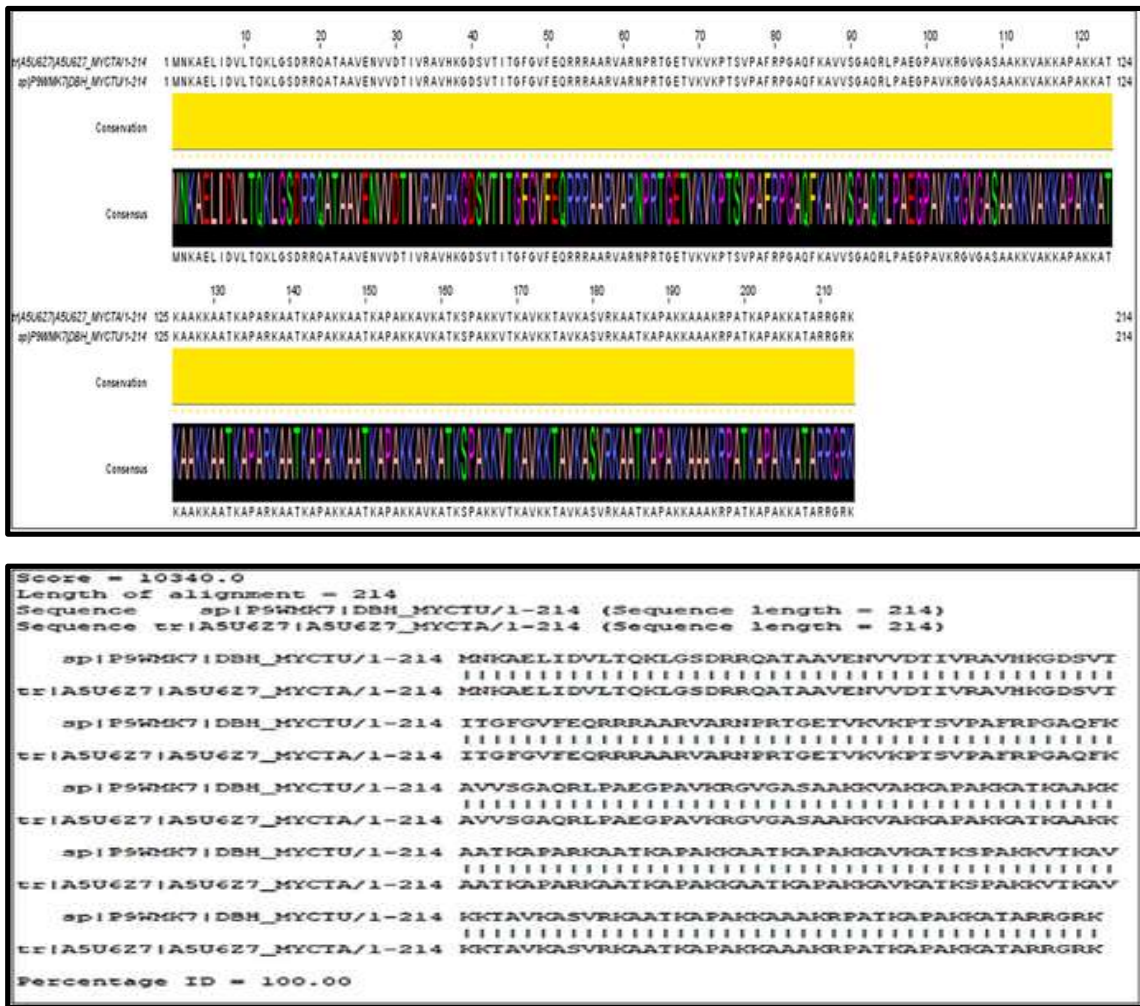


Figure 7. Pairwise Sequence Alignment of DNA binding protein HU between *Mycobacterium tuberculosis* H37Rv and H37Ra strains

3.B.2.12. Potential Binding mode of RRA268

Biochemical experiments on recombinant, purified HupB_{Mtb} showed that it exhibits properties of nucleoid-associated proteins (NAPs) in terms of non-specific DNA binding activity [38]. The HU protein is characterized by its interaction with DNA and plays an important role in regulating its expression. Our docking interaction has clearly indicated that RRA 268 interacts with HU protein into its DNA binding cleft in Figure 8. The compound showed the hydrogen bonding interaction with the Pro 77 and Phe 79 residues. The hydrophobic interaction is composed of interactions with the Pro 81, Phe 79, Ala 78, Pro 77, and Val 76. The compound also interacted with the basic positively charged residues of Arg 55, Arg 53, and Lys 86, as shown in Table 6. The study revealed that residues of DNA binding cleft might be essential for the activity of 1,2,4-triazole derivatives. Here, the computational (theoretical) prediction data from the molecular modelling study was replicated in target identification by the pull-down method.

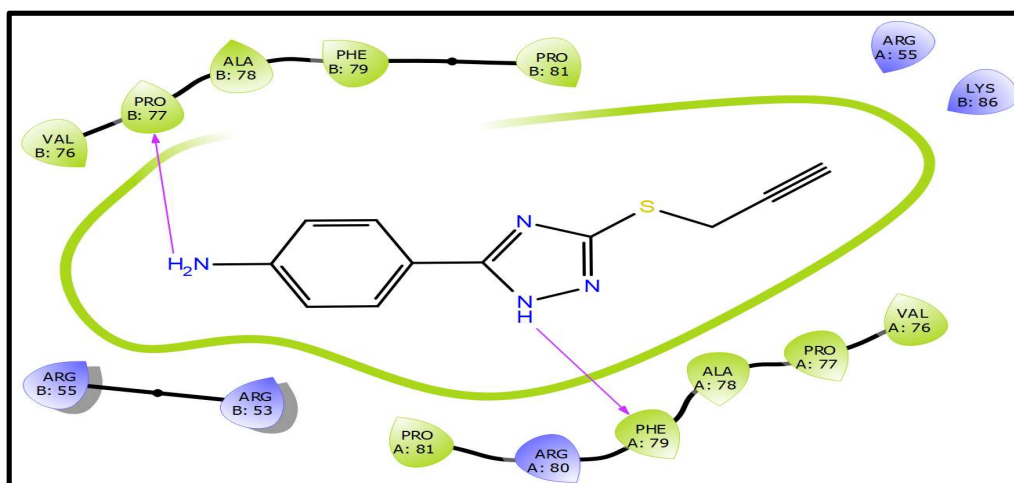


Figure 8. Interactions observed in the binding of compound RRA268 into the DNA-binding cleft

Table 6. Docking scores

Shown is the docking score for the highest-ranked solution. Notably, the lower the score, the better the dock is proposed to be.

Compound code	Docking Score (kcal/mol)	Binding interaction residues
RRA268	-3.107	Hydrogen bonding interaction with the Pro 77 and Phe 79 residues. The hydrophobic interaction with the Pro 81, Phe 79, Ala 78, Pro 77, and Val 76.

3.B.3. Discussion

Target identification and characterization started with the discovery of novel potent inhibitors to increase the understanding of the role of potential therapeutic targets (i.e., protein/gene/receptors/metabolites/enzymes) in the disease [39]. Various techniques are reported for target identification, such as affinity chromatography/affinity pull-down method, expression-cloning, protein microarray, phage, and mRNA display, biochemical suppression, siRNA, DNA microarray, reverse transfected cell microarray, and system biology [36,37]. Additionally, in-silico drug discovery uses machine-learning techniques to identify targets and their linked ligands deposited in multiple-target [40-42]. We have used the affinity pull-down method because of the commercial availability of different linkers and established methods to easily bind with the proposed candidate molecule and capture the target protein. Various classes of biomolecules such as enzymes, proteins, lipids, and DNA are identified as drug-target playing a crucial role in the growth of Mtb. Examples include the enoyl-acyl carrier protein reductase (InhA), a recognized anti-TB target involved in the biosynthesis of mycolic acids; it is also the target for isoniazid and ethionamide [43]. Bing Zhang and coworkers identified the drug target for SQ109 (in phase 2b-3 clinical trials) as Mycobacterial membrane proteins Large (MmpL3), which play crucial roles in transporting lipids, polymers, and immunomodulators using expression, purification, and crystallization techniques [44]. Furthermore, kinetic modelling of biochemical pathways was used to assess potential anti-Tb drug targets that interfere with the TCA cycle and glyoxylate bypass pathway enzymes of Mtb [45]. However, experimental confirmation of the projected targets for most of the compounds in the studies mentioned above is limited in many cases. Hence,

more studies are required to explore this area and understand the mechanism of candidate drugs.

In our study, compound RRA2 inhibited the active and dormant stage Mtb, and RRA268 specifically inhibited dormant stage Mtb. At the same time, the compound RRA2 used in the present study acts against both active and dormant stages of Mtb and is only known to bind specifically with groEL2 protein [27]. The spectrum of activity results confirmed the specificity of the selected compounds towards mycobacteria only (Table 2). Furthermore, the in-vitro cytotoxicity results found no toxic effect for the compounds tested for the concentration up to 100 µg/ml, suggesting the RRA compound's use for further in-vivo studies (Table 3). Our target specificity analysis found no competition between RRA2, RRA267, and RRA268 for the identified target HU protein (Figure 7). This proves that RRA 268 with a specific moiety such as the NH₂ group in the six-membered ring structure may play a crucial role in target (Hu protein) selection and binding compared with the other scaffold derivatives. Literature reports suggest that HU protein plays a significant role in different species at the beginning of DNA replication [46], SOS response cell division [47,48], and galactose metabolism [49]. It could play an essential role in inhibiting interaction with proteins and nucleic acids, ultimately leading to the global regulation of bacterial viability.

A recent study identified the core area within the HU-DNA edge that can be pursued as a drug target using stilbene derivatives. These derivatives specifically prevent HU-DNA binding, interrupt nucleoid architecture, and decrease Mtb growth; they ultimately have been suggested as a potential target for the development of therapies against TB [50]. However, these compound's target and action mechanisms have not been identified yet, which further complicates its usage for in-vivo studies during the drug discovery program. In our study, due to the higher efficacy against dormant stage Mtb (Table 1) and the presence of the alkyne group, RRA 268 was selected to identify its specific target from the dormant stage of Mtb culture. Furthermore, we identified the target for the RRA268 compound as HU protein by LC-MS/MS method (Table 4). Earlier studies explored the importance of the hupB gene (HU-coding gene; gene id: 15610123) to be essential for the growth of Mtb [51]. Another study highlighted the significance of HU protein and Lsr2 (a small, basic protein) in Mtb, wherein the HU protein and Lsr2 interact to form a complex and regulate the expression of

A/T-rich portions of the mycobacterial gene expression [52]. These studies suggest the important role of HU protein in the survival of Mtb and could be considered a drug target.

The importance of HU protein identified in the literature in bacterial metabolic cell cycles has been proven at the DNA, RNA, and protein levels. It is abundant among the most class of NAPs in bacterial metabolic cell cycles [53]. However, this raises a question about conservation patterns at the protein level. To address this, we have performed the MSA of HU protein found in different mycobacterial species. Our results from the MSA study found a significant difference in the sequence conservation pattern of HU protein analyzed through the MSA study when compared against ten closely related species of the same Mycobacteria. (Figure 6). It also has been suggested that HU protein is recognized as a transcription factor and controls the transcription regulation of expression of Hu protein [53]. Even though sequence conservation at the genome level, Hu protein can modulate the transcription and controls the expression of most of the other proteins [54,55]. These significant differences are further replicated in differences pertaining to structural, functional, and evolutionary relationships among closely related species of Mycobacteria. To understand this, we have done a pairwise sequence alignment study of HU protein and identified 100% similarity at the protein level in Mtb H37 Ra and Rv strain. This gives a hint for the evolutionary relationships and common patterns between the species of mycobacteria (Figure 7). Furthermore, our study on docking interactions of the RRA268 predicts the significance of the DNA binding cleft region required for anti-tubercular activity (Figure 8). Given the remarkable sequence conservation at the genome level found among HUs from various pathogenic mycobacterial species, including *M.bovis*, *M.lepre*, and other pathogenic actinobacteria, such as *Nocardia*, particularly at the N-terminal DNA binding region [50], we anticipate that the inhibitor design and drug-target identification strategy outlined in the present study can serve as a template to target HU protein in these organisms.

To summarise the present study, RRA268 showed significant inhibitory activity in both in-vitro and ex-vivo assays against dormant stage Mtb. The spectrum of activity study confirms its specificity towards mycobacteria. Furthermore, cytotoxicity results showed that RRA268 is less toxic and can be further explored in in-vivo studies. Using the affinity pull-down method and LC-MS/MS approach, we identified DNA binding protein HU as the target site of the RRA268 compound in dormant stage Mtb, and further possible interaction of RRA268 inhibitor predicted through molecular modeling studies. The findings of this study revealed

that the combined analysis was supportive of explaining RRA268's efficacy in suppressing Mtb cells and interpreting their likely mode of action. This study opens up new avenues to examine the role of HU protein as a possible target for drugs.

3.B.4. Materials and methods

3.B.4.1. Chemicals and materials

All the chemicals such as XTT, DMSO, rifampicin, isoniazid, and M phlei media components, including KH₂PO₄, trisodium citrate, MgSO₄, asparagine, and glycerol, were purchased from Sigma Aldrich USA unless otherwise mentioned. Dubos medium was purchased from DIFCO, USA. RPMI 1640 cell culture media and fetal bovine serum (FBS) were purchased from GIBCO, USA. Stock solutions (10mg/ml) of all the synthesized compounds were freshly prepared in DMSO and used the same day after mixing.

3.B.4.2. Bacterial strains, media, and inoculum preparation

M. tuberculosis H37Ra (ATCC 25177) was obtained from Astra Zeneca, Bangalore, India. The THP-1 (Human leukemia monocytic cell line), A 549 (Human lung cancer cell line), PANC-1 (Human pancreatic cancer cell line), and HeLa (Human cervical cancer cell line) were obtained from the National Center for Cell Science (NCCS), Pune, India. Subculturing of all mycobacterial strains was routinely done in Dubos albumin agar slants or plates. The stock was maintained at -70 °C and sub-cultured once in a liquid medium before inoculation in the experimental culture medium. The liquid inoculum was prepared in Dubos broth with 5 % glycerol, and 10 % Albumin dextrose catalase (ADC) enrichment medium, incubated in a shaker incubator rotating at a speed of 150 rpm at 37 °C till the logarithmic phase (OD₆₂₀ ~ 1.0) was reached. For in-vitro screening before inoculation to an experimental culture, Mtb was subcultured in M.pheli medium. The M.pheli medium contains 0.5 gm Potassium dihydrogen orthophosphate, 0.25 gm Sodium citrate, 60 mg Magnesium chloride, 0.5 gm Asparagine, and 2% (v/v) glycerol in 100 ml of distilled water at pH 6.6 ± 0.2. 1% of 1.0 OD₆₂₀ of the culture was used as standard inoculum size for all the experiments, yielding final inoculum of approximately 1X10⁵ CFU/ml.

3.B.4.3. In-vitro anti-tubercular activity of synthesized 1,2,4-triazole derivatives against the active and dormant stage of *Mycobacterium tuberculosis*

For anti-tubercular activity screening, stock solutions (10 mg/ml) of all the synthesized compounds were freshly prepared in DMSO and evaluated for their dose-response effect

against active and dormant stage Mtb using an established microplate-based technique using tetrazolium salt 2,3-bis[2-methoxy-4-nitro-5-sulphophenyl]-2H-tetrazolium-5-carboxanilide (XTT) and menadione to determine the viability of Mtb [28]. Briefly, 2.5 μ L of the test solution (10mg/ml) was added to 247.5 μ L of *M. phlei* medium containing bacilli and incubated for 8 days for the active stage and 12 days for the dormant stage at 37 °C. Post incubation, an XRMA assay was performed. The reduction of XTT is directly proportional to the cell concentration in the presence of menadione. This method allows rapid screening of inhibitors against mycobacterial cultures against active and dormant stage Mtb. Mtb culture was grown in *M. Phlei* broth up to the log phase and was subjected to brief sonication in a water bath sonicator to break the clumps. This sonicated culture was further used for inoculation in *M. Phlei* broth for assay, where the final assay volume was 250 μ L in each well of sterile 96 well plates, which helped to maintain the headspace ratio of 0.5 [34,56]. 200 μ M XTT was added to each well and incubated for 20 min at 37 °C. After incubation, 60 μ M menadione was added and incubated further at 37 °C for 40 min. The plate was read on SpectraMax Plus 384, Molecular Devices, Inc., using a 470 nm filter against a blank prepared from cell-free wells. MIC and IC₅₀ values of the selected compound were calculated from their dose-response curves by using OriginPro 2019b software. The assay was carried out in triplicates, and the percentage inhibition was calculated using a similar formula as per the described method below in the calculation of percent inhibition. The data shown are representative of three independent experiments.

3.B.4.4. Screening of 1,2,4-triazole derivatives against intracellular *M.tuberculosis* inside THP-1 macrophage by nitrate reductase assay (Ex-vivo assay).

THP-1 was used to examine the inhibitory activity of the compounds against intracellular bacilli by following a method described earlier [29]. Briefly, 3 mL of THP-1 cells ($\sim 5 \times 10^4$ cells/ml) were treated with 100 nM of phorbol myristate acetate (PMA) in a culture flask for 24 h to convert them into macrophages. These macrophages were further incubated for 12 h with *M. tuberculosis* H₃₇Ra at MOI (multiplicity of infection) of 1: 100 for infection. Extracellular bacilli were removed by washing twice with sterile PBS and then adding fresh medium to adhered cells. Compounds were then added to these infected macrophages at different concentrations. In order to check the effect of inhibitors on the growth of intracellular bacilli, compounds were added at 0 h (for identification of active stage inhibitors) and after 120 h (for identification of dormant stage inhibitors) of infection. Unless mentioned otherwise, the effect of the compound was monitored by determining the bacterial

load within macrophages by lysing them with hypotonic buffer (10 mM HEPES, 1.5 mM MgCl₂, and 10 mM KCl) at different time points and spreading 100 µL of the samples on Dubos agar plates to enumerate colonies after 21 days.

3.B.4.5. The spectrum of activity of 1,2,4-triazole derivatives against non-mycobacterial species

To determine the spectrum of activity against non-mycobacterial species, all the eight derivatives of 1,2,4-triazole (RRA2, RRA3, RRA4, RRA121, RRA267, RRA268, RRA226, and RRA232) were screened for their in-vitro anti-bacterial activity in 96-well plates against four bacterial strains (Gram-negative strains: *Escherichia coli* (NCIM 2065; ATCC 8739) and *Pseudomonas aeruginosa* (NCIM 5029; ATCC 27853); Gram-positive strains: *Staphylococcus aureus* (NCIM 2901; ATCC 29737) and *Bacillus subtilis* (NCIM 2920; ATCC 605) obtained from the National Collection of Industrial Microorganisms (NCIM), Pune, India. Once the cultures reached OD₆₂₀ of 1, 0.1 % of bacterial culture was used to determine anti-bacterial activity. The synthesized compounds were screened to monitor the dose-response effect and incubated for 8 h at 37 °C. Post-incubation OD₆₂₀ was measured for both Gram-positive and Gram-negative bacteria. The percentage inhibition was calculated using the following equation: percentage inhibition = [(absorbance of control-absorbance of the test sample)/ (absorbance of control - absorbance of blank)] X 100, where control denotes the medium with bacilli together with the vehicle, test denotes the medium with bacilli together with compound and blank denotes the cell-free medium. Here reference drugs in clinical use, Ampicillin and Kanamycin, served as standards, and DMSO was used as solvent control. The data shown are representative of three independent experiments.

3.B.4.6. In-vitro cytotoxicity of 1,2,4-triazole derivatives against human cancer cell lines

Eight derivatives of 1,2,4-triazole (RRA2, RRA3, RRA4, RRA121, RRA267, RRA268, RRA226, and RRA232) were further screened for in-vitro cytotoxicity against four human cancer cell lines namely, THP-1 (Human leukemia monocytic cell line), A 549 (Human lung cancer cell line), PANC-1 (Human pancreatic cancer cell line), and HeLa (Human cervical cancer cell line) by 3-(4,5-dimethylthiazol-2-yl)-2,5-diphenyltetrazolium bromide (MTT) assay method [32,33]. Briefly, the toxicity of the active compounds was done by examining their effect on the proliferation of the individual cell line. Briefly, 100 µL of cells from each cell line (5 × 10⁴ cells/ml) culture was dispensed in each 96-well plate, and 2.5 µL of each was added up to 10 × higher concentration of their MIC along with the inoculums in a dose-dependent manner and vehicle control. The cell culture plates were then incubated at 37 °C,

5% CO₂, 95% humidity-maintained incubator for three days. MTT assay was done after three days of incubation. Ten µL of MTT dye solution (5 mg/ml) was added to each well and incubated for one h in a humidified atmosphere (37 °C, 5% CO₂, 95%). 200 µL of isopropanol was added to each well and kept for four h to dissolve the formazan crystal. Thoroughly mix the formazan in the solvent and take the violet color absorbance of the culture at 490 nm to examine their effect on proliferation. The Paclitaxel was used as standard, and DMSO was used as vehicle control.

3.B.4.7. In-vitro culture method to generate (hypoxic) dormant *M.tuberculosis* cultures

A preliminary experiment was done to confirm limiting oxygen conditions in agitated liquid cultures of Mtb. To obtain dormant cultures, Mtb culture was grown in Dubos broth with 5 % glycerol, and 10 % Albumin dextrose catalase (ADC) enrichment medium, incubated in a shaker incubator rotating at a speed of 150 rpm at 37 °C till the logarithmic phase (OD₆₂₀ ~ 1.0) was reached. Wayne's in-vitro oxygen depletion method was followed to generate hypoxic (dormant) Mtb cultures [16,57]. Briefly, Mtb culture was grown in Dubos broth and inoculated in test tubes (20mm X 125 mm, with an overall fluid capacity of 25.5 ml). Test tubes were initially filled with 17 ml of Dubos broth containing Mtb culture leaving 8.5 ml of head space to give a head to air space ratio of 0.5. After inoculation, the tubes were tightly sealed through a sterile rubber septum and incubated at 37 °C. Sterile 8-mm Teflon -coated magnetic beads were added to each Wayne tube to gently stir the culture at 120 rpm. This stirring maintains the equal distribution, and the rate of O₂ depletion was under control.

The O₂ depletion was examined by the reduction and decolorization of the methylene blue indicator. A sterile solution of methylene blue (Sigma-Aldrich, St. Louis, MO, USA) was added at a final concentration of 1µg/ml into the Wayne tubes containing dormant Mtb culture at the beginning of incubation. Earlier reports highlighted the methylene blue reduction and decolorization in in-vitro cultures of Mtb when the oxygen concentration is declined below 3% [57]. Therefore, significant decolorization of methylene blue was considered to indicate oxygen depletion. Growth was measured at OD₆₂₀, and visual methylene blue decolorization (for dormant culture only) was also monitored for up to 24 days for both active and dormant cultures. Triplicate cultures of both active and dormant were set up during the study.

3.B.4.8. Preparation of Conjugate (RRA268-biotin linker conjugate)

Copper-catalysed alkyne-azide cycloaddition protocol was used to prepare biotin-linked RRA268 conjugate (RRA268-biotin linker) [58,59]. Briefly, Azide-PEG3-Biotin (5 mg/0.011 mmol) was dissolved in 0.5 mL anhydrous Tetrahydrofuran (THF) in a 5 mL round bottom test tube at room temperature. 0.5 ml copper sulphate solution (125 mmol) was added to this 5 mL test tube and mixed properly. Next, 10 mg of sodium ascorbate was added, and this complete solution was stirred on a magnetic stirrer at room temperature. A 2:1 ratio of RRA268 and Biotin was used for the reaction. So, 10 mg of the inhibitor was added to this reaction mixture, and the reaction was allowed to proceed and stirred for 8 h at room temperature.

3.B.4.9. Purification of Biotin Linker-Inhibitor complex by HPLC

Chromatographic separation and analysis of the product and components of the reaction were done using reverse-phase X bridge C₁₈ (5 μm, 46 x250 mm) column in preparative HPLC (binary pump-1525, UV detector-2489, sampler-2707, Waters, India). Organic solvents employed to prepare mobile phases were HPLC-grade, and the HPLC column used was reverse-phase X bridge C₁₈ (5 μM, 46x250 mm). The optimized mobile phase composition used was in, 'A' solution - water (100, 60, 60, 45, 40, 0) % and 'B' solution – acetonitrile (0, 40, 40, 55, 60, 100) %. The analysis was carried out in gradient elution mode at a 1 ml/min flow rate with column run-off monitored at 254 nm wavelength. The retention time for inhibitor RRA268 (Figure 3A) and Azide-PEG3-biotin (Figure 3B) were observed at 23.2 and 16.2min, respectively, which could help in comparison with the reaction mixture of the conjugate (Figure 3C). After injecting the reaction mixture of conjugate into the column, one foreign peak was observed at 11.5 min retention time along with the biotin and inhibitor peak. This foreign peak (Figure 3C) represented the neat conjugate (inhibitor-biotin linker complex) and was collected for further experiments.

3.B.4.10. Mass confirmation by HR-MS analysis

HR-MS analysis was done by the modified method as reported earlier [60]. The purified inhibitor-biotin linker complex was dissolved in acetonitrile (mass spectrometry grade) followed by separation using the Accela ultrahigh performance liquid chromatography (UHPLC) system (Thermo Fisher, Waltham, USA) using a C₁₈ Hypersil Gold column (3 μm, 3 × 100mm, Thermo fisher) coupled with a Q Executive- Orbitrap mass spectrometer (Thermo Fisher, Germany). The separation is carried out in optimized mobile phase

composition of solvent A (acetonitrile with 0.1% of formic acid) against 70-30% of solvent B (water with 0.1% of formic acid) at a flow rate of 500 $\mu\text{L}/\text{min}$ and a temperature of 45 °C for 5 min. The molecular weight was identified by electrospray ionization positive (ESI+) mode with a mass scan range set from 100 to 1500 m/z . The data acquisition and processing were performed using the Thermo Scientific Xcalibur software (version 3.0). The tandem mass spectrometry (data-dependent MS/MS) data were collected with collision energy between 30 and 40 eV. The raw data from the instrument were converted to the mzxml file format by using ProteoWizard. The mass confirmation was carried out with the HPLC purified fractions for RRA268 Inhibitor (Figure 4A), Azide-PEG3 Biotin (Figure 4B), and neat conjugate (Figure 4C), respectively, were then analyzed for mass confirmation by HR-MS method. The RRA268 Inhibitor (Figure 4A) and Azide-PEG3-Biotin (Figure 4B) showed their corresponding mass of 231.04 Da and 445.22 Da. The mass of neat conjugate was found at 675.51 Da, confirming the separation of the Biotin linker-inhibitor conjugate from the mixture. The confirmed mass of conjugate from HR-MS analysis helped to process for the next step of the experiment.

3.B.4.11. Binding of RRA268-Biotin conjugate with the dormant culture of *Mycobacterium tuberculosis*

The RRA268-Biotin conjugate obtained from HPLC purification was allowed to dry the solvent in speed vac for 30 min, dissolved in 100 μL DMSO, and finally added to the dormant Mtb culture. Using a sterile syringe and needle in an aseptic condition, the RRA268-Biotin conjugate dissolved in DMSO was added at MIC concentration through the tightly sealed septum of the Wayne tube. For dormant culture preparation, 5 mL spheroplast solution (0.0006%) was added in 0.4- 0.6 OD_{620} Mtb culture and incubated for 12-16 h. This Biotin linker-inhibitor conjugate was also added to the control culture, which was already treated with an RRA268 inhibitor. To bind the target protein, both control and test samples were kept for 30 minutes in an incubator shaker at 37 °C and 150 RPM. Both the cultures were sonicated in protein extraction buffer (100mM HEPES buffer, 5 mM EDTA 1 %, SDS, 100 mM NaCl 0.5%, Triton X-100, and freshly prepared 1% protease inhibitor cocktail) at 45 Hz with 10 Sec. pulse ON and 5 Sec. pulse OFF in ice-cold condition for 15 min and centrifuged the cell extract at 14,000 rpm for 1 h at 4 °C to get the intracellular protein in supernatant. The supernatant containing the target protein with Biotin-Inhibitor conjugate was taken out and dialyzed against PBS to remove the excess unbound Biotin-Inhibitor conjugate and inhibitor molecules at 25 °C for 3 h.

3.B.4.12. Purification of RRA268-Biotin conjugate tagged target Proteins by MagnaBind™ Streptavidin Beads

MagnaBind Streptavidin Beads are convenient for affinity purification or separation methods involving biotin-labeled molecules obtained from Thermo Scientific MagnaBind Streptavidin Beads (Cat. No. 21344) were added in the supernatant containing the target protein already bound with Biotin-Inhibitor conjugate allowed to pull down by using an external magnetic field overnight at 4 °C. Then, the beads were washed with sterile PBS 2-3 times to remove the unwanted proteins. To release our target protein attached with Biotin-Inhibitor conjugate, we added an excess of free 10 mM biotin molecule in shaking condition at 25 °C for 30 min before dialysis against water for 3 h. Dialyzed sample was collected and further processed for protein precipitation.

3.B.4.13. Chloroform-Methanol Precipitation of Target proteins

The chloroform-methanol precipitation method was followed to remove salt and detergents. 100 µL sample was added to 400 µL methanol, vortexed well, then 100 µL chloroform was added, and vortexed. 300 µL Milli Q water was added and again vortexed for 2 min Spin was given for 1 min at 14,000g. Removed the top aqueous layer (protein is between layers), then 400 µL methanol was added and vortexed. 2 min at 14,000 g spin was given and removed the MeOH without disturbing the pellet. The sample was dried in speed-Vac. and 1X sample buffer (125 mM Tris•HCl, pH 6.8, 20% Glycerol, 1% SDS, 10% β-Mercaptoethanol, 0.5 mg/ml Bromophenol Blue) was added for SDS-PAGE [61].

3.B.4.14. Protein estimation

Protein quantification was done by the Bradford method (Bio-Rad Protein Assay; Cat. No. 500-0006) according to the manufacturer's instructions (Bio-Rad, Hercules, CA) [62].

3.B.4.15. SDS-PAGE and Proteomic Analysis of Captured Proteins

Individual proteins in the sample were separated by carrying out SDS-PAGE (Figure 4) [63]. Briefly, 80 µg (5µL) of each protein sample was first mixed with 1X loading (sample) buffer containing 5% β-mercaptoethanol (Sigma, MO, USA). The samples were then incubated for 10 min at 80 °C. Next, 20 µL (64 µg) samples were loaded onto 12.5% Bis-Tris pre-cast polyacrylamide gels, and the SDS-PAGE was carried out using Mini-PROTEAN® Electrophoresis System-Bio-Rad (Catalog.1658000). After electrophoresis, the gel was subjected to Coomassie staining for overnight. Protein bands seen within the gel were

appropriately cut and subjected to trypsin digestion using the earlier protocol [64], followed by peptide extraction and proteomic analysis in Liquid chromatography-mass spectrometry (LC-MS).

3.B.4.16. Target specificity analysis

To determine the target specificity of RRA268, four-hit derivatives of 1,2,4-triazolethiols (RRA2, RRA267, RRA226, and RRA232) were selected from in-vitro screening (Table 1). These derivatives also have significant inhibitory activity against the active and dormant stage of Mtb H37Ra. Therefore, all these four compounds are specific compounds of either the active stage or dormant stage of the bacilli. To confirm the specificity of the RRA268 compound, the purified biotin linker-RRA268 conjugate was separately added to the dormant Mtb culture, which has already been treated with the RRA268 compound (control) and without the RRA268 compound (test) along with four similar scaffolds of 1,2,4-triazolethiols compounds (Table 1). A similar protocol was used to pull the purified target protein (mentioned in the above section) and perform the SDS-PAGE. Presumably, if all or any of the compounds had the same target as RRA268, it should not show any band in the SDS-PAGE because the target site is not available to bind to purified conjugate (Figure 5).

3.B.4.17. LC-MS analysis

2 μ L digested peptides with a final concentration of 100 ng/ μ L were analyzed by nano LC-MS using nanoACQUITY online coupled to SYNAPT HDMS system (Waters Corporation, MA, USA) equipped with a nanolockspray ion source with a flow rate of 300 nL/ min (external lock mass standard: Glu-fibrinopeptide) [65]. Peptide samples were injected online onto a 5 μ m Symmetry C18 trapping column (180 μ m x 2 cm length) at a flow rate of 15 μ L/min. Peptides were separated by in-line gradient elution onto BEH (Bridged Ethyl Hybrid) C-18 1.7 μ m x 75 μ m x 150 mm nanoACQUITY analytical column at a flow rate of 300 nL/ min using a linear gradient from 5 to 40% B over 35 min (A. 0.1% formic acid in water, B. 0.1% formic acid in acetonitrile). The acquisition was performed in positive V mode in a mass range of 50-1990 m/z with a scan time of 1 second with alternating low (5 eV) and high (15-40 eV) collision energy. MS data were processed with ProteinLynx Global Server (PLGS version 2.4. Waters Corporation, MA, USA). The processed data were allowed to search against the *Mycobacterium tuberculosis* H37Ra subset of the UniProt database containing all 44,987 protein entries for protein identification described by Silva et. al. [66].

3.B.4.18. Multiple Sequence Alignment of HU protein from different species of Mycobacteria

Multiple sequence alignment (MSA) is often used to measure common features between sequence conservation of protein domains, tertiary and secondary structures, and even individual amino acids or nucleotides to find sequence similarity, homology, and evolutionary association. The MSA was manually edited using default parameters in Jalview software V 2.11.2.0 [67]. FASTA files of HU protein were imported from the UniProt database for 10 closely related Mycobacterial species. (1. *M. tuberculosis* H37RV; 2. *M. tuberculosis* H37Ra; 3. *M. bovis*; 4. *M. ulcerans*; 5. *M. smegmatis*; 6. *M. leprae*; 7. *M. marinum*; 8. *M. avium*; 9. *M. abscessus*; 10. *M. canetti*)

3.B.4.19. Pairwise Sequence Alignment of HU protein from *Mycobacterium tuberculosis* H37Ra and Rv strain

To identify the pairwise sequence similarity of HU protein from *Mycobacterium tuberculosis*, H37 Ra and Rv strains were done using FASTA files of GroE11 and GroE12 were imported from the UniProt database using Jalview software V 2.11.2.0. Every unique pair of sequences is implemented in MUSCLE [68], ClustalW [69], and computes the identity of each pair of sequences.

3.B.4.20. Molecular Modelling

The docking study was performed in order to identify the crucial interactions between the protein structure of MtbHU and the target compound (RRA268). The protein structure with PDB ID: 4PT4 (<https://www.rcsb.org/structure/4PT4>), having better resolution (2.04 Å), was selected for our study. The entire study was performed using the trial version of the maestro software version 12.9 (Schrodinger_Suites_2021-3). The ligand was optimized using the OPLS4 force field in the LigPrep tool of the software. The protein structure was prepared using the protein preparation workflow. The prepared protein was further subjected to the grid generation step. The centroids of active site residues were specified for grid generation. The specified residues were comprised of core residues of DNA binding cleft, namely., Lys 3, Arg 53, 55, 58, 61, 64, 80, and Lys 86. Finally, the docking was performed using the glide module of the software using the standard precision method.

3.B.5. References

1. World Health Organization, Global tuberculosis report 2021. Geneva; World Health Organization, 2021.
2. Chakaya, Jeremiah, Mishal Khan, Francine Ntoumi, Eleni Aklillu, Razia Fatima, Peter Mwaba, Nathan Kapata et al. "Global Tuberculosis Report 2020—Reflections on the Global TB burden, treatment and prevention efforts." *International Journal of Infectious Diseases* 113 (2021): S7-S12.
3. Stead, William W., Gerald R. Kerby, Donald P. Schlueter, and Clarence W. Jordahl. "The clinical spectrum of primary tuberculosis in adults: confusion with reinfection in the pathogenesis of chronic tuberculosis." *Annals of internal medicine* 68, no. 4 (1968): 731-745.
4. Wayne, Lawrence G., and Charles D. Sohaskey. "Nonreplicating persistence of *Mycobacterium tuberculosis*." *Annual Reviews in Microbiology* 55, no. 1 (2001): 139-163.
5. Lecoecur, H. F., P. H. Lagrange, Ch Truffot-Pernot, M. Gheorghiu, and J. Grosset. "Relapses after stopping chemotherapy for experimental tuberculosis in genetically resistant and susceptible strains of mice." *Clinical and experimental immunology* 76, no. 3 (1989): 458.
6. McCune Jr, Robert M., Ralph Tompsett, and Walsh McDermott. "The fate of *Mycobacterium tuberculosis* in mouse tissues as determined by the microbial enumeration technique: II. The conversion of tuberculous infection to the latent state by the administration of pyrazinamide and a companion drug." *The Journal of experimental medicine* 104, no. 5 (1956): 763-802.
7. Alnimr, Amani M. "Dormancy models for *Mycobacterium tuberculosis*: A minireview." *Brazilian Journal of Microbiology* 46 (2015): 641-647.
8. McCune Jr, Robert M., and Ralph Tompsett. "Fate of *Mycobacterium tuberculosis* in mouse tissues as determined by the microbial enumeration technique: I. The persistence of drug-susceptible tubercle bacilli in the tissues despite prolonged antimicrobial therapy." *The Journal of experimental medicine* 104, no. 5 (1956): 737-762.
9. Balaban, Nathalie Q., Sophie Helaine, Kim Lewis, Martin Ackermann, Bree Aldridge, Dan I. Andersson, Mark P. Brynildsen et al. "Definitions and guidelines for research on antibiotic persistence." *Nature Reviews Microbiology* 17, no. 7 (2019): 441-448.

10. Goossens, Sander N., Samantha L. Sampson, and Annelies Van Rie. "Mechanisms of drug-induced tolerance in *Mycobacterium tuberculosis*." *Clinical Microbiology Reviews* 34, no. 1 (2020): e00141-20.
11. Adams, Kristin N., Kevin Takaki, Lynn E. Connolly, Heather Wiedenhoft, Kathryn Winglee, Olivier Humbert, Paul H. Edelstein, Christine L. Cosma, and Lalita Ramakrishnan. "Drug tolerance in replicating mycobacteria mediated by a macrophage-induced efflux mechanism." *Cell* 145, no. 1 (2011): 39-53.
12. Burger, Divan Aristo, and Robert Schall. "A Bayesian *nonlinear* mixed-effects regression model for the characterization of early bactericidal activity of tuberculosis drugs." *Journal of Biopharmaceutical Statistics* 25, no. 6 (2015): 1247-1271.
13. Barr, David A., Mercy Kamdolozi, Yo Nishihara, Victor Ndhlovu, Margaret Khonga, Geraint R. Davies, and Derek J. Sloan. "Serial image analysis of *Mycobacterium tuberculosis* colony growth reveals a persistent subpopulation in sputum during treatment of pulmonary TB." *Tuberculosis* 98 (2016): 110-115.
14. Sonawane AD, Rode ND, Nawale L, Joshi RR, Joshi RA, Likhite AP, Sarkar D. Synthesis and biological evaluation of 1,2,4-triazole-3-thione and 1,3,4-oxadiazole-2-thione as antimycobacterial agents. *Chem Biol Drug Des.* 2017 Aug;90(2):200-209. doi: 10.1111/cbdd.12939. Epub 2017 Feb 16.
15. Rode, Navnath D., Amol D. Sonawane, Laxman Nawale, Vijay M. Khedkar, Ramesh A. Joshi, Anjali P. Likhite, Dhiman Sarkar, and Rohini R. Joshi. "Synthesis, biological evaluation, and molecular docking studies of novel 3-aryl-5-(alkyl-thio)-1H-1, 2, 4-triazoles derivatives targeting *Mycobacterium tuberculosis*." *Chemical Biology & Drug Design* 90, no. 6 (2017): 1206-1214.
16. Wayne, Lawrence G., and Ladonna G. Hayes. "An in-vitro model for sequential study of shift-down of *Mycobacterium tuberculosis* through two stages of nonreplicating persistence." *Infection and immunity* 64, no. 6 (1996): 2062-2069.
17. Piccaro, Giovanni, Federico Giannoni, Perla Filippini, Alessandro Mustazzolu, and Lanfranco Fattorini. "Activities of drug combinations against *Mycobacterium tuberculosis* grown in aerobic and hypoxic acidic conditions." *Antimicrobial agents and chemotherapy* 57, no. 3 (2013): 1428-1433.

18. Iona, Elisabetta, Federico Giannoni, Manuela Pardini, Lara Brunori, Graziella Orefici, and Lanfranco Fattorini. "Metronidazole plus rifampin sterilizes long-term dormant *Mycobacterium tuberculosis*." *Antimicrobial agents and chemotherapy* 51, no. 4 (2007): 1537-1540.
19. Kumar, Vinod, Kamalneet Kaur, Girish Kumar Gupta, and Anil Kumar Sharma. "Pyrazole containing natural products: Synthetic preview and biological significance." *European Journal of Medicinal Chemistry* 69 (2013): 735-753.
20. Nagesh, Hunsur Nagendra, Kalaga Mahalakshmi Naidu, Damarla Harika Rao, Jonnalagadda Padma Sridevi, Dharmarajan Sriram, Perumal Yogeewari, and Kondapalli Venkata Gowri Chandra Sekhar. "Design, synthesis and evaluation of 6-(4-((substituted-1H-1, 2, 3-triazol-4-yl) methyl) piperazin-1-yl) phenanthridine analogues as antimycobacterial agents." *Bioorganic & medicinal chemistry letters* 23, no. 24 (2013): 6805-6810.
21. Nakashima, Emi, Akira Tsuji, Masato Nakamura, and Tsukinaka Yamana. "Physicochemical properties of amphoteric β -lactam antibiotics. IV. First-and second-order degradations of cefaclor and cefatrizine in aqueous solution and kinetic interpretation of the intestinal absorption and degradation of the concentrated antibiotics." *Chemical and pharmaceutical bulletin* 33, no. 5 (1985): 2098-2106.
22. Lewis, Robert P., Richard D. Meyer, and Linda L. Kraus. "Anti-bacterial activity of selected beta-lactam and aminoglycoside antibiotics against cephalothin-resistant Enterobacteriaceae." *Anti-microbial Agents and Chemotherapy* 9, no. 5 (1976): 780-786.
23. Keri, Rangappa S., Siddappa A. Patil, Srinivasa Budagumpi, and Bhari Mallanna Nagaraja. "Triazole: a promising antitubercular agent." *Chemical biology & drug design* 86, no. 4 (2015): 410-423.
24. Stead, William W. "Pathogenesis of a first episode of chronic pulmonary tuberculosis in man: recrudescence of residuals of the primary infection or exogenous reinfection?." *American Review of Respiratory Disease* 95, no. 5 (1967): 729-745.
25. Sutherland, Hamish S., Adrian Blaser, Iveta Kmentova, Scott G. Franzblau, Baojie Wan, Yuehong Wang, Zhenkun Ma, Brian D. Palmer, William A. Denny, and Andrew M. Thompson. "Synthesis and structure-activity relationships of anti-tubercular 2-nitroimidazooxazines bearing heterocyclic side chains." *Journal of medicinal chemistry* 53, no. 2 (2010): 855-866.

26. Quan, Diana, Gayathri Nagalingam, Richard Payne, and James A. Triccas. "New tuberculosis drug leads from naturally occurring compounds." *International Journal of Infectious Diseases* 56 (2017): 212-220.
27. Sarkar, Sampa, Sagar Swami, Sarvesh Kumar Soni, Jessica K. Holien, Arshad Khan, Arvind M. Korwar, Anjali P. Likhite, Ramesh A. Joshi, Rohini R. Joshi, and Dhiman Sarkar. "Detection of a target protein (GroEl2) in Mycobacterium tuberculosis using a derivative of 1, 2, 4-triazolethiols." *Molecular Diversity* (2021): 1-14.
28. Singh, Upasana, Shamim Akhtar, Abhishek Mishra, and Dhiman Sarkar. "A novel screening method based on menadione mediated rapid reduction of tetrazolium salt for testing of anti-mycobacterial agents." *Journal of microbiological methods* 84, no. 2 (2011): 202-207.
29. Sarkar, Sampa, and Dhiman Sarkar. "Potential use of nitrate reductase as a biomarker for the identification of active and dormant inhibitors of Mycobacterium tuberculosis in a THP1 infection model." *Journal of Biomolecular Screening* 17, no. 7 (2012): 966-973.
30. Gao, Feng, Tengfei Wang, Jiaqi Xiao, and Gang Huang. "Anti-bacterial activity study of 1, 2, 4-triazole derivatives." *European journal of medicinal chemistry* 173 (2019): 274-281.
31. Bácskay, Ildikó, Dániel Nemes, Ferenc Fenyvesi, Judit Váradi, Gábor Vasvári, Pálma Fehér, Miklós Vecsernyés, and Zoltán Ujhelyi. *Role of cytotoxicity experiments in pharmaceutical development*. InTech: London, UK, 2018.
32. Molinari, Aurora, Alfonso Oliva, Claudia Ojeda, José M. Miguel del Corral, M. Angeles Castro, Carmen Cuevas, and Arturo San Feliciano. "Synthesis and Cytotoxic Evaluation of 6-(3-Pyrazolylpropyl) Derivatives of 1, 4-Naphthohydroquinone-1, 4-diacetate." *Archiv der Pharmazie: An International Journal Pharmaceutical and Medicinal Chemistry* 342, no. 10 (2009): 591-599.
33. Manjula, S. N., N. Malleshappa Noolvi, K. Vipani Parihar, SA Manohara Reddy, Vijay Ramani, Andanappa K. Gadad, Gurdial Singh, N. Gopalan Kutty, and C. Mallikarjuna Rao. "Synthesis and antitumor activity of optically active thiourea and their 2-aminobenzothiazole derivatives: A novel class of anticancer agents." *European Journal of Medicinal Chemistry* 44, no. 7 (2009): 2923-2929.
34. Wayne, Lawrence G., and Ladonna G. Hayes. "An in vitro model for sequential study of shift-down of Mycobacterium tuberculosis through two stages of nonreplicating persistence." *Infection and immunity* 64, no. 6 (1996): 2062-2069.

35. Leistikow, Rachel L., Russell A. Morton, Iona L. Bartek, Isaac Frimpong, Karleen Wagner, and Martin I. Voskuil. "The Mycobacterium tuberculosis DosR regulon assists in metabolic homeostasis and enables rapid recovery from nonrespiring dormancy." *Journal of bacteriology* 192, no. 6 (2010): 1662-1670.
36. Cuatrecasas, Pedro. "Affinity chromatography and purification of the insulin receptor of liver cell membranes." *Proceedings of the National Academy of Sciences* 69, no. 5 (1972): 1277-1281.
37. Field, Stephen K. "Bedaquiline for the treatment of multidrug-resistant tuberculosis: great promise or disappointment?." *Therapeutic advances in chronic disease* 6, no. 4 (2015): 170-184.
38. Kumar, Sandeep, Abhijit A. Sardesai, Debashree Basu, Kalappagowda Muniyappa, and Seyed E. Hasnain. "DNA clasping by mycobacterial HU: the C-terminal region of HupB mediates increased specificity of DNA binding." *PLoS One* 5, no. 9 (2010): e12551.
39. Gashaw, Isabella, Peter Ellinghaus, Anette Sommer, and Khusru Asadullah. "What makes a good drug target?." *Drug discovery today* 16, no. 23-24 (2011): 1037-1043.
40. Chen, Xing, Chenggang Clarence Yan, Xiaotian Zhang, Xu Zhang, Feng Dai, Jian Yin, and Yongdong Zhang. "Drug–target interaction prediction: databases, web servers, and computational models." *Briefings in bioinformatics* 17, no. 4 (2016): 696-712.
41. Yao, Zhi-Jiang, Jie Dong, Yu-Jing Che, Min-Feng Zhu, Ming Wen, Ning-Ning Wang, Shan Wang, Ai-Ping Lu, and Dong-Sheng Cao. "TargetNet: a web service for predicting potential drug–target interaction profiling via multi-target SAR models." *Journal of computer-aided molecular design* 30, no. 5 (2016): 413-424.
42. Rifaioglu, Ahmet Sureyya, Esra Nalbat, Volkan Atalay, Maria Jesus Martin, Rengul Cetin-Atalay, and Tunca Doğan. "DEEPScreen: high performance drug–target interaction prediction with convolutional neural networks using 2-D structural compound representations." *Chemical science* 11, no. 9 (2020): 2531-2557.
43. Takayama, Kuni, Lynn Wang, and Hugo L. David. "Effect of isoniazid on the in vivo mycolic acid synthesis, cell growth, and viability of Mycobacterium tuberculosis." *Antimicrobial agents and chemotherapy* 2, no. 1 (1972): 29-35.

44. Zhang, Bing, Jun Li, Xiaolin Yang, Lijie Wu, Jia Zhang, Yang Yang, Yao Zhao et al. "Crystal structures of membrane transporter MmpL3, an anti-TB drug target." *Cell* 176, no. 3 (2019): 636-648.
45. Singh, Vivek Kumar, and Indira Ghosh. "Kinetic modeling of tricarboxylic acid cycle and glyoxylate bypass in Mycobacterium tuberculosis, and its application to assessment of drug targets." *Theoretical Biology and Medical Modelling* 3, no. 1 (2006): 1-11.
46. Bonnefoy, Eliette, and Josette Rouvière-Yaniv. "HU, the major histone-like protein of E. coli, modulates the binding of IHF to oriC." *The EMBO journal* 11, no. 12 (1992): 4489-4496.
47. Preobrajenskaya, Olga, Annie Boullard, Fatima Boubrik, Manfred Schnarr, and Josette Rouvière-Yaniv. "The protein HU can displace the LexA repressor from its DNA-binding sites." *Molecular microbiology* 13, no. 3 (1994): 459-467.
48. Oberto, Jacques, Sabrina Nabti, Valerie Jooste, Herve Mignot, and Josette Rouvière-Yaniv. "The HU regulon is composed of genes responding to anaerobiosis, acid stress, high osmolarity and SOS induction." *PloS one* 4, no. 2 (2009): e4367.
49. Aki, Tsunehiro, Hyon E. Choy, and Sankar Adhya. "Histone-like protein HU as a specific transcriptional regulator: co-factor role in repression of gal transcription by GAL repressor." *Genes to Cells* 1, no. 2 (1996): 179-188.
50. Bhowmick, T., Ghosh, S., Dixit, K., Ganesan, V., Ramagopal, U.A., Dey, D., Sarma, S.P., Ramakumar, S. and Nagaraja, V., 2014. Targeting Mycobacterium tuberculosis nucleoid-associated protein HU with structure-based inhibitors. *Nature communications*, 5(1), pp.1-13.
51. Bhowmick, Tuhin. "Crystal Structure Of Mycobacterium Tuberculosis Histone Like Protein HU And Structure-Based Design Of Molecules To Inhibit MtbHU-DNA Interaction: Leads For A New Target. Structure Aided Computational Analysis Of Metal Coordinated Complexes Containing Amino Acids And Organic Moieties Designed For Photo Induced DNA Cleavage." Ph.D. diss., 2015.
52. Datta, Chandreyee, Rajiv Kumar Jha, Wareed Ahmed, Sohini Ganguly, Soumitra Ghosh, and Valakunja Nagaraja. "Physical and functional interaction between nucleoid-associated proteins HU and Lsr2 of Mycobacterium tuberculosis: altered DNA binding and gene regulation." *Molecular Microbiology* 111, no. 4 (2019): 981-994.

53. Stojkova, Pavla, Petra Spidlova, and Jiri Stulik. "Nucleoid-associated protein HU: A lilliputian in gene regulation of bacterial virulence." *Frontiers in cellular and infection microbiology* 9 (2019): 159.
54. Majdalani, Nadim, Christofer Cuning, Darren Sledjeski, Tom Elliott, and Susan Gottesman. "DsrA RNA regulates translation of RpoS message by an anti-antisense mechanism, independent of its action as an antisilencer of transcription." *Proceedings of the National Academy of Sciences* 95, no. 21 (1998): 12462-12467.
55. Lease, Richard A., and Marlene Belfort. "A trans-acting RNA as a control switch in Escherichia coli: DsrA modulates function by forming alternative structures." *Proceedings of the National Academy of Sciences* 97, no. 18 (2000): 9919-9924.
56. Wayne, L. G. "Dormancy of Mycobacterium tuberculosis and latency of disease." *European Journal of Clinical Microbiology and Infectious Diseases* 13, no. 11 (1994): 908-914.
57. Devasundaram, Santhi, Akilandeswari Gopalan, Sulochana D. Das, and Alamelu Raja. "Proteomics analysis of three different strains of Mycobacterium tuberculosis under in vitro hypoxia and evaluation of hypoxia associated antigen's specific memory T cells in healthy household contacts." *Frontiers in microbiology* 7 (2016): 1275.
58. Meldal, Morten, and Christian Wenzel Tornøe. "Cu-catalyzed azide-alkyne cycloaddition." *Chemical reviews* 108, no. 8 (2008): 2952-3015.
59. Hong, Vu, Stanislav I. Presolski, Celia Ma, and M. G. Finn. "Analysis and optimization of copper-catalyzed azide-alkyne cycloaddition for bioconjugation." *Angewandte Chemie* 121, no. 52 (2009): 10063-10067.
60. Dan, Vipin Mohan, Vinodh JS, Sandesh CJ, Rahul Sanawar, Asha Lekshmi, R. Ajay Kumar, T. R. Santhosh Kumar, Uday Kiran Marelli, Syed G. Dastager, and M. Radhakrishna Pillai. "Molecular networking and whole-genome analysis aid discovery of an angucycline that inactivates mTORC1/C2 and induces programmed cell death." *ACS chemical biology* 15, no. 3 (2020): 780-788.
61. Wessel, D. M., and U. I. Flügge. "A method for the quantitative recovery of protein in dilute solution in the presence of detergents and lipids." *Analytical biochemistry* 138, no. 1 (1984): 141-143.

62. Bradford, N. J. A. B. "A rapid and sensitive method for the quantitation microgram quantities of a protein isolated from red cell membranes." *Anal. Biochem* 72, no. 248 (1976): e254.
63. Vila, Andrew, Keri A. Tallman, Aaron T. Jacobs, Daniel C. Liebler, Ned A. Porter, and Lawrence J. Marnett. "Identification of protein targets of 4-hydroxynonenal using click chemistry for ex vivo biotinylation of azido and alkynyl derivatives." *Chemical research in toxicology* 21, no. 2 (2008): 432-444.
64. Shevchenko, Andrej, Henrik Tomas, Jan Havli, Jesper V. Olsen, and Matthias Mann. "In-gel digestion for mass spectrometric characterization of proteins and proteomes." *Nature protocols* 1, no. 6 (2006): 2856-2860.
65. Ramdas, Vidya, Rashmi Talwar, Vijay Kanoje, Rajesh M. Loriya, Moloy Banerjee, Pradeep Patil, Advait Arun Joshi et al. "Discovery of Potent, Selective, and State-Dependent NaV1. 7 Inhibitors with Robust Oral Efficacy in Pain Models: Structure–Activity Relationship and Optimization of Chroman and Indane Aryl Sulfonamides." *Journal of medicinal chemistry* 63, no. 11 (2020): 6107-6133.
66. Silva, Jeffrey C., Richard Denny, Craig Dorschel, Marc V. Gorenstein, Guo-Zhong Li, Keith Richardson, Daniel Wall, and Scott J. Geromanos. "Simultaneous qualitative and quantitative analysis of the Escherichia coli proteome: A sweet tale." *Molecular & cellular proteomics* 5, no. 4 (2006): 589-607.
67. Waterhouse, Andrew M., James B. Procter, David MA Martin, Michèle Clamp, and Geoffrey J. Barton. "Jalview Version 2—a multiple sequence alignment editor and analysis workbench." *Bioinformatics* 25, no. 9 (2009): 1189-1191.
68. Edgar, Robert C. "MUSCLE: multiple sequence alignment with high accuracy and high throughput." *Nucleic acids research* 32, no. 5 (2004): 1792-1797.
69. Larkin, Mark A., Gordon Blackshields, Nigel P. Brown, R. Chenna, Paul A. McGettigan, Hamish McWilliam, Franck Valentin et al. "Clustal W and Clustal X version 2.0." *Bioinformatics* 23, no. 21 (2007): 2947-2948.

Chapter 4

*Drug metabolism and
pharmacokinetics study of novel
triazole hits against Mycobacterium
tuberculosis*

4.1. Introduction:

Tuberculosis (TB), a potentially infectious bacterial disease caused by the respiratory pathogen *Mycobacterium tuberculosis* (Mtb), most often affects the lungs. Globally, an estimated 10 million individuals fell ill with TB worldwide in 2020, with 3.3 million women, 5.6 million men, and 1.1 million children [1]. First-line TB medications such as rifampicin, isoniazid, pyrazinamide, ethambutol, and streptomycin are now being used for treatment. However, the primary cause of concern is a systematic and frequent development of resistance to these drugs creating (Multidrug-resistant) MDR-TB cases [2]. In 2019, WHO recommended new consolidated guidelines on the second-line drugs to treat MDR-TB. These second-line drugs include bedaquiline, levofloxacin, linezolid, moxifloxacin, delamanid, and pretomanid [3]. There have also been instances of extremely drug-resistant *M. tuberculosis* strains (XDR-TB) that are resistant to rifampicin, isoniazid, and second-line treatments such as fluoroquinolones (for example, kanamycin, amikacin, and capreomycin) [4,5]. Moreover, long-duration drug regimens, low efficacy, high cost, high toxicity, and burden of MDR-TB/XDR-TB continue to exhibit many challenges to physicians and national TB programs. Therefore, there is an urgent need for a new class of drugs/repurposing of existing drugs and effective strategies that can reduce treatment time and complexity of treatment and also effectively treat MDR-TB and XDR-TB.

The triazole nucleus has gathered interest among pharmacists and biologists in recent years. It is one of the important building components in its structure due to its medicinal values [6,7]. The unique properties of triazoles are colorless compound, high chemical stability, broad-spectrum, usually inert to basic or acidic hydrolysis, and stable in most redox conditions [8-10]. Among heterocyclic compounds, the two isomers 1,2,3-triazole and 1,2,4-triazole have received wide interest in recent years due to their effectiveness in different areas of biological activities such as anti-microbial [11-15], anticonvulsant [16], antitubercular [17], anticancer [18-19], anti-inflammatory and analgesic activities [20]. 1,2,4-triazole derivatives such as 3-(3-pyridyl)-5-(4-methylphenyl)-4-(N-4-chloro-1,3-benzothiazol-2-amino)-4H-1,2,4-triazole when tested under in-vitro conditions demonstrated significant anti-TB activity as compared to rifampicin [21]. Kumar and associates described the synthesis of triazole-isoniazid conjugates and further in-vitro evaluated for their possible likeliness property as an anti-TB drug. In their study, compound (12) was reported as the most active derivative (MIC=0.195-0.39 μ M), with comparatively better activity than isoniazid (INH, MIC=0.39 μ M) [22].

We have recently reported the biological activity of the 1,2,4-triazole derivatives against Mtb and *M. bovis* BCG [23-25]. Also, we have reported a library of novel 3-aryl-5-(alkyl-thio)-1H-1,2,4-triazoles and screened their anti-TB activity against *M.bovis* BCG and Mtb H37Ra both in the active and dormant stage. The screening results found 25 compounds that exhibited lower toxicity ($>100 \mu\text{g/ml}$) and promising anti-TB activity in the range of IC_{50} values of $0.03\text{-}5.88 \mu\text{g/ml}$ for the dormant stage and $0.03\text{-}6.96 \mu\text{g/ml}$ for the active stage [23]. However, the pharmacokinetic properties of these synthesized derivatives have not yet been evaluated. To address this issue, in the present study, we have screened the library of ~ 300 compounds of 1,2,4-triazole derivatives and decided to pursue only 30 compounds that showed significant anti-TB activity identified through the in-vitro and ex-vivo study for further pharmacokinetics study.

Preclinical PK assays help to understand the absorption, distribution, metabolism, and excretion [ADME] of a compound in animals following intravenous or oral administration [26]. In the present study, ADME of 30 RRA compound was done to analyze its concentration-time profile in blood or plasma, such as peak concentration (C_{max}), exposure (AUC), and elimination half-life ($t_{1/2}$) concerning pharmacological potency (e.g., MIC or intracellular MIC for Mtb), which directly determines the magnitude of efficacy (pharmacodynamics) and toxicity of the compound. Evaluating PK at the early stages of discovery helps to weed out compounds that show poor PK and thus lack the potential to show efficacy and helps medicinal chemists to optimize compounds for better PK. In a typical PK study, animals are dosed orally or intravenously, and blood samples are drawn at pre-defined time points for 24 hrs. In the present study, the selected 30 compounds were evaluated for their PK properties, such as metabolic stability of the compound, plasma protein binding to check the metabolism of the drug, and in-vitro determination of passive diffusion drug or drug permeability across a biological membrane through parallel artificial membrane permeability (PAMPA) assay.

In summary, based on the preliminary findings of PK properties, the 30 RRA compounds were further evaluated to assess dosage format, and the compounds will be taken for efficacy studies in mice. The MTD analysis for the selected RRA compounds showed no mortalities for single oral dose administration of $50\text{-}500 \text{mg/kg}$ in mice up to 72 hrs post-dosing and identified MTD of at least 500mg/kg body weight. Based on single oral dose estimation and MTD studies at last four RRA compounds RRA79, RRA242, RRA267, and RRA268, were selected for oral PK and dose proportionality analysis in mice and estimated

the final dose for further efficacy studies. Further PK studies proved the efficacy of the selected RRA compounds for further clinical trials, and hence more studies are required to confirm the actual potential as antitubercular leads.

4.2. Results:

4.2.1. Screening of novel triazole derivatives against the active and dormant stage of *Mycobacterium tuberculosis*

In order to search the novel antitubercular compounds, screening was done from the diverse chemical library of triazole derivatives at our facility. From our in-house library of compounds, we have identified 30 derivatives of 1,2,4-triazole based on their inhibition in our preliminary studies. The selection criteria we have used are based on its MIC value. Those compounds that showed significant inhibition with a MIC value of ≤ 100 $\mu\text{g/ml}$ concentration against active and dormant stage Mtb were selected for further study. Then, these 30 compounds were further screened using in-vitro assay (XTTRMA assay) against active and dormant stage Mtb [27] and ex-vivo assay (nitrate reductase NR assay) [28] against the dormant stage Mtb (described in method section). The dose-response effect was monitored for all these 30 compounds applying a concentration range between 100 $\mu\text{g/ml}$ to 0.03 $\mu\text{g/ml}$, and the screening results are shown in Table 1.

Table 1: Screening of novel triazole derivatives against the active and dormant stage of *Mycobacterium tuberculosis*

Sr. No.	Compound Code	In-vitro Mtb (Dormant)		In-vitro Mtb (Active)		Ex-vivo Mtb (Dormant)	
		IC ₅₀ ($\mu\text{g/ml}$)	MIC ($\mu\text{g/ml}$)	IC ₅₀ ($\mu\text{g/ml}$)	MIC ($\mu\text{g/ml}$)	IC ₅₀ ($\mu\text{g/ml}$)	MIC ($\mu\text{g/ml}$)
1	RRA-2	<0.03	15.67± 1.65	<0.03	9.64± 07	0.019± 0.04	6.09± 2.55
2	RRA-7	0.164± 0.04	1.88± 0.64	1.16±0.03	13.02± 3.27	0.06± 0.001	1.91± 0.07
3	RRA-8	0.09± 0.03	8.83± 2.1	<0.03	3.29± 1.53	0.09± 0.02	2.72± 1.2
4	RRA-36	0.18± 0.05	3.11± 0.8	<0.03	6.73± 1.22	0.056± 0.02	4.16± 1.03

5	RRA-50	1.09± 0.2	4.72± 1.3	11.32± 4.22	>30	0.22± 0.08	9.18± 3.21
6	RRA-55	0.35± 0.1	13.54± 3.4	1.98±0.23	>30	NT	NT
7	RRA-62	1.07± 0.3	6.28± 1.2	1.25±0.65	>30	0.19± 0.05	5.62± 1.32
8	RRA-79	0.43± 0.13	1.93± 0.33	0.66±0.12	20.69± 6.32	0.19± 0.06	2.99± 0.65
9	RRA-90A	0.035± 0.01	0.334± 0.02	0.04±0.02	2.67± 1.42	0.013± 0.07	0.9± 0.02
10	RRA-96	1.24± 0.3	3.91± 1.2	0.93±0.43	9.67± 3.21	0.16± 0.06	6.99± 1.32
11	RRA-101	0.64± 0.2	8.64± 3.2	1.62±0.76	11.36± 4.22	0.16± 0.06	8.42± 2.11
12	RRA-117	0.87± 0.13	5.22± 1.4	0.97±0.21	>30	0.2± 0.01	2.78± 0.57
13	RRA-163	0.095± 0.032	3.105± 1.1	0.745±0.23	24.14±3. 21	0.09± 0.02	8.53± 3.25
14	RRA-165	0.096± 0.022	>30	7.78±1.43	>30	NT	NT
15	RRA-193	0.078± 0.013	2.24± 0.98	NT	NT	NT	NT
16	RRA-242	0.68± 0.03	2.47± 0.43	NT	NT	NT	NT
17	RRA-263	17.18± 4.24	68.64± 7.34	NT	NT	NT	NT
18	RRA-264	0.45± 0.12	0.8± 0.03	NT	NT	0.015± 0.04	0.71± 0.04
19	RRA-265	<0.03	0.44± 0.07	NT	NT	0.018± 0.02	0.79± 0.043
20	RRA-266	<0.03	0.58± 0.03	NT	NT	0.016± 0.08	0.77± 0.23

21	RRA-267	0.12± 0.03	0.46± 0.01	NT	NT	0.019± 0.04	0.29± 0.15
22	RRA-268	<0.03	0.11± 0.06	NT	NT	0.011± 0.03	0.34± 0.12
23	RRA-272	<0.03	0.78± 0.06	NT	NT	0.01± 0.002	0.29± 0.14
24	RRA-284	0.68± 0.04	2.24± 1.04	NT	NT	0.12± 0.05	2.62± 0.03
25	RRA-287	0.057± 0.01	0.68± 0.06	NT	NT	0.017± 0.08	0.86± 0.02
26	RRA-288	0.35± 0.06	1.33± 0.09	NT	NT	0.055± 0.02	2.99± 0.13
27	RRA-289	0.58± 0.03	2.8± 0.85	NT	NT	0.024± 0.03	2.21± 0.18
28	RRA-293	0.84± 0.3	1.94± 0.06	0.63±0.08	2.15± 0.13	NT	NT
29	RRA-295	0.71±0.2	2.7± 0.19	0.6± 0.005	2.7± 0.19	NT	NT
30	RRA-304	0.33± 0.05	8.13± 2.47	0.328±0.13	1.96± 0.32	NT	NT

NT-Not tested; Standard deviations were used to generate error bars are the mean ± SEM (n=3).

4.2.2. The spectrum of activity of triazole derivatives against non-mycobacterial species

Drugs having a broader and often unexpected range of biological activity may cause adverse effects, rendering their usage unsuitable for treatment. Thus, we are interested in the compound's broader specificity; hence, these 30 hits were further evaluated for the spectrum of activity against non-mycobacterial species. Proper dose-dependent effect of these compounds was examined against four bacterial strains such as Gram-negative strains- *Escherichia coli*, *Pseudomonas aeruginosa*, and Gram-positive strains- *Staphylococcus aureus* and *Bacillus subtilis*. The results for inhibition activity are presented in Table 2.

Table 2: Anti-bacterial activity of synthesized triazole derivatives against non-mycobacterial species

Sr. No	Compound Code	Anti-bacterial activity			
		Gram + ve bacteria		Gram - ve bacteria	
		<i>Staphylococcus aureus</i>	<i>Bacillus subtilis</i>	<i>Escherichia coli</i>	<i>Pseudomonas aeruginosa</i>
		MIC ($\mu\text{g/ml}$)	MIC ($\mu\text{g/ml}$)	MIC ($\mu\text{g/ml}$)	MIC ($\mu\text{g/ml}$)
1	RRA-2	>30	>30	>30	>30
2	RRA-7	>30	>30	>30	>30
3	RRA-8	17.24	29.41	>30	13.6
4	RRA-36	>30	>30	>30	>30
5	RRA-50	>30	>30	>30	>30
6	RRA-55	9.6	>30	>30	8.49
7	RRA-62	>30	>30	>30	>30
8	RRA-79	>30	>30	>30	28.91
9	RRA-90A	>30	>30	>30	>30
10	RRA-96	>30	>30	>30	>30
11	RRA-101	9.61	12.48	>30	>30
12	RRA-117	>30	>30	>30	>30
13	RRA-163	>30	>30	>30	>30
14	RRA-165	>30	>30	>30	>30
15	RRA-193	>30	>30	>30	>30
16	RRA-242	>30	9.28	>30	>30
17	RRA-263	>30	>30	>30	>30
18	RRA-264	27.37	>30	>30	>30
19	RRA-265	>30	>30	>30	>30
20	RRA-266	>30	>30	>30	>30
21	RRA-267	>30	>30	>30	>30
22	RRA-268	>30	>30	>30	>30
23	RRA-272	>30	>30	>30	>30
24	RRA-284	>30	>30	>30	>30

25	RRA-287	>30	>30	>30	>30
26	RRA-288	>30	>30	>30	>30
27	RRA-289	>30	>30	>30	>30
28	RRA-293	>30	>30	>30	>30
29	RRA-295	>30	>30	>30	>30
30	RRA-304	>30	>30	>30	>30
	Ampicillin ^a	5.09±0.19	7.45±0.19	3.59±0.44	6.89±0.34
	Kanamycin ^a	8.24±0.65	6.27±0.76	4.93±0.86	3.93±0.17

^a Positive control drugs; standard 1) Ampicillin, 2) Kanamycin

4.2.3. In-vitro cytotoxicity of synthesized triazole derivatives against human cancer cell lines

In-vitro tests must be well-characterized and accurate predictors of in-vivo effects, with a low rate of false-positive or negative outcomes. In order to proceed further, the compound's toxicity was assessed. Hence, we screened the 30 hit compounds for in-vitro cytotoxicity in a dose-dependent manner against four human cancer cell lines, namely, THP-1 (Human leukemia monocytic cell line), A549 (Human lung cancer cell line), PANC-1 (Human pancreatic cancer cell line), and HeLa (Human cervical cancer cell line) by 3-(4,5-dimethylthiazol-2-yl)-2,5-diphenyltetrazolium bromide (MTT) assay method [29,30]. The result (shown in Table 3) clearly indicated that these compounds have no significant cytotoxic effect on mammalian cell lines.

Table 3: In-vitro cytotoxicity of synthesized 1,2,4-triazole derivatives against different human cancer cell line

Sr. No	Compound Code	Cytotoxic- activity % GI ₅₀ ^a			
		THP-1 (Human leukemia monocytic cell line)	A549 (Human lung cancer cell line)	PANC-1 (Human pancreatic cancer cell line)	HeLa (Human cervical cancer cell line)
		(µg/ml)	(µg/ml)	(µg/ml)	(µg/ml)
1	RRA-2	>100	>100	>100	>100
2	RRA-7	>100	>100	>100	69.49

3	RRA-8	>100	>100	>100	>100
4	RRA-36	>100	>100	>100	>100
5	RRA-50	>100	>100	>100	>100
6	RRA-55	>100	>100	>100	42.27
8	RRA-79	>100	>100	>100	>100
9	RRA-90A	>100	>100	>100	>100
10	RRA-96	>100	>100	>100	>100
11	RRA-101	>100	>100	>100	25.76
12	RRA-117	>100	>100	>100	>100
13	RRA-163	>100	>100	>100	>100
14	RRA-165	>100	>100	>100	>100
15	RRA-193	>100	>100	>100	>100
16	RRA-242	>100	>100	>100	>100
17	RRA-263	>100	>100	>100	>100
18	RRA-264	>100	>100	>100	>100
19	RRA-265	>100	>100	>100	42.14
20	RRA-266	>100	>100	>100	89.16
21	RRA-267	>100	>100	>100	>100
22	RRA-268	>100	>100	>100	>100
23	RRA-272	>100	>100	>100	>100
24	RRA-284	>100	>100	>100	8.22
25	RRA-287	>100	>100	>100	76.23
26	RRA-288	>100	>100	>100	8.63
27	RRA-289	>100	>100	>100	>100
28	RRA-293	>100	>100	>100	>100
29	RRA-295	>100	>100	>100	>100
30	RRA-304	>100	>100	>100	>100
	Paclitaxel ^b	0.084±0.02	0.077±0.04	4.54±0.26	0.069±0.03

^a Inhibitor concentrations responsible for 50 % growth inhibition were assessed by MTT assay at 72 h. The values were calculated with data from at least three independent experiments.

^b Positive control drug

4.2.4. Metabolic Stability of selected triazole derivatives in Human and Mouse Liver Microsomes

The majority of inhibitors face the initial barriers from 1) non-specific binding with blood proteins, then 2) clearance by liver microsomes, and 3) high permeability across membranes to effectively apply on curing activity. The major goal at this level is to put the above compounds in 3 categories, High, Medium, and Low, to select the appropriate compounds for

the next level. Results of the selected RRA compounds for the stability assay in human liver microsomes are presented (Table 4), and in mouse liver, microsomes are presented (Table 5).

Table 4: Metabolic Stability of RRA compounds in Human Liver Microsomes

Compound ID	Mean Values N=3				Classification of Intrinsic Clearance [CLint]
	Percent metabolized (%)	t _{1/2} (min)	Ke=0.693/t	Clint (μL/min/mg)	
RRA-2	65	20.5	0.03	67.7	Moderate
RRA-7	50	32.9	0.02	42.2	Moderate
RRA-8	<5	NA	NE	NE	Low
RRA-36	75	15.1	0.05	92.2	Moderate
RRA-50	13	NE	NE	NE	Low
RRA-55	3	NE	NE	NE	Low
RRA-62	81	12.6	0.05	110.0	High
RRA-79	11	NE	NE	NE	Low
RRA-90A	94	7.5	0.09	183.9	High
RRA-96	94	7.7	0.09	180.0	High
RRA-101	NE	NE	NE	NE	NE
RRA-117	81	13.1	0.05	106.0	High
RRA-163	67	20.3	0.03	68.3	Moderate
RRA-165	NE	NE	NE	NE	NE
RRA-193	94	7.7	0.09	179.5	High
RRA-242	8	NE	NE	NE	Low
RRA-263	<5	NE	NE	NE	Low
RRA-264	62	21.8	0.03	63.7	Moderate
RRA-265	87	10.6	0.07	131.6	High
RRA-266	80	14.9	0.05	93.6	Moderate
RRA-267	10	NE	NE	NE	Low

RRA-268	42	41.5	0.02	33.4	Low
RRA-272	95	7.1	0.10	196.3	High
RRA-284	100	NE	NE	NE	High
RRA-287	NE	NE	NE	NE	NE
RRA-288	50	34.1	0.02	42.9	Moderate
RRA-289	NE	NE	NE	NE	NE
RRA-293	48	34.9	0.02	39.7	Low
RRA-295	46	34.9	0.02	40	Low
RRA-304	93	8.1	0.09	171.4	High
Verapamil (Positive control)	81	13	0.05	107	High

NE: Not Estimated either because the compound was metabolized too rapidly or due to lack of metabolism (stable)

In human liver microsomes, RRA compounds 62, 90A, 96, 117, 193, 265, 272 and 304 showed high intrinsic clearance ($CL_{int} > 100 \mu\text{L}/\text{min}/\text{mg}$); RRA 2, 7, 36, 163, 264, 266 and 288 showed moderate intrinsic clearance ($CL_{int} > 40$ and $< 100 \mu\text{L}/\text{min}/\text{mg}$), and **RRA 8, 50, 55, 79, 242, 263, 267, 268, 293, and 295** showed low intrinsic clearance ($CL_{int} < 40 \mu\text{L}/\text{min}/\text{mg}$).

Table 5: Metabolic Stability of selected triazole derivatives in Mouse Liver Microsomes

Compound ID	Mean Values N=3				Classification of Intrinsic Clearance [CL _{int}]
	Percent metabolized (%)	t _{1/2} (min)	Ke=0.693/t	Cl _{int} ($\mu\text{L}/\text{min}/\text{mg}$)	
RRA-2	79	13.7	0.05	101.6	High
RRA-7	<5	NE	NE	NE	Low
RRA-8	1	NE	NE	NE	Low
RRA-36	80	13.7	0.05	101.4	High
RRA-50	18	108.8	0.01	12.8	Low

RRA-55	9	NE	NE	NE	Low
RRA-62	74	15.4	0.04	90.3	Moderate
RRA-79	10	NE	NE	NE	Low
RRA-90A	99	4.9	0.14	282.2	High
RRA-96	100	4.8	0.14	288.7	High
RRA-101	NE	NE	NE	NE	NE
RRA-117	99	NE	NE	NE	High
RRA-163	76	15.3	0.05	90.6	Moderate
RRA-165	NE	NE	NE	NE	NE
RRA-193	99	4.3	0.16	324.7	High
RRA-242	18	102	0.01	15	Low
RRA-263	0	NE	NE	NE	Low
RRA-264	99	5	0.14	271	High
RRA-265	99	6	0.11	219	High
RRA-266	99	NE	NE	NE	High
RRA-267	16	135.5	0.01	10.3	Low
RRA-268	96	7	0.10	193	High
RRA-272	99	6	0.12	245	High
RRA-284	100	NE	NE	NE	High
RRA-287	NE	NE	NE	NE	NE
RRA-288	>95	NE	NE	NE	High
RRA-289	NE	NE	NE	NE	NE
RRA-293	84	12	0.06	119	High
RRA-295	89	9	0.08	153	High
RRA-304	99	5	0.13	266	High
Verapamil (Positive control)	95	8	0.09	181	High

NE: Not Estimated either because the compound was metabolized too rapidly or due to lack of metabolism (stable)

In mouse liver microsomes, RRA compounds 2, 36, 90A, 96, 117, 193, 264, 265, 266, 268, 272, 288, 293, 295 and 304 showed high intrinsic clearance ($CL_{int} > 100 \mu\text{L}/\text{min}/\text{mg}$); RRA 62 and 163 showed moderate intrinsic clearance and compounds **RRA 7, 8, 50, 55, 79, 242, 263** and **267** showed low intrinsic clearance ($CL_{int} < 40 \mu\text{L}/\text{min}/\text{mg}$).

4.2.5. Plasma Protein Binding of selected compounds in Human and Mouse plasma

Table 6: Mean Plasma Protein Binding of selected compounds in Human Plasma

Compound ID	% Unbound (Mean, n=3)	Classification of Plasma Protein Binding
Warfarin (Positive control)	1.0	High
Diclofenac (Positive control)	1.6	Very High
RRA-2	1.2	High
RRA-7	Unstable in plasma	NE because of instability in Plasma
RRA-8	Unstable in plasma	NE because of instability in Plasma
RRA-36	Unstable in plasma	NE because of instability in Plasma
RRA-50	18.7	Moderately high
RRA-55	3.9	High
RRA-62	2.8	High
RRA-79	2.4	High
RRA-90A	0.8	Very High
RRA-96	0.6	very high
RRA-101	Mass not Found	Didn't optimize on LC-MS/MS
RRA-117	8.6	High
RRA-163	Unstable in plasma	NE because of instability in Plasma
RRA-165	Mass not Found	Didn't optimize on LC-MS/MS

RRA-193	4.3	High
RRA-242	4.6	High
RRA-263	8.5	High
RRA-264	7.6	High
RRA-265	1.4	High
RRA-266	3.7	High
RRA-267	9.3	Moderately high
RRA-268	20.7	Moderately high
RRA-272	2.8	High
RRA-284	Unstable in plasma	NE because of instability in Plasma
RRA-287	Mass not Found	Didn't optimize on LC-MS/MS
RRA-288	Unstable in plasma	NE because of instability in Plasma
RRA-289	Mass not Found	Didn't optimize on LC-MS/MS
RRA-293	2.0	High
RRA-295	10.4	High
RRA-304	Unstable in plasma	NE because of instability in Plasma

NA: Not Applicable; NE: Not Estimated

A significant number of compounds showed high to moderately high protein binding in human plasma. Seven compounds (RRA 7, 8, 36, 163, 284, 288, and 304) were unstable in human plasma.

Table 7: Mean Plasma Protein Binding of RRA compounds in Mouse Plasma

Compound ID	% Unbound (Mean, n=3)	Classification of Plasma Protein Binding
Warfarin (Positive control)	7.1	High
Diclofenac	0.9	Very High

(Positive control)		
RRA-2	3.4	High
RRA-7	Unstable in plasma	NE because of instability in Plasma
RRA-8	Unstable in plasma	NE because of instability in Plasma
RRA-36	Unstable in plasma	NE because of instability in Plasma
RRA-50	32.7	low
RRA-55	5.3	High
RRA-62	2.5	High
RRA-79	5.1	High
RRA-90A	3.5	High
RRA-96	0.9	very high
RRA-101	Mass not Found	Didn't optimize on LC-MS/MS
RRA-117	11.3	Moderately high
RRA-163	Unstable in plasma	NE because of instability in Plasma
RRA-165	Mass not Found	Didn't optimize on LC-MS/MS
RRA-193	6.3	High
RRA-242	11.8	Moderately high
RRA-263	6.8	High
RRA-264	8.7	High
RRA-265	1.9	High
RRA-266	4.1	High
RRA-267	27.6	Moderately high
RRA-268	14.0	Moderately high
RRA-272	3.3	High
RRA-284	Unstable in plasma	NE because of instability in Plasma
RRA-287	Mass not Found	Didn't optimize on LC-MS/MS
RRA-288	Unstable in plasma	NE because of instability in Plasma

RRA-289	Mass not Found	Didn't optimize on LC-MS/MS
RRA-293	Mass not Found	Didn't optimize on LC-MS/MS
RRA-295	Unstable in plasma	NE because of instability in Plasma
RRA-304	Unstable in plasma	NE because of instability in Plasma

NE: Not Estimated

A significant number of compounds showed high to moderately high protein binding in mouse plasma. Eight compounds (RRA 7,8,36,163,284,288,295,304) were unstable in mouse plasma.

4.2.6. Parallel artificial membrane permeability assay (PAMPA) of selected compounds

Table 8: Mean Permeability of RRA compounds in PAMPA assay

Compound ID	Mean P_{app} (n=3) (X10⁻⁶cm/sec)	classification*
Propranolol (Positive control)	3.2	High
RRA-2	6.5	High
RRA-7	3.8	High
RRA-8	0.0	Low
RRA-36	9.0	High
RRA-50	0.0	Low
RRA-55	1.4	Low
RRA-62	8.5	High
RRA-79	3.5	High
RRA-90A	3.7	High
RRA-96	3.1	High
RRA-101	Did not optimize on LCMS	

RRA-117	3.3	High
RRA-163	5.0	High
RRA-165	Did not optimize on LCMS	
RRA-193	6.9	High
RRA-242	7.6	High
RRA-263	1.3	Low
RRA-264	6.3	High
RRA-265	2.8	Moderate
RRA-266	4.2	High
RRA-267	0.0	Low
RRA-268	7.8	High
RRA-272	1.3	Low
RRA-284	4.2	High
RRA-287	Did not optimize on LCMS	
RRA-288	5.1	High
RRA-289	Did not optimize on LCMS	
RRA-293	7.2	High
RRA-295	7.0	High
RRA-304	1.4	Low

The apparent permeability coefficient $*P_{app} < 2 \times 10^{-6}$ cm/s = low permeability. $P_{app} > 3 \times 10^{-6}$ cm/s = high permeability

In general, most of the compounds showed high permeability, with seven compounds (RRA 8, 50, 55, 263, 267, 272, and 304) showing low permeability in the PMPA assay. Fifteen compounds were selected for oral pharmacokinetics studies based on the above results.

4.2.7. Oral Pharmacokinetics of Fifteen Selected Compounds of 20 mg/kg in Mice

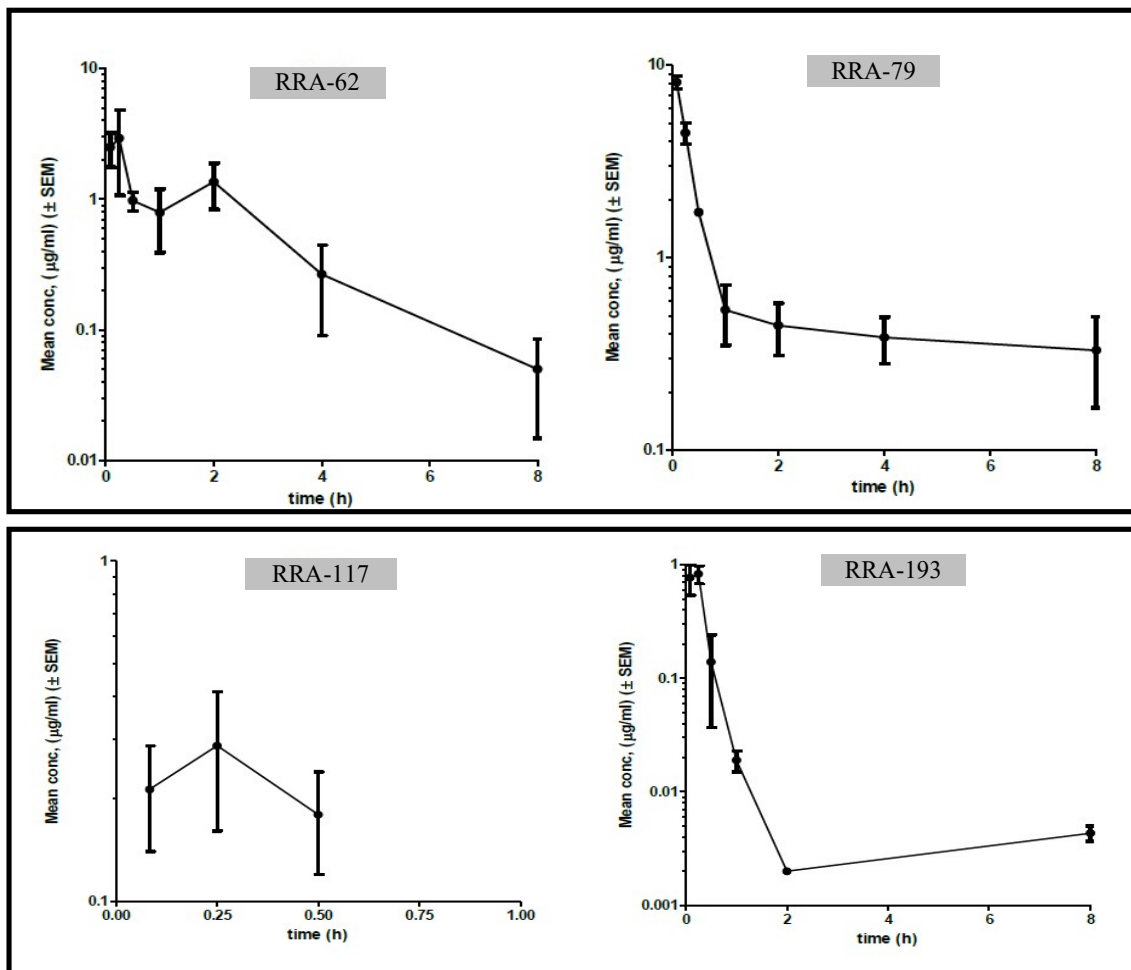
Table 9: PK parameters for the RRA compounds in mice following a single oral dose of 20 mg/kg body weight

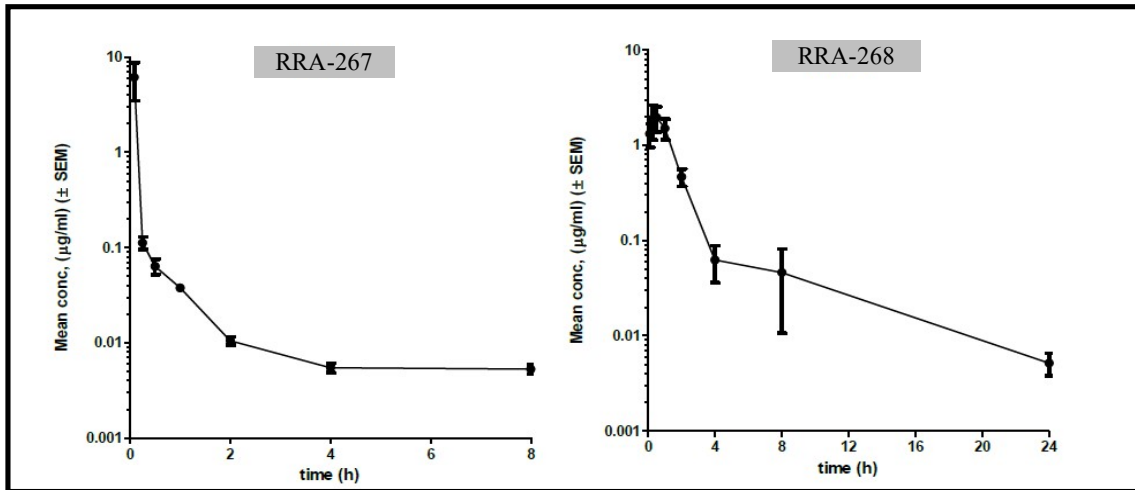
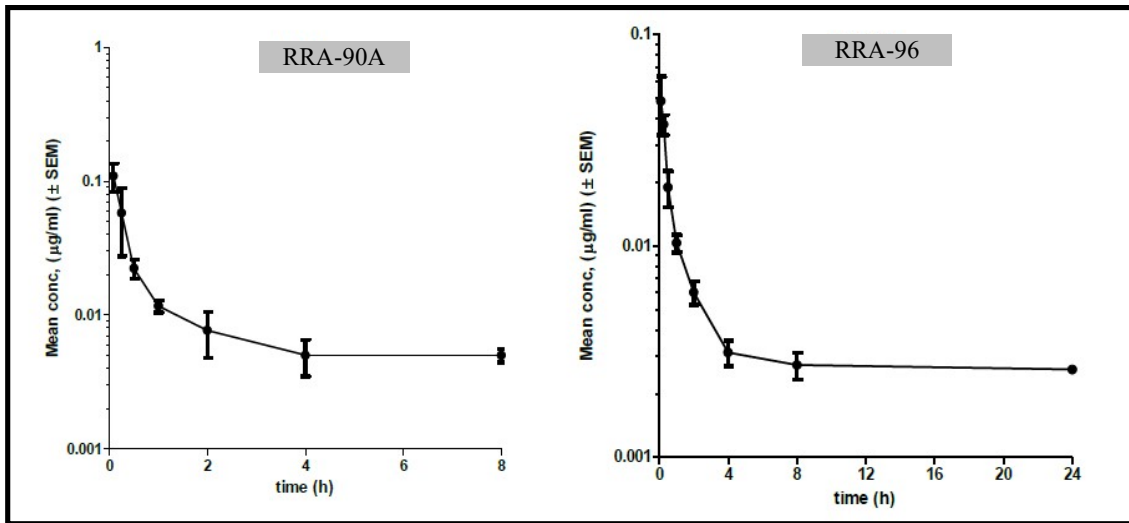
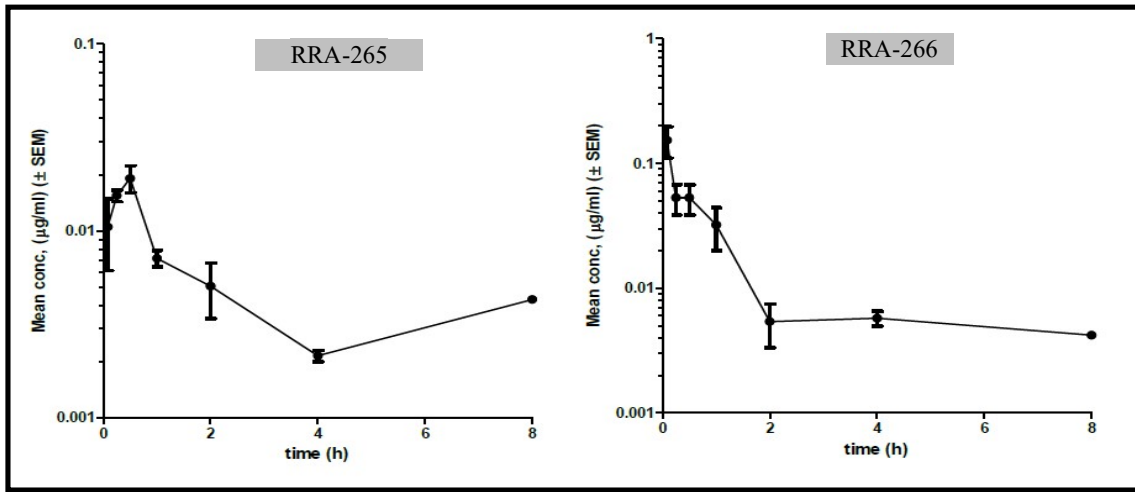
Compound	C _{max} (µg/ml)	T _{max} (h)	AUC(0-t) (µg.h/ml)	AUC(t-∞) (µg.h/ml)	AUC(0-∞) (µg.h/ml)	extrapolate dAUC (%)	k _e (h)	t _{1/2} (h)
RRA 62	2.9	0.25	4.7	0.089	4.8	1.9	0.55	1.3
RRA 79	8.2	0.083	5.15	4.82	10.0	48.3	0.069	10.1
RRA 90A	0.11	0.083	0.075	0.06	0.139	45.9	0.078	8.9
RRA 96	0.05	0.083	0.093	NE	NE	NE	NE	NE
RRA 117	0.29	0.25	0.100	NE	NE	NE	NE	NE
RRA 193	0.83	0.25	0.32	NE	NE	NE	NE	NE
RRA 242	7.3	0.25	7.15	0.01	7.16	0.2	0.246	2.8
RRA 264	0.58	0.083	0.22	0.02	0.24	9.0	0.205	3.4
RRA 265	0.02	1.0	0.04	0.01	0.05	11.7	0.404	1.7
RRA 266	0.15	0.083	0.1	0.10	0.20	51.0	0.041	17.1
NCL 267	6.1	0.083	0.63	0.05	0.68	6.7	0.116	6.0
RRA 268	2.0	0.5	3.76	0.04	3.80	1.1	0.125	5.5
RRA 272	0.10	0.083	0.04	0.004	0.04	8.1	1.352	0.5
RRA 289	0.10	0.083	0.02	NE	NE	NE	NE	NE
RRA 293	1.3	0.25	1.17	0.02	1.19	1.4	0.534	1.3

NE: Not Estimated either because the compound was metabolized too rapidly or due to lack of metabolism (stable)

Whereas C_{max}-Peak concentration in plasma, t_{max}-Time of peak concentration in plasma, AUC_{0-t} Area Under the Plasma Concentration Time Curve from t=0 to C_{last}, AUC_{0-∞} Area Under the Plasma Concentration Time Curve from t=0 to infinity, K_e-First order Elimination rate constant, t_{1/2} Elimination half-life NE: Not estimated due to lack of a clear declining terminal linear phase.

The Pk of compounds RRA 62, 72, 90A, 96, 117, 193, 242, 264, 265, 266, 267, 268, 272, 289, and 293 were performed in BALB/c mice at an oral dose of 20 mg/kg body weight. Post dose and results are shown in Table 7. All the compounds were rapidly absorbed with the time of peak concentrations in plasma (T_{max}) ranging between 5 min and 0.5 h, except RRA 265, which showed a T_{max} = 1.0 h. RRA 79 showed the highest peak concentration in plasma (C_{max}) = 8.2 $\mu\text{g}/\text{ml}$, followed by RRA 242 (7.3 $\mu\text{g}/\text{ml}$), RRA 267 (6.1 $\mu\text{g}/\text{ml}$), with RRA 265 and RRA 264 showing the lowest C_{max} of 0.02 and 0.05 $\mu\text{g}/\text{ml}$, respectively. The highest Area under the Plasma Concentration Time Curve ($AUC_{(0-t)}$) was achieved by RRA 242 (7.15 $\mu\text{g}\cdot\text{h}/\text{ml}$), followed by RRA 79 (5.2 $\mu\text{g}\cdot\text{h}/\text{ml}$), and RRA 268 (3.8 $\mu\text{g}\cdot\text{h}/\text{ml}$), RRA 289 (0.02 $\mu\text{g}\cdot\text{h}/\text{ml}$), RRA 272 (0.04 $\mu\text{g}\cdot\text{h}/\text{ml}$) and RRA 265 (0.04 $\mu\text{g}\cdot\text{h}/\text{ml}$) showing the lowest. The terminal half-life ranged between 1.3 h and ~ 10 h. Animals were dosed with compounds RRA 62, 72, 90A, 96, 117, 193, 242, 264, 265, 266, 267, 268, 272, 289, and 293 were normal throughout the study. Six compounds were selected for the maximum tolerated dose study based on the above results.





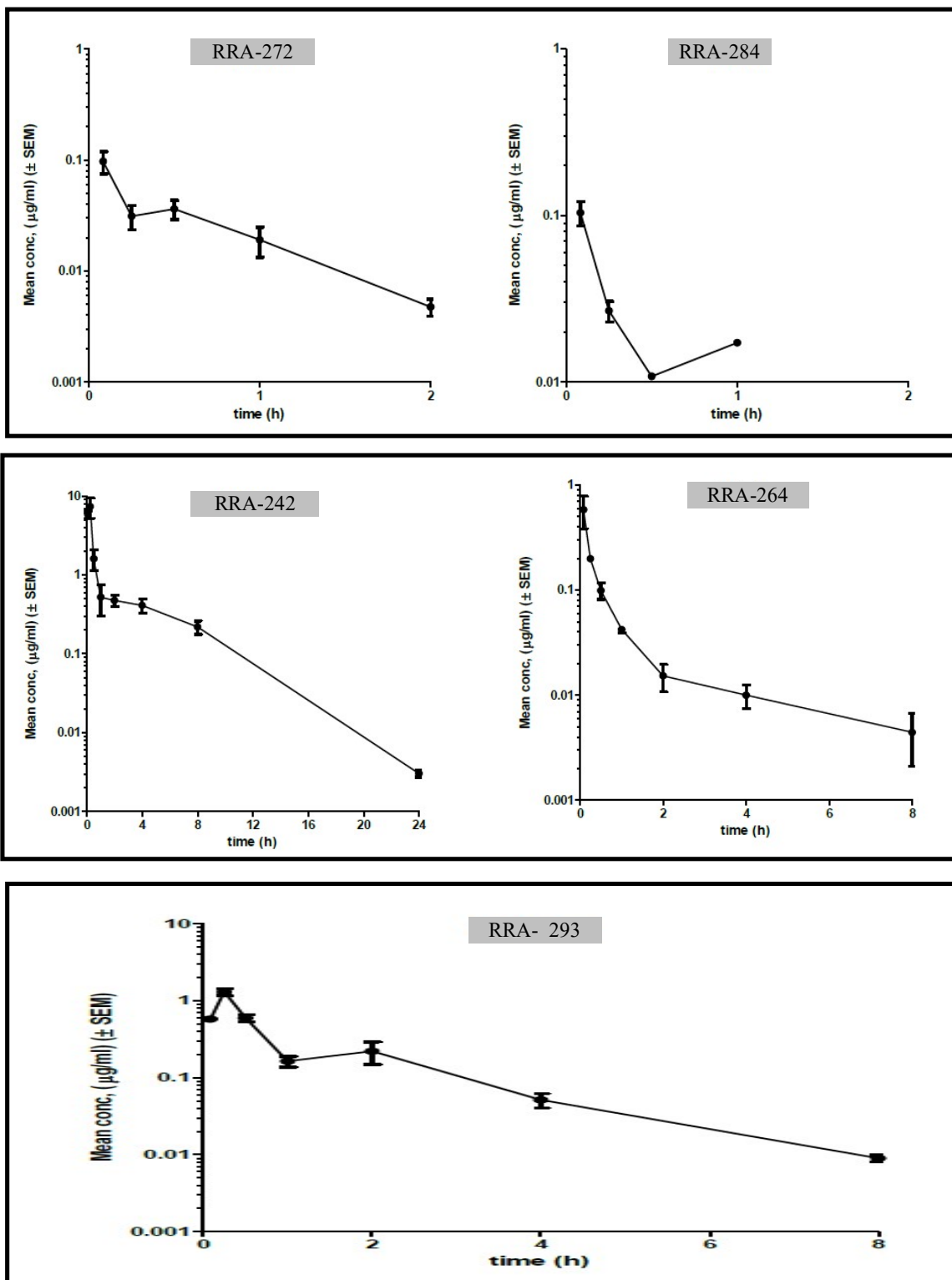


Figure 1: Mean concentration-time profiles of RRA compounds following a single oral dose of 20 mg/kg in mice. During the post-infusion period, distribution and elimination phases

(plasma concentration Vs. time curve). Standard deviations were used to generate error bars for each time point are the mean \pm SEM (n=3).

4.2.8. The maximum tolerated dose (MTD) of selected RRA compounds

The MTD analysis estimated the highest dose or treatment that does not affect any side effects. In clinical studies, the maximum tolerated dose is determined by evaluating escalating doses on several groups of patients until the highest dose with tolerable side effects is discovered. The MTD of RRA79,242,267,268,62,293 was performed in BALB/c mice following escalating oral single doses of 50, 100, 200, 400, and 500 mg/kg. This study aims to determine the MTD of selected compounds, as earlier mentioned, following escalating oral single doses in mice.

Table 10: Clinical signs post escalating doses of selected RRA compounds in mice

The body weights of animals, the dose volumes administered, and the mortality results are shown in Table 10

Compound	Group	Treatment Dose (mg/kg)	No. of Animals /group	Clinical Signs on Days			Mortality
				Day 1	Day 2	Day 3	
Vehicle	G1	0	5	N	N	N	0/5
RRA79	G2	50	5	N	N	N	0/5
	G3	100	5	N	N	N	0/5
	G4	200	5	N	N	N	0/5
	G5	400	5	N	N	N	0/5
	G6	500	5	N	N	N	0/5
RRA242	G7	50	5	N	N	N	0/5
	G8	100	5	N	N	N	0/5
	G9	200	5	N	N	N	0/5
	G10	400	5	N	N	N	0/5
	G11	500	5	N	N	N	0/5
RRA267	G12	50	5	N	N	N	0/5

	G13	100	5	N	N	N	0/5
	G14	200	5	N	N	N	0/5
	G15	400	5	N	N	N	0/5
	G16	500	5	N	N	N	0/5
RRA268	G17	50	5	N	N	N	0/5
	G18	100	5	N	N	N	0/5
	G19	200	5	N	N	N	0/5
	G20	400	5	N	N	N	0/5
	G21	500	5	N	N	N	0/5
RRA62	G22	50	5	N	N	N	0/5
	G23	100	5	N	N	N	0/5
	G24	200	5	N	N	N	0/5
	G25	400	5	N	N	N	0/5
	G26	500	5	N	N	N	0/5
RRA293	G27	500	5	N	N	N	0/5
	G28	400	5	N	N	N	0/5

N: Apparently Normal

No significant adverse clinical signs or mortalities were seen in mice following single-dose oral administrations of 50, 100, 200, 400, and 500 mg/kg of RRA 62, 79, 242, 267, 268, and 400, and 500 mg/kg for RRA293 up to 72 h post-dosing. The MTD of RRA 62, 79, 242, 267, 268, and 293 was at least 500 mg/kg in mice following oral administration. Four compounds were selected for the oral dose escalation PK study in mice based on the above results.

4.2.9 Oral Dose Escalation Pharmacokinetics of selected RRA compounds in Mice

In this study, the oral PK and dose proportionality of AUC and C_{max} of four RRA compounds RRA79, RRA242, RRA267, and RRA268 in mice at 50, 100, 200, and 400mg/kg body weight of BALB/c mice. The bioanalytical methods for four RRA compounds, RRA79, RRA242, RRA267, and RRA268, were sensitive, linear, accurate, and precise in the concentration ranges tested and met all the acceptance criteria. The lower limit of quantitation

of four RRA compounds RRA79, RRA242, RRA267, and RRA268 were 0.026, 0.0067, 0.025, and 0.081 µg/ml, respectively (data not shown).

Compound RRA79 showed rapid absorption followed by bi-exponential disposition (Figure 2). The terminal elimination phases at 100, 200, and 400mg/kg were flat. The concentrations at 24 h were below the limit of quantitation (BLOQ) at all the doses.

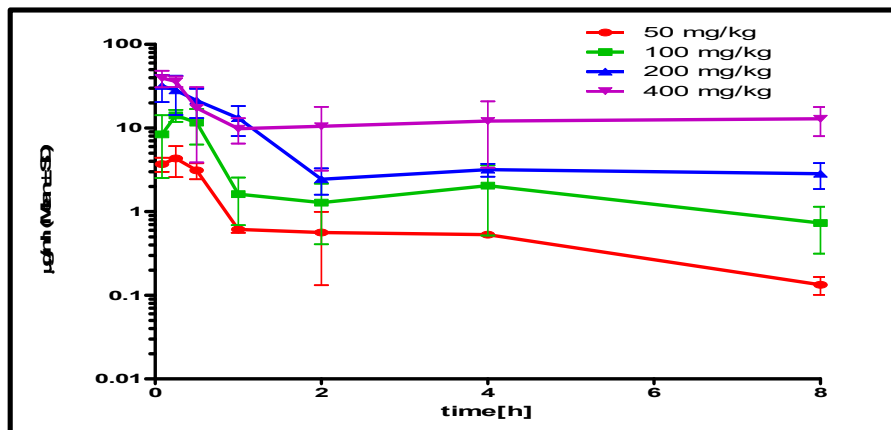


Figure 2: Mean concentration-time profiles of RRA79 following single oral doses of 50,100,200 and 400 mg/kg in mice. Error bars are SD.

Compound RRA79 showed more than dose-proportional linear [$r^2=0.999$] increase in AUC_{0-8h} , with the $AUC/dose$ increasing between 50 and 400 mg/kg [31]; C_{max} showed more than dose proportional linear increase [$r^2=0.999$] between 50 and 200 mg/kg, and plateauing at 400mg/kg [Figure 3, Table 11].

Table 11: Relationship between dose and AUC and C_{max} for RRA79 in mice

Dose [mg/kg]	$t_{1/2}$ [h]	T_{max} [h]	C_{max} (µg/ml)	AUC [µg.h/ml]
50	2.74	0.25	4.3	5.35
100	6.86	0.25	14.2	17.87
200	5.07	0.08	31.8	44.9
400	NE	0.08	39.5	103.61

NE: Not estimated

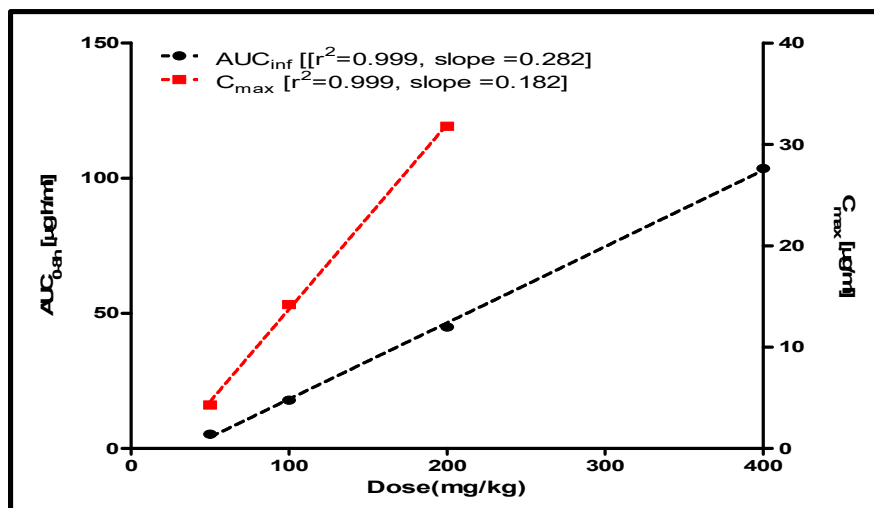


Figure 3: Relationship of AUC_{0-8h} and C_{max} with a dose of RRA79 in mice. The dashed lines are regression lines

Compound RRA242 showed rapid absorption [$t_{max}=0.25h$] post-dose followed by approximately bi-exponential decline with first-order kinetics at all the doses (Figure 4). The terminal elimination phases at 50,100 and 400mg/kg were parallel suggesting linear PK between 50 and 400 mg/kg.

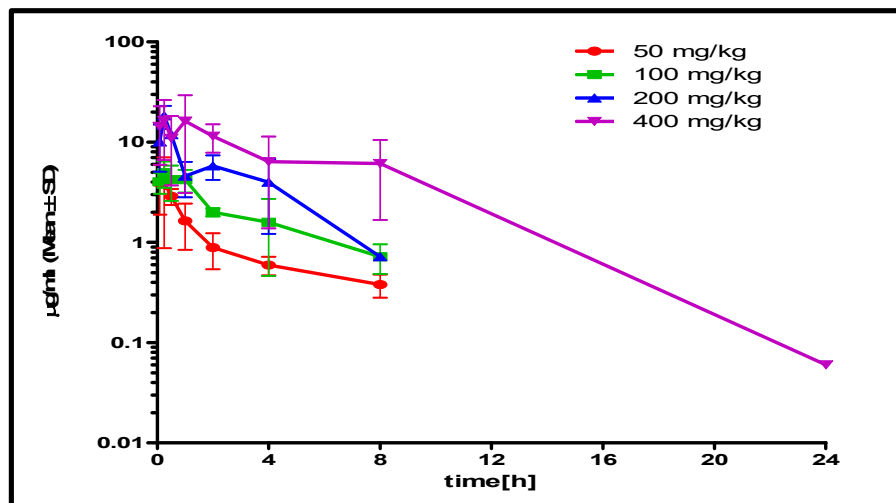


Figure 4: Mean concentration time-profiles of RRA242 following single oral doses of 50,100,200 and 400 mg/kg in mice. Error bars are SD.

Compound RRA242 showed approximately a dose-proportional linear [$r^2=0.98$] increase in AUC_{0-inf}, with the AUC/dose increasing between 50 and 400mg/kg body weight of mice [31]. In contrast, the C_{max} showed more than the dose-proportional linear increase between 50 and

200mg/kg and plateauing at 400mg/kg body weight of mice, as shown in Figure 5 and Table 12.

Table 12: Relationship between dose and AUC and C_{max} for RRA242 in mice

Dose [mg/kg]	t _{1/2} (h)	T _{max} (h)	C _{max} (µg/ml)	AUC _{INF} (h*µg/ml)	CI/F (L/h/kg)
50	5.0	0.25	4.0	10.1	4.967
100	3.1	0.25	5.0	18.2	5.505
200	1.9	0.25	18.3	35	5.720
400	2.8	0.25	16.5	90.6	4.413

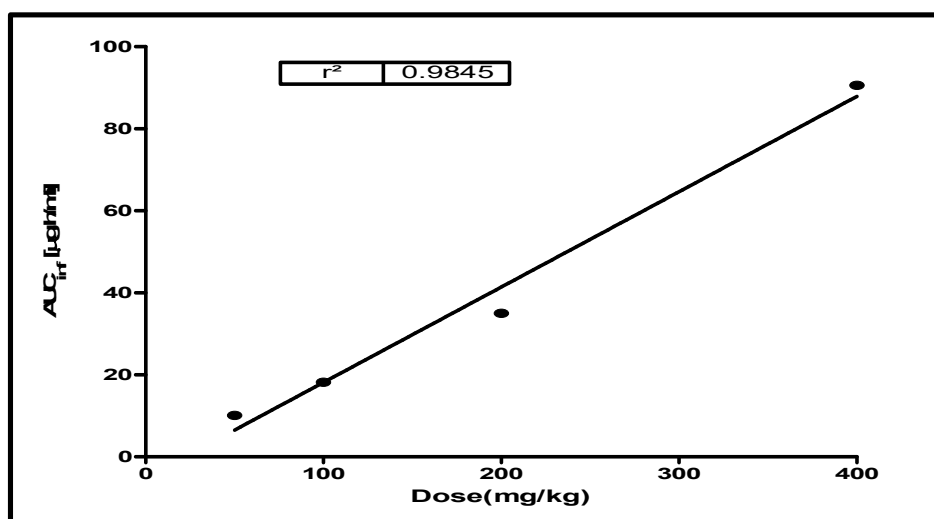


Figure 5: Relationship of AUC_{0-∞} and dose of RRA242 in mice

Compound RRA267 showed rapid absorption [$t_{max}=5min$] followed by a bi-exponential decline (Figure 6). Concentrations were BLOQ at 1 for 50mg/kg dose, as a result of which a complete profile was not obtained for characterization. The terminal elimination phases at 100,200 and 400mg/kg were flat, so accurate estimation of k_e , $t_{1/2}$, and AUC_{inf} was not possible. The non-compartmental analysis (NCA) PK parameters are summarised in Table 13.

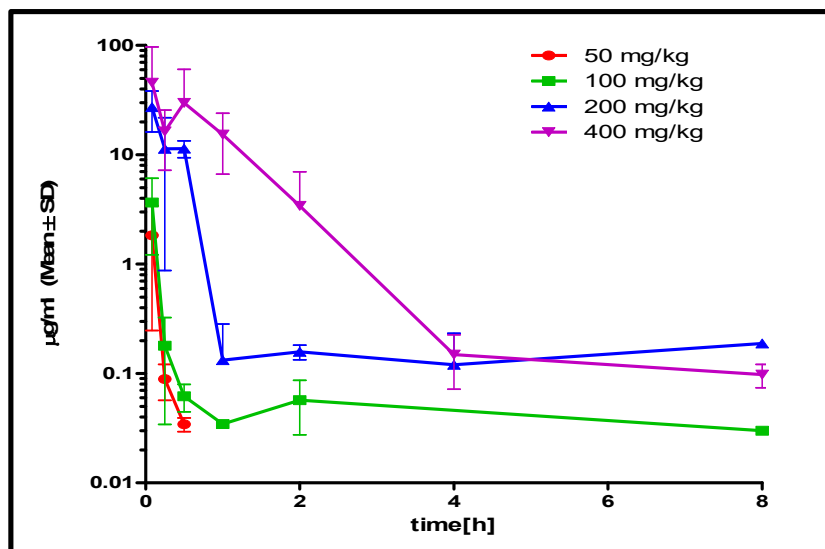


Figure 6: Mean concentration time profiles of RRA267 following single oral doses of 50,100,200 and 400 mg/kg in mice. Error bars are SD.

Compound RRA267 showed more than dose-proportional linear increase in AUC_{0-8h} with the $AUC/dose$ increasing with dose, whereas the C_{max} showed more than the dose-proportional linear increase between 50 and 400 mg/kg body weight of mice, as shown in Figure 7 and Table 13.

Table 13: Relationship between dose and AUC and C_{max} for RRA267 in mice

Dose [mg/kg]	$t_{1/2}$ (h)	T_{max} (h)	C_{max} ($\mu\text{g/ml}$)	T_{last} (h)	AUC_{last} ($h^* \mu\text{g/ml}$)
50	0.076	0.083	1.83	0.5	0.19
100	5.189	0.083	3.65	8	0.69
200	2.540	0.083	27.21	8	9.30
400	1.325	0.083	45.62	8	33.81

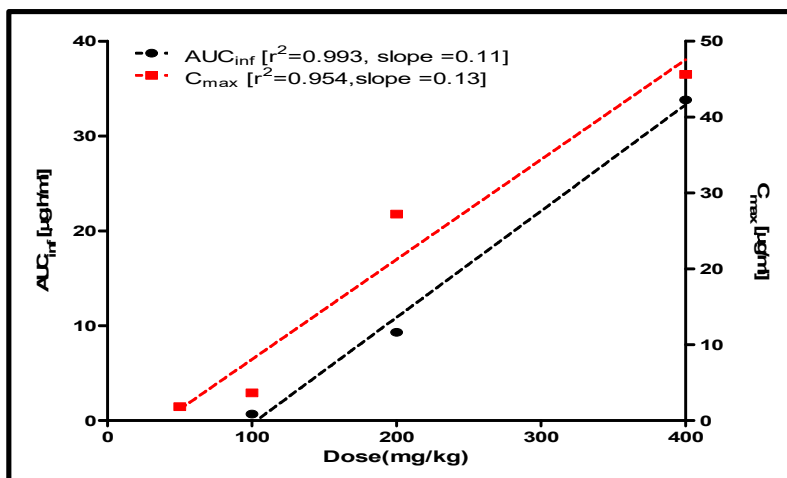


Figure 7: Relationship of AUC_{0-8h} and C_{max} with a dose of RRA267 in mice. The dashed lines are regression lines

Compound RRA268 showed moderately rapid absorption [$t_{max}= 0.5-2h$] post-dose followed by approximately bi-exponential disposition, except at 100mg/kg, with first-order kinetics [Figure 8]. The terminal elimination phases at 50,200 and 400mg/kg were parallel suggesting linear PK between 50 and 400 mg/kg. Twin peaks were observed post-dose at 50 and 100mg/kg body weight of mice.

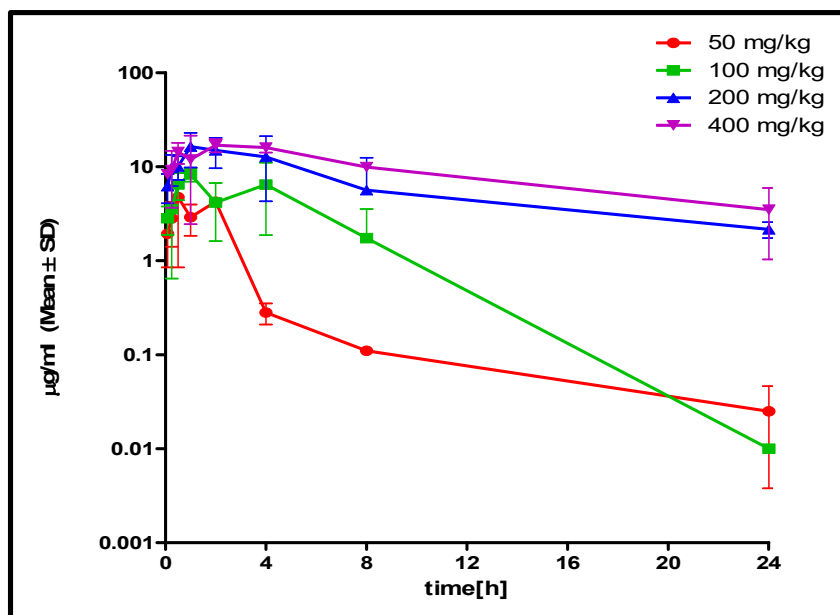


Figure 8: Mean concentration time profiles of RRA268 following single oral doses of 50,100,200 and 400 mg/kg in mice. Error bars are SD.

Compound RRA268 showed more than dose dose-proportional linear [$r^2=0.98$] increase in AUC_{0-inf} between 50 and 200mg/kg, and plateauing at 400mg/kg. The $AUC/dose$ increased between 50 and 100 and decreased at 400mg/kg. C_{max} showed a dose-proportional linear increase between 50 and 200 mg/kg and plateauing at 400 mg/kg of body weight of mice, as shown in Figure 9 and Table 14.

Table 14. Relationship between dose and AUC and C_{max} for RRA267 in mice

Dose [mg/kg]	$t_{1/2}$ (h)	T_{max} (h)	C_{max} ($\mu\text{g/ml}$)	AUC_{INF} ($\text{h}^*\mu\text{g/ml}$)
50	4.32	0.5	4.75	16.28
100	2.08	1	8.27	52.76
200	6.24	1	16.35	209.46
400	7.64	2	16.9	236.7

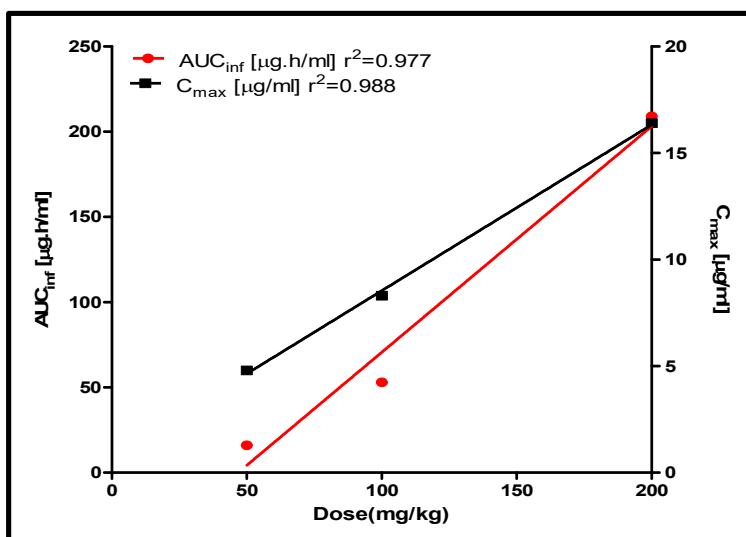


Figure 9: Relationship between AUC_{0-inf} and dose of RRA268 in mice

4.3. Discussion

Many potential drug candidates fail in the early stages of drug discovery due to undesirable toxicity and inadequacies caused by absorption, distribution, metabolism, and excretion (ADME) properties [32]. Therefore, robust pharmacokinetics information on modern drugs

with challenging targets can aid in developing and selecting in-vitro pharmacological models to evaluate molecular pathways in a kinetically practical method [33-35]. Pharmacokinetic studies are developed to evaluate the fate of the newly synthesized drug, which determines the effective concentration of the active substance at its target site, which plays a crucial therapeutic role. An in-vitro ADME and in-vivo Pk study for novel TB-active Decoquinare derivatives was reported earlier in drug discovery against Mtb [36]. Nowadays, the regulatory authorities mandate the data to evaluate safety, efficacy, and quality to get the basic idea for the proposed drug. The present work used a quick, sensitive, and specific LC-MS/MS method to estimate the compound concentration in mice plasma. The method was suitable for studying tissue distribution, plasma pharmacokinetics, and protein binding of RRA compounds in mice and can be used with modifications for thorough PK studies of other triazole derivatives.

The compound is extracted from blood or plasma by solvent extraction or protein precipitation and subjected to bioanalysis by LC-MS to quantify compound concentrations. Based on the concentration-time profile, PK parameters are estimated. In the present study, 30 RRA compounds were evaluated for their metabolic stability analysis (intrinsic clearance CL_{int}) in liver microsomes in mice and humans. Results suggest that there is significant variation in CL_{int} with respect to pharmacodynamic constituents in the structure. The CL_{int} also depends on interspecies differences, i.e., species-specific microsomes in human and mouse liver microsomes during drug metabolism. RRA 267 with a maximum $t_{1/2}$ of 135.5 min suggest higher in-vivo stability and lower clearance rate among the other tested compound.

Further studies are required to explore the excretion profile of RRA compounds and understand the potential influence of different intestinal content on metabolism. Species-specific protein binding analysis in the present study in human and mice plasma predicts the interaction of RRA compounds to proteins with blood. The unbound fraction of the compound undergoes metabolism in the liver and other tissues. This protein binding can influence the compound's biological half-life and may be affected by the degree to which it binds. Parallel artificial membrane permeability (PAMPA) analysis in our study identified the suitable candidates for passive drug permeability [37-40]. Two compounds, RRA 268 and RRA 242 showed maximum permeability P_{app} values of 7.8×10^{-6} cm/s and 7.6×10^{-6} cm/s, suggesting the increased possibility of transport across the cell membrane through the

gastrointestinal tract, blood-brain barrier as well as general passive transport across the cell membrane. This indicates that the -SH group for RRA 243 and -NH₂ group present in RRA 268 may allow compounds to permeate the cell membrane and mycolic cell wall of Mtb. RRA 8 and RRA 267 showed no permeability indicating a further need for structural modifications to improve their in-vivo characteristics.

An NCA PK analysis was performed using MS Excel to calculate the PK parameters for RRA compounds. The maximum tolerable dose in the present study was done to estimate a single intravenous dose administration with subsequent formulations of RRA compounds in the range of 0-500 mg/kg in mice. After a single intravenous dose, the RRA compound was promptly reduced from the plasma of mice. The bioanalytical methods for all the compounds were sensitive, linear, accurate, and precise in the concentration ranges to be tested and met all the acceptance criteria. The concentration-time data and other PK parameters for the RRA compounds are shown in Table 7. The highest Area Under the Plasma Concentration Time Curve (AUC_(0-t)) following a single oral dose of 20 mg/kg in mice was achieved highest by RRA 242 (7.15 µg.h/ml) and RRA 265 (0.04 µg.h/ml), showing the lowest resulting in variation of distribution and elimination post-infusion period (Figure1). Furthermore, our MTD analysis of selected RRA compounds was identified in mice following single-dose oral administrations of 50-500 mg/kg was at least 500 mg/kg. This confirms the efficacy of the compounds for in-vivo analysis for up to 500mg/kg. At last, based on the single-dose analysis and MTD study for RRA compounds, i.e., RRA79, RRA242, RRA267, and RRA268 were selected for the oral dose escalation study to get the final dose concentration to be given for further efficacy studies. Our results of an oral dose-escalation study for RRA 79 suggest 400, 150, 50 mg/kg dosed twice daily, for RRA242 suggests 400, 150, 50 mg/kg dosed twice daily, for RRA267 400, 150, 50 mg/kg dosed twice daily and for RRA 268 200, 60, 20 mg/kg dosed once daily (Figure 2-9 and Table 14).

In summary, the library of triazole (RRA) compounds was screened for anti-TB activity against active and dormant stage Mtb and identified 30 RRA compounds with significant inhibition against Mtb. Further PK study was done for the same compounds to understand the stability, protein binding efficiency, and possibility of passive diffusion in the cell membrane. RRA 242, RRA 267, and RRA 268 for further efficacy studies. The data provided in the present work helps to select the appropriate dosing of a compound for in-vitro pharmacological studies considered a suitable drug. Future experiments are required using

virulent strains of Mtb to explore the true potential of the RRA compounds as potential candidates for anti-TB therapy.

4.4. Materials and methods

4.4.1. Chemicals and materials

All the chemicals such as XTT, DMSO, rifampicin, isoniazid, and M phlei media components, including KH_2PO_4 , trisodium citrate, MgSO_4 , asparagine, and glycerol, were purchased from Sigma Aldrich USA unless otherwise mentioned. Dubos medium was purchased from DIFCO, USA. RPMI 1640 cell culture media and fetal bovine serum (FBS) were purchased from GIBCO, USA. Stock solutions (10mg/ml) of all the synthesized compounds were freshly prepared in DMSO and used the same day after mixing.

4.4.2. In-vivo Test System

Species: Mice

Strain: Balb/c

Weight: 20-24 g

Age: 6-8 weeks

Sex: Female

4.4.3. Animal welfare

This study was performed at TheraIndx Lifesciences Private Limited, a CPCSEA-approved laboratory (Registration number 1852/PO/Rc/S/16/CPCSEA), following all ethical practices laid down in the guidelines for animal care [41,42]. The study has been approved by the Institutional Animals Ethics Committee (IAEC) of the test facility under the Project entitled “Maximum Tolerated Dose studies of TN series (TN 01- TN 15) of compounds in Mice” (Protocol No. IAEC/01/2016/002)

4.4.4. Husbandry

Conditions: The animal room environment was monitored twice a day for temperature and relative humidity. The temperature range was 22 ± 2 °C, and the humidity range was between 45 and 60%. The animals were provided with 12 h of light and 12 h of dark artificial photoperiod.

Animals were housed in IVC systems and acclimatized for seven days after the veterinary examination for the study. Only animals without any visible signs of abnormalities were used

for the study. Housing: Groups of 3 animals in polypropylene cages (approximately 100 sq cm area for each animal) Diet: Nutrilab Rodent Feed from M/s. Provimi Animal Nutrition India Pvt. Ltd., Bangalore, was provided *ad libitum*. Water: Bisleri water was provided *ad libitum*.

4.4.5. Treatment/Animal dosage

Animals were dosed orally, by gavage, from the lowest to the highest dose, with half-hour intervals between each dose for clinical observations [43,44]. Post each dose, animals were observed for 72 h and were compared with the vehicle control group for the following parameters: a) Bodyweight just before dosing and at 24 h post-dosing; b) Clinical signs (gait, posture, excretions, and secretions, morbidity) before and immediately after dosing up to 72 h; c) Mortality

4.4.6. Bacterial strains, media, and inoculum preparation

M. tuberculosis H37Ra (ATCC 25177) was obtained from Astra Zeneca, Bangalore, India. The THP-1 cell line was obtained from the National Collection of Industrial Microorganisms (NCIM), Pune, India. Subculturing of all mycobacterial strains was routinely done in Dubos albumin agar slants or plates. The liquid inoculum was prepared in Dubos broth containing 2% glycerol (v/v) and 10 % albumin-dextrose-catalase (ADC), incubated in a shaker incubator rotating at a speed of 150 rpm at 37 °C. For in-vitro screening subculture in M.pheli medium containing 0.5 gm Potassium dihydrogen orthophosphate, 0.25 gm Sodium citrate, 60 mg Magnesium chloride, 0.5 gm Asparagine, and 2% (v/v) glycerol in 100 ml of distilled water at pH 6.6 ± 0.2. The stock culture was maintained at -70°C and subcultured once in a liquid medium before inoculation to an experimental culture. The stock was maintained at -70 °C and sub-cultured once in a liquid medium before inoculation in the experimental culture medium at 37 °C till the logarithmic phase (OD₆₂₀ ~ 1.0) was reached. 1% of 1.0 OD₆₂₀ of the culture was used as standard inoculum size for all the experiments, yielding final inoculum of approximately 10⁵ CFU/ml.

4.4.7. In-vitro antitubercular activity of synthesized triazoles derivatives against the active and dormant stage of *Mycobacterium tuberculosis*

For antitubercular activity screening, stock solutions of all the synthesized compounds were freshly prepared in DMSO and evaluated for their in-vitro antitubercular activity against the active and dormant stage Mtb using an established microplate-based technique using

tetrazolium salt 2,3-bis[2-methoxy-4-nitro-5-sulphophenyl]-2H-tetrazolium-5-carboxanilide (XTT) and menadione to determine the viability of Mtb [27]. Briefly, 2.5 μ l of the test solutions at different concentrations between 100-0 μ g/ml were added to 247.5 μ l of M. phlei medium containing bacilli and incubated for 8 days for the active stage and 12 days for the dormant stage at 37 °C. Post incubation, an XRMA assay was performed. The plate was read on SpectraMax Plus 384, Molecular Devices, Inc., using a 470 nm filter against a blank prepared from cell-free wells. MIC and IC₅₀ values of the selected compound were calculated from their dose-response curves by using OriginPro 2019b software. The assay was carried out in triplicates, and the percentage inhibition was calculated using a similar formula as per the described method below in the calculation of percent inhibition. The data shown are representative of three independent experiments.

4.4.8. Screening of active molecules against intracellular *Mycobacterium tuberculosis* inside THP-1 macrophage by (Nitrate reduction) NR assay (Ex-vivo assay)

THP-1 was used to examine the inhibitory activity of the compounds against intracellular bacilli by following a method described earlier [28]. Briefly, 3 ml of THP-1 cells (~5x10⁴ cells/ml) were treated with 100 nM of phorbol myristate acetate (PMA) in a culture flask for 24 h to convert them into macrophages. These macrophages were further incubated for 12 h with *M. tuberculosis* H₃₇Ra at MOI (multiplicity of infection) of 1: 100 for infection. Extracellular bacilli were removed by washing twice with sterile PBS and then adding fresh medium to adhered cells. Compounds were then added to these infected macrophages at different concentrations. In order to check the effect of inhibitors on the growth of intracellular bacilli, compounds were added at 0 h (for identification of active stage inhibitors) and after 120 h (for identification of dormant stage inhibitors) of infection. Unless mentioned otherwise, the effect of the compound was monitored by determining the bacterial load within macrophages by lysing them with hypotonic buffer (10 mM HEPES, 1.5 mM MgCl₂, and 10 mM KCl) at different time points and spreading 100 μ L of the samples on Dubos agar plates to enumerate colonies after 21 days.

4.4.9. Anti-bacterial Activity

To determine specificity, we have used optical density-based measurements to assess bacterial growth inhibition for screening compounds for their anti-bacterial activity against Gram-positive and Gram-negative bacteria [45]. All the synthesized compounds were screened for their in-vitro anti-bacterial activity in 96-well plates against four bacterial strains

(Gram-negative strains: *Escherichia coli* (NCIM 2065; ATCC 8739) and *Pseudomonas aeruginosa* (NCIM 5029; ATCC 27853); Gram-positive strains: *Staphylococcus aureus* (NCIM 2901; ATCC 29737) and *Bacillus subtilis* (NCIM 2920; ATCC 605). Once the cultures reached OD₆₂₀ of 1, 0.1 % of bacterial culture was used as inoculum to determine anti-bacterial activity. The synthesized compounds were screened to monitor the dose-response effect and incubated for 8 h at 37 °C. Post-incubation OD₆₂₀ was measured for both Gram-positive and Gram-negative bacteria. Here reference drugs in clinical use, Ampicillin and Kanamycin, served as standard. The data shown are representative of three independent experiments.

4.4.10. Cytotoxicity of the active molecules

The cytotoxicity compound was examined by examining their effect on the proliferation of THP-1 (Human leukemia monocytic cell line), A549 (Human lung cancer cell line), PANC-1 (Human pancreatic cancer cell line), and HeLa (Human cervical cancer cell line) by 3-(4,5-dimethylthiazol-2-yl)-2,5-diphenyltetrazolium bromide (MTT) assay method [29,30]. Briefly, growing cells from individual cell lines (1x10⁶ cells/ml) were used to monitor the dose-response effect of the inhibitors. DMSO was used as vehicle control. The 96 well-plates were then incubated for 72 h in the incubator (37 °C, 5% CO₂, 95% humidity) to adhere to the well bottom. After adding MTT dye solution (50 µg/ml) to each well, the plate was incubated for 1h in an incubator. 200 µL of isopropanol was added to each well and kept for 4 h to dissolve the formazan crystal. The read-out was taken after 72 h of incubation at 490nm. The GI₅₀ values of the selected compound were calculated from their dose-response curves by using OriginPro 2019b software. The assay was carried out in triplicates, and the percentage inhibition was calculated using a similar formula as per the described method below in the calculation of percent inhibition. The data shown are representative of three independent experiments.

4.4.11. Calculation of percent inhibition

The percentage inhibition was calculated using the following equation: percentage inhibition = [(Average absorbance of control- Average absorbance of the test sample)/ (Average absorbance of control - Average absorbance of blank)] X 100, where control denotes the medium with bacilli together with the vehicle, test denotes the medium with bacilli together with compound and blank denotes the cell-free medium.

4.4.12. Microsomal Metabolic Stability Assay in Human Liver Microsomes

Human liver microsomes were removed from a -75 °C deep freezer and thawed on an ice bath. Following thawing, 27.5 µL microsomes (20 mg/ml) were mixed in ~971.5 µL of 66.7 mM potassium phosphate buffer (pH 7.4), getting a concentration of ~ 0.5 mg/ml of microsomal protein. 1.1 µL of test compound/Verapamil (1 mM) was added to the reaction mixture to obtain a final concentration of 1 µM. Aliquots of 180 µl were drawn from the reaction mixture and placed into separate Eppendorf tubes labeled as Tc (negative control), T0 (0 min), T5 (5 min), T15 (15 min), and T30(30 min). All the tubes were pre-incubated at 37 °C for 5 min in a shaking water bath along with the test compound/reference standard. Following the pre-incubation, the reaction was initiated by adding 20 µL of NADPH (10 mM) to tubes T0, T5, T15, and T30. To the Tc tube, 20 µL of potassium phosphate buffer (PPB) was added instead of NADPH and incubated for 30 min. At the end of each of the incubation times (Tc, T0, T5, T15, and T30), the reaction in the corresponding tubes was terminated by adding 200 µL of quenching solution. The samples were centrifuged at 4000 rpm for 10 min, and 200 µL of the supernatant from each vial was analysed by API 4000 LC-MS/MS. The assay was done in duplicates.

4.4.13. Microsomal Metabolic Stability Assay in Mouse Liver Microsomes

Mouse liver microsomes were removed from a -75 °C deep freezer and thawed on an ice bath. Following thawing, 27.5 µL microsomes (20 mg/ml) were mixed in ~971.5 µL of 66.7 mM PPB (pH 7.4), get a concentration of ~ 0.5 mg/ml of microsomal protein. 1.1 µL of test compound/Verapamil (1 mM) was added to the reaction mixture to obtain a final concentration of 1 µM. Aliquots of 180 µL were drawn from the reaction mixture and placed into separate Eppendorf tubes labeled as Tc (negative control), T0 (0 min), T5 (5 min), T15 (15 min), and T30 (30 min). All the tubes were pre-incubated at 37 °C for 5 min in a shaking water bath along with the test compound/reference standard. Following the pre-incubation, the reaction was initiated by adding 20 µL of NADPH (10 mM) to tubes T0, T5, T15, and T30. To the Tc tube, 20 µL of PPB was added instead of NADPH and incubated for 30 min. At the end of each of the incubation times (Tc, T0, T5, T15, and T30), the reaction in the corresponding tubes was terminated by adding 200 µL of quenching solution. The samples were centrifuged at 4000 rpm for 10 min, and 200 µL of the supernatant from each vial was analysed by API 4000 LC-MS/MS. The assay was done in duplicates.

4.4.14. Human Plasma Protein Binding

Human Plasma protein binding was done using the Rapid Equilibrium Device described earlier [46]. The membranes were soaked in Milli-Q water for 60 min and subsequently in 20% ethanol in Milli-Q water for 30 min. The membranes were rinsed well with Milli-Q water twice before loading onto the HT dialyzer. 150 μ L of mouse plasma (n=3) containing 3 μ M final concentration of test compound/reference standard was placed into the first half of the 96-well Micro-Equilibrium Dialysis Device [Reusable 96-well Micro-Equilibrium Dialysis Device HTD 96: HT Dialysis LLC-HTD 96b-1006]. 150 μ L (n=3) of blank sodium phosphate buffer was placed into the buffer half of the same well of the above plate and equilibrated at 37 ± 5 °C for 4.5 h, with constant rotation at 130 rpm on an orbital shaker. After equilibration, 10 μ L of a plasma sample from the plasma half of the well was pipetted to a vial/plate containing 200 μ L of quenching solution, and 50 μ L of blank buffer was added to it. Similarly, 50 μ L of buffer sample from the buffer half of the wells was pipetted to a vial/plate containing 200 μ L of quenching solution, and 10 μ L of blank plasma was added to it. The samples were centrifuged at 14,000 rpm for 5 min, and the supernatants were transferred to LC-MS vials or plates for analysis by LC-MS/MS. For recovery experiments, 10 μ L of plasma from the plasma half and 50 μ L from the buffer half of the same well were added to a vial plate containing 200 μ L of quenching solution, centrifuged at 14000 rpm and the supernatants were analysed by API 4000 LC-MS/MS.

4.4.15. Mouse Plasma Protein Binding

Mouse Plasma protein binding was done using the Rapid Equilibrium Device as described in the earlier method [46]. The membranes were soaked in Milli-Q water for 60 min and subsequently in 20% ethanol in Milli-Q water for 30 min. The membranes were rinsed well with Milli-Q water twice before loading onto the HT dialyzer. 150 μ L of mouse plasma (n=3) containing 3 μ M final concentration of test compound/reference standard was placed into the first half of the 96-well Micro-Equilibrium Dialysis Device [Reusable 96-well Micro-Equilibrium Dialysis Device HTD 96: HT Dialysis LLC-HTD 96b-1006]. 150 μ L (n=3) of blank sodium phosphate buffer was placed into the buffer half of the same well of the above plate and equilibrated at 37 ± 5 °C for 4.5 h, with constant rotation at 130 rpm on an orbital shaker. After equilibration, 10 μ L of a plasma sample from the plasma half of the well was pipetted to a vial/plate containing 200 μ L of quenching solution, and 50 μ L of blank buffer was added to it. Similarly, 50 μ L of buffer sample from the buffer half of the wells was

pipetted to a vial/plate containing 200 μL of quenching solution, and 10 μL of blank plasma was added to it. The samples were centrifuged at 14,000 rpm for 5 min, and the supernatants were transferred to LC-MS/MS vials or plates for analysis by LC-MS. For recovery experiments, 10 μL of plasma from the plasma half and 50 μL from the buffer half of the same well were added to a vial/ plate containing 200 μL of quenching solution, centrifuged at 14000 rpm, and the supernatants were analysed by API 4000 LC-MS/MS. The experiment was done in triplicates.

4.4.16. Permeability in Parallel artificial membrane permeability assay (PAMPA assay)

The Lipid-PAMPA method is a non-cell-based assay designed to predict drugs' passive, transcellular permeability in early drug discovery. The assay is carried out in a 96- well Multiscreen Permeability plate and measures the ability of compounds to diffuse from a Donor to an Acceptor compartment separated by a PVDF membrane filter pretreated with a lipid-containing organic solvent. A 1 to 4% solution (w/v) of lecithin in dodecane (~500 $\mu\text{L}/\text{plate}$) was prepared; 5 μL of the lecithin/dodecane mixture was placed into each Donor plate well, avoiding pipette tip contact with the membrane. Immediately after applying the artificial membrane (within 10 minutes maximum), 150 μL of drug-containing donor solutions (drugs dissolved in 5% DMSO, PBS) were added to each well of the Donor plate. 300 μL of aqueous buffer was added to each well of the PTFE Acceptor plate. The drug-filled Donor plate was placed carefully into the Acceptor plate. The plate lid was replaced, and the setup was incubated at room temperature for 16 h. After incubation, the acceptor plate was analyzed by API 4000 LC-MS/MS. The experiment was done in triplicates.

4.4.17. Test item preparation

The vehicle was 0.25% CMC (RRA 62, 79) or 0.25% CMC containing 2 % DMSO for compounds (RRA 90A, 96, 117, 193, 242, 264, 265, 266, 267, 268, 272, 289 and 293) that did not yield homogenous suspensions. Each compound was weighed and transferred into a mortar; appropriate volumes of 0.25% CMC were added in aliquots while grinding with a pestle. The final uniform suspension (concentration 2.0 mg/ml) was transferred to a vial.

4.4.18. Study design to evaluate single-dose administration

Groups of animals (n=12/compound) were administered single oral doses of 20 mg/kg, of each compound, at a dose volume of 10 ml/kg. Post dose, blood samples were collected from the mice at 5 min, 15 min, 30 min, 1 h, 2, 4, 8, and 24 h. Before sampling, mice were

anesthetized with isoflurane at the indicated time points. From each mouse, two blood samples were drawn; the 1st was non-terminal (~0.1 ml blood) done by saphenous vein puncture and the 2nd terminal, by retro-orbital plexus puncture using heparinized mice capillary tubes. Blood was collected in 2 ml Eppendorf tubes containing 0.01 ml of 10% K₂EDTA as an anticoagulant, mixed gently, and placed in ice before centrifugation. Blood was centrifuged at 10,000 r.p.m. for 5 min, and plasma was harvested and stored at -80 °C until analysis.

4.4.19. The maximum tolerated dose (MTD) of selected RRA compounds

The vehicle was 0.25% Carboxymethylcellulose (CMC) containing 2% DMSO. A 50 mg/ml suspension was prepared for each compound and homogenized in DMSO using a mortar and pestle. The subsequent formulations were prepared by diluting 50 mg/ml formulation to 40, 20, 10, and 5 mg/ml using the same vehicle. For this, the animals were divided into 23 groups, as shown in Table 11. Care was taken to vortexing each formulation suspension prior to dilution to ensure homogeneity of the suspensions.

Table 15: Study design for Maximum tolerable dose study

Compound	Group	Dose (mg/kg)	Concentration of compound in formulation (mg/ml)	No. of Animals/group	
Vehicle	G1	0	0	5	
	RRA79	G2	50	5	5
		G3	100	10	5
		G4	200	20	5
		G5	400	40	5
		G6	500	50	5
NCL242	G7	50	0	5	
	G8	100	5	5	
	G9	200	10	5	
	G10	400	20	5	
	G11	500	40	5	

NCL267	G12	50	0	5
	G13	100	5	5
	G14	200	10	5
	G15	400	20	5
	G16	500	40	5
NCL268	G17	50	0	5
	G18	100	5	5
	G19	200	10	5
	G20	400	20	5
	G21	500	40	5
NCL 62	G22	50	0	5
	G23	100	5	5
	G24	200	10	5
	G25	400	20	5
	G26	500	40	5
NCL293	G27	500	50	5
	G28	400	40	5

4.4.20. Oral Dose Escalation Pharmacokinetics of selected RRA compounds in Mice

A. Test Item preparation

In this study, the vehicle was 0.25% CMC. A 50 mg/ml suspension was prepared for each compound and homogenized in DMSO using a mortar and pestle. The final uniform suspensions were transferred to vials. All formulations were prepared on the day of the study. The final concentrations of each compound in the formulations were 5,10,20 and 40 mg/ml for the 50, 100, 200 and 400mg/kg doses, respectively. The dose-volume was 10ml/kg.

C. Study design

Compound	Oral Dose [mg/kg]	No. of mice/dose	No of mice /time point	Time points for blood collection
RRA79	50, 100, 200, 400	12	3	5 min, 15 min, 30 min, 1 h, 2, 4, 8 and 24 h.
RRA242	50, 100, 200 400	12	3	5 min, 15 min, 30 min, 1 h, 2, 4, 8 and 24 h.
RRA267	50, 100, 200 400	12	3	5 min, 15 min, 30 min, 1 h, 2, 4, 8 and 24 h.
RRA268	50, 100, 200 400	12	3	5 min, 15 min, 30 min, 1 h, 2, 4, 8 and 24 h.

Post dose, blood samples were collected from the mice at 5min,15min,1h,2h,4h,8h, and 24h. At the indicated time points and before sampling, mice were anesthetized with isoflurane. From each mouse, two blood samples were drawn; the 1st was non-terminal (0.1ml blood)done by saphenous vein puncture and the 2nd terminal, by retro-orbital plexus puncture using heparinized mice capillary tubes. Blood was collected in 2ml Eppendorf tubes containing 0.01ml of 10% K₂EDTA as an anticoagulant, mixed gently, and placed in ice before centrifugation. Blood was centrifuged at 10,000 r.p.m. for 5 min, and plasma was harvested and stored at -80°C until analysis.

C. Pharmacokinetic analysis

Mean data were used for PK analysis. NCA PK was performed using Phoenix WinNolin version 6.4.0.768 [certara] using the NCA PK model-Plasma Data, Extravascular Administration. The linear up-log down method was used to estimate AUC [31]. A minimum of 3 concentrations on the terminal liner phase were used to estimate the terminal elimination rate constant (λ_z) and half-life [$t_{1/2}$]. Dose proportionality was assessed using graphical plots of AUC_{0-inf} and C_{max} versus dose and the ratio of AUC/Dose and C_{max}/Dose [31].

4.5. References

1. World Health Organization, Global tuberculosis report 2021.Geneva; World Health Organization,2021.
2. Jnawali, Hum Nath, and Sungweon Ryoo. "First-and second-line drugs and drug resistance." *Tuberculosis-Current Issues in Diagnosis and Management* 20 (2013): 163-80.

3. World Health Organization. WHO consolidated guidelines on drug-resistant tuberculosis treatment. No. WHO/CDS/TB/2019.7. *World Health Organization*, 2019.
4. Eker, Barbara, Johannes Ortmann, Giovanni B. Migliori, Giovanni Sotgiu, Ralf Muetterlein, Rosella Centis, Harald Hoffmann et al. "Multidrug-and extensively drug-resistant tuberculosis, Germany." *Emerging infectious diseases* 14, no. 11 (2008): 1700.
5. Ramachandran, Geetha, and Soumya Swaminathan. "Safety and tolerability profile of second-line anti-tuberculosis medications." *Drug safety* 38, no. 3 (2015): 253-269.
6. Holla, Bantwal Shivarama, Manjathuru Mahalinga, Mari Sithambaram Karthikeyan, Boja Poojary, Padiyath Mohammed Akberali, and Nalilu Suchetha Kumari. "Synthesis, characterization and anti-microbial activity of some substituted 1, 2, 3-triazoles." *European journal of medicinal chemistry* 40, no. 11 (2005): 1173-1178.
7. Sanghvi, Yogesh S., Birendra K. Bhattacharya, Ganesh D. Kini, Steven S. Matsumoto, Steven B. Larson, Weldon B. Jolley, Roland K. Robins, and Ganapathi R. Revankar. "Growth inhibition and induction of cellular differentiation of human myeloid leukemia cells in culture by carbamoyl congeners of ribavirin." *Journal of medicinal chemistry* 33, no. 1 (1990): 336-344.
8. Ali, Abdul Aziz. *1, 2, 3-triazoles: Synthesis and biological application*. IntechOpen, 2020.
9. Bozorov, Khurshed, Jiangyu Zhao, and Haji A. Aisa. "1, 2, 3-Triazole-containing hybrids as leads in medicinal chemistry: A recent overview." *Bioorganic & medicinal chemistry* 27, no. 16 (2019): 3511-3531.
10. Staśkiewicz, Agnieszka, Patrycja Ledwoń, Paolo Rovero, Anna Maria Papini, and Rafal Latajka. "Triazole-modified peptidomimetics: an opportunity for drug discovery and development." *Frontiers in Chemistry* 9 (2021).
11. Holla, B. Shivarama, Richard Gonsalves, and Shalini Shenoy. "Studies on some N-bridged heterocycles derived from bis-[4-amino-5-mercapto-1, 2, 4-triazol-3-yl] alkanes." *Il Farmaco* 53, no. 8-9 (1998): 574-578.
12. Sahu, Jagdish K., Swastika Ganguly, and Atul Kaushik. "Triazoles: A valuable insight into recent developments and biological activities." *Chinese journal of natural medicines* 11, no. 5 (2013): 456-465.

13. Ashok, Mithun, and B. Shivarama Holla. "Convenient synthesis of some triazolothiadiazoles and triazolothiadiazines carrying 4-methylthiobenzyl moiety as possible anti-microbial agents." *J Pharmacol Toxicol* 2, no. 3 (2007): 256-263.
14. Prasad, D. Jagadeesh, Mithun Ashok, Prakash Karegoudar, Boja Poojary, B. Shivarama Holla, and Nalilu Sucheta Kumari. "Synthesis and anti-microbial activities of some new triazolothiadiazoles bearing 4-methylthiobenzyl moiety." *European journal of medicinal chemistry* 44, no. 2 (2009): 551-557.
15. Turan-Zitouni, Gülhan, Zafer Asım Kaplancıklı, Mehmet Taha Yıldız, Pierre Chevallet, and Demet Kaya. "Synthesis and antimicrobial activity of 4-phenyl/cyclohexyl-5-(1-phenoxyethyl)-3-[N-(2-thiazolyl) acetamido] thio-4H-1, 2, 4-triazole derivatives." *European Journal of Medicinal Chemistry* 40, no. 6 (2005): 607-613.
16. Amir, Mohd, and Kumar Shikha. "Synthesis and anti-inflammatory, analgesic, ulcerogenic and lipid peroxidation activities of some new 2-[(2, 6-dichloroanilino) phenyl] acetic acid derivatives." *European journal of medicinal chemistry* 39, no. 6 (2004): 535-545.
17. Walczak, Krzysztof, Andrzej Gondela, and Jerzy Suwiński. "Synthesis and anti-tuberculosis activity of N-aryl-C-nitroazoles." *European journal of medicinal chemistry* 39, no. 10 (2004): 849-853.
18. Holla, B. Shivarama, K. Narayana Poojary, B. Sooryanarayana Rao, and M. K. Shivananda. "New bis-aminomercaptotriazoles and bis-triazolothiadiazoles as possible anticancer agents." *European Journal of Medicinal Chemistry* 37, no. 6 (2002): 511-517.
19. Holla, B. Shivarama, B. Veerendra, M. K. Shivananda, and Boja Poojary. "Synthesis characterization and anticancer activity studies on some Mannich bases derived from 1, 2, 4-triazoles." *European Journal of Medicinal Chemistry* 38, no. 7-8 (2003): 759-767.
20. Almasirad, Ali, Sayyed A. Tabatabai, Mehrdad Faizi, Abbas Kebriaeezadeh, Nazila Mehrabi, Afshin Dalvandi, and Abbas Shafiee. "Synthesis and anticonvulsant activity of new 2-substituted-5-[2-(2-fluorophenoxy) phenyl]-1, 3, 4-oxadiazoles and 1, 2, 4-triazoles." *Bioorganic & medicinal chemistry letters* 14, no. 24 (2004): 6057-6059.
21. Patel, Navin B., Imran H. Khan, and Smita D. Rajani. "Pharmacological evaluation and characterizations of newly synthesized 1, 2, 4-triazoles." *European Journal of Medicinal Chemistry* 45, no. 9 (2010): 4293-4299.

22. Kumar, Deepak, Garima Khare, Saqib Kidwai, Anil K. Tyagi, Ramandeep Singh, and Diwan S. Rawat. "Synthesis of novel 1, 2, 3-triazole derivatives of isoniazid and their in vitro and in vivo antimycobacterial activity evaluation." *European journal of medicinal chemistry* 81 (2014): 301-313.
23. Rode, Navnath D., Amol D. Sonawane, Laxman Nawale, Vijay M. Khedkar, Ramesh A. Joshi, Anjali P. Likhite, Dhiman Sarkar, and Rohini R. Joshi. "Synthesis, biological evaluation, and molecular docking studies of novel 3-aryl-5-(alkyl-thio)-1H-1, 2, 4-triazoles derivatives targeting Mycobacterium tuberculosis." *Chemical Biology & Drug Design* 90, no. 6 (2017): 1206-1214.
24. Sonawane, Amol D., Navnath D. Rode, Laxman Nawale, Rohini R. Joshi, Ramesh A. Joshi, Anjali P. Likhite, and Dhiman Sarkar. "Synthesis and biological evaluation of 1, 2, 4-triazole-3-thione and 1, 3, 4-oxadiazole-2-thione as antimycobacterial agents." *Chemical Biology & Drug Design* 90, no. 2 (2017): 200-209.
25. Sarkar D, Deshapande SR et al. 1, 2, 4-Triazole Derivatives and their anti mycobacterial activity. US Patent Appl US 2013/0060045 A1 (2013).
26. Jang, Graham R., Robert Z. Harris, and David T. Lau. "Pharmacokinetics and its role in small molecule drug discovery research." *Medicinal research reviews* 21, no. 5 (2001): 382-396.
27. Singh, Upasana, Shamim Akhtar, Abhishek Mishra, and Dhiman Sarkar. "A novel screening method based on menadione mediated rapid reduction of tetrazolium salt for testing of anti-mycobacterial agents." *Journal of microbiological methods* 84, no. 2 (2011): 202-207.
28. Sarkar, Sampa, and Dhiman Sarkar. "Potential use of nitrate reductase as a biomarker for the identification of active and dormant inhibitors of Mycobacterium tuberculosis in a THP1 infection model." *Journal of Biomolecular Screening* 17, no. 7 (2012): 966-973.
29. Molinari, Aurora, Alfonso Oliva, Claudia Ojeda, José M. Miguel del Corral, M. Angeles Castro, Carmen Cuevas, and Arturo San Feliciano. "Synthesis and Cytotoxic Evaluation of 6-(3-Pyrazolylpropyl) Derivatives of 1, 4-Naphthohydroquinone-1, 4-diacetate." *Archiv der Pharmazie: An International Journal Pharmaceutical and Medicinal Chemistry* 342, no. 10 (2009): 591-599.
30. Manjula, S. N., N. Malleshappa Noolvi, K. Vipani Parihar, SA Manohara Reddy, Vijay Ramani, Andanappa K. Gadad, Gurdial Singh, N. Gopalan Kutty, and C. Mallikarjuna Rao.

"Synthesis and antitumor activity of optically active thiourea and their 2-aminobenzothiazole derivatives: A novel class of anticancer agents." *European Journal of Medicinal Chemistry* 44, no. 7 (2009): 2923-2929.

31. Gabrielsson, Johan, and Daniel Weiner. *Pharmacokinetic and pharmacodynamic data analysis: concepts and applications*. CRC press, 2001.

32. Li, Albert P. "Screening for human ADME/Tox drug properties in drug discovery." *Drug discovery today* 6, no. 7 (2001): 357-366.

33. Hao, Haiping, Xiao Zheng, and Guangji Wang. "Insights into drug discovery from natural medicines using reverse pharmacokinetics." *Trends in pharmacological sciences* 35, no. 4 (2014): 168-177.

34. Aggarwal, Bharat B., and Bokyoung Sung. "Pharmacological basis for the role of curcumin in chronic diseases: an age-old spice with modern targets." *Trends in pharmacological sciences* 30, no. 2 (2009): 85-94.

35. Jones, Quinton RD, Jordan Warford, HP Vasantha Rupasinghe, and George S. Robertson. "Target-based selection of flavonoids for neurodegenerative disorders." *Trends in pharmacological sciences* 33, no. 11 (2012): 602-610.

36. Tanner, Lloyd, Richard K. Haynes, and Lubbe Wiesner. "An in vitro ADME and in vivo pharmacokinetic study of novel TB-active decoquinate derivatives." *Frontiers in pharmacology* 10 (2019): 120.

37. Kansy, Manfred. "Physicochemical high throughput screening: parallel artificial membrane permeation assay in the description of passive absorption processes." *J Med Chem* 41 (1998): 1007-1010.

38. Wohnsland, Frank, and Bernard Faller. "High-throughput permeability pH profile and high-throughput alkane/water log P with artificial membranes." *Journal of medicinal chemistry* 44, no. 6 (2001): 923-930.

39. Sugano, Kiyohiko, Yoshiaki Nabuchi, Minoru Machida, and Yoshinori Aso. "Prediction of human intestinal permeability using artificial membrane permeability." *International journal of pharmaceutics* 257, no. 1-2 (2003): 245-251.

40. Ottaviani, Giorgio, Sophie Martel, and Pierre-Alain Carrupt. "Parallel artificial membrane permeability assay: a new membrane for the fast prediction of passive human skin permeability." *Journal of medicinal chemistry* 49, no. 13 (2006): 3948-3954.
41. Care, V. "CPCSEA guidelines for laboratory animal facility." *Indian J Pharmacol* 35 (2003): 257-274.
42. National Research Council. "Guide for the care and use of laboratory animals." (2010).
43. Guidance Document on the Recognition, Assessment and Use of Clinical signs as humane endpoints for Experimental Animals used in Safety Evaluation. ENV/JM/MONO(2000)7. OECD, (2000).
44. Schedule, Y. "of The Drugs and Cosmetics Act, 1940, amendment June, 2005." New Delhi: Ministry of Health and Family Welfare (2005).
45. Campbell, Jennifer. "High-throughput assessment of bacterial growth inhibition by optical density measurements." *Current protocols in chemical biology* 2, no. 4 (2010): 195-208.
46. Waters, Nigel J., Rachel Jones, Gareth Williams, and Bindi Sohal. "Validation of a rapid equilibrium dialysis approach for the measurement of plasma protein binding." *Journal of pharmaceutical sciences* 97, no. 10 (2008): 4586-4

ABSTRACT

Name of the Student: Mr. Sagar Swami

Faculty of Study: Biological Science

AcSIR academic center/

CSIR Lab: CSIR-NCL

Registration No. : 10BB17J26055

Year of Submission: 2022

Name of the Supervisor(s): Dr.D Sarkar

Title of the thesis: Biological evaluation of novel small molecule inhibitors against *Mycobacterium tuberculosis*

Mycobacterium tuberculosis (Mtb), the causative agent of tuberculosis (TB), has co-evolved with humans for thousands of years, avoiding the immune system in a dormant or latent state. According to World Health Organization (WHO), TB is a worldwide pandemic; and it is anticipated that at least one-quarter of the world's population could be infected with latent TB.

In my thesis, we tried to address two major issues: 1. the urgent need for new candidate molecules that can act on the active and dormant stage of Mtb, 2. a poor understanding of the target for the proposed hits after thorough screening procedures. We have screened >300 compounds of different categories against the active and dormant stages of Mtb by using in-vitro, ex-vivo, and in-vivo methods to identify the potential candidate showing significant stage-specific inhibitory activity. We further selected two compounds conjugated with a linker molecule. Using the pull-down method and mass spectrometry analysis, we identified GroEl2 protein as a potential target for RRA2 inhibitor in active stage Mtb and DNA binding HU protein as a target for RRA268 inhibitor in dormant stage Mtb. Further, we analyzed the conservation pattern of target protein among other species of mycobacteria and between Mtb H37Ra and Rv strain. At last, we have predicted the binding site and type of interaction of the inhibitor with its target site using molecular modeling studies. Our findings may open up new avenues to examine the role of GroEl2 and HU protein as possible targets for drugs.

Many potential drug candidates fail in the early stages of drug discovery due to undesirable toxicity and inadequacies caused by ADME properties. Hence in the present study, we have selected 30 RRA compounds based on their inhibition properties, checked for specificity against non-mycobacterial species, and evaluated for toxicity effect against different cancer cell lines. We characterized these compounds' PK properties using the in vitro, ex-vivo, and in-vivo methods in mice. At last, we determined the effective concentration of dose required for further efficacy studies.

A. Publications emanating from the thesis work-

1. Sarkar, Sampa*, **Sagar Swami***, Sarvesh Kumar Soni, Jessica K. Holien, Arshad Khan, Arvind M. Korwar, Anjali P. Likhite, Ramesh A. Joshi, Rohini R. Joshi, and Dhiman Sarkar. "Detection of a target protein (GroEl2) in *Mycobacterium tuberculosis* using a derivative of 1, 2, 4-triazolethiols." **Molecular Diversity** (2021): 1-14.
2. Puranik, Ninad V.*, **Sagar Swami***, Ashwini V. Misar, Ritu Mamgain, Swapnaja S. Gulawani, Dhiman, Sarkar, and Pratibha Srivastava. "The first synthesis of podocarflavone A and its analogs and evaluation of their antimycobacterial potential against *Mycobacterium tuberculosis* with the support of virtual screening." **Natural Product Research** (2021): 1-8.
3. Waghmode, Samadhan, **Sagar Swami**, Dhiman Sarkar, Mangesh Suryavanshi, Sneha Roachlani, Prafulla Choudhari, and Surekha Satpute. "Exploring the pharmacological potentials of biosurfactant derived from *Planococcus maritimus* SAMP MCC 3013." **Current microbiology** 77, no. 3 (2020): 452-459.
4. **Sagar Swami**, Rahul Aher, Dhiman Sarkar. Detection of target protein (DNA binding protein HU) in the dormant stage of *Mycobacterium tuberculosis* using a derivative of 1, 2, 4-triazole. (**Manuscript under submission**)
5. **Sagar Swami**, Dhiman Sarkar. Drug Metabolism And Pharmacokinetics Study Of Novel Triazole Hits Against *Mycobacterium tuberculosis* (**Manuscript under submission**)
6. Ritu Mamgain*, **Sagar Swami***, R. J. Waghole, Swapnaja Gulwani, Garima Mishra, Dhiman Sarkar, Pratibha Srivastava: Design, synthesis, and in vitro biological evaluation of Phenanthridin-trione-epoxide conjugates as antitubercular agents against *Mycobacterium tuberculosis*. (**Manuscript under submission**)
7. Abhay Bavishi, **Sagar Swami**, Shailesh Thakrar, Hardev Vala, Dhiman Sarkar, Anamik Shaha. Synthesis of Some Pyrazole derivatives of 5-Chloro-2-Methoxy Phenyl Hydrazide and its Biological Evaluation. (**Under review**)
8. Abhay Bavishi, **Sagar Swami**, Shailesh Thakrar, Hardev Vala, Dhiman Sarkar, Anamik Shaha. Synthesis of some coumarins derivatives and their biological evaluation. (**Under submission**)
9. Abhay Bavishi, **Sagar Swami**, Shailesh Thakrar, Hardev Vala, Dhiman Sarkar, Anamik Shaha. Antitubercular and antimicrobial activity of pyrazole scaffolds hybrid with 1,4-dihydropyridine and 4-hydroxycoumarin: in-vitro and in silico studies. (**Under submission**)
10. Abhay Bavishi, **Sagar Swami**, Shailesh Thakrar, Hardev Vala, Dhiman Sarkar, Anamik Shaha. Synthesis of azipine clubbed coumarin derivatives and its antitubercular and antimicrobial activity: in-vitro and in silico studies. (**Under submission**)

B. Publications emanating out of the thesis work-

1. Puranik, Ninad V., Pratibha Srivastava, **Sagar Swami**, Amit Choudhari, and Dhiman Sarkar. "Molecular modeling studies and in-vitro screening of dihydrorugosaflavonoid and its

derivatives against *Mycobacterium tuberculosis*." RSC advances 8, no. 19 (2018): 10634-10643.

List of Poster presentations

1. Participated in a poster presentation at **National Science Day** arranged by **CSIR-National Chemical laboratory-Feb. 2019**.

Title- Detection of a target protein (GroEl2) in *Mycobacterium tuberculosis* using a derivative of 1,2,4-triazolethiols.

Abstract: Mycobacterial chemotherapy is complicated due to both the requirement for prolonged treatment with a combination of drugs and the emergence of drug-resistant strains. However, a major need in global health is to eradicate persistent or non-replicating subpopulations of Mtb bacilli. In the preliminary analysis, an in-house library of 1, 2, 4-triazolethiol derivatives was screened against *M. bovis* BCG, and *Mycobacterium tuberculosis* showed significant antitubercular activity. Notably, the RRA-2 inhibitor was found to be inhibiting both replicating and non-replicating Mtb bacilli with MIC values of $4.46 \pm 0.17 \mu\text{g/ml}$ and $4.79 \pm 0.6 \mu\text{g/ml}$, respectively. In addition, the affinity pooling of target protein was achieved by linking the Azide PEG-3 biotin with RRA-2 and found ~60 kD protein band in SDS-PAGE analysis. Further work for the identification and validation of the captured protein is in progress.

2. Participated in a poster presentation at **International Conference on Infectious Diseases and Immunopathology** organized by SPPU Pune- **Apr.2021**.

Title: Detection of a target protein (GroEl2) in *Mycobacterium tuberculosis* using a derivative of 1,2,4-triazolethiols.

Abstract- Herein, we evaluated a limited series of 54 allyl and propargyl derivatives of alkyl, aryl, and heteroaryl-substituted 1,2,4-triazolethiols for in-vitro and ex-vivo mycobactericidal activity. A structure-activity relationship (SAR) study using 54 analogs against *Mycobacterium bovis* BCG indicated thiopropargylation/thioallylation at C-3 with simultaneous modification in the phenyl group attached at the C-5 position of the 1,2,4-triazole ring had very effective mycobactericidal activity. Compounds RRA2, RRA3, and RRA7 had mycobactericidal activity against *Mycobacterium bovis* BCG and *Mycobacterium tuberculosis* (Mtb) with minimum inhibitory concentration (MIC) values of 2, 0.2, and 2 $\mu\text{g/ml}$ respectively. At MIC concentrations, RRA2, RRA3, and RRA7 compounds yielded 0.82, 1.43, and 0.88 log cfu reduction against non-replicating *Mycobacterium tuberculosis*, respectively. These three compounds are selective and non-toxic, having little effect on the

growth of *Mycobacterium smegmatis*, *Escherichia coli* (*E. coli*), or THP-1 macrophages. Moreover, these molecules were similarly effective against intracellular Mtb in THP-1 macrophages. Using “click” chemistry via a biotin linker-inhibitor conjugate with the RRA2 inhibitor, we pulled down the GroEl 2 protein from Mtb whole-cell extract. When applied at their respective MIC level, all three inhibitors abrogate the ATPase activity of purified GroEl 2. Furthermore, computational molecular modelling indicated that these compounds were able to interact with GroEl 2 in a manner that explains the structure-activity relationship seen with this compound class. Overall, this study has unlocked a new opportunity for tuberculosis treatments by identifying 1,2,4-triazolethiols as potential anti-tuberculosis compounds and their novel target protein GroEl 2.

List of Conferences attained

1. Received “**Best oral presentation award**” with a cash prize in Virtual Conference on Proteomics in Agriculture and Healthcare-2021 arranged by School of Life Science, University of Hyderabad

Title: Identification of a growth responsible *Mycobacterium tuberculosis* target protein ‘GroEl 2’ and its inhibition via a series of 1,2,4-triazolethiols.

Abstract- Herein, we evaluated a limited series of 54 allyl and propargyl derivatives of alkyl, aryl, and heteroaryl-substituted 1,2,4-triazolethiols for in-vitro and ex-vivo mycobactericidal activity. A structure-activity relationship (SAR) study using 54 analogs against *Mycobacterium bovis* BCG indicated that thiopropargylation/thioallylation at C-3 with simultaneous modification in the phenyl group attached at the C-5 position of the 1,2,4-triazole ring had very effective mycobactericidal activity. Compounds RRA2, RRA3, and RRA7 had mycobactericidal activity against *Mycobacterium tuberculosis* (Mtb) with minimum inhibitory concentration (MIC) values of 2, 0.2, and 2 µg/ml, respectively. At MIC concentrations, RRA2, RRA3 and RRA7. These three compounds are selective and non-toxic, having little effect on the growth of *Mycobacterium smegmatis*, *Escherichia coli* (*E. coli*), or THP-1 macrophages. Moreover, these molecules were similarly effective against intracellular Mtb in THP-1 macrophages. Using “click” chemistry via a biotin linker-inhibitor conjugate with the RRA2 inhibitor, we pulled down the GroEl 2 protein from Mtb whole-cell extract. When applied at their respective MIC level, all three inhibitors abrogate the ATPase activity of purified GroEl 2. Furthermore, computational

molecular modelling indicated that these compounds were able to interact with GroEl 2 in a manner that explains the structure-activity relationship seen with this compound class. Overall, this study has unlocked a new opportunity for tuberculosis treatments by identifying 1,2,4-triazolethiols as potential anti-tuberculosis compounds and their novel target protein GroEl 2.

2. Received “**First prize**” for oral presentation at **International Science Symposium-2021** on Recent Trends in Science and Technology arranged by Christ College, Rajkot.

Title: IDENTIFICATION OF A GROWTH RESPONSIBLE *Mycobacterium tuberculosis* TARGET PROTEIN ‘GROEL 2’ AND IT’S INHIBITION VIA A SERIES OF 1,2,4-TRIAZOLETHIOLS

Abstract- Herein, we evaluated a limited series of 54 allyl and propargyl derivatives of alkyl, aryl, and heteroaryl-substituted 1,2,4-triazolethiols for in-vitro and ex-vivo mycobactericidal activity. A structure-activity relationship (SAR) study using 54 analogs against *Mycobacterium bovis* BCG indicated that thiopropargylation/thioallylation at C-3 with simultaneous modification in the phenyl group attached at the C-5 position of the 1,2,4-triazole ring had very effective mycobactericidal activity. Compounds RRA2, RRA3, and RRA7 had mycobactericidal activity against *Mycobacterium bovis* BCG and *Mycobacterium tuberculosis* (Mtb) with minimum inhibitory concentration (MIC) values of 2, 0.2, and 2 µg/ml respectively. At MIC concentrations, RRA2, RRA3, and RRA7 compounds yielded 0.82, 1.43, and 0.88 log reduction of cfu against non-replicating *Mycobacterium tuberculosis*, respectively. These three compounds are selective and non-toxic, having little effect on the growth of *Mycobacterium smegmatis*, *Escherichia coli* (*E. coli*), or THP-1 macrophages. Moreover, these molecules were similarly effective against intracellular Mtb in THP-1 macrophages. Using “click” chemistry via a biotin linker-inhibitor conjugate with the RRA2 inhibitor, we pulled down the GroEl 2 protein from Mtb whole-cell extract. When applied at their respective MIC level, all three inhibitors abrogate the ATPase activity of purified GroEl 2. Furthermore, computational molecular modelling indicated that these compounds were able to interact with GroEl 2 in a manner, which explains the structure-activity relationship seen with this compound class. Overall, this study has unlocked a new opportunity for tuberculosis treatments by identifying 1,2,4-triazolethiols as potential anti-tuberculosis compounds and their novel target protein GroEl 2.

3. Participated in an online conference organized by **NCL Research Foundation Annual Students conference-2021** as an oral presentation.

Title: Detection of a target protein (GroEl2) in *Mycobacterium tuberculosis* using a derivative of 1,2,4-triazolethiols.

Abstract- Herein, we identified a potential lead compound, RRA2, within a series of 54 derivatives of 1,2,4-triazolethiols (exhibit good potency as an anti-mycobacterial agent) against intracellular *Mycobacterium tuberculosis* (Mtb). Compound RRA2 showed significant mycobactericidal activity against active stage *Mycobacterium bovis* BCG and Mtb with minimum inhibitory concentration (MIC) values of 2.3 and 2.0 µg/ml, respectively. At MIC concentration, the RRA2 compound yielded a 0.82 log reduction of cfu against non-replicating Mtb. Furthermore, the RRA2 compound was selected for further target identification due to the presence of the alkyne group, showing higher selectivity index ($>66.66 \pm 0.22$ in the non-replicating stage). Using “click” chemistry, we synthesized the biotin linker -RRA2 conjugate, purified it with the HPLC method and confirmed the conjugation of the biotin linker-RRA2 complex by HR-MS analysis. Furthermore, we successfully pulled down and identified a specific target protein, GroEl2, from Mtb whole-cell extract. Furthermore, computational molecular modelling indicated RRA2 could interact with GroEl2, which explains the structure-activity relationship observed in this study.

4. Participated in **International Conference on Infectious Diseases and Immunopathology** organized by SPPU Pune-2021 with oral presentation.

Title: Detection of a target protein (GroEl2) in *Mycobacterium tuberculosis* using a derivative of 1,2,4-triazolethiols.

Abstract- Herein, we evaluated a limited series of 54 allyl and propargyl derivatives of alkyl, aryl, and heteroaryl-substituted 1,2,4-triazolethiols for in-vitro and ex-vivo mycobactericidal activity. A structure-activity relationship (SAR) study using 54 analogs against *Mycobacterium bovis* BCG indicated that thiopropargylation/thioallylation at C-3 with simultaneous modification in the phenyl group attached at the C-5 position of the 1,2,4-triazole ring had very effective mycobactericidal activity. Compounds RRA2, RRA3, and RRA7 had mycobactericidal activity against *Mycobacterium bovis* BCG and *Mycobacterium tuberculosis* (Mtb) with minimum inhibitory concentration (MIC) values of 2, 0.2, and 2 µg/ml respectively. At MIC concentrations, RRA2, RRA3, and RRA7 compounds yielded 0.82, 1.43, and 0.88 log reduction of cfu against non-replicating *Mycobacterium tuberculosis*, respectively. These three compounds are selective and non-toxic, having little effect on the

growth of *Mycobacterium smegmatis*, *Escherichia coli* (*E. coli*), or THP-1 macrophages. Moreover, these molecules were similarly effective against intracellular Mtb in THP-1 macrophages. Using “click” chemistry via a biotin linker-inhibitor conjugate with the RRA2 inhibitor, we pulled down the GroEl 2 protein from Mtb whole-cell extract. When applied at their respective MIC level, all three inhibitors abrogate the ATPase activity of purified GroEl 2. Furthermore, computational molecular modelling indicated that these compounds were able to interact with GroEl 2 in a manner that explains the structure-activity relationship seen with this compound class. Overall, this study has unlocked a new opportunity for tuberculosis treatments by identifying 1,2,4-triazolethiols as potential anti-tuberculosis compounds and their novel target protein GroEl2 protein as a potential target for RRA2 compound and DNA binding protein HU as a target for RRA268



Detection of a target protein (GroEL2) in *Mycobacterium tuberculosis* using a derivative of 1,2,4-triazolethiols

Sampa Sarkar^{1,2} · Sagar Swami^{2,3} · Sarvesh Kumar Soni¹ · Jessica K. Holien¹ · Arshad Khan^{2,4} · Arvind M. Korwar⁵ · Anjali P. Likhite⁶ · Ramesh A. Joshi⁶ · Rohini R. Joshi⁶ · Dhiman Sarkar^{2,3}

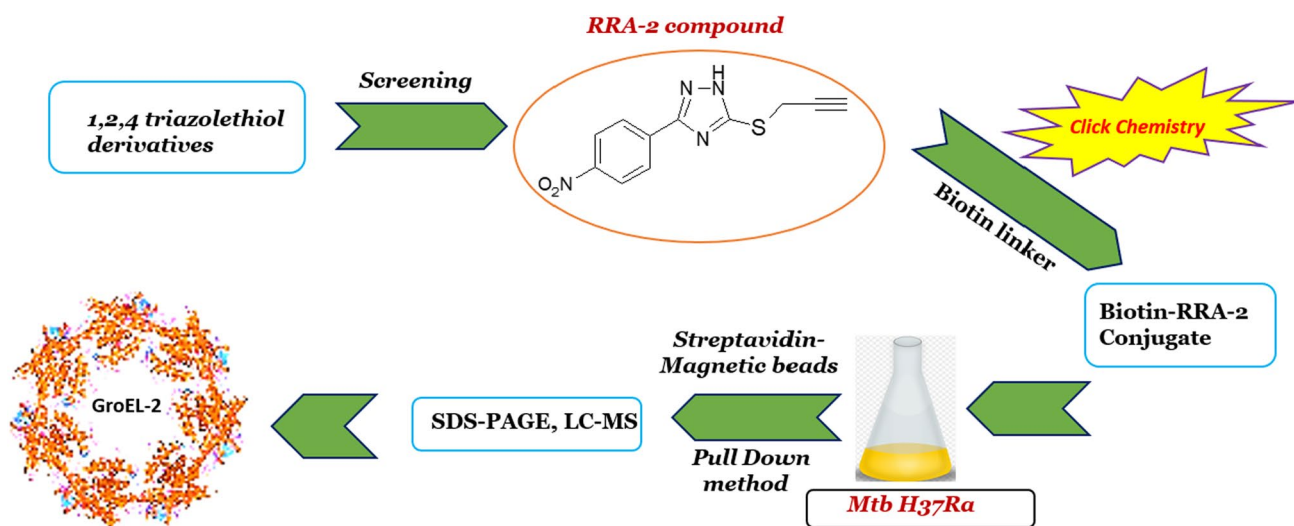
Received: 22 September 2021 / Accepted: 8 November 2021
© The Author(s), under exclusive licence to Springer Nature Switzerland AG 2021

Abstract

Herein, we identified a potent lead compound RRA2, within a series of 54 derivatives of 1,2,4-triazolethiols (exhibit good potency as an anti-mycobacterial agents) against intracellular *Mycobacterium tuberculosis* (Mtb). Compound RRA2 showed significant mycobactericidal activity against active stage *Mycobacterium bovis* BCG and Mtb with minimum inhibitory concentration (MIC) values of 2.3 and 2.0 µg/mL, respectively. At MIC value, RRA2 compound yielded 0.82 log reduction of colony-forming unit (cfu) against non-replicating Mtb. Furthermore, RRA2 compound was selected for further target identification due to the presence of alkyne group, showing higher selectivity index ($> 66.66 \pm 0.22$, in non-replicating stage). Using “click” chemistry, we synthesized the biotin linker-RRA2 conjugate, purified with HPLC method and confirmed the conjugation of biotin linker-RRA2 complex by HR-MS analysis. Furthermore, we successfully pulled down and identified a specific target protein GroEL2, from Mtb whole-cell extract. Furthermore, computational molecular modeling indicated RRA2 could interact with GroEL2, which explains the structure–activity relationship observed in this study.

Graphical abstract

GroEL-2 identified a potent and specific target protein for RRA 2 compound in whole cell extract of Mtb H37Ra.



Keywords 1,2,4-triazolethiols · Mycobactericidal activity · *Mycobacterium bovis* BCG · *Mycobacterium tuberculosis* · GroEL2

Sampa Sarkar and Sagar Swami have contributed equally.

Extended author information available on the last page of the article

Published online: 25 November 2021

Springer

Introduction

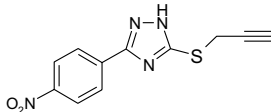
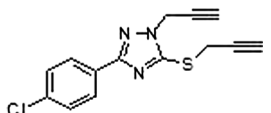
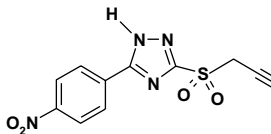
Tuberculosis is a major public health problem in developing countries and requires an innovative treatment to eradicate this infection [1–3]. Past 20 years, the advent of new technologies has failed to provide many novel anti-tubercular molecules or molecular targets [4]. In recent days, 1,2,4-triazoles have been reported to show anti-tubercular activity against *Mycobacterium tuberculosis* (Mtb), keeping on the sight of biological importance of azoles [5]. In addition, it was highlighted the possibility of azoles exert anti-tubercular activity through inhibition of CYP51 and CYP121 by a mechanism in which the heterocyclic nitrogen (N3: imidazole or N4: 1,2,4-triazole) binds to the sixth coordination site of the heme iron atom of porphyrin in the substrate-binding site of the enzyme [6–10]. The 1,2,4-triazole core has drawn great attention due to its diversified pharmacological activities and low toxicity. This core is known as a therapeutic drug in the market, including voriconazole, triazolam, fluconazole, itraconazole, alprazolam, etizolam, etc. [11–13]. Several groups worldwide have synthesized novel triazole derivatives and assayed them for anti-mycobacterial activity [14–16]. Structure–activity relationship (SAR) studies for this compound class have shown that numerous features are important for the anti-tubercular activity, including the presence of the hydrogen bond acceptor subunit, the position in the aromatic ring and, the planarity of triazole and phenyl rings. Interestingly, small structural changes to the 1,2,4-triazole scaffold have been found to inhibit different molecular targets (e.g., CYP51 and CYP121) [16–18].

Recently, we have patented the synthesis process and the anti-mycobacterial activity of whole library of 1,2,4-triazole derivatives against *Mycobacterium tuberculosis* H37Ra and *Mycobacterium bovis* BCG (both active and dormant stage, presented in the Supporting Information Table No. S1) [19]. In another study, Rode et al. [20] reported the complete synthesis of 3-aryl-5-(alkyl-thio)-1*H*-1,2,4-triazoles derivatives; they also investigated the anti-mycobacterial potency against the active and dormant stage of *Mycobacterium tuberculosis* H37Ra strain and *Mycobacterium bovis* BCG. They found 25 compounds that exhibited promising anti-TB activity and lower cytotoxicity. Additionally, a molecular docking study was carried out using similar chemical entities against a potential target Mtb CYP121 which seemed to show relevance between the binding score and biological activity. Based on primary (Supporting Information Table No. S1) and secondary screening results, (Table 1) in this study, we have selected three derivatives, RRA2 (2d, Table No. S1), RRA3 (4f, Table No. S1) [19], and RRA7 (11d, Table No. S1) [20], from the above-mentioned 1,2,4-triazole

derivatives library those were active against the non-replicating dormant phase of *Mycobacterium tuberculosis* H37Ra and *Mycobacterium bovis* BCG. However, the target and the action mechanism of these compounds have not been identified yet. Due to the higher efficacy and presence of alkyne group, RRA2 was selected to identify its specific target from Mtb whole-cell culture.

Biotinylated RRA2 conjugate was used for pulling down the target protein GroEL2 from Mtb whole-cell extract and confirmed by SDS-PAGE and liquid chromatography–mass spectrometry (LC–MS) analysis. Earlier research reported that GroEL2 has homology with members of a family of heat shock proteins (HSPs) that is known as the chaperonin-60 (Cpn60/GroEL) family, which serves as an essential molecular chaperone (Cpn) for maintaining cellular homeostasis in normal and stressed conditions among different proteins. Mtb contains two copies of the *cpn60* gene [21]. One of these, *cpn60.1*, is an operon with *cpn 10*, while the second *cpn60.2* occurs independently on the chromosome. The regulation of HSPs in Mtb has shown overexpression of the two *Cpn60s* upon thermal shock [22] and phagocytosis by macrophages [23]. These reports suggest that the Cpn60 of Mtb contributes to its defense response against external stress conditions. Furthermore, evidence uncovered that both proteins Cpn 60.1 (GroEL1) and 60.2 (GroEL2) of Mtb are highly antigenic and potent cytokine inducers [24, 25]. Earlier studies also focused on the role of the full-length (FL) Mtb protein GroEL2 indicates that a cleaved form of GroEL2 [GroEL(c1)] predominates in wild-type and that the cleavage of the same protein GroEL2 tends to inhibit the innate immune response to infection [26]. Furthermore, the FL GroEL2 protein produced strong proinflammatory responses from dendritic cells and promoted DC maturation and antigen presentation to T cells [27]. Similar to GroEL2(c1), Fong et al. [28] reported that HSP70 is secreted from cells and can activate the immunoreceptors on monocytes and neutrophils. So, targeting GroEL2 may open up new avenues for the treatment of tuberculosis. In this concern, a series of inhibitors were also reported for dual-targeting GroEL/ES along with protein tyrosine phosphatase B (PtpB), which act as virulence factors and show effective inhibition against active and dormant stages of tuberculosis [29]. Interestingly, our present in vitro and ex-vivo studies showed that RRA2 efficiently inhibits the active stage and dormant stage Mtb bacilli.

Table 1 Secondary screening characterization and MIC identification of identified lead molecules

Compound code	Compound Structure	MIC ^c against active stage ^c (μg/mL)			Inhibition against dormant stage ^d (CFU/mL)		
		<i>M. bovis</i> BCG	<i>M. tuberculosis</i>	<i>M. smegmatis</i>	<i>E. coli</i>	<i>M. bovis</i> BCG	<i>M. tuberculosis</i>
RRA2		2.31 ± 0.3	2.0 ± 0.2	> 100	> 100	0.91 ± 0.2	0.82 ± 0.1
RRA3		2.35 ± 0.1	2.27 ± 0.1	> 100	> 100	1.2 ± 0.4	1.43 ± 0.4
RRA7		2.61 ± 0.4	2.45 ± 0.2	> 100	> 100	1.1 ± 0.2	0.91 ± 0.2
Rifampicin ^a		0.22 ± 0.2	0.12 ± 0.05	0.23 ± 0.2	0.51 ± 0.1	0.64 ± 0.3	0.53 ± 0.1
Isoniazid ^a		0.31 ± 0.1	0.25 ± 0.01	0.31 ± 0.1	2.1 ± 0.1	0.66 ± 0.1	0.75 ± 0.1
Metronidazole ^b		> 100	> 100	> 100	> 100	0.56 ± 0.4	0.61 ± 0.4
Itaconic anhydride ^b		> 100	> 100	> 100	> 100	0.94 ± 0.2	0.93 ± 0.1

^aPositive control for aerobic stage of *M. tuberculosis*

^bPositive control for dormant stage of *M. tuberculosis*

^cConcentration of compounds exhibiting 90% inhibition on mycobacterial growth

^dCFU counts were determined after 4 days of treatment with compounds

Results and discussion

Identification of triazolethiol actives against *M. bovis* BCG

Fifty-four derivatives of 1,2,4-triazolethiol (Supporting Information Table No. S1) from our in-house chemical library has been screened out using a simple and rapid bio-assay, i.e., Active and Dormant Antitubercular Screening (ADAS) [30] protocol (described in method section) with a range of concentration (1, 10, 30, and 100 μg/mL) against *M. bovis* BCG. From this primary screening, 17 active compounds showed > 90% inhibition. In particular, three of them (RRA2, RRA3, and RRA7) were showing > 98% inhibition in this detection method. Further, secondary screening (Table 1) results identified RRA2, RRA3, and RRA7 as lead compounds within 54 derivatives and pursued for further characterization.

The study of structure–activity relationship (SAR) of the 1,2,4-triazole ring [31, 32], demonstrated that the structures with thiopropargyl group at the C-3 position of the 1,2,4-triazole ring lacked any major influencing effect against mycobacterial survival under the aerobically growing stage. Oxidation of this S-propargyl compound did not perturb the inhibitory action of the molecule. So, the SAR results evidently indicated that S-propargyl moiety is not

involved in pharmacophoric recognition with target protein/s in Mtb cells [31]. This observation was gainfully utilized in a click chemistry approach for target identification. SAR study also indicated that allylation at 1 and 2 positions were inversely related to the molecule's potency. At its para-position, a phenyl substitution with an electron-withdrawing group was required at the C-5 position in the triazole ring. Replacing –NO₂ group by Cl- with simultaneous change of propargyl to allyl group attached to sulfur at position C-3 in the 1,2,4-triazole ring has increased the molecule's potency by tenfold as an anti-tuberculous agent [31, 32].

Determination of MIC of RRA2, RRA3, and RRA7 against *M. bovis* BCG

The MIC values of RRA2, RRA3, and RRA7 were determined against aerobically growing *M. bovis* BCG 2.31, 2.35, and 2.61 μg/mL, respectively (Table 1). The three leads were separately applied to hypoxia-induced dormant bacilli in Wayne's tube culture [33]. The tube model of dormancy provided the flexibility of adding compound at any stage of culture without significantly disturbing its oxygen environment. RRA2, RRA3, and RRA7 (at their MIC concentration) reduced the viability of dormant Mtb bacilli by 0.91 ± 0.2, 1.20 ± 0.4, and 1.1 ± 0.2 logs CFU, respectively (Table 1). Although the propargyl or allyl groups were present in these

three leads triazole structures, they could not achieve inhibition against bacilli, which suggested that a different substituent at the C-5 position may be responsible for its activity. Although different groups were tried at the C-5 position, only p-nitrophenyl (RRA2) showed the desired activity. In compound RRA3, the replacement of propargyl moiety by the allyl group could retain the extent of inhibition against the bacilli. The sulfone derivative (RRA7) of this p-nitrophenyl compound was equally potent against actively growing *M. bovis* BCG, which indicated that oxidation of sulfur did not negatively impact its biological activity.

Spectrum of activity against *M. tuberculosis*, *M. smegmatis*, and *E. coli*

To further verify the spectrum of activity for RRA2, RRA3, and RRA7 was assayed against an actively growing and hypoxic Wayne's tube model (dormant bacilli) of Mtb culture. The MIC values of RRA2, RRA3, and RRA7 were obtained 2.0 ± 0.2 , 2.27 ± 0.1 , and 2.45 ± 0.2 $\mu\text{g}/\text{mL}$, respectively, against aerobic Mtb bacilli (Table 1). The calculated reduction of viable cell counts of dormant Mtb bacilli were found to be 0.82 ± 0.1 , 1.43 ± 0.4 , and 0.91 ± 0.2 log CFU values, respectively. The inhibitory effect of these compounds against both *M. bovis* BCG and *M. tuberculosis* indicated an inductive effect of the group attached to the para-position of the phenyl ring connected to the C-5 position of 1,2,4-triazolethiol is crucial in bringing the potent inhibitory effect against the bacilli. Earlier studies using well-known antifungal triazole drugs had clearly established that 14- α -demethylase belonging to the Cytochrome P-450 class of proteins are the targets in mycobacteria. Interestingly, our lead compounds were not effective on *M. smegmatis* even though *M. smegmatis* has 51 copies of those proteins, whereas, in *M. tuberculosis* and *M. bovis* BCG, only 22 copies are present [34, 35]. Furthermore, the lead compounds were also assayed against gram-negative bacteria *E. coli* as test organism to check their specificity against non-mycobacterial species. None of the lead compounds had any significant effect on the growth of either organism up to the concentration of 100 $\mu\text{g}/\text{mL}$ (Table 1). Hence, the result confirmed that the effectiveness of RRA2, RRA3, and RRA7 were specific for non-mycobacterial species *M. bovis* BCG and *M. tuberculosis*. Interestingly, RRA2 showed more potency against an actively growing and hypoxic Wayne's tube model (dormant bacilli) of Mtb culture and was further used for its target identification from whole-cell Mtb culture [36]. Rifampicin, isoniazid, metronidazole, and itaconic anhydride were used as standards (positive controls) in these assays [36].

Efficacy of the leads (RRA2, RRA3, and RRA7) against Mtb inside THP-1 macrophage

To check the effectiveness of these three leads against dormant bacilli, an *ex-vivo* infection model was used to provide information about the level of efficacy that may be achieved before the compounds were applied to animal models. We analyzed the three lead compounds with positive control rifampicin and isoniazid against THP-1 macrophages infected with Mtb bacilli (Fig. 1). RRA3 and RRA7 compounds could completely sterilize the intracellular Mtb (residing inside THP-1 macrophage) bacilli at 5 $\mu\text{g}/\text{mL}$ concentration within 8 days of infection, whereas RRA2 could achieve sterilization at as low as 1.5 $\mu\text{g}/\text{mL}$ concentration. The minimum bactericidal concentration (MBC) value of RRA2 was almost comparable with rifampicin and isoniazid in this experimental setting. To ensure these results were not due to nonspecific lethal effects on THP-1 macrophages, the three lead compounds were assayed against the human THP-1 monocyte cell line.

Cytotoxicity against the human THP-1 monocyte cell line

In Fig. 2, the cytotoxicity results were indicated no significant effect on the cell viability of THP-1 monocytes at > tenfold MIC concentration. In particular, out of three lead compounds, RRA2 demonstrated significant potency against the hard to kill intracellular Mtb bacilli and was found to be nontoxic to the monocyte cell line. Moreover, cytotoxicity studies enabled us to calculate the selectivity index (SI) for the compounds RRA 2, RRA 3, and RRA 7. The SI of each compound was determined by the ratio of IC_{50} (on THP-1 cell cytotoxicity) to MIC (anti-TB activity) (Table 2). In the drug susceptibility study, Orme et al. [37] suggested that compounds as a new candidate drugs must have an index ≥ 10 , with MIC < 6.25 mg/mL and low cytotoxicity considered safe and effective. Therefore, SI is a significant parameter used to estimate the therapeutic window to identify drug candidates for further studies. For example, in Table-2 RRA 3 compound showed maximum SI (> 500) value in active strains (A), whereas RRA 2 showed higher SI ($> 66.66 \pm 0.22$) value in dormant strains (D) of *Mycobacterium tuberculosis* H37Ra as compared to RRA 3 and RRA 7, which makes them potential candidates for the further biological studies.

Time-kill kinetics of RRA2 on Mtb within infected THP-1 macrophage

Up to date, it has been established that hypoxia generates within macrophages during the growth of bacilli [38]. Achieving dormancy within the intracellular environment

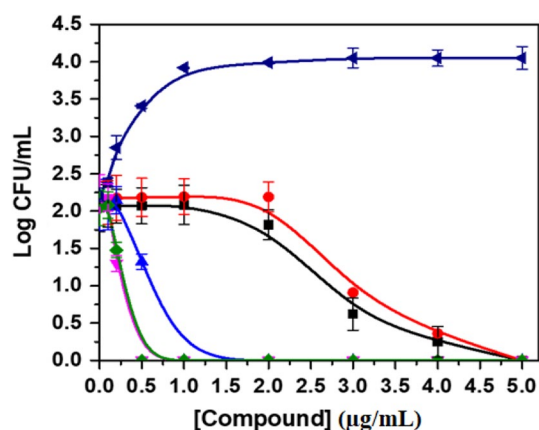


Fig. 1 Dose–response effect of compounds on growth of intracellular Mtb bacilli. The intracellular Mtb bacilli are growing in THP-1 macrophages were monitored in the absence of compounds, i.e., control (\blacktriangle), in the presence of different concentrations of RRA2 (\blacktriangle), RRA3 (\blacksquare), RRA7 (\bullet), Rifampicin (\blacktriangledown), and Isoniazid (\blacklozenge). The details of the experimental procedure for the growth of intracellular *M. tuberculosis* are described in “Materials and Methods”. The results described here as mean \pm SD of three identical experiments

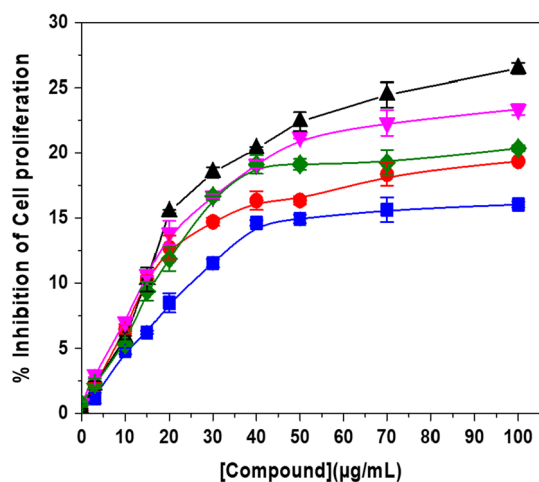


Fig. 2 Dose–response effect of compounds on cell proliferation of THP-1 monocyte. The proliferation of THP-1 cells was monitored in the presence of different concentrations of RRA2 (\blacksquare), RRA3 (\blacktriangle), RRA7 (\bullet), Rifampicin (\blacktriangledown), and Isoniazid (\blacklozenge). The details of the experimental procedure for cytotoxicity on THP-1 are described in “Materials and Methods”. The results are mean \pm SD of three identical experiments

makes bacilli resistant to most anti-tubercular drugs [38–40]. Therefore, we further investigated the time-kill kinetics on Mtb bacilli within the THP-1 macrophage infection model (Fig. 3). As mentioned above, the RRA2 compound showed a higher selective index (SI) in the dormant stage; due to that, only RRA2 has been used for further time-kill kinetics experiments. RRA2 was added in two different stages of infection, at 0 h and after 120 h at its MIC value

($1.5 \pm 0.1 \mu\text{g/mL}$). The result indicated that effective killing of intracellular bacilli in THP-1 macrophages took place immediately after the addition of the compound (RRA2). The complete sterilization of aerobic bacilli occurred within ~ 70 h and ~ 170 h of incubation, respectively. This result (Fig. 3) clearly indicated that the RRA2 triazolethiol derivative could be used as potential anti-tubercular leads for further explorations.

Identification of target protein for RRA2 from the whole-cell extract of *Mycobacterium tuberculosis* H37Ra by using conjugate (biotin linker-inhibitor)

In order to aid future lead optimization of the RRA2 scaffold, the identification of the specific target of RRA2 compound was carried out with whole-cell Mtb culture. Among the different approaches known for identifying the target of a novel compound, affinity pooling could be a traditional and simple procedure to lead a protein target. RRA2 compound possesses an acetylenic group in the side chain, which could be utilized in a copper-catalyzed alkyne-azide cycloaddition reaction, i.e., “click chemistry,” with Azide-PEG3-Biotin to form a covalent linkage (Scheme 1). The reaction mixture (biotin linker-RRA2) was purified using preparative HPLC, and mass was confirmed via mass spectrometry. The purified biotin linker-RRA2 conjugate was then added to the *Mycobacterium tuberculosis* H37Ra whole-cell extract. Proteins were hooked with RRA2 were then pulled down via MagnaBind Streptavidin beads (Thermo Fisher Scientific) and washed with PBS 2–3 times to remove the unwanted nonspecific proteins. SDS-PAGE analysis indicated a major protein band at ~ 60 kDa molecular weight (Fig. 4). As a control, we added our biotin-linked-RRA2 to a whole Mtb cell culture previously treated with RRA2. Notably, no band was seen on the SDS-PAGE, presumably as RRA2 was already bound to the target protein's active site, leaving no room for conjugate (biotin-linked-RRA2) binding and subsequent pull-down.

Target specificity analysis

To determine the target specificity of RRA2, four hit derivatives of 1,2,4-triazolethiols (RRA79, RRA242, RRA267, and RRA268) were selected from an in-house library (Supporting Information Table S2). These derivatives also have significant inhibitory activity against active and dormant stage of *Mycobacterium tuberculosis* H37Ra. Therefore, all these four compounds are specific compounds of either the active stage or dormant stage of the bacilli. To confirm the specificity of the RRA2 compound, the purified biotin linker-RRA2 conjugate was separately added to the *Mycobacterium tuberculosis* H37Ra whole-cell culture, which

Table 2 Calculation of selectivity index (SI) for RRA 2, RRA3, and RRA 7 compounds

Compound code	Anti-TB activity(a)		Cytotoxicity THP-1(b)	Selectivity index THP-1(c)	
	A	D		A	D
RRA2	2.0±0.2	1.5±0.1	> 100	> 50	> 66.66±0.22
RRA3	2.27±0.1	5.0±0.3	> 100	> 500	> 20±0.12
RRA7	2.45±0.2	5.0±0.2	> 100	> 50	> 20±0.77

[a] Anti-TB activity against active (A) and dormant (D) strains of *Mycobacterium tuberculosis* H37Ra as MIC ($\mu\text{g/mL}$); [b] Cytotoxicity studies for THP-1 IC₅₀ ($\mu\text{g/mL}$); [c] Selectivity Index IC₅₀ (cytotoxicity)/MIC (anti-TB) for THP-1 for both A and D strains

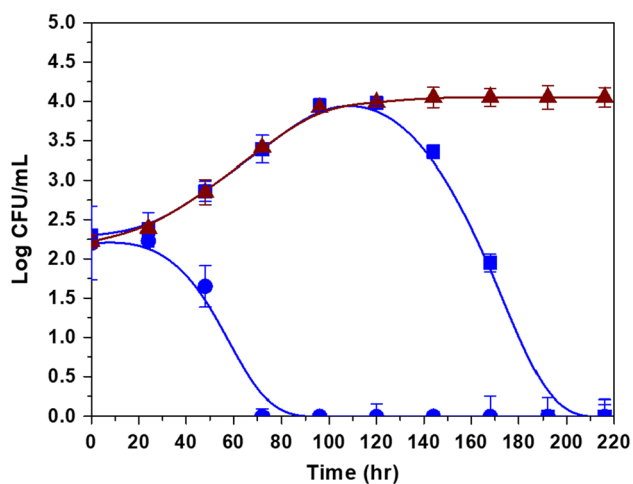
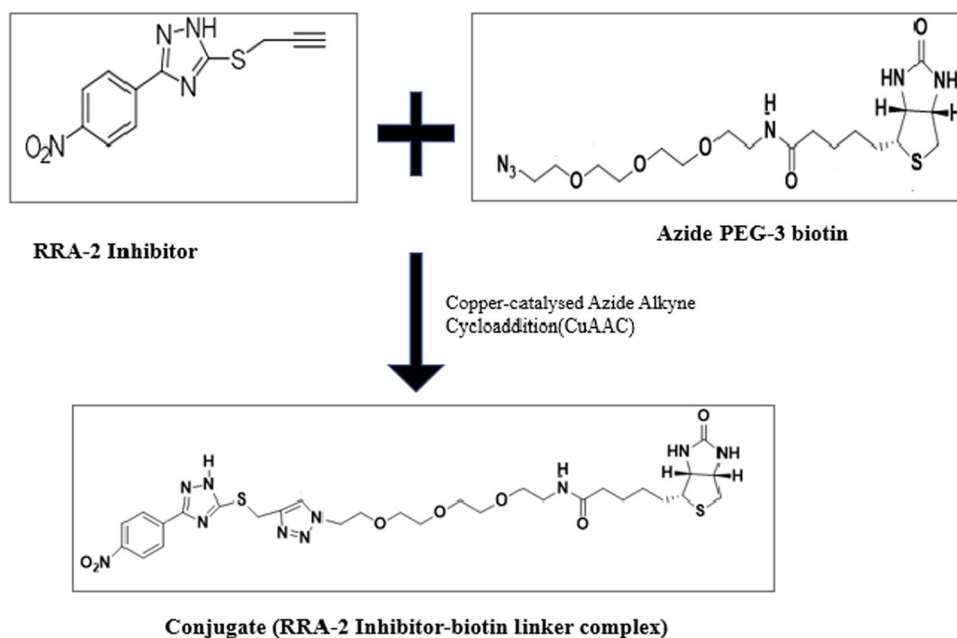


Fig. 3 Time-kill Kinetics of intracellular Mtb (residing inside THP-1 macrophage) bacilli in the presence of RRA2 compound. The viable count of the bacilli measured in terms of log CFU in control (\blacktriangle), RRA2 compound added immediately after infection (0 h) (\bullet) and after 5 days of infection (\blacksquare) at MIC value (1 $\mu\text{g/mL}$). The results described here mean \pm SD of three identical experiments

has already been treated with RRA2 compound (control) and without RRA2 compound (test) along with four similar scaffolds of 1,2,4-triazolethiols compounds (Supporting Information Table S2). A similar protocol was used to pull the purified target protein (mentioned in the above section) and performed the SDS-PAGE. (Fig. 5). Presumably, if all or any of the compounds had the same target as RRA2, it should not show any band in the SDS-PAGE because the target site is not available to bind to purified conjugate.

Interestingly, Fig. 5 showed the cleared bands with all four compounds like test samples of RRA2 except in the control sample. Even though the other four similar scaffolds of 1,2,4-triazolethiols compounds had an inhibitory effect against the active and dormant stage of *Mycobacterium tuberculosis* H37Ra, but their protein target sites were different. This result demonstrated the robust specificity of the RRA2 target.

Scheme 1 Proposed mechanism for the formation of conjugate RRA2 inhibitor-Biotin linker complex via copper-catalyzed Azide Alkyne Cycloaddition reaction



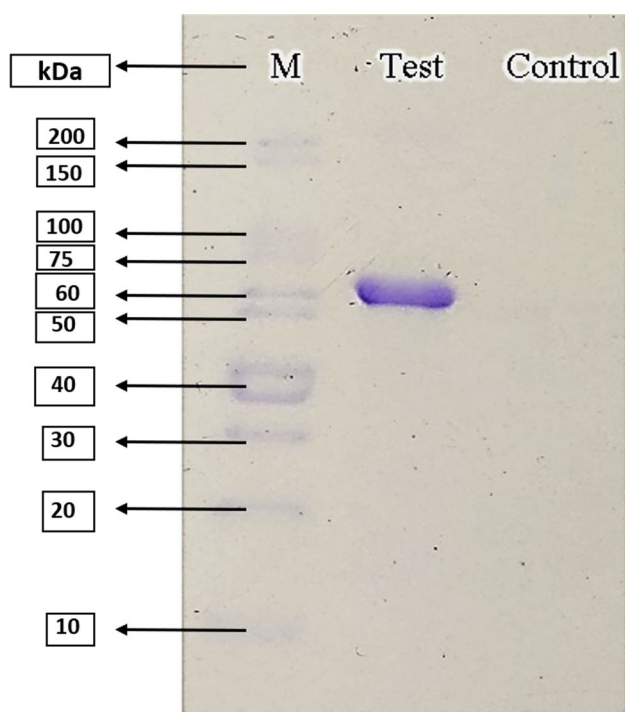


Fig. 4 Separation of target protein isolated from *Mycobacterium tuberculosis* H37Ra whole-cell extract on SDS-PAGE. The gel image represents the final target protein sample obtained in addition to conjugate (biotin linker-RRA2) from the whole-cell extract previously treated with RRA2 compound (Control), untreated with RRA2 compound (Test), and M is represented by molecular weight protein markers

Validation of *Mycobacterium tuberculosis* GroE12 as a potential target of RRA2 triazolethiols

The single protein band was taken out of SDS-PAGE, representing a molecular weight of ~60 kDa. Notably, GroE11 was also picked up as a possible protein target from LC-MS analysis (Supporting Information Figure S3). Both GroE11 and GroE12 are functionally similar proteins belonging to the ~60 kDa HSP family of chaperonins (Supporting Information Figure S4). Moreover, both have ATPase activity and protect citrate synthase agglutination during heat shock [41]. Multiple sequence alignments using CLUSTAL 2.1 showed the similarity aligned score between GroE12 and GroE11 is 60% (Supporting Information Figure S4 A). The LC-MS (Gel free) analysis of the tryptic digest of purified protein identified chaperonin 20S *Mycobacterium tuberculosis* GN GroL 2 PE 1 SV 2 by using PLGS score (Figure S4 B). In order to validate the LC-MS data (Supporting Information Figure S4), ATPase inhibition of purified GroE11 and GroE12 activity was monitored in the presence of RRA2 (Table 3). At 2 ± 0.02 $\mu\text{g}/\text{mL}$ (MIC value) RRA2 inhibited the ATPase activity of purified GroE12. However, it did not exhibit any significant effects on GroE11 (Table 3).

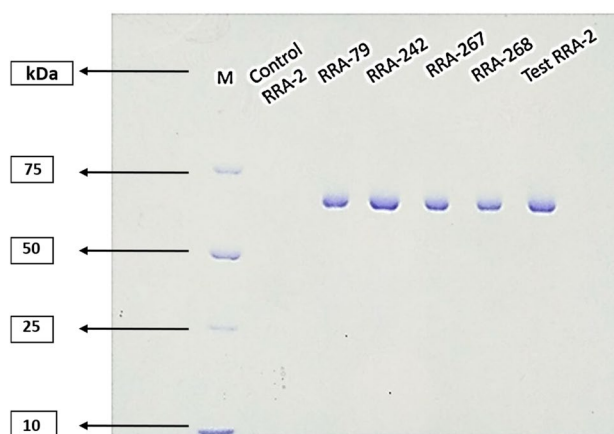


Fig. 5 Target specificity analysis of RRA2 in the presence of four similar scaffolds of 1,2,4-triazolethiols compounds by SDS PAGE. M represents different molecular weight protein markers, whole-cell culture treated with purified conjugate mixture added to previously treated with RRA2 compound (control), RRA79, RRA242, RRA267, and RRA268. In test, the whole-cell extracts were previously untreated with an RRA2 compound

Therefore, this result confirmed the GroE12 is the potential target for RRA2 compound for *Mycobacterium tuberculosis* H37Ra.

Potential Binding mode of RRA2

To determine where RRA2 might interact with GroE12, we conducted some preliminary molecular docking. There were two major sites, which are also the hinge sites of the protein [41], where compounds could potentially interact with GroE12 (Fig. 6a). The first is where ATP has been proposed to interact and was crystallized in the analogous *E. Coli* GroE11 protein (PDB:1KP8) [42]. The second was where Mg was found in the *M. tuberculosis* GroE12 X-ray structure (PDB:3rtk) [43]. Both sites were utilized to dock RRA2. Interestingly, RRA2 compound was able to have a consistent binding mode in both sites. Although the Mg site scored lower across the board than the ATP site (Table 4), for the RRA2 complex, the ATP site was lower energy than the Mg site (-13,355.62 kcal/mol for ATP site vs -13,292.40 kcal/mol for Mg site).

Table 3 ATPase activity on purified GroE11 and GroE12

ATPase activity ^a		
Compound code	GroE11 ^b (% Inhibition)	GroE12 (% Inhibition)
RRA2	2.56 ± 2.81	85.64 ± 3.21

^a Concentration of compounds exhibiting 90% inhibition of ATPase activity

^b Positive control: Purified GroE11

Furthermore, numerous studies have suggested that movement in the equatorial domain, which binds ATP, is essential for its function [43]. Therefore, it would be expected that a compound binding in this region would interfere with ATP binding and affect the function of GroEl2. Together, this suggests the ATP site is the likely binding site for this compound class. In this site, RRA2 is positioned with I451 stacking over the phenyl group and putative hydrogen bonds between the nitro moiety of RRA2 to Q450 and the triazine D483 (Fig. 6b). The alkyne is pointed out of the pocket, having little effect on the interaction energy. This is important as it is essential to be exposed for the biotin-linking experiment to be viable. Although beyond the scope of this paper, future experiments (e.g., mutagenesis, X-ray crystallization) will be needed to confirm this binding mode.

Conclusion

Our findings summarized, three nontoxic lead compounds (RRA2, RRA3, and RRA7) of 1,2,4-triazolethiols (alkyl-substituted) having a significant effect on the active and dormant stage of *M. bovis* BCG and *M. tuberculosis* bacilli. They were found to be more specific against Mtb bacilli rather than *M. smegmatis* and *E. coli*. Among these three lead compounds, due to higher efficacy, significant SI value, and the presence of alkyne group in its structure, RRA2 was used for pool down technique for target identification. Using the LC-MS approach, we identified GroEl2, a chaperonin, as the target of RRA2 compound in Mtb and validated it through ATPase activity and molecular modeling studies.

Table 4 Docking scores. Shown is the docking score for the highest-ranked solution

Compound code	ATP site (kcal/mol)	Mg site (kcal/mol)
RRA2	-4.893	-3.608

Notably, the lower the score, the better the dock is proposed to be

The outcome of this study disclosed that the consolidated analysis was found to be supportive of explaining the efficacy of RRA2 in inhibiting Mtb cells for interpreting their possible mechanism of action. Therefore, the RRA2 compound could be considered as a potential candidate molecule to take ahead before the in vivo trial study.

Experimental section

Bacterial strains, media, and inoculum preparation

M. bovis BCG (ATCC 35,745), *M. smegmatis* (ATCC 607) were obtained from Astra Zeneca, Bangalore, India, and *M. tuberculosis* H37Ra (ATCC 25,177) was obtained from Microbial Type Culture Collection, Chandigarh, India. *E. coli* strain DH5 α was obtained from National Collection of Industrial Microorganisms (NCIM), Pune, India. RPMI 1640 cell culture media, fetal bovine serum (FBS) were purchased from GIBCO, USA. Dubos albumin agar powder was purchased from Sigma, USA. Subculturing of all mycobacterial strains was routinely done in Dubos albumin agar slants or plates. The liquid inoculum was prepared in Dubos tween

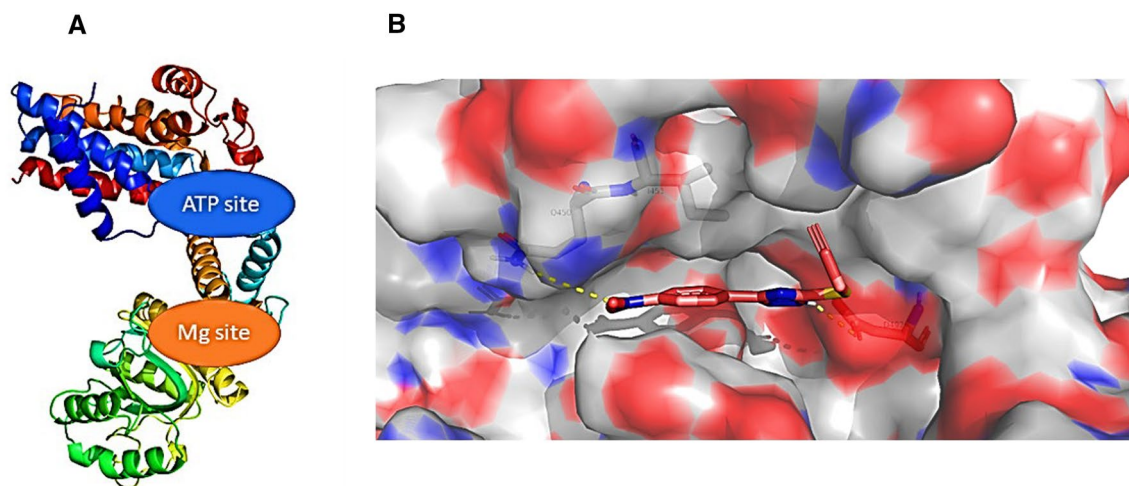


Fig. 6 **a** Structure of GroEl2 colored via rainbow from N to C terminus. This structure was prepared from the PDB:1KP8 and shown is the location of the two docking sites, as detected via Site ID which correspond to the ATP site and the Mg site (Schrodinger LLC). **b** Proposed docking orientation of RRA2 (peach) in the ATP site of

GroEl2. Shown via yellow dashed lines are the putative hydrogen bonds between the nitro moiety of RRA2 to Q450 and the triazine D483, and highlighted via sticks are the amino acids involved in the most predominant interactions, including these putative hydrogen bonds and the stacking interaction with I451"

albumin broth, incubated in a shaker incubator rotating at a speed of 150 rpm at 37 °C. 1% of 1.0 O.D. at 620 nm of the culture was used as standard inoculum size for all the experiments, yielding final inoculum of approximately 10^5 CFU/mL. THP-1 human monocyte cell line was obtained from National Centre for Cell Science (NCCS), Pune, India. Cells were maintained routinely in RPMI 1640 cell culture medium supplemented with 10% FBS.

Screening compounds for anti-mycobacterial activity

An earlier study demonstrated that the growth pattern in a high throughput assay platform completely mimics the nitrate reductase (NR) activity of *M. bovis* BCG in Wayne's model [30]. Active and dormant stage inhibitors against *M. bovis* BCG were identified using ADAS and NR assay protocol developed in our lab to screen the compounds. Briefly, 2.5 μ L of compound solution in DMSO was aseptically transferred to individual wells of sterile 96-well plates. 247.5 μ L of bacterial culture containing $\sim 10^5$ cells/mL, supplemented with 40 mM NaNO₃, was aseptically transferred to each well to make up the total volume to 250 μ L, and the plate was covered with a plate sealer. 125 μ L space is left in each well to make the headspace to culture volume ratio exactly 0.5. After sealing, these culture plates were incubated at 37 °C. After 8 days of incubation, culture OD was read using a cutoff filter of 620 nm after sonication for 2 min in a bath sonicator (Bandelin Electronic, Germany). Then, 80 μ L of culture was taken out from each well and transferred to a separate 96-well plate. Then, 80 μ L of 1% sulfanilic acid and 80 μ L of 0.1% NEDD (*N*-(1-Naphthyl) ethylenediamine dihydrochloride) solution were added in each well, and the plate was incubated for 15 min at room temperature to develop pink color. The color was read in Spectramax plus 384 Molecular Devices, USA at 540 nm to measure nitrate reduction (NR) activity.

Confirmation of inhibitors active against non-replicating *Mycobacterium bovis* BCG

The inhibitory effect of compounds against dormant bacilli was carried out using Wayne's 0.5 HSR (headspace ratio) in test tubes, as described earlier [44]. Briefly, 17.5 mL of diluted culture containing $\sim 10^5$ bacilli per mL of *M. bovis* BCG was transferred to 20 \times 125 mm tubes. Culture tubes were then sealed with rubber septa and gently stirred with the help of 8 mm magnetic beads rotating at 100 rpm on a magnetic stirring platform at 37 °C. After 8 days of incubation, when the culture reached the non-replicating phase, 10 μ L of compound solution in DMSO was added using a

Hamilton syringe with a 24-gauge needle and incubated for another 4 days. Culture samples were then spread on Dubos agar plates, and colonies were enumerated on day 21 to examine the effect of compound on dormant stage.

Spectrum of activity of active molecules against *Mycobacterium tuberculosis*, *Mycobacterium smegmatis*, and *E. coli*

M. smegmatis and *Escherichia coli* (*E. coli*) were used as representatives of nonpathogenic mycobacteria and non-mycobacterial strains, respectively, to examine the specific action of molecules by following methods described earlier [45]. Briefly, diluted culture containing 10^5 cells/mL was transferred to 20 mm \times 125 mm tubes. Compounds were added at the time of inoculation at doses ranging from 0.1 μ g/mL to 10 μ g/mL in *M. smegmatis* and *E. coli* culture, and growth was measured by reading the absorbance at 620 nm after 6 h and 72 h for *E. coli* and *M. smegmatis*, respectively.

Cytotoxicity of the active molecules

Toxicity of the active compounds was done by examining their effect on the proliferation of monocyte THP-1 cell line [46]. Briefly, 100 μ L of THP-1 cell (5×10^4 cells/mL) culture was dispensed in each 96-well plate, 2.5 μ L of each inhibitor (RRA 2, RRA 3, and RRA 7) was added up to $10 \times$ higher concentration of their MIC along with the inoculums in a dose-dependent manner and vehicle control. The cell culture plates were then incubated for 5 days at 37 °C, 5% CO₂, 95% humidity-maintained incubator. MTT assay was done after 5 days of incubation. 10 μ L of MTT dye solution (5 mg/mL) was added to each well and incubated for 1 h in a humidified atmosphere (37 °C, 5% CO₂, 95%). 200 μ L of isopropanol was added to each well and kept for 4 h to dissolve the formazan crystal. Thoroughly mix the formazan in the solvent and take the violet color absorbance of the culture at 490 nm to examine their effect on proliferation.

SI calculation

The selectivity index (SI) for the inhibitors (RRA 2, RRA 3, and RRA 7) were calculated by using the following formula:

$$SI = \frac{IC_{50}(\text{cytotoxicity}) \text{ value of inhibitor}}{MIC(\text{anti-TB activity}) \text{ value of inhibitor}}$$

Inhibitory effect of active molecules against intracellular *Mycobacterium tuberculosis* inside THP-1 macrophage

THP-1 was used to examine the inhibitory activity of the compounds against intracellular bacilli by following a method described earlier [1, 46]. Briefly, 3 mL of THP-1 cells ($\sim 5 \times 10^4$ cells/mL) was treated with 100 nM of phorbol myristate acetate (PMA) in a culture flask for 24 h to convert them into macrophages. These macrophages were further incubated for 12 h with *M. tuberculosis* H37Ra at MOI (multiplicity of infection) of 1: 100 for infection. Extracellular bacilli were removed by washing twice with sterile PBS and then adding fresh medium to adhered cells. Compounds were then added to these infected macrophages at different concentrations. In order to check the effect of inhibitors on the growth of intracellular bacilli, compounds were added at 0 h (for identification of active stage inhibitors) and after 120 h (for identification of dormant stage inhibitors) of infection; unless mentioned otherwise, the effect of the compound was monitored by determining the bacterial load within macrophage by lysing them with hypotonic buffer (10 mM HEPES, 1.5 mM $MgCl_2$, and 10 mM KCl) at different time points and spreading 100 μ L of the samples on Dubos agar plates to enumerate colonies after 21 days.

Preparation of Conjugate (RRA2-biotin linker complex)

Copper-catalyzed alkyne-azide cycloaddition protocol was used to prepare biotin-linked RRA2 conjugate (RRA2-biotin linker) [47, 48]. Briefly, Azide-PEG3-Biotin (5 mg, 0.011 mmol) was dissolved in 0.5 mL anhydrous tetrahydrofuran (THF) in a 5 mL round bottom test tube at room temperature. 0.5 mL copper sulfate solution (125 mmol) was added to this 5 mL test tube and mixed properly. Next, 10 mg of sodium ascorbate was added, and this complete solution was stirred on a magnetic stirrer at room temperature. 2:1 ratio of RRA2 and Biotin was used for the reaction. So, 10 mg of the inhibitor was added to this reaction mixture, and the reaction was allowed to proceed and stirred for 8 h at room temperature.

Purification of Biotin Linker-Inhibitor complex by HPLC

Chromatographic separation and analysis of the product and components of the reaction were done using reverse-phase X bridge C_{18} (5 μ m, 46 \times 250 mm) column in preparative HPLC (binary pump-1525, UV detector-2489, sampler-2707, Waters, India). Organic solvents employed to prepare mobile phases were HPLC-grade, and the HPLC column used was reverse-phase X bridge C_{18} (5 μ m,

46 \times 250 mm). The optimized mobile phase composition used was in, "A" solution–water (100, 60, 60, 45, 40, 0) % and "B" solution – acetonitrile (0, 40, 40, 55, 60, 100) %. The analysis was carried out in gradient elution mode as flow rate 1 mL/min with column runoff monitored at 254 nm wavelength. The retention time for vehicle control DMSO (Figure S1 A), inhibitor RRA2 (Figure S1B), and Azide-PEG3-biotin (Figure S1C) were observed at 2.1, 28, 13.5 min, respectively, which could help in comparison with the reaction mixture of the conjugate (Figure S1 D). After injecting the reaction mixture of conjugate into the column, one foreign peak was observed at 7 min retention time along with the biotin and inhibitor peak. This foreign peak (Figure S1 D) represented the neat conjugate (inhibitor-biotin linker complex) and was collected for further experiments.

Mass confirmation by HR-MS analysis

HR-MS analysis was done by the modified method as reported earlier [49]. The purified inhibitor-biotin linker complex was dissolved in acetonitrile (mass spectrometry grade) followed by separation using the Accela ultrahigh performance liquid chromatography (UHPLC) system (Thermo Fisher, Waltham, USA) using a C_{18} Hypersil Gold column (3 μ m, 3 \times 100 mm, Thermo fisher) coupled with a Q Exactive- Orbitrap mass spectrometer (Thermo Fisher, Germany). The separation is carried in optimized mobile phase composition of solvent A (acetonitrile with 0.1% of formic acid) against 70–30% of solvent B (water with 0.1% of formic acid) at a flow rate of 500 μ L/min and a temperature of 45 $^{\circ}$ C for 5 min. The molecular weight was identified by electrospray ionization positive (ESI+) mode with a mass scan range set from 100 to 1500 m/z. The data acquisition and processing were performed using the Thermo Scientific Xcalibur software (version 3.0). The tandem mass spectrometry (data-dependent MS/MS) data were collected with collision energy between 30 and 40 eV. The raw data from the instrument were converted to the mzxml file format by using ProteoWizard. The mass confirmation was carried out with the HPLC purified samples (Figure S2). HPLC samples fractions for RRA2 Inhibitor (Figure S2 A), Azide-PEG3 Biotin (Figure S2 B), and neat conjugate (Figure S2 C), respectively, were then analyzed for mass confirmation by HR-MS method. The RRA2 Inhibitor (Figure S2 A) and Azide-PEG3-Biotin (Figure S2 B) showed their corresponding mass 261.04 Da and 445.22 Da. The mass of neat conjugate was found 705.25 Da confirming separation of the Biotin linker-inhibitor conjugate from the mixture. Confirmed mass of conjugate from HR-MS analysis helped to process for the next step of the experiment.

Binding of conjugate RRA2-Biotin complex with crude whole-cell extract of *Mycobacterium tuberculosis*

The RRA2-Biotin conjugate obtained from HPLC purification was allowed to dry up the solvent in speed-Vac for 30 min, then dissolved in 100 μ L DMSO and then added to the whole-cell extract of Mtb. For whole-cell extract preparation, 5 mL spheroplast solution (0.0006%) was added in 100 mM ~ 1.0 OD Mtb culture and incubated for 12–16 h. This Biotin linker-inhibitor conjugate was also added to the control culture, which was already treated with RRA-2 inhibitor. Both control and test samples were kept for 30 min. in an incubator shaker at 37 °C and 150 RPM for binding to the target protein. Both the cultures were sonicated in protein extraction buffer (100 mM HEPES buffer, 5 mM EDTA, 1% SDS, 100 mM NaCl, 0.5% Triton X-100, and freshly prepared 1% protease inhibitor cocktail) at 45 Hz with 10 Sec. pulse ON and 5 Sec. pulse OFF in ice-cold condition for 15 min and centrifuged the cell extract at 14,000 rpm for 1 h at 4 °C to get the intracellular protein in supernatant. The supernatant containing the target protein with Biotin-Inhibitor conjugate was taken out and dialyzed against PBS to remove the excess unbound Biotin-Inhibitor conjugate and inhibitor molecules at 25 °C for 3 h.

Purification of RRA2-biotin conjugate tagged target proteins by magnaBind™ streptavidin beads

MagnaBind Streptavidin Beads are convenient for affinity purification or separation methods involving biotin-labeled molecules obtained from Thermo Scientific MagnaBind Streptavidin Beads (Cat no 21344) were added in the supernatant containing the target protein already bound with Biotin-Inhibitor conjugate allowed to pull down by using an external magnetic field overnight at 4 °C. Then, the beads were washed with sterile PBS 2–3 times to remove the unwanted proteins. To release our target protein attached with Biotin-Inhibitor conjugate, we added an excess of free 10 mM biotin molecule in shaking condition at 25 °C for 30 min. before dialysis against water at 25 °C for 3 h. Dialyzed sample was collected and further processed for protein precipitation.

Chloroform–Methanol precipitation of target proteins

The chloroform–methanol precipitation method has been followed to remove salt and detergents. 100 μ L sample was added to 400 μ L methanol, vortexed well, then 100 μ L chloroform was added and vortexed. 300 μ L mili Q water was added and again vortexed for 2 min. spin was given for 1 min at 14,000 g. Removed the top aqueous layer (protein

is between layers), then 400 μ L methanol was added and vortexed. 2 min at 14,000 g spin was given and removed the MeOH without disturbing the pellet. The sample was dried in speed-Vac. 1X sample buffer was added for SDS PAGE [50].

Protein estimation

Protein quantification was done by Bradford method (Bio-Rad Protein Assay; cat no. 500–0006) [51]. The measurements were taken according to the manufacturer's instructions (Bio-Rad, Hercules, CA).

SDS-PAGE and Proteomic Analysis of Captured Proteins

Individual proteins in the sample were separated by carrying out SDS-PAGE [52]. Briefly, 80 μ g (5 μ L) of each protein sample was first mixed with 1X loading (sample) buffer containing 5% β -mercaptoethanol (Sigma, MO, USA). The samples were then incubated for 10 min at 80 °C. Next, 20 μ L (64 μ g) samples were loaded onto 12.5% Bis–Tris precast polyacrylamide gels, and the SDS-PAGE was carried out using Mini-PROTEAN® Electrophoresis System–Bio-Rad (Catalog.1658000). After electrophoresis, the gel was subjected to Coomassie staining for overnight. Protein bands seen within the gel were cut properly and subjected to trypsin digestion, followed by peptide extraction and proteomic analysis in liquid chromatography–mass spectrometry (LC–MS).

LC–MS analysis

2 μ L digested peptides with a final concentration of 100 ng/ μ L was analyzed by nano LC–MS using nanoACQUITY online coupled to SYNAPT HDMS system (Waters Corporation, MA, USA) equipped with a nanolockspray ion source with a flow rate of 300 nL/min (external lock mass standard: Glu-fibrinopeptide) [53]. Peptide samples were injected online onto a 5 μ m Symmetry C18 trapping column (180 μ m \times 2 cm length) at a flow rate of 15 μ L/min. Peptides were separated by in-line gradient elution onto BEH (Bridged Ethyl Hybrid) 130 C18 1.7 μ m \times 75 μ m \times 150 mm nanoACQUITY analytical column, at a flow rate of 300 nL/min using a linear gradient from 5 to 40% B over 35 min (A. 0.1% formic acid in water, B. 0.1% formic acid in acetonitrile). The acquisition was performed in positive V mode in a mass range of 50–1990 m/z with a scan time of 1 s with alternating low (5 eV) and high (15–40 eV) collision energy. MS data were processed with ProteinLynx Global Server (PLGS version 2.4. Waters Corporation, MA, USA). The processed data were allowed to search against *Mycobacterium tuberculosis* H37Ra subset of UniProt database

containing all 44,987 protein entries for protein identification as described by Silva et al. [54].

ATPase activity assay

The ATPase activity of the purified GroEl1 and GroEl2 from *M.tuberculosis* H37Rv (gifted by Dr. Shekhar Mande, NCCS, Pune) was quantified with a colorimetric assay performed as described previously [54]. Briefly, 25 μ L of the reaction buffer containing 50 mM Tris–HCL (pH 8.0), 10 mM KCL, 10 mM MgCl₂, and 2.5 μ M of each GroEl were incubated 1 mM ATP at 37 °C for 20 min. Enzymatic reactions were terminated by the addition of 100 μ L of an acidic solution of malachite green. The amount of inorganic phosphate liberated was measured at 655 nm. In control, a reaction was performed in the absence of ATP and GroEl proteins. The estimation of liberated phosphate was done from the standard curve generated using monobasic potassium phosphate with each experiment.

Molecular modeling

The crystal structure of *M.tuberculosis* GroEl2 (PDB: 1KP8) was downloaded from the Protein Data Bank (rcsb.org). All docking was conducted within Maestro v12.0.012 (Schrodinger LLC, New York, NY, 2020). Specifically, the protein was prepared using the Protein Preparation Wizard, Site ID was used to find potential binding pockets, and the Receptor Grid-Generation was utilized to create a docking receptor using default parameters. Ligands were drawn in Maestro v12.0.012 (Schrodinger LLC, New York, NY, 2020) and prepared using ILgprep from the Schrodinger suite. These compounds were then docked into each receptor using the standard precision docking in Glide, with ten poses to be written out for each ligand. Docks were then visually analyzed for their ability to cluster and their interactions. The energy was calculated using the refine protein–ligand complex within Prime (Schrodinger, LLC, New York, NY, 2020). Figures were constructed using The PyMOL Molecular Graphics System, Version 4.6.0, Schrodinger, LLC.

Supplementary Information The online version contains supplementary material available at <https://doi.org/10.1007/s11030-021-10351-y>.

Acknowledgements We are thankful to AstraZeneca, Bangalore, MTCC Chandigarh, India, and Dr. Shekhar Mande, NCCS, Pune (DG CSIR), for providing *M. bovis* BCG (ATCC 35745), *M. smegmatis* (ATCC 607) and, *M. tuberculosis* H37Ra (ATCC 25177) and purified GroEl1 and GroEl2 from *M.tuberculosis* H37Rv, respectively. Thanks to the Rebecca L Cooper Medical Research Foundation and Director, National Chemical Laboratory, Pune, India, for providing financial support.

Author contributions Dhiman Sarkar has conceived the experiments and provided an interpretation of the results. Sampa Sarkar, Sagar

Swami, Arshad Khan, Sarvesh Soni and Jessica Holien performed the experiments and analysed the data. Sarvesh Soni and Jessica Holien assisted with analysis and interpretation. Dhiman Sarkar, Sampa Sarkar, Sarvesh Soni and Sagar Swami wrote the final manuscript draft.

Funding Sarvesh K Soni is the recipient of research grants from Rebecca L Cooper Medical Research Foundation (PG2018098) and ATSE- Priming grant PG181. Sagar Swami has been awarded Senior Research Fellowship (SRF) File no: 31/011(0983)2017/EMR-01) from the Council of Scientific & Industrial Research (CSIR) New Delhi, India.

Declarations

Conflicts of interest The authors declare that there is no conflict of interest.

References

- Muñoz-Elías EJ, Timm J et al (2005) Replication dynamics of *Mycobacterium tuberculosis* in chronically infected mice. *Infect Immun* 73:546–551. <https://doi.org/10.1128/iai.73.1.546-551.2005>
- Rogerson BJ, Jung Y et al (2006) Expression levels of *Mycobacterium tuberculosis* antigen-encoding genes versus production levels of antigen-specific T cells during stationary level lung infection in mice. *Immunology* 118:195–201. <https://doi.org/10.1111/j.1365-2567.2006.02355.x>
- McCune RM, Feldmann FM et al (1966) Microbial persistence. I. The capacity of tubercle bacilli to survive sterilization in mouse tissues. *J Exp Med* 123:445–468. <https://doi.org/10.1084/jem.123.3.445>
- Cong F, Cheung AK et al (2012) Chemical genetics-based target identification in drug discovery. *Annu Rev Pharmacol Toxicol* 52:57–78. <https://doi.org/10.1146/annurev-pharmtox-010611-134639>
- Chaudhary PM, Chavan SR et al (2008) Structural elucidation of propargylated products of 3-substituted-1,2,4-triazole-5-thiols by NMR techniques. *Magn Reson Chem* 46:1168–1174. <https://doi.org/10.1002/mrc.2307>
- Bellamine A, Lepesheva GI et al (2004) Fluconazole binding and sterol demethylation in three CYP51 isoforms indicate differences in active site topology. *J Lipid Res* 45:2000–2007. <https://doi.org/10.1194/jlr.M400239-JLR200>
- Deng XQ, Song MX et al (2018) Recent developments on triazole nucleus in anticonvulsant compounds: a review. *J Enzyme Inhib Med Chem* 33:453–478. <https://doi.org/10.1080/14756366.2017.1423068>
- Slivka MV, Korol NI et al (2020) Fused bicyclic 1,2,4-triazoles with one extra sulfur atom: synthesis, properties, and biological activity. *J Heterocycl Chem* 57:3236–3254. <https://doi.org/10.1002/jhet.4044>
- Vanjare BD, Mahajan PG et al (2020) Novel 1,2,4-triazole analogues as mushroom tyrosinase inhibitors: synthesis, kinetic mechanism, cytotoxicity and computational studies. *Mol Diversity* 118:195–201. <https://doi.org/10.1007/s11030-020-10102-5>
- Dunford AJ, McLean KJ et al (2007) Rapid P450 Heme Iron Reduction by Laser Photoexcitation of *Mycobacterium tuberculosis* CYP121 and CYP51B1 analysis of co complexation reactions and reversibility of the p450/p420 equilibrium. *J Biol Chem* 282:24816–24824. <https://doi.org/10.1074/jbc.m702958200>

11. Kharb R, Sharma PC et al (2011) Pharmacological significance of triazole scaffold. *J Enzyme Inhib Med Chem* 26:1–21. <https://doi.org/10.3109/14756360903524304>
12. Pagniez F, Lebouvier N et al (2020) Biological exploration of a novel 1,2,4-triazole-indole hybrid molecule as antifungal agent. *J Enzyme Inhib Med Chem* 35:398–403. <https://doi.org/10.1080/14756366.2019.1705292>
13. Kaur P, Chawla A (2017) 1,2,4-Triazole: a review of pharmacological activities. *Int. Res. J. Pharm.* 8:10–29. <https://doi.org/10.7897/2230-8407.087112>
14. Guardiola-Diaz HM, Foster LA et al (2001) Azole-antifungal binding to a novel cytochrome P450 from *Mycobacterium tuberculosis*: implications for treatment of tuberculosis. *Biochem Pharmacol* 61:1463–1470. [https://doi.org/10.1016/s0006-2952\(01\)00571-8](https://doi.org/10.1016/s0006-2952(01)00571-8)
15. Gülerman NN, Dogan HN et al (2001) Synthesis and structure elucidation of some new thioether derivatives of 1,2,4-triazoline-3-thiones and their antimicrobial activities. *Farmaco* 56:953–958. [https://doi.org/10.1016/s0014-827x\(01\)01167-3](https://doi.org/10.1016/s0014-827x(01)01167-3)
16. Akhtar T, Hameed S et al (2010) Design, synthesis, and urease inhibition studies of some 1,3,4-oxadiazoles and 1,2,4-triazoles derived from mandelic acid. *J Enzyme Inhib Med Chem* 25:572–576. <https://doi.org/10.3109/14756360903389864>
17. Wu J, Liu X et al (2007) Synthesis of novel derivatives of 4-amino-3-(2-furyl)-5-mercapto-1,2,4-triazole as potential HIV-1 NNRTIs. *Molecules* 12:2003–2016. <https://doi.org/10.3390/12082003>
18. Moulin A, Demange L et al (2008) Trisubstituted 1,2,4-triazoles as ligands for the ghrelin receptor: on the significance of the orientation and substitution at position 3. *Bioorg Med Chem Lett* 18:164–168. <https://doi.org/10.1016/j.bmcl.2007.10.113>
19. Sarkar D, Deshapande SR et al (2013) 1, 2, 4-Triazole Derivatives and their anti mycobacterial activity. US Patent Appl US. 0060045 A1
20. Rode ND, Sonawane AD et al (2017) Synthesis, biological evaluation, and molecular docking studies of novel 3-aryl-5-(alkyl-thio)-1H-1,2,4-triazoles derivatives targeting *Mycobacterium tuberculosis*. *Chem Biol Drug Des* 90:1206–1214. <https://doi.org/10.1111/cbdd.13040>
21. Kong TH, Coates AR et al (1993) *Mycobacterium tuberculosis* expresses two chaperonin-60 homologs. *Proc Natl Acad Sci USA* 90:2608–2612. <https://doi.org/10.1073/pnas.90.7.2608>
22. Stewart GR, Wernisch L et al (2002) Dissection of the heat-shock response in *Mycobacterium tuberculosis* using mutants and microarrays. *Microbiology* 148:3129–3138. <https://doi.org/10.1099/00221287-148-10-3129>
23. Monahan IM, Betts J et al (2001) Differential expression of mycobacterial proteins following phagocytosis by macrophages. *Microbiology* 147:459–471. <https://doi.org/10.1099/00221287-147-2-459>
24. Lewthwaite JC, Coates AR et al (2001) *Mycobacterium tuberculosis* chaperonin 60.1 is a more potent cytokine stimulator than chaperonin 60.2 (Hsp 65) and contains a CD14-binding domain. *Infect Immun* 69:7349–7355. <https://doi.org/10.1128/IAI.69.12.7349-7355.2001>
25. Young DB, Garbe TR (1991) Heat shock proteins and antigens of *Mycobacterium tuberculosis*. *Infect Immun* 59:3086–3093. <https://doi.org/10.1128/IAI.59.9.3086-3093.1991>
26. Naffin-Olivos JL, Georgieva M et al (2014) *Mycobacterium tuberculosis* Hip1 modulates macrophage responses through proteolysis of GroEL2. *PLoS Pathog* 10:e1004132–e1004132. <https://doi.org/10.1371/journal.ppat.1004132>
27. Georgieva M, Sia JK, Bizzell E, Madan-Lala R, Rengarajan J (2018) *Mycobacterium tuberculosis* modulates GroEL2 Dendritic Cell Responses. *Infect Immun* 86:e00387–e00317. <https://doi.org/10.1128/IAI.00387-17>
28. Fong JJ, Sreedhara K et al (2015) Immunomodulatory activity of extracellular Hsp70 mediated via paired receptors Siglec-5 and Siglec-14. *The EMBO J.* 34:2775–2788. <https://doi.org/10.15252/emboj.201591407>
29. Washburn A, Abdeen S et al (2019) Dual-targeting GroEL/ES chaperonin and protein tyrosine phosphatase B (PtpB) inhibitors: A polypharmacology strategy for treating *Mycobacterium tuberculosis* infections. *Bioorganic Med Chem Lett* 29(13):1665–1672. <https://doi.org/10.1016/j.bmcl.2019.04.034>
30. Khan A, Sarkar D (2008) A simple whole cell based high throughput screening protocol using *Mycobacterium bovis* BCG for inhibitors against dormant and active tubercle bacilli. *J Microbiol Methods* 73:62–68. <https://doi.org/10.1016/j.mimet.2008.01.015>
31. Gao F, Wang T, Xiao J, Huang G (2019) Antibacterial activity study of 1,2,4-triazole derivatives. *Eur J Med Chem* 173:274–281. <https://doi.org/10.1016/j.ejmech.2019.04.043>
32. Aher RB, Sarkar D (2021) 2D-QSAR modeling and two-fold classification of 1,2,4 triazole derivatives for antitubercular potency against the dormant stage of *Mycobacterium tuberculosis*. *Mol Divers*. <https://doi.org/10.1007/s11030-021-10254-y>
33. Wayne LG, Sohaskey CD (2001) Nonreplicating persistence of mycobacterium tuberculosis. *Annu Rev Microbiol* 55:139–163. <https://doi.org/10.1146/annurev.micro.55.1.139>
34. Jackson CJ, Lamb DC et al (2003) Conservation and cloning of CYP51: a sterol 14 alpha-demethylase from *Mycobacterium smegmatis*. *Biochem Biophys Res Commun* 301:558–563. [https://doi.org/10.1016/s0006-291x\(02\)03078-4](https://doi.org/10.1016/s0006-291x(02)03078-4)
35. Poupin P, Ducrocq V, Hallier-Soulier S, Truffaut N (1999) Cloning and characterization of the genes encoding a cytochrome P450 (PipA) involved in piperidine and pyrrolidine utilization and its regulatory protein (PipR) in *Mycobacterium smegmatis* mc2155. *J Bacteriol* 181:3419–3426. <https://doi.org/10.1128/JB.181.11.3419-3426.1999>
36. Sarkar D, Sarkar S (2012) A method of screening anti-tubercular compound. WIPO Patent Appl WO 2012(123971):A2
37. Orme I, Tuberculosis Drug Screening P (2001) Search for new drugs for treatment of tuberculosis. *Antimicrob Agents Chemother* 45:1943–1946. <https://doi.org/10.1128/AAC.45.7.1943-1946.2001>
38. Prosser G, Brandenburg J et al (2017) The bacillary and macrophage response to hypoxia in tuberculosis and the consequences for T cell antigen recognition. *Microbes Infect* 19:177–192. <https://doi.org/10.1016/j.micinf.2016.10.001>
39. Jakkala K, Ajitkumar P (2019) Hypoxic non-replicating persistent *Mycobacterium tuberculosis* develops thickened outer layer that helps in restricting rifampicin entry. *Front Microbiol*. <https://doi.org/10.3389/fmicb.2019.02339>
40. Rustad TR, Sherrid AM, Minch KJ, Sherman DR (2009) Hypoxia: a window into *Mycobacterium tuberculosis* latency. *Cell Microbiol* 11:1151–1159. <https://doi.org/10.1111/j.1462-5822.2009.01325.x>
41. Qamra R, Mande SC (2004) Crystal structure of the 65-kilodalton heat shock protein, chaperonin 60.2, of *Mycobacterium tuberculosis*. *J Bacteriol* 186:8105–8113. <https://doi.org/10.1128/JB.186.23.8105-8113.2004>
42. Wang J, Boisvert DC (2003) Structural basis for GroEL-assisted protein folding from the crystal structure of (GroEL-KMgATP)₁₄ at 2.0 Å resolution. *J Mol Biol* 327:843–855. [https://doi.org/10.1016/s0022-2836\(03\)00184-0](https://doi.org/10.1016/s0022-2836(03)00184-0)
43. Shahar A, Melamed-Frank M, Kashi Y, Shimon L, Adir N (2011) The dimeric structure of the Cpn60.2 chaperonin of *Mycobacterium tuberculosis* at 2.8 Å reveals possible modes of function. *J Mol Biol* 412:192–203. <https://doi.org/10.1016/j.jmb.2011.07.026>

44. Wayne LG, Hayes LG (1996) An in vitro model for sequential study of shutdown of *Mycobacterium tuberculosis* through two stages of nonreplicating persistence. *Infect Immun* 64:2062–2069. <https://doi.org/10.1128/IAI.64.6.2062-2069.1996>
45. Sarkar D (2014) Nitrite-reductase (nirb) as potential anti-tubercular target and a method to detect the severity of tuberculosis disease. WIPO Patent Appl WO. 2014:132263
46. McDonough KA, Kress Y, Bloom BR (1993) Pathogenesis of tuberculosis: interaction of *Mycobacterium tuberculosis* with macrophages. *Infect Immun* 61:2763–2773. <https://doi.org/10.1128/iai.61.7.2763-2773.1993>
47. Meldal M, Tornøe CW (2008) Cu-catalyzed azide-alkyne cycloaddition. *Chem Rev* 108:2952–3015. <https://doi.org/10.1021/cr0783479>
48. Hong V, Presolski SI, Ma C, Finn MG (2009) Analysis and Optimization of copper-catalyzed azide-alkyne cycloaddition for bioconjugation. *Angew Chem Int Ed* 48:9879–9883. <https://doi.org/10.1002/anie.200905087>
49. Dan VM, Vinodh JS et al (2020) Molecular networking and whole-genome analysis aid discovery of an angucycline that inactivates mTORC1/C2 and induces programmed cell death. *ACS Chem Biol* 15:780–788. <https://doi.org/10.1021/acscchembio.0c00026>
50. Wessel D, Flüggé UI (1984) A method for the quantitative recovery of protein in dilute solution in the presence of detergents and lipids. *Anal Biochem* 138:141–143. [https://doi.org/10.1016/0003-2697\(84\)90782-6](https://doi.org/10.1016/0003-2697(84)90782-6)
51. Bradford MM (1976) A rapid and sensitive method for the quantitation of microgram quantities of protein utilizing the principle of protein-dye binding. *Anal Biochem* 72:248–254. [https://doi.org/10.1016/0003-2697\(76\)90527-3](https://doi.org/10.1016/0003-2697(76)90527-3)
52. Vila A, Tallman KA et al (2008) Identification of protein targets of 4-hydroxynonenal using click chemistry for ex vivo biotinylation of azido and alkynyl derivatives. *Chem Res Toxicol* 21:432–444. <https://doi.org/10.1021/tx700347w>
53. Ramdas V, Talwar R et al (2020) Discovery of potent, selective, and state-dependent NaV1.7 inhibitors with robust oral efficacy in pain models: structure activity relationship and optimization of chroman and indane aryl sulfonamides. *J Med Chem*. 63:6107–6133. <https://doi.org/10.1021/acs.jmedchem.0c00361>
54. Silva JC, Denny R et al (2006) Simultaneous qualitative and quantitative analysis of the *Escherichia coli* proteome: a sweet tale. *Mol Cell Proteomics* 5:589–607. <https://doi.org/10.1074/mcp.M500321-MCP200>

Publisher's Note Springer Nature remains neutral with regard to jurisdictional claims in published maps and institutional affiliations.

Authors and Affiliations

Sampa Sarkar^{1,2}  · Sagar Swami^{2,3}  · Sarvesh Kumar Soni¹ · Jessica K. Holien¹ · Arshad Khan^{2,4} · Arvind M. Korwar⁵ · Anjali P. Likhite⁶ · Ramesh A. Joshi⁶ · Rohini R. Joshi⁶ · Dhiman Sarkar^{2,3} 

✉ Dhiman Sarkar
d.sarkar@ncl.res.in

¹ School of Science, STEM College, Engineering and Health, RMIT University, GPO Box 2476, Melbourne, VIC 3001, Australia

² Combi-Chem Bio-Resource Centre, Organic Chemistry Division, CSIR-National Chemical Laboratory, Pune, Maharashtra 411 008, India

³ Academy of Scientific and Innovative Research (AcSIR), Ghaziabad 201 002, India

⁴ Institute of Academic Medicine and Weill Cornell Medical College, Houston, Houston, TX 77030, USA

⁵ Biochemical Sciences Division, CSIR-National Chemical Laboratory, Pune, Maharashtra 411 008, India

⁶ Organic Chemistry Division, CSIR-National Chemical Laboratory, Pune, Maharashtra 411 008, India



The first synthesis of podocarflavone A and its analogs and evaluation of their antimycobacterial potential against *Mycobacterium tuberculosis* with the support of virtual screening

Ninad V. Puranik^{a,d*}, Sagar Swami^{b,c*}, Ashwini V. Misar^a, Ritu Mangain^a, Swapnaja S. Gulawani^a, Dhiman, Sarkar^{b,c} and Pratibha Srivastava^{a,d}

^aBioprospecting Group, Agharkar Research Institute, Pune, Maharashtra, India; ^bAcademy of Scientific and Innovative Research (AcSIR), Ghaziabad, India; ^cCombi-Chem Bio-Resource Center, Organic Chemistry Division, CSIR-National Chemical Laboratory, Pune, Maharashtra, India; ^dSavitribai Phule Pune University, Pune, Maharashtra, India

ABSTRACT

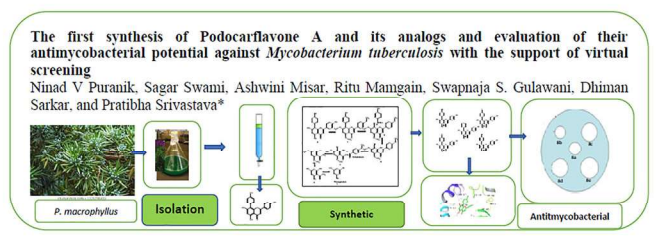
The first synthetic route developed for Podocarflavone A reported from *Podocarpus macrophyllus* and its analogs in 7 steps. Computational analysis for binding with the pantothenate kinase (3AVO) of *Mycobacterium tuberculosis* showed their docking score (ds) in the range of -8.9 to -9.3 Kcal/mol. MD simulations delineated the stability of the protein-ligand complexes in the TIP3P model. MMGBSA and MMPBSA values of **8d** were -42.46 Kcal/mol and -14.58 Kcal/mol, respectively. Further in-vitro antitubercular screening of compounds **8a**, **8d**, and **8e** against *M. tuberculosis* H37Ra using XRMA protocol exhibited promising antimycobacterial activity with IC₅₀ values 21.82 μ g/mL, 15.55 μ g/mL, and 16.56 μ g/mL, respectively. Compounds **8a**, **8d**, and **8e** showed antibacterial activity with IC₅₀ values 41.56 μ g/mL, 24.72 μ g/mL, and 72.45 μ g/mL respectively against the *Staphylococcus aureus*. **8a** and **8d** showed inhibition with IC₅₀ values 39.6 μ g/mL and 27.64 μ g/mL, respectively, against *Bacillus subtilis*. The present study could help in the further development of lead molecules against tuberculosis.

ARTICLE HISTORY

Received 30 December 2020
Accepted 17 February 2021


KEYWORDS

Podocarflavone A synthesis; antimycobacterial activity; docking; MD simulations; MMPBSA; and MMGBSA



CONTACT Pratibha Srivastava psrivastava@aripune.org; Dhiman Sarkar d.sarkar@ncl.res.in

*Both Ninad V. Puranik and Sagar Swami have equal contribution in this piece of work.

 Supplemental data for this article can be accessed at <https://doi.org/10.1080/14786419.2021.1893317>.

© 2021 Informa UK Limited, trading as Taylor & Francis Group

1. Introduction

Natural products are a dynamic source for innumerable novel pharmaceutical agents (Ahmad et al. 2016, 2017; Newman and Cragg 2016). Their isolation from natural resources is essential for their identification, characterization, and evaluation of biological potential. Every time, their isolation from the plants causes overexploitation of medicinal plants. With natural product synthesis, potential natural products can be available throughout the year (Maier 2015). The flavonoid class of compounds is prevalent among natural products (Crozier et al. 2009).

Podocarflavone A is an 8-aryl flavone reported from the leaves and twigs of plant *Podocarpus macrophyllus maki* and tested for different activities (Qiao et al. 2014). This plant belongs to the Podocarpaceae family and is distributed over tropical and subtropical regions of eastern Asia and Australia. The structures of some of the compounds isolated from this plant are presented in the following figure (Figure 1). Thus, considering the promising biological activities, we contemplated developing a synthetic protocol of podocarflavone A.

Tuberculosis (TB) is an acute infectious disease worldwide, and the causative agent is *Mycobacterium tuberculosis* (Mtb) (WHO 2020a). In 2019, 10 million people got infected, and 1.4 million people died from TB, though it is curable and preventable. An estimated 58 million people have been saved from TB. A complete cure of TB is still beyond reach, and the emergence of new pandemics such as COVID-19 can create hurdles to accomplish it. The DOTS (Directly Observed Treatment, Short Course) therapy announced by the World Health Organization (WHO) has shown an immense effect in achieving more than 90% treatment rates. However, the lengthy period (6–9 months) of the DOTS therapy and reoccurring gene mutations in pathogenic strains became the prime cause of drug resistance (WHO 2020b). Hence, the burst-out cases of multi-drug resistance (MDR) and extensive drug resistance (XDR) have

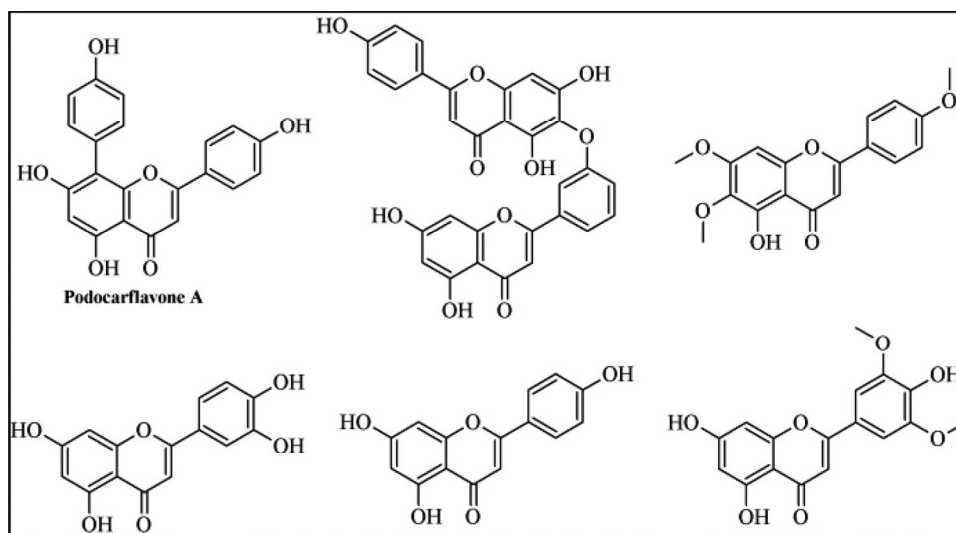


Figure 1. Structures of compounds isolated from *Podocarpus macrophyllus*.

emerged in recent years. The continuous search for potential new molecules with reduced toxicity can eradicate TB from the world.

In the present study, we have reported the total synthesis of natural product podocarflavone A and its analogs and evaluated them for in-vitro antitubercular screening Singh et al. 2011. The essential targets of Mtb are enzymes of the cell wall. Therefore, docking studies of these molecules' with cell wall enzyme pantothenate kinase (PDB 3AVO) carried out to understand their interactions (Chetnani et al. 2011). MMGBSA, MMPBSA approach determined the thermodynamic stability of the receptor-ligand complex, and MD simulations studies of 50 ns demonstrated the stability of the complex in the TIP3P model.

2. Results and discussion

Retrosynthetic analysis of podocarflavone A was planned, which confirmed 8-bromo flavone (**6**) is a critical scaffold to synthesize the target molecule (**8a**). It could be possible either by bromination of suitably substituted flavone (**5**) (Route 1) or by the cyclization of suitably substituted bromo chalcone (**5**) as shown in Route 2.

2.1. Retrosynthetic analysis

Retrosynthesis Route 1 involves the demethylation (Figure 2) of its methoxy analog (**7a**), which can be synthesized from the Suzuki cross-coupling reaction (Hooshmand et al. 2019) of 4-hydroxy phenylboronic acid with 8-bromo-5, 7-dimethoxy-2-(4-methoxyphenyl)-4H-1-benzopyran-4-one (**6**). The 8-bromo flavone (**6**) intermediate can be prepared from bromination of 5,7-dimethoxy-2-(4-methoxyphenyl)-4H-1-benzopyran-4-one (**5**), which further can be obtained from cyclization of substituted chalcone i.e., 1-(4,6-dimethoxy-2-hydroxyphenyl)-3-(4-methoxyphenyl)prop-2-en-1-one (**4**) (Arai et al. 2017). The chalcone can be synthesized using the aldol condensation of 1-(4,6-dimethoxy phenyl-2-hydroxy)- ethanone (**3**) with anisaldehyde using sodium hydroxide as a base (Gurung et al. 2009). Intermediate 4, 6-dimethoxy-2-

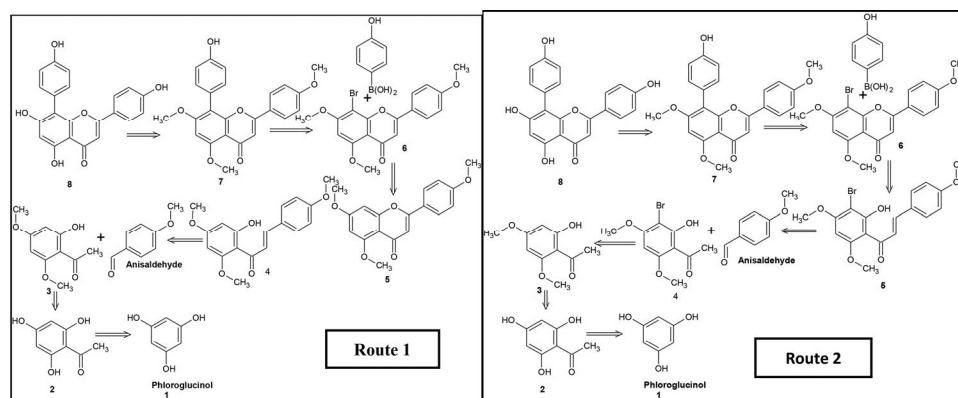
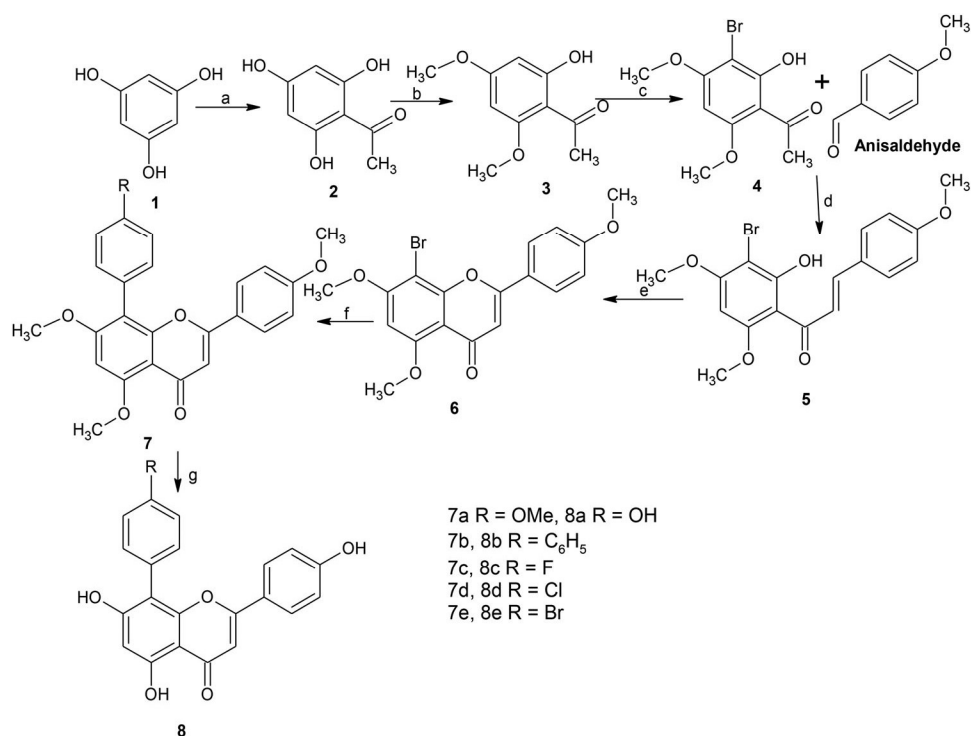


Figure 2. Retrosynthetic route (Route1 and Route 2) considered for the synthesis of natural product Podocarflavone A.



Scheme 1. Synthesis of podocarflavone A and its analogues; Reagents: (a) AlCl₃, acetyl chloride, nitrobenzene: DCM (1:1), 0°C-90°C, 2 h; (b) DMS, K₂CO₃, acetone, reflux, 8 h; (c) Br₂, acetic acid, 0°C to RT, 1 h; (d) NaOH, ethanol, RT, 72 h; (e) I₂, DMSO, 100°C, 1 h; (f) substituted phenylboronic acid, Pd(PPh₃)₄, Cs₂CO₃, DMF, 110°C, 6-12 h; (g) BBr₃, DCM, RT, 12 h.

hydroxyacetophenone (**3**) can be prepared (Sheng et al. 2017) from acetylated phloroglucinol (**2**), which can be synthesized by acylation of phloroglucinol using the reported method (Zhou et al. 2017).

Route 1 could not succeed due to the formation of 6, 8-dibromo flavone instead of monosubstituted 8-bromo flavone even on applying various parameters. This result incited us to consider retrosynthetic route **2** for the preparation of the targeted natural molecule.

Scheme 1 represents a detailed protocol for the synthesis of podocarflavone A and its analogs via **Route 2**. In this route, bromination, chalcone preparation, cyclization, and Suzuki coupling are the key steps. The acylation of phloroglucinol using AlCl₃, acetyl chloride in dichloromethane, and nitrobenzene delivered acetylated phloroglucinol (**2**). The yield was 75% (Zhou et al. 2017). Selective O-methylation (Sheng et al. 2017) of **2** using dimethyl sulfate, K₂CO₃, in acetone produced 4,6-dimethoxy-2-hydroxyacetophenone (**3**) with a 90% yield. Bromination of intermediate **3** in the presence of Br₂/acetic acid at 0 °C elicited into 3-bromo-4,6-dimethoxy-2-hydroxyacetophenone (**4**) with an 80% yield (Cechinel-Filho et al. 1996). This step provided **4** having bromo substituent at the desired position. Synthesis of 1-(3-bromo-4, 6-dimethoxy-2-hydroxyphenyl)-3-(4-methoxyphenyl)-2-propen-1-one (**5**) was done by base-catalyzed aldol condensation (Bandgar et al. 2012) of **4** with anisaldehyde, and the chalcone (**5**)

obtained with 95% yield. The cyclization of chalcone (**5**) in the presence of iodine and dimethylsulfoxide on heating resulted into 8-bromo-5,7-dimethoxy-2-(4-methoxyphenyl)-4H-benzopyran-4-one (**6**) (Gurung et al. 2009). The Suzuki cross-coupling reaction (Pan et al. 2017; Hooshmand et al. 2019) was performed for the C-C bond formation at the 8th position of the intermediate **6** with 4-hydroxyphenyl boronic acid produced methylated natural product Podocarflavone A (**7a**). The desired natural molecule Podocarflavone A obtained by deprotection of methyl group using BBr₃/DCM/12h (Ravishankar et al. 2016). Different 4-substituted phenylboronic acids were used to prepare the analogs of Podocarflavone A in the Suzuki coupling step (**Scheme-1**). Podocarflavone A and analogs were characterized by spectroscopic analysis. The spectral data were cross-checked with the natural product reported for confirmation, and it was found in agreement with the isolated natural product. Podocarflavone A (**8a**) was obtained after synthesis as the white powdered solid. The LC-MS of **8a** displayed a single peak and confirmed the mass of m/z 363.0. The FTIR spectra also showed two significant peaks at 3310 cm⁻¹ and 1651 cm⁻¹ for hydroxyl and carbonyl groups respectively. The ¹H NMR (400 MHz, DMSO-d₆) spectrum displayed a singlet δ 6.37 (s, 1H, 6-H), and another singlet for proton 3-H of ring A merged with a doublet of 3',5' H of the 4-hydroxyphenyl ring (**C**) and came as multiplet 6.78-6.80 (m, 3H, 3-H, 3',5' H). The three doublets 6.84 (d, J = 8.4 Hz, 3'', 5'' H), 7.25 (d, J = 8.8 Hz, 2'', 6'' H), 7.62 (d, J = 8.8 Hz, 2', 6' H), belong to aromatic protons of ring C and ring D respectively. Elegantly, we also got separate peaks for four hydroxyl groups, which are present at 7th position of B ring at 9.49s, OH, 7-OH), 4th position of ring D 10.33 (s, OH, 4''), 4th position of ring C at 10.66 (s, OH, 4'), and 5th position of ring B at 13.11 (s, OH, 5-OH) respectively. **Table S1** showed the comparative analysis of ¹H NMR, ¹³CNMR, and IR spectra. The ¹³C NMR displayed signals for 21 carbons, which contains the signals of a carbonyl carbon (δ 182.7) and 20 sp² carbons. The spectral analysis confirmed the total synthesis of Podocarflavone A and was found in agreement with the isolated Podocarflavone A (Qiao et al. 2014).

2.2. Antitubercular activity

Amongst the tested compounds, compounds **8a**, **8b**, **8c**, **8d**, and **8e** exhibited promising antimycobacterial activity with IC₅₀ values 21.82 μg/mL, 4.84 μg/ml with 24.84 μg/ml, 22.54 μg/ml, 15.55 μg/mL, and 16.56 μg/mL, respectively (**Table S2**). The compounds **8d** and **8e** were found more potent than the natural Podocarflavone A to inhibit Mtb. The results showed that the conversion of the hydroxyl group with the methoxy group restrict their inhibitory property. Replacement of the hydroxyl group at 4th position in ring D of **8a** with chloro or bromo group enhances its inhibitory potential against Mtb. We observed the same kind of results when we checked with dihydroflavonoids derivatives (Puranik et al. 2018).

2.3. Antibacterial activity

During the screening, three compounds **8a**, **8d**, and **8e**, showed potential against Gram +ve bacteria while there was no inhibitory activity towards Gram-ve bacteria.

Compound **8a** showed IC₅₀ at 41.56 µg/mL 39.6 µg/mL against *S. aureus* and *B. subtilis*, respectively. **8d** showed IC₅₀ at 24.72 µg/mL and 27.64 µg/mL against *S. aureus* and *B. subtilis*, respectively. **8e** showed IC₅₀ at 72.45 µg/mL against *S. aureus*. Data are presented in [Table S3](#).

2.4. Molecular modelling

Pantothenate kinase (3AVO) is an essential enzyme for Mtb and catalyzes the ATP-based phosphorylation of pantothenate. It is a crucial step in the biosynthetic pathway of coenzyme A from pantothenic acid. All the compounds were docked at the binding pocket to identify ligand-receptor interactions. Podocaflavone A and its analogs displayed strong binding properties to PanK with docking scores -7.2 to -9.3 Kcal/mole. The docking image of **8a**, **8c**, **8d**, and **8e** are displayed in [Figure S1](#). The interacting residues and docking scores are presented in [Table S2](#). Mostly all compounds showed hydrogen-bonded interactions with Arg 238. Essential residues are Asp 129, Lys147, Tyr 235, Arg 238, Asn 277 of the active binding pocket. All the compounds are surrounded by these amino acid residues and displayed interactions ([Figure S1](#)). Based on their binding profiles, these compounds are screened for anti-TB activity. Only compounds **8a**, **8c**, **8d**, and **8e** showed inhibitory activity. Therefore, the MD simulations of active compounds (**8a**, **8c**, **8d**, and **8e**) were performed.

2.5. Molecular dynamics simulations

The docked complexes of the compounds **8a**, **8c**, **8d**, and **8e** were subjected to analyze their stability in the TIP3P water model for 50 ns. The MD simulations on minimized and equilibrated complexes of **8a**, **8c**, **8d**, and **8e** were subjected to MD simulations for 50 ns Wang et al. 2006. RMSD versus time graph of the trajectories displayed in [Figure S2](#). The complexes' trajectories showed stability in the MD simulations, and RMSD values are determined ([Table S4](#)).

2.6. MMGBSA and MMPBSA analysis

The thermodynamic stability of proteins was determined by MMGBSA and MMPBSA analysis using Amber 20 Software Miller et al. 2012. The free energy values were calculated with the help of the mmpbsa.py script of Amber 20 by using a number of frames generated during MD simulations. It gave information about the thermodynamic stability of the complex. The MMPBSA and MMGBSA values of complexes are presented in [Table S4](#).

3. Experimental section

All the procedures for the intermediates from 2-8 are prepared and characterized by NMR. Their methodology is given in [supplementary file 1 \(Supplementary file 1\)](#). It

also contains [Figure S1](#) and [S2](#), [Tables S1–S4](#), the Mass (LC-MS), ^1H NMR, and ^{13}C NMR spectra of **7a–7e** and **8a–8e**.

4. Conclusion

The flavonoids are widely distributed in fruits and vegetables and are essential for human health. Therefore, we have reported the first synthetic route involving bromination followed by chalcone preparation, cyclization, and Suzuki coupling as the key steps to synthesize natural product Podocarflavone A, which is reported from *Podocarpus macrophyllus*. The natural product **8a** was successfully prepared in 7 steps. During the synthesis, their analogs are prepared following the same route. The halogenated Podocarflavone A showed better results in comparison to the natural product **8a**. The computational studies and in-vitro antimycobacterial screening results confirm inhibitory activity against Mtb. These molecules can serve to discover the lead molecules as antitubercular agents.

Disclosure statement

No potential conflict of interest was reported by the authors.

Funding

The authors are thankful to the Director, ARI, and the Director, NCL, Pune, India, for providing infrastructure and financial support. S. Swami (File no: 31/011(0983)2017/EMR-01) is grateful to the CSIR, New Delhi, India, for Senior Research Fellowship support. Dr. R. Mamgain is thankful to the Department of Science and Technology, New Delhi, India, for WOS-A project SR/WOS-A/CS-107/2018 and Ms. S.S. Gulawani for the support of UGC fellowship.

References

- Ahmad H, Ahmad S, Khan E, Shahzad A, Ali M, Tahir MN, Shaheen F, Ahmad M. 2017. Isolation, crystal structure determination and cholinesterase inhibitory potential of isotalatizidine hydrate from *Delphinium denudatum*. *Pharm Biol.* 55(1):680–686.
- Ahmad S, Ahmad H, Khan HU, Shahzad A, Khan E, Shah SAA, Ali M, Wadud A, Ghufuran M, Naz H, et al. 2016. Crystal structure, phytochemical study and enzyme inhibition activity of Ajaconine and Delectinine. *J Mol Struct.* 1123:441–448.
- Arai MA, Yamaguchi Y, Ishibashi M. 2017. Total synthesis of agalloside, isolated from *Aquilaria agallocha*, by the 5-O-glycosylation of flavan. *Org Biomol Chem.* 15(23):5025–5032.
- Bandgar BP, Hote BS, Dhole NA, Gacche RN. 2012. Synthesis and biological evaluation of novel series of chalcone derivatives as inhibitors of cyclooxygenase and LPS-induced TNF- α with potent antioxidant properties. *Med Chem Res.* 21(9):2292–2299.
- Cechinel-Filho V, Vaz ZR, Zunino L, Calixto JB, Yunes RA. 1996. Synthesis of xanthoxyline derivatives with antinociceptive and antiedematogenic activities. *Eur J Med Chem.* 31(10):833–839.
- Chetnani B, Kumar P, Abhinav KV, Chhibber M, Surolia A, Vijayan M. 2011. Location and conformation of pantothenate and its derivatives in *Mycobacterium tuberculosis* pantothenate kinase: insights into enzyme action. *Acta Crystallogr D Biol Crystallogr.* 67(Pt 9):774–783.
- Crozier A, Jaganath IB, Clifford MN. 2009. Dietary phenolics: chemistry, bioavailability and effects on health. *Nat Prod Rep.* 26(8):1001–1043.

- Gurung SK, Kim HP, Park H. 2009. Inhibition of prostaglandin E2 production by synthetic wogonin analogs. *Arch Pharm Res.* 32(11):1503–1508.
- Hooshmand SE, Heidari B, Sedghi R, Varma RS. 2019. Recent advances in the Suzuki-Miyaura cross-coupling reaction using efficient catalysts in eco-friendly media. *Green Chem.* 21(3): 381–405.
- Maier ME. 2015. Design and synthesis of analogues of natural products. *Org Biomol Chem.* 13(19):5302–5343.
- Miller BR, III McGee TD, Jr. Swails JM, Homeyer N, Gohlke H, Roitberg AE. 2012. MMPBSA.py: An efficient program for end-state free energy calculations. *J Chem Theory Comput.* 8(9): 3314–3321.
- Newman DJ, Cragg GM. 2016. Natural products as sources of new drugs from 1981 to 2014. *J Nat Prod.* 79(3):629–661.
- Pan G, Li X, Zhao L, Meng W, Chao S, Xuzhe L, Yongmin Z, Peng Y, Yuou T, Kui L. 2017. Synthesis and anti-oxidant activity evaluation of (±)-Anastatins A, B and their analogs. *Eur J Med Chem.* 138:577–589.
- Puranik NV, Srivastava P, Swami S, Choudhari A, Sarkar D. 2018. Molecular modeling studies and in-vitro screening of dihydrorugosaf flavonoids and its derivatives against *Mycobacterium tuberculosis*. *RSC Adv.* 8(19):10634–10643.
- Qiao Y, Sun WW, Wang JF, Zhang JD. 2014. Flavonoids from *Podocarpus macrophyllus* and their cardioprotective activities. *J Asian Nat Prod Res.* 16(2):222–229.
- Ravishankar D, Watson KA, Greco F, Osborn HMI. 2016. Novel synthesized flavone derivatives provide significant insight into the structural features required for enhanced anti-proliferative activity. *RSC Adv.* 6(69):64544–64556.
- Sheng X, Jia XY, Tang F, Wang Y, Hou AJ. 2017. The total synthesis of (±) sanggenol F. *Tetrahedron.* 73(25):3485–3491.
- Singh U, Akhtar S, Mishra A, Sarkar D. 2011. A novel screening method based on menadione mediated rapid reduction of tetrazolium salt for testing of anti-mycobacterial agents. *J Microbiol Methods.* 84(2):202–207.
- Wang J, Wang W, Kollman PA, Case DA. 2006. Automatic atom type and bond type perception in molecular mechanical calculations. *J Mol Graph Model.* 25(2):247–260.
- World Health Organization. 2020a. *Global tuberculosis report*.
- World Health Organization. 2020b. Tuberculosis. <http://www.who.int/mediacentre/factsheets/fs104/en/>.
- Zhou WL, Tan HB, Qiu SX, Chen GY, Liu HX, Zheng C. 2017. Biomimetic total synthesis and structure conformation of myrtucommulone K. *Tetrahedron Let.* 58(19):1817–1821.



Exploring the Pharmacological Potentials of Biosurfactant Derived from *Planococcus maritimus* SAMP MCC 3013

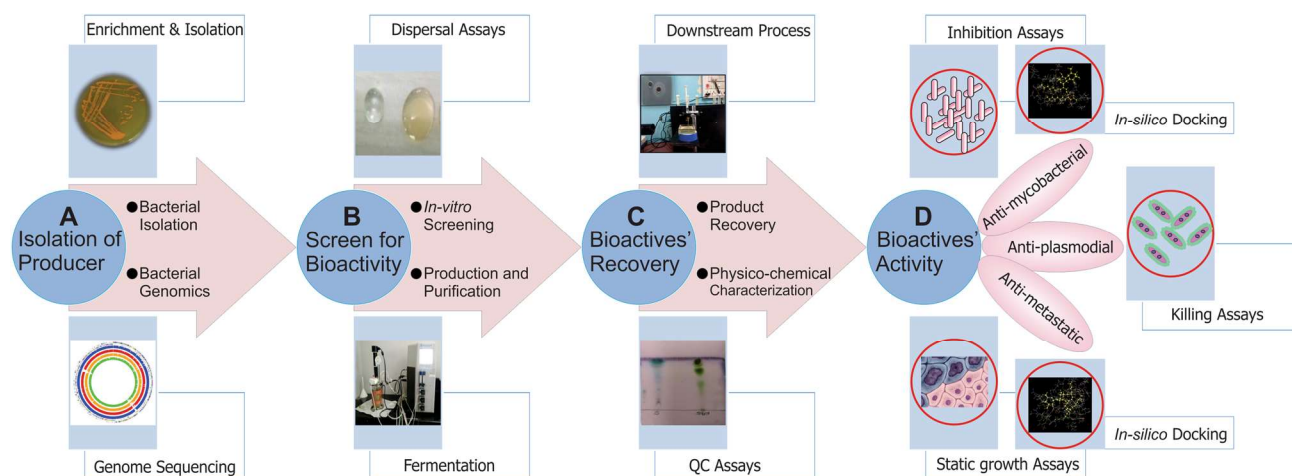
Samadhan Waghmode¹ · Sagar Swami^{2,3} · Dhiman Sarkar^{2,3} · Mangesh Suryavanshi⁴ · Sneha Roachlani⁵ · Prafulla Choudhari⁵ · Surekha Satpute⁶

Received: 25 July 2019 / Accepted: 17 December 2019
© Springer Science+Business Media, LLC, part of Springer Nature 2020

Abstract

Therapeutic potential of biosurfactant (BS) has been improved in recent years. Our present study deals with production of BS from *Planococcus maritimus* SAMP MCC 3013 in a mineral salt medium (MSM) supplemented with glucose (1.5% w/v). Further, BS has been purified and partially characterized as glycolipid type through our previous publication. Current research article aimed to evaluate biological potential of BS against *Mycobacterium tuberculosis*, *Plasmodium falciparum* and cancerous cell lines. *Planococcus* derived glycolipid BS was found to be a promising inhibitor of *M. tuberculosis* (MTB) H37Ra at IC₅₀ 64.11 ± 1.64 µg/mL and MIC at 160.8 ± 1.64 µg/mL. BS also showed growth inhibition of *P. falciparum* at EC₅₀ 34.56 ± 0.26 µM. Additionally, BS also displayed the cytotoxicity against HeLa (IC₅₀ 41.41 ± 4.21 µg/mL), MCF-7 (IC₅₀ 42.79 ± 6.07 µg/mL) and HCT (IC₅₀ 31.233 ± 5.08 µg/mL) cell lines. Molecular docking analysis was carried for the most popular glycolipid type BS namely Rhamnolipid (RHL) aiming to interpret the possible binding interaction for anti-tubercular and anti-cancer activity. This analysis revealed the involvement of RHL binding with *enoyl reductase* (InhA) of *M. tuberculosis*. Docking studies of RHL with tubulin directed several hydrophobic and Vander Waal interactions to exhibit anti-cancer potential. The present study will be helpful for further development of marine bioactive molecules for therapeutic applications. Their anti-tubercular, anti-plasmodial and cytotoxic activities make BS molecules as a noteworthy candidate to combat several diseases. To the best of our knowledge, this is the first report on projecting the pharmacological potential of *Planococcus* derived BS.

Graphic Abstract



✉ Surekha Satpute
drsureshasatpute@gmail.com; satputesk@unipune.ac.in

Extended author information available on the last page of the article

Introduction

The marine environments exhibit a number of macro and microorganisms for finding unique bioactive metabolites comprising antibiotics, compatible solutes, enzymes, vitamins, drugs and so forth [1, 2]. Halophilic bacteria have been demonstrated for their abundant biotechnological applications including production of biosurfactant (BS), pigments, enzymes, terpenoids, bacteriocins, biopolymers and exopolysaccharides [3, 4]. The marine microbial products act as primary resources for innovative medicines to treat dreaded diseases like cancer, AIDS, malaria, arthritis and so forth [5, 6]. Globally, marine natural products have gained rigorous awareness from scientific communities due to their feasibility in diverse field. BS are especially known as anti-biofilm, anti-adhesive and anti-microbial agents which needs to be explored further for several pharmacological applications [7, 8].

Tuberculosis (TB) is a wide spread infectious disease, caused by *M. tuberculosis* (MTB) where a contagious airborne is transmitted through the air and hard to control [9, 10]. World Health Organization (WHO) introduced the DOTS (Directly Observed Treatment, Short Course) strategy for the treatment of TB. Despite the available treatments, the spontaneous gene mutation in the pathogenic strains introduces the emergence of resistant strains to the currently available drugs and antibiotics. At present, there are very few drugs available to treat such drug-resistant TB [11]. Therefore, to overcome the current scenario, it is mandatory to explore the successful anti-tubercular treatment, where the marine natural product appears to be the promising one.

Malaria is a vector-borne disease caused by *Plasmodium* sp. and is transmitted through female Anopheles sp. Mosquito. According to WHO, in 2017 there were 219 million cases of malaria reported in 87 countries [12]. The increasing clinical resistance to commonly used frontline anti-malarial drugs, e.g. Chloroquine, Sulphadoxine-Pyrimethamine (SP) and so forth by these parasites cause difficulties in its treatment [13]. Therefore, it necessitates to develop new, safe and efficient drugs against malarial parasite.

Worldwide, another dreaded condition like cancer is the major concern. Currently, the vast majority of the drugs used to target the cancer cells through DNA damage, disturbance in cell division cycle leading the cell death [14]. Most cancer drugs are deliberately developed as specific molecular targets. The developments of anti-cancer drugs pose the most significant market in the pharmaceutical industry [15]. In cancer therapy, natural products of marine origin perhaps appear to be a suitable solution to tackle the severe diseases.

Literature survey primarily illustrates the hydrocarbon-degrading and emulsifying potential (with hydrocarbons

and oils) of BS derived from the Genus *Planococcus* [16, 17]. It is clear that the *Planococcus* derived BS has not been explored thoroughly for pharmaceutical potentials. We recently reported a research article on BS production from *Planococcus maritimus* with its physico-chemical properties [18]. The promising functional characteristics of *P. maritimus* BS encouraged us to exploit its therapeutic potentials. Due to sparse literature with respect to structural details of *Planococcus* BS; it is extremely challenging to interpret their possible pharmacological mechanisms of actions. In view of this background; we performed molecular docking analysis of Rhamnolipid (RHL) (well-known glycolipid type BS) as a reference compound. Through this reports, we tried to infer the possible anti-tubercular and anti-cancer mechanism of action of RHLBS.

Materials and Methods

Isolation and Identification of Marine Bacterium

The isolation of halophilic bacteria was carried out by using enrichment culture technique in Mineral Salt Medium (MSM) supplemented with glucose (1.5% w/v) [16]. The morphological trait of the isolated bacteria was observed under a scanning electron microscope (SEM). The identification of the selected isolate was carried out by 16S rRNA gene sequencing [19]. In order to identify the metabolic pathways encoded on the draft genome, whole genome sequencing (WGS) analysis was carried out [20] and published in our recent report [18].

Extraction and Purification of Biosurfactant

Initial screening of *P. maritimus* for BS production was carried out using surface tension (ST), drop collapse (DC) and oil displacement (OD) techniques [7]. The production of BS was carried out in MSM supplemented with glucose (1.5% w/v) as sole carbon source at 30 °C, 120 rpm for 7 days as per the method described earlier [16]. After seven days of fermentation process, the product was extracted from cells free broth, purified by Silica gel (Merck, mesh size 60–120) column chromatography. The structural characterization of product was carried out by FT-IR, NMR and LC-MS techniques [18]. The purified product was further used for biopharmaceutical related applications.

Pharmacological Screening of Biosurfactant

Chemicals, for example, sodium salt benzene sulfonic acid hydrate (XTT) and (3-[4,5-dimethylthiazol-2-yl]-2,5-diphenyltetrazolium bromide (MTT), Dimethyl sulfoxide

(DMSO). Paclitaxel and Rifampicin were procured from Sigma-Aldrich, US and Dubos medium from DIFCO, USA. Stock solution (10 mg/mL) of BS was made in DMSO and used further for anti-tubercular activity.

Anti-tubercular Activity

Reference culture of *M. tuberculosis* H37Ra (ATCC 25177) was procured from AstraZeneca, India. MTB stock cultures were grown and the *in vitro* anti-tubercular activity of BS measured at various concentrations (1–1000 µg/mL) as per the method described earlier [21, 22]. Rifampicin served as a positive control. The *in vitro* anti-tubercular activity was carried out in triplicate and the IC₅₀ and MIC values were determined using Origin 6.1 software. The data shown are representative of three independent experiments.

Anti-plasmodial Activity

Asexual stage of *Plasmodium falciparum* strain 3D7 was maintained under standard conditions at 2% haematocrit with 'O⁺' human erythrocytes in RPMI1640 containing 15 mM HEPES, 50 mg/L hypoxanthine, 2 g/L sodium bicarbonate and 2.5 g/L AlbuMAX II [23, 24]. Assays are typically set up in 96-well plate format and 200 µL of 2% of parasitized culture used per well. Stock solution of the BS compound was prepared in DMSO (100 µM). Standard anti-malarial drug Chloroquine (1 µM) used as positive control and 1% DMSO (equivalent to the DMSO present in the compound-treated samples) was used as a negative control [24]. Results are reported as percentages of growth inhibition and active compound further tested to determine the EC₅₀ values.

Cell Culture and Cytotoxicity Assay

HeLa (cervical cancer), HCT (colon cancer) and MCF-7 (breast cancer) cell lines were procured from the National Centre for Cell Science (NCCS), Pune. *In vitro* cytotoxicity of BS was measured at various concentrations (0.78–100 µg/mL) by MTT assay [25]. Here, Paclitaxel PTX was used as a reference compound for cytotoxicity study. The *in vitro* cytotoxicity activity was carried out in triplicate and the IC₅₀ and MIC values were determined using Origin 6.1 software. The data shown are representative of mean ± SD of three independent experiments.

Molecular Docking

Molecular docking analysis was performed to investigate the possible binding interaction for anti-tubercular and anti-cancer activity [26]. Crystal structure of *Mycobacterium tuberculosis* enoyl reductase (InhA) complexed with

n-(3-chloro-2-methylphenyl)-1-cyclohexyl-5-oxopyrrolidine-3-carboxamide (PDB ID 4TZT) and tubulin (PDB ID 4O2B) was utilized for docking analysis [26, 27]. Crystal structures of targeted proteins are downloaded from the free protein database www.rcsb.org. Both protein structures are refined via addition of hydrogen and removal of water molecules prior to the docking analysis.

Results

Identification of the Bacterium

The *P. maritimus* SAMP is 0.1 µm in size and possesses small cocci shaped morphology. The physiological features along with 16S rRNA sequence analysis confirmed that the strain SAMP belonging to *P. maritimus* (NCBI GenBank accession no. MINM00000000.1). Whole genome sequencing identified the metabolic pathways encoded in the draft genome. The presence of genes for the secondary metabolite having terpene like molecule was found [18].

Extraction and Purification of Biosurfactant

Various screening procedures viz. DC, OD and SFT measurement proved the surfactant activity of the BS obtained from *P. maritimus* SAMP MCC 3013. BS was extracted successfully from seven days old culture grown in MSM broth (30 °C with 120 rpm) using acid precipitation technique. The viscous honey coloured BS was obtained by solvent extraction, purified by column chromatography. Characterization of purified BS through analytical techniques proved terpene like molecule [18]. The purified BS was further used for pharmacological screening.

Pharmacological Applications of Biosurfactant

Anti-tuberculosis Activity

The terpene containing BS produced by *P. maritimus* was screened for *in vitro* anti-tubercular activity against *M. tuberculosis* H37Ra with a conventional XTT Reduction Menadione Assay (XRMA). BS exhibited IC₅₀ value at 64.11 ± 1.64 µg/mL and MIC at 160.8 ± 1.64 µg/mL concentration. Here, Rifampicin used as a reference molecule for anti-TB studies exhibited MIC at 0.04 µg/mL.

Anti-plasmodial Activity

BS produced from *P. maritimus* further tested to evaluate their anti-malarial activity against *P. falciparum* 3D7 strain. BS showed > 80% growth inhibition, after data normalization with background and control values. Next, we

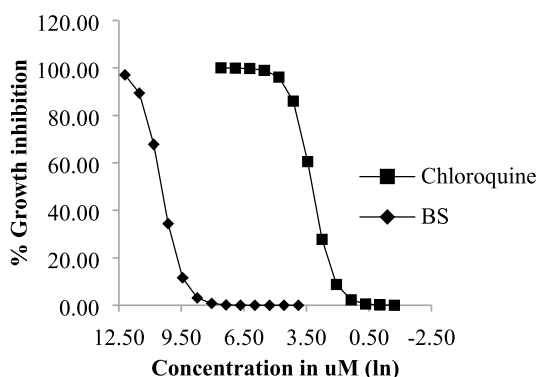


Fig. 1 In vitro anti-plasmodial activity (EC_{50}) of biosurfactant against *P. falciparum* 3D7 strain

Table 1 The cytotoxic effects of different concentrations of biosurfactant on the HeLa, HCT and MCF-7 cell lines

Cell line	Cytotoxicity ($\mu\text{g/mL}$)	
	IC_{50}	PTX Standard
MCF-7	42.793 ± 6.072	0.001 ± 0.003
HeLa	41.41 ± 4.214	0.0061 ± 0.01
HCT	31.233 ± 5.083	1.69 ± 0.18

carried out dose assay for BS using serial twofold dilution from $100 \mu\text{M}$ to $0.48 \mu\text{M}$ to determine EC_{50} value. BS dose assay data were analyzed in Microsoft excel and it showed EC_{50} at $34 \pm 0.26 \mu\text{M}$. (Fig. 1) represents sigmoidal curve BS compounds plotted using log dilution values vs. % growth inhibition values.

Cytotoxicity

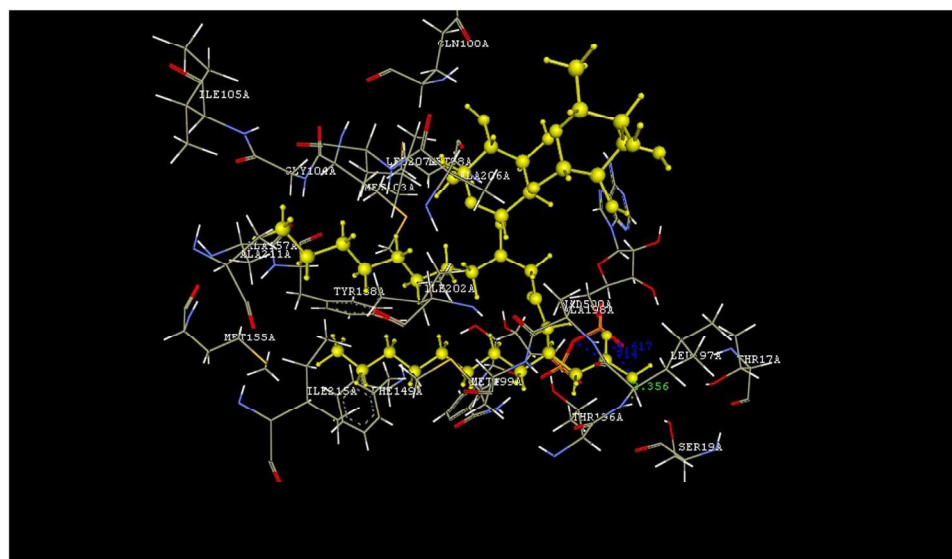
The results of cytotoxic activity of BS were recorded on three human cancer cell lines as IC_{50} (concentration of the drug required for 50% growth inhibition) (Table 1). BS was found to be cytotoxic to HeLa, MCF-7, HCT cells with concentrations $41.41 \pm 4.214 \mu\text{g/mL}$, $42.793 \pm 6.072 \mu\text{g/mL}$ and $31.233 \pm 5.083 \mu\text{g/mL}$ respectively. Here, Paclitaxel PTX used as a reference compound for cytotoxicity study.

Molecular Docking Study

Docking analysis was utilized to predict the possible mechanism of action of RHL type BS for anti-cancer and anti-tubercular activities. The RHLBS, a glycolipid type BS which has been reported extensively in the literature. In our studies, we also partially characterized the *Planococcus* BS and found to be glycolipid in nature [18]. This is the first report highlighting few details on structural aspects of *Planococcus* derived BS. Therefore, for molecular docking studies, we used a well-known type of glycolipid BS i.e. RHL. Docking studies of RHLBS on *M. tuberculosis* enoyl reductase (PDB 4TZT) revealed its anti-tubercular potential through hydrogen bond interaction (green colour) with GLN100, THR196; hydrophobic interaction with ILE16, THR17, SER19, ARG43, SER20, GLN100, MET103, PRO193, THR196, LEU197, ALA198, MET199, ILE202, LEU207, ILE215, LEU218 and Vander Waal interaction with PHE149, PHE97, MET98, PRO99, PHE149, TYR158, ILE194, with ILE16, THR17, SER19, ARG43, SER20, GLN100, MET103, PRO193, THR196, LEU197, ALA198, MET199, ILE202, LEU207, ILE215, LEU218 (Fig. 2).

Rhamnolipid when docked on tubulin (PDB ID 4O2B) to screen anti-cancer potential, it exhibited hydrogen bond

Fig. 2 Binding Interaction of Rhamnolipid with *M. tuberculosis* enoyl reductase (InhA)



interactions (green colour) with ARG2, ARG48, TYR202, LEU248, ASN249, ALA250; hydrophobic interaction with ARG2, ILE4, PHE20, TRP21, ILE24, HIS28, ARG48, ILE49, VAL51, TYR52, GLN136, MET235, VAL238, THR239, CYS241, LEU242, ARG243, LEU248, ASN249, ALA250, ASP251, LEU252, LYS254, LEU255 and Vander Waal interactions with GLN133, ASN167, PHE169, GLU200, TYR202, ARG2, ILE4, PHE20, TRP21, ILE24, HIS28, ARG48, ILE49, VAL51, TYR52, GLN136, MET235, VAL238, THR239, CYS241, LEU242, ARG243, LEU248, ASN249, ALA250, ASP251, LEU252, LYS254, LEU255 (Fig. 3).

Discussion

Halophiles are one of the substantial groups of extremophiles that tolerate high salt concentrations. Most of the secondary metabolites produced by these halobacteria possess valuable pharmacological properties [28, 29]. BS possesses anti-bacterial, anti-fungal, anti-viral, anti-cancer, anti-adhesive and anti-oxidants [8]. A good example is BS produced by marine *B. circulans* exhibit anti-microbial activity against gram-positive and gram-negative pathogens including multidrug-resistant (MDR) strains [30, 31].

The BS of *Planococcus* sp. was exploited against asexual stage of *P. falciparum* for determining the killing efficacies in whole-organism. We are reporting the EC_{50} ($34 \pm 0.26 \mu\text{M}$) value for *Planococcus* origin BS against *P. falciparum*. Many other existing anti-plasmodial compounds proved to be effective ranging between 5 and 50 μM concentration [12]. So, observations of our present study are comparable with the previous literature documenting anti-plasmodial efficacy (other than BS) [8]. Thus, it will be an

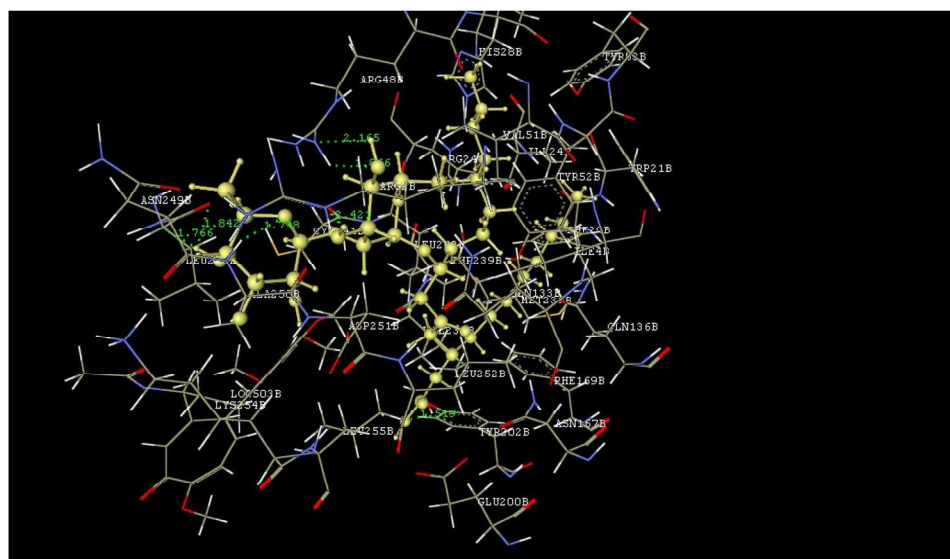
interesting to investigate the molecular detailed mechanism which lead the death of *P. falciparum*.

Drug discovery and development in TB is still challenging due to the shortage of predictive animal models, multiple physiological states and the slow growth rate of an organism. Therefore, to discover the drugs with new mode of action, it is mandatory to broaden the target areas [4, 10]. Here, we have explored one of the possibilities in the drug regimen using BS produced by *P. maritimus*. The in vitro XRMA activity was confirmed in *M. tuberculosis* H37Ra. To the best of our knowledge; this is the first report on BS produced by *P. maritimus* for its anti-tubercular agent. Such natural compounds have been explored for positive synergistic results of the existing anti-tubercular agents [32].

Molecular docking studies were accomplished to disclose the binding possibility of the RHLBS against interacting molecules. The docking analysis demonstrated that RHLBS docked with the active pockets of *M. tuberculosis* enoyl reductase (PDB 4TZZ) and interacted with active amino acids in various ways. RHLBS exhibited hydrogen bond interaction (green colour) (Fig. 2), hydrophobic interaction and Vander Waal interaction with several amino acids. Therefore, the interaction of inhibitors with certain amino acids is necessary for *M. tuberculosis* inhibition. The docking scores of **5a**, **5c**, **5d** and **6c** with 1UZN were found to be -8.296 , -8.366 , -8.175 and -7.398 kcal/mol respectively.

In comparison with anti-tubercular and anti-plasmodial study of BS; the work on cytotoxicity is reported frequently. Donio et al. demonstrated anti-cancer activity of BS obtained from halophilic *Bacillus* sp. BS3 using mammary epithelial carcinoma cell [33]. Anti-cancer activity was achieved at 0.25 $\mu\text{g}/\text{mL}$ concentration. Further, Donio et al. worked on *Halomonas* sp. BS4 originated BS to

Fig. 3 Binding Interaction of Rhamnolipid with tubulin protein of cancerous cells



demonstrate its anti-bacterial, anti-fungal, anti-viral and anti-cancer activities [34]. Their pharmacological screening studies confirmed the suppression of mammary epithelial carcinoma cell at a concentration (46.77% inhibition at 2.5 µg/mL). A naturally occurring BS with such interesting biological properties could be used as a lead molecule for the improvement of innovative anti-cancer agents. The cytotoxic effect of BS derived from marine microbes has been reported earlier [35] but the terpene containing BS not yet previously acknowledged. In this work, we are reporting the cytotoxic activity of terpene containing BS of *Planococcus* against HeLa, MCF-7, HCT cells with concentrations 41.41±4.214 µg/mL, 42.793±6.072 µg/mL and 31.233±5.083 µg/mL respectively. To screen anti-cancer potential, RHL which was docked on tubulin (PDB ID 4O2B) exhibited hydrogen bond interactions (green colour) (Fig. 3). with few amino acids viz. Arginine, Tyrosine, Leucine, Asparagine, Alanine and also exhibited hydrophobic interaction, Vander Waal interactions with several amino acids.

In the present study, we docked and evaluated in silico against *M. tuberculosis* enoyl reductase (PDB 4T2T) and anti-cancer potential, on tubulin (PDB ID 4O2B). The outcome of this integrated analysis was found to be supportive to explain the efficacy of the RHLBS in inhibiting MTB and cancerous cell lines. To the best of our knowledge, this is possibly the first report on molecular docking of RHLBS against *M. tuberculosis* and cancerous cell lines to interpret their possible mechanisms of action.

We also agree that the current study is reporting higher MIC values as compared with standard drugs. However, it is important to note that, the standard or reference drugs have undergone through extensive research and chemical modifications e.g. Rifampicin is chemically derived from natural product Rifamycins initially isolated from *Streptomyces mediterani* in 1957 [36, 37]. The early members of the family are undesirable for therapeutic applications due to poor potency, solubility, bioavailability and short half-life compared with current advanced stage of Rifampicin. So, as per our study the higher MIC may be reduced by future developments through chemical modifications in natural product or making synthetic derivatives of it. Further study is required in this area.

Newly discovered marine natural products like BSs have progressed through several clinical trials, although few of them must go through preclinical studies. One of the major problem for development is the “continuous supply”. Large quantities of compounds are required to carry out biological assay, to study site of action, identify the specific targets, selectivity of the compounds and its cytotoxicity. Throughout the world, several synthetic chemists are continuously trying to develop the synthetic and semi-synthetic strategies to overcome the supply issue and bring such molecules to

preclinical stage and further development for use in commercial and pharmaceutical areas.

Development of ‘drug-like’ molecules is possible by chemically altering the marine derived BS with several bios-teric structural units. Similarly, ongoing developments in mariculture (farming the growth of an organism in its natural environment) and aquaculture (culturing an organism under artificial conditions) have been tried to solve the problem of continuous supply of microorganisms. However, the natural condition of the sea makes cultivation or maintenance of isolated microorganisms is extremely difficult and even challenging oftenly.

Conclusion

The promising activity of *Planococcus* derived BS against tuberculosis, malaria and in cancer suggests its potential as a lead candidate for the development of novel “drug-like” molecules. Nevertheless, the chemical characteristics of a novel glycolipid molecule also make them acquiescent to the subsequent medicinal chemistry purposes. In vitro studies conducted against *P. falciparum*, *M. tuberculosis* H37Ra and cancerous cell lines (HeLa, HCT and MCF-7) proved the therapeutic potential of BS isolated from *Planococcus*. Molecular docking studies of RHLBS may provide avenues to explore the possible target sites for effective drug–receptor interactions and have created a new rational approach to design the drug. These approaches would be helpful to utilize unexplored BS like molecules for various therapeutic purposes.

Compliance with Ethical Standards

Conflict of interest The authors declare that they have no conflict of interest.

References

1. Adnan M, Alshammari E, Patel M, Ashraf SA, Khan S, Hadi S (2018) Significance and potential of marine microbial natural bioactive compounds against biofilms/biofouling: necessity for green chemistry. *Peer J* 6:e5049
2. Antoniou E, Fodelianakis S, Korkakaki E, Kalogerakis N (2015) Biosurfactant production from marine hydrocarbon-degrading consortia and pure bacterial strains using crude oil as carbon source. *Front Microbiol* 6:274
3. Dwivedi N, Mishra S, Mishra BN, Singh RB, Katoch VM (2011) 3D QSAR Based study of potent growth inhibitors of terpenes as antimycobacterial agents. *Open Nutraceuticals J* 4:119–124
4. Koul A, Arnoult E, Lounis N, Guillemont J, Andries K (2011) The challenge of new drug discovery for tuberculosis. *Nature* 469:483
5. Hamza F, Satpute S, Banpurkar A, Kumar AR, Zinjjarde S (2017) Biosurfactant from a marine bacterium disrupts biofilms

- of pathogenic bacteria in a tropical aquaculture system. FEMS Microbiol Ecol 93:11
6. Kalyani P, Hemalatha KPJ (2016) Marine microbial bioactive compounds. Int J Eng Sci Res Technol 5:124–133
 7. Satpute SK, Bhawsar BD, Dhakephalkar PK, Chopade BA (2008) Assessment of different screening methods for selecting biosurfactant producing marine bacteria. Indian J Mar Sci 37:243–250
 8. Satpute S, Mone N, Das P, Banpurkar A, Banat I (2018) *Lactobacillus acidophilus* derived biosurfactant as a biofilm inhibitor: a promising investigation using microfluidic approach. Appl Sci 8:1555
 9. Getahun H, Matteelli A, Chaisson RE, Raviglione M (2015) Latent *Mycobacterium tuberculosis* infection. N Engl J Med 372:2127–2135
 10. Rawat DS (2013) Antituberculosis drug research: a critical overview. Med Res Rev 33:693–764
 11. Palomino J, Martin A (2014) Drug resistance mechanisms in *Mycobacterium tuberculosis*. Antibiot 3:317–340
 12. World Health Organization (2017) A framework for malaria elimination. World Health Organization, Geneva, Switzerland
 13. Aratikatla EK, Valkute TR, Puri SK, Srivastava K, Bhattacharya AK (2017) Norepinephrine alkaloids as antiplasmodial agents: synthesis of syncarpamide and insight into the structure-activity relationships of its analogues as antiplasmodial agents. Eur J Med Chem 138:1089–1105
 14. Xu J, Mao W (2016) Overview of research and development for anticancer drugs. J Cancer Ther 7:762
 15. Ruiz-Torres V, Encinar J, Herranz-López M, Pérez-Sánchez A, Galiano V, Barrajón-Catalán E, Micol V (2017) An updated review on marine anticancer compounds: the use of virtual screening for the discovery of small-molecule cancer drugs. Molecules 22:1037
 16. Ebrahimipour G, Gilavand F, Karkhane M, Kavyanifard AA, Teymouri M, Marzban A (2014) Bioemulsification activity assessment of an indigenous strain of halotolerant *Planococcus* and partial characterization of produced biosurfactants. Int J Env Sci Technol 11:1379–1386
 17. Engelhardt MA, Daly K, Swannell RP, Head IM (2001) Isolation and characterization of a novel hydrocarbon-degrading, Gram-positive bacterium, isolated from intertidal beach sediment, and description of *Planococcus alkanoclasticus* sp. nov. J Appl Microbiol 90:237–247
 18. Waghmode S, Suryavanshi M, Dama L, Kansara S, Ghattargi V, Das P, Banpurkar A, Satpute SK (2019) Genomic insights of halophilic *Planococcus maritimus* SAMP MCC 3013 and detail investigation of its biosurfactant production. Front Microbiol 10:235
 19. Suryavanshi MV, Paul D, Doijad SP, Bhute SS, Hingamire TB, Gune RP, Shouche YS (2017) Draft genome sequence of *Lactobacillus plantarum* strains E2C2 and E2C5 isolated from human stool culture. Stand Genomic Sci 12:15
 20. Waghmode S, Dama L, Hingamire T, Bharti N, Doijad S, Suryavanshi M (2017) Draft genome sequence of a biosurfactant producing, *Bacillus aquimaris* strain SAMP MCC 3014 isolated from Indian Arabian coastline sea water. J Genomics 5:124
 21. Puranik NV, Srivastava P, Swami S, Choudhari A, Sarkar D (2018) Molecular modeling studies and in vitro screening of dihydrogosa flavonoid and its derivatives against *Mycobacterium tuberculosis*. RSC Adv 8:10634–10643
 22. Singh U, Akhtar S, Mishra A, Sarkar D (2011) A novel screening method based on menadione mediated rapid reduction of tetrazolium salt for testing of anti-mycobacterial agents. J Microbiol Methods 84:202–207
 23. Sanders NG, Sullivan DJ, Mlambo G, Dimopoulos G, Tripathi AK (2014) Gametocytocidal screen identifies novel chemical classes with *Plasmodium falciparum* transmission blocking activity. PLoS ONE 9:e105817
 24. Van Voorhis WC, Adams JH, Adelfio R, Ah Yong V, Akabas MH, Alano P, Alday A, Resto YA, Alsibae A, Alzualde A, Andrews KT (2016) Open source drug discovery with the malaria box compound collection for neglected diseases and beyond. PLoS Pathog 12:e1005763
 25. Choudhari AS, Suryavanshi SA, Kaul-Ghanekar R (2013) The aqueous extract of *Ficus religiosa* induces cell cycle arrest in human cervical cancer cell lines SiHa (HPV-16 Positive) and apoptosis in HeLa (HPV-18 Positive). PLoS ONE 7:e70127
 26. He X, Alian A, Stroud R, de Montellano OPR (2006) Pyrrolidine carboxamides as a novel class of inhibitors of enoyl acyl carrier protein reductase from *Mycobacterium tuberculosis*. J Med Chem 49:6308–6323
 27. Prota AE, Danel F, Bachmann F, Bargsten K, Buey RM, Pohlmann J, Reinelt S, Lane H, Steinmetz MO (2014) The novel microtubule-destabilizing drug BAL27862 binds to the colchicine site of tubulin with distinct effects on microtubule organization. J Mole Biol 426:1848–1860
 28. Cragg GM, Newman DJ (2013) Natural products: a continuing source of novel drug leads. Biochim Biophys Acta-General Subjects 6:3670–3695
 29. Manikandan P, Senthilkumar PK (2017) On overview of saltpan halophilic bacterium. Int J Biol Res 2:28–33
 30. Das P, Mukherjee S, Sen R (2008) Antimicrobial potential of a lipopeptide biosurfactant derived from a marine *Bacillus circulans*. J Appl Microbiol 6:1675–1684
 31. Vasileva-Tonkova E, Gesheva V (2007) Biosurfactant production by antarctic facultative anaerobe *Pantoea* sp. during growth on hydrocarbons. Curr Microbiol 54:136–141
 32. Sieniaswska E, Sawicki R, Swatko-Ossor M, Napiorkowska A, Przekora A, Ginalska G, Augustynowicz-Kopec E (2018) The effect of combining natural terpenes and antituberculous agents against reference and clinical *Mycobacterium tuberculosis* strains. Molecules 23:176
 33. Donio MB, Ronica FA, Viji VT, Velmurugan S, Jenifer JS, Michaelbabu M, Dhar P, Citarasu T (2013) *Halomonas* sp. BS4, A biosurfactant producing halophilic bacterium isolated from solar salt works in India and their biomedical importance. Springer Plus 1:149
 34. Donio MB, Ronica SF, Viji VT, Velmurugan S, Jenifer JA, Michaelbabu M, Citarasu T (2013) Isolation and characterization of halophilic *Bacillus* sp. BS3 able to produce pharmacologically important biosurfactants. Asian Pac J Trop Med 6:876–883
 35. Waters AL, Hill RT, Place AR, Hamann MT (2010) The expanding role of marine microbes in pharmaceutical development. Curr Opin Biotechnol 21:780–786
 36. Sensi P (1983) History of the development of rifampin. Rev Infect Dis Suppl 3:S402–S406
 37. Ramasami P, Gupta Bhown M, Jhaumeer Laulloo S, Li Kam Wah H (eds) (2019) Chemistry for a Clean and Healthy Planet. In: International conference on pure and applied chemistry—review on tuberculosis: trends in the discovery of new and efficient chemotherapeutic agents. Springer Nature, Basel, pp 197–227

Publisher's Note Springer Nature remains neutral with regard to jurisdictional claims in published maps and institutional affiliations.

Affiliations

Samadhan Waghmode¹ · Sagar Swami^{2,3} · Dhiman Sarkar^{2,3} · Mangesh Suryavanshi⁴ · Sneha Roachlani⁵ · Prafulla Choudhari⁵ · Surekha Satpute⁶ 

¹ Department of Microbiology, Elphinstone College, Fort, Mumbai 400032, India

² Combi-Chem BioResource Center, Organic Chemistry Division, CSIR-National Chemical Laboratory, Pune, Maharashtra 411 008, India

³ Academy of Scientific and Innovative Research (AcSIR), Ghaziabad, India

⁴ Yenepoya Research Centre, Yenepoya Deemed to be University, Deralakatte, Mangalore 575018, India

⁵ Department of Pharmaceutical Chemistry, Bharati Vidyapeeth College of Pharmacy, Kolhapur 416013, India

⁶ Department of Microbiology, Savitribai Phule Pune University, Pune 411007, India